

INVESTIGATING THE ROLE OF THE
CONDENSIN COMPLEXES DURING
MEIOSIS IN *ARABIDOPSIS THALIANA*

By

SARAH JANE SMITH

A thesis submitted to

The University of Birmingham

for the degree of

DOCTOR OF PHILOSOPHY

School of Biosciences
University of Birmingham
September 2011

UNIVERSITY OF
BIRMINGHAM

University of Birmingham Research Archive

e-theses repository

This unpublished thesis/dissertation is copyright of the author and/or third parties. The intellectual property rights of the author or third parties in respect of this work are as defined by The Copyright Designs and Patents Act 1988 or as modified by any successor legislation.

Any use made of information contained in this thesis/dissertation must be in accordance with that legislation and must be properly acknowledged. Further distribution or reproduction in any format is prohibited without the permission of the copyright holder.

ABSTRACT

Meiosis is a specialised cell division essential for sexual reproduction. During meiosis the chromosomes are highly organised and correct chromosome architecture is required for meiotic recombination and faithful segregation of chromosomes at anaphase. Condensin is involved in chromosome organisation during meiotic and mitotic cell divisions. Three condensin subunits, including condensin I and II specific subunits *AtCAPD2* and *AtCAPD3* respectively, have been studied for their role in meiosis using T-DNA insertion plants and an RNAi approach.

The condensin subunit *AtSMC4* localised to meiotic chromosomes at metaphase I, where it coated the entire chromosome and remained until telophase. Some evidence of centromere localisation of *AtSMC4* was also seen during prophase I and metaphase I. *AtSMC4^{RNAi}* lines were able to condense their chromosomes into metaphase bivalents which were essentially normal. However at anaphase the chromosomes appeared to lose structural integrity such that a thin curtain of lagging chromatin was seen to trail behind the segregating chromosomes. As in *AtSMC4^{RNAi}* lines, both condensin I and II specific subunits were also required for chromosome segregation at anaphase I and II. However their roles in this process differed. *AtCAPD2^{RNAi}* resembled *AtSMC4^{RNAi}* lines but *Atcapd3* plants had a unique anaphase phenotype. It is possible that these two phenotypes represent different manifestations of the same role of maintaining chromosome organisation. Condensin I, but not condensin II was also shown to be required for the organisation of the rDNA and to maintain the structure of the centromeres at metaphase.

ACKNOWLEDGEMENTS

I would like to thank my supervisors Chris Franklin and Sue Armstrong for all of their help and guidance throughout my PhD and for giving me the opportunity to do my project.

I would also especially like to thank Kim Osman and Eugenio Sanchez-Moran, who have shared their time, expertise and advice over the years and James Higgins for his help in the lab, useful discussions and willingness to sing karaoke. I thank Steve Price for all of his technical support, especially in the last few months of my project, Ruth Perry for her guidance and support throughout my PhD (and for her amazing Guinness and Chocolate cake!) and Karen Staples for looking after my plants. I would also like to thank all members of the Franklin, Franklin-Tong and Coates' labs past and present for their advice and friendship. I am grateful to Mathilda Grelon at INRA for allowing me to come to her lab and Liudmila Chelysheva for showing me the immunolocalisation technique on fixed buds which proved essential for analysing my antibody. My project was funded by the Biotechnological and Biological Sciences Research Council (BBSRC).

I also thank my family and partner Luke for their love and support throughout my PhD, especially during difficult times, and my friends for fun times along the way.

CONTENTS

CHAPTER 1

1	INTRODUCTION	1
1.1	The significance of meiosis	1
1.2	An overview of meiosis.....	2
1.3	Meiosis in <i>Arabidopsis</i>	6
1.4	Meiotic recombination	8
1.4.1	Processing of DSBs in the CO pathway	10
1.4.2	Single end invasion (SEI)	10
1.4.3	There is an excess of DSBs compared to COs formed	12
1.4.4	CO interference	13
1.4.5	Two recombination pathways exist in many species	15
1.4.6	The class I pathway of CO formation.....	16
1.4.7	The class II pathway of CO formation.....	17
1.4.8	Relative contribution of the two pathways.....	17
1.4.9	Double Holliday junction resolution.....	18
1.4.10	Factors influencing CO distribution.....	19
1.5	The chromosome axes are highly organised.....	20
1.6	Recombination and Chromosome organisation	24
1.6.1	SC proteins mediate meiotic recombination	25
1.6.2	Recombination initiates pairing and synapsis	27
1.7	Condensin is involved in chromosome organisation during meiosis and mitosis.....	29
1.7.1	The condensin complexes	29
1.7.2	Identification of the condensin complexes	31
1.7.3	Structural Maintenance of Chromosome proteins.....	32
1.7.4	Condensin and chromosome condensation.....	37
1.7.5	Condensin I and II play different roles during mitotic cell divisions	42

1.7.6	Condensin is specifically required for rDNA organisation in yeast.....	43
1.7.7	Condensin is required for correct centromere and kinetochore function	47
1.7.8	Condensin and chromosome segregation	51
1.7.9	Condensin recruitment onto DNA	53
1.7.10	Regulation of condensin during mitotic divisions	55
1.7.11	Condensin and gene regulation.....	56
1.7.12	Condensin in meiosis	57
1.8	Project aims	64

CHAPTER 2

2	MATERIALS AND METHODS	65
2.1	Plant cultivation	65
2.1.1	Sterilisation of seeds for plating on MS media	65
2.2	Cytological procedures.....	65
2.2.1	Preparation of slides	66
2.2.2	Cytology: chromosome spreading	66
2.2.3	Nick translation of Fluorescence <i>in situ</i> hybridisation FISH probes	67
2.2.4	Fluorescence <i>in situ</i> hybridisation.....	68
2.2.5	Immunolocalisation by spreading.....	69
2.2.6	Immunolocalisation on fixed bud material.....	70
2.2.7	Alexander staining of pollen.....	70
2.3	DNA and RNA manipulations	71
2.3.1	Plant DNA extractions.....	71
2.3.2	RNA extraction.....	71
2.3.3	cDNA synthesis	72
2.3.4	Agarose Gel electrophoresis for DNA.....	72
2.3.5	Agarose Gel electrophoresis for RNA.....	73

2.3.6	Primer design.....	73
2.3.7	Polymerase Chain Reactions (PCR).....	73
2.4	Cloning procedures	74
2.4.1	Amplification of sequence specifically for cloning	74
2.4.2	Extraction of amplified DNA from agarose gels	74
2.4.3	Quantification of nucleic acids	75
2.4.4	Cloning Vectors	75
2.4.5	Ligation into pZErO cloning vector.....	76
2.4.6	Ligation into pET-21b, pHANNIBAL and pPF404	77
2.4.7	Preparation of competent <i>E. coli</i> cells.....	77
2.4.8	Transformation of <i>E. coli</i> competent cells by heat-shock.....	78
2.4.9	Production of electro-competent <i>A. tumefaciens</i> cells	78
2.4.10	Transformation of electro-competent <i>A. tumefaciens</i> cells	79
2.4.11	Bacterial Growth media	79
2.4.12	Colony PCR.....	80
2.4.13	Purification of plasmid DNA.....	80
2.4.14	Sequencing of plasmid DNA.....	80
2.4.15	Sequence analysis	81
2.4.16	Restriction digests	81
2.4.17	Phenol chloroform extraction.....	81
2.5	Protein manipulations.....	82
2.5.1	Induction of recombinant protein from <i>E. coli</i> cells.....	82
2.5.2	Recombinant protein extraction from bacteria cells	82
2.5.3	SDS-PAGE gel electrophoresis	83
2.5.4	Coomassie staining	84
2.5.5	Isolation of HIS-tagged proteins using Ni-NTA resin (QIAGEN)	84
2.5.6	Dialysis of purified recombinant proteins	85
2.5.7	Protein quantification	86

2.5.8	Protein extraction from plant material:	86
2.5.8.1	Large-scale extraction protocol	86
2.5.8.2	Protein extraction from anthers	86
2.5.9	Western transfer analysis	87
2.5.10	Antibody labelling	87
2.5.10.1	Alkaline phosphatase detection.....	87
2.5.10.2	Enhanced chemiluminescence (ECL) detection.....	88
2.5.11	Affinity purification of antibody.....	88
2.5.12	Purification of antibody using Immobilized <i>E. coli</i> Lysate Kit (Thermo scientific) 89	
2.5.13	Plant transformation	89
2.6	Statistical procedures	90
2.7	List of websites:.....	90

CHAPTER 3

3	PRODUCTION AND ANALYSIS OF AN ANTI-ATSMC4 ANTIBODY.....	91
3.1	INTRODUCTION.....	91
3.2	RESULTS.....	94
3.2.1	Cloning <i>AtSMC4</i> C-terminus for antibody production	94
3.2.2	Production of <i>AtSMC4</i> C-terminal recombinant protein	96
3.2.3	Determining the cellular localisation of the expressed <i>AtSMC4</i> recombinant protein	97
3.2.4	Large scale purification of <i>AtSMC4</i> recombinant protein	98
3.2.5	Testing the specificity of the <i>AtSMC4</i> antibody.....	101
3.2.6	Immunolocalisation of <i>AtSMC4</i> on pollen mother cells (PMCs).....	103
3.2.7	Purification of <i>AtSMC4</i> -Ab.....	105
3.2.8	Immunolocalisation of <i>AtSMC4</i> during meiosis using fixed bud material 108	
3.2.9	<i>AtSMC4</i> localisation to mitotic cells	114

3.2.10	Western blot analysis on plant protein extract	117
3.3	DISCUSSION.....	119
3.3.1	Origin of non-specific axis-associated signal in the pre-immune serum 119	
3.3.2	<i>E. coli</i> column antibody purification was more successful than affinity purification	119
3.3.3	<i>AtSMC4</i> -Ab recognises recombinant <i>AtSMC4</i> protein and a protein corresponding to the size of <i>AtSMC4</i> from plant extracts.	120
3.3.4	Condensin localisation during meiosis in <i>Arabidopsis</i>	121
3.3.5	Condensin localisation during mitotic cell divisions.....	123
3.3.6	Future perspectives	124
3.3.7	Conclusions	125

CHAPTER 4

4	THE CONDENSIN SUBUNIT <i>ATSMC4</i> IS ESSENTIAL FOR MEIOTIC CHROMOSOME ORGANISATION IN <i>ARABIDOPSIS THALIANA</i>	126
4.1	INTRODUCTION.....	126
4.2	RESULTS.....	129
4.2.1	Isolation and Characterisation of an <i>AtSMC4</i> T-DNA insertion line	129
4.2.2	Fertility of <i>AtSMC4</i> ^{+/-} plants.....	131
4.2.3	Meiosis in <i>AtSMC4</i> ^{+/-} plants	132
4.2.4	Synapsis and the chromosome axis appear normal in <i>AtSMC4</i> ^{+/-}	134
4.2.5	RNA interference: a form of post-transcriptional gene silencing	136
4.2.6	Choosing and cloning the <i>AtSMC4</i> sense and antisense sequence	138
4.2.7	Screening of pPF408-empty lines.....	140
4.2.8	Initial screening of <i>AtSMC4</i> ^{RNAi} lines.....	143
4.2.9	Checking for the presence of the RNAi insert by PCR and cloning of the PCR band	145
4.2.10	Screening transformants for meiotic phenotypes	147

4.2.11	Mitotic defects in <i>AtSMC4^{RNAi}</i> lines.....	148
4.2.12	Selection of <i>AtSMC4^{RNAi}</i> lines for further analysis.....	151
4.2.13	Western blot analysis of extracts from <i>AtSMC4^{RNAi}</i> lines.....	152
4.2.14	Localisation of <i>AtSMC4</i> -Ab on fixed buds of <i>AtSMC4^{RNAi}</i> lines	156
4.2.15	Detailed phenotypic analysis of selected lines	158
4.2.15.1	Fertility and pollen viability of <i>AtSMC4^{RNAi}</i> lines	158
4.2.15.2	Full cytological atlas of <i>AtSMC4^{RNAi}</i> lines	160
4.2.15.3	<i>AtSMC4^{RNAi}</i> lines appeared to have normal prophase I chromosome axes	162
4.2.15.4	<i>AtSMC4^{RNAi}</i> lines show a slight reduction in chiasmata	167
4.2.15.5	The rDNA appears disorganised in the <i>AtSMC4^{RNAi}</i> lines	172
4.2.16	Centromere organisation in the <i>AtSMC4^{RNAi}</i> lines.....	175
4.2.17	Investigating the origin of the anaphase defects	179
4.3	DISCUSSION.....	182
4.3.1	The <i>DMC1</i> promoter is 'leaky'.....	183
4.3.2	<i>AtSMC4^{RNAi}</i> lines have reduced <i>AtSMC4</i> protein levels as shown by western blot and immunolocalisation	183
4.3.3	Chromosome axes appear normal in <i>AtSMC4^{RNAi}</i> lines.....	185
4.3.4	<i>AtSMC4^{RNAi}</i> lines have a slight reduction in chiasmata.....	186
4.3.5	Effect of reducing <i>AtSMC4</i> on chromosome organisation	187
4.3.5.1	Centromere structure is compromised in <i>AtSMC4^{RNAi}</i> lines.....	187
4.3.5.2	The rDNA appears disorganised in the <i>AtSMC4^{RNAi}</i> lines	189
4.3.5.3	Origin of the anaphase defects	190
4.3.6	Future perspectives	192
4.3.7	Conclusions	194

CHAPTER 5

5	PRODUCTION AND ANALYSIS OF RNAi LINES FOR DEPLETION OF THE <i>ATCAPD2</i> SUBUNIT OF CONDENSIN I.....	195
5.1	INTRODUCTION.....	195

5.2	RESULTS.....	199
5.2.1	Search for T-DNA insertion lines of condensin I subunits.....	199
5.2.2	Production of an RNAi construct to deplete <i>AtCAPD2</i>	200
5.2.3	Checking for the presence of the RNAi inserts by PCR.....	200
5.2.4	Cytological screening of <i>AtCAPD2^{RNAi}</i> lines	202
5.2.5	<i>AtCAPD2^{RNAi}</i> lines have disorganised rDNA regions	206
5.2.6	<i>AtCAPD2^{RNAi}</i> lines have defective centromeric DNA	208
5.3	DISCUSSION.....	211
5.3.1	An <i>Atcapg</i> homozygote insertion mutant appears to be lethal.....	211
5.3.2	Chromosome organisation in the <i>AtCAPD2^{RNAi}</i> lines.....	211
5.3.3	Condensin I is required for the structural stability of the centromeres ..	212
5.3.4	Condensin I is required for correct organisation of the rDNA in <i>Arabidopsis</i>	212
5.3.5	Chromosome segregation defects are seen in condensin I-deficient cells	213
5.3.6	Future perspectives	214
5.3.7	Conclusions	216

CHAPTER 6

6	ANALYSIS OF AN <i>ATCAPD3</i> T-DNA LINE AND <i>ATCAPD3^{RNAi}</i> LINES	217
6.1	INTRODUCTION.....	217
6.2	RESULTS.....	220
6.2.1	Isolation and characterisation of <i>AtCAPD3</i> T-DNA lines.....	220
6.2.2	Confirming the position of the T-DNA insertion site	221
6.2.3	Confirming the number of inserts in the <i>Atcapd3</i> insertion line.....	222
6.2.4	Analysis of <i>AtCAPD3</i> transcript levels in wild-type and <i>Atcapd3</i> plants	223
6.2.5	<i>Atcapd3</i> mutants have developmental defects	224

6.2.6	Fertility was reduced in <i>Atcapd3</i> and <i>AtCAPD3^{+/-}</i> plants	226
6.2.7	<i>Atcapd3</i> plants had a reduced seed germination frequency compared to wild-type and <i>AtCAPD3^{+/-}</i> plants.	228
6.2.8	Cytological analysis of <i>Atcapd3</i> and <i>AtCAPD3^{+/-}</i>	229
6.2.9	<i>AtCAPD3^{+/-}</i> plants had a mild meiotic phenotype	229
6.2.10	<i>Atcapd3</i> plants had misshapen chromosomes and connections between chromosomes at metaphase I.	230
6.2.11	Mitotic <i>Atcapd3</i> cells had anaphase defects.....	234
6.2.12	Producing <i>AtCAPD3^{RNAi}</i> lines	236
6.2.13	Checking for the presence of the inserts by PCR and cloning the PCR bands	236
6.2.14	<i>AtCAPD3^{RNAi}</i> lines confirm the phenotype of <i>Atcapd3</i> plants	238
6.2.15	<i>Atcapd3</i> does not appear to be involved in rDNA organisation	241
6.2.16	Analysis of centromeric DNA in <i>Atcapd3</i> plants	243
6.2.17	Prophase I chromosome axes in <i>Atcapd3</i> plants appear normal	245
6.2.18	Attempting to make an <i>AtCAPD3</i> recombinant protein for antiserum production	247
6.3	DISCUSSION	251
6.3.1	<i>Atcapd3</i> plants are viable and have developmental defects	251
6.3.2	<i>AtCAPD3^{+/-}</i> and <i>Atcapd3</i> plants both had reduced fertility	253
6.3.3	<i>Atcapd3</i> does not appear to have prophase I defects.....	254
6.3.4	Chromosome organisation problems in <i>Atcapd3</i> plants.....	254
6.3.5	Condensin II does not play a role in rDNA or centromeric organisation	256
6.3.6	<i>Atcapd3</i> plants appear to lose chromosome integrity at anaphase.....	257
6.3.7	<i>Atcapd3</i> phenotypes differed from those of <i>AtSMC4</i> and <i>AtCAPD2^{RNAi}</i> lines	258
6.3.8	<i>AtCAPD3</i> C-terminal recombinant protein appeared to be lethal to the <i>E. coli</i> expression cells	259
6.3.9	Future perspectives	259
6.3.10	Conclusions.....	261

CHAPTER 7

7	GENERAL DISCUSSION	262
7.1	Introduction	262
7.2	Condensin does not appear to have a role in prophase I chromosome organisation	266
7.3	A role for condensin in recombination?	266
7.4	A role for condensin in maintaining chromosome architecture	267
7.5	Condensin I and II have different roles in meiotic chromosome organisation 269	
7.6	Future perspectives	271
7.7	Concluding remarks	273

CHAPTER 8

8	REFERENCE LIST	274
---	----------------------	-----

CHAPTER 9

9	APPENDIXES	294
9.1	BUFFERS	294
9.2	TABLE OF PRIMERS	297
9.3	TABLE OF T-DNA LINES	296

FIGURES

Figure 1.1: Schematic representation of a mitotic cell division..	3
Figure 1.2: Schematic representation of a meiotic cell division	4
Figure 1.3: Schematic representation of the meiotic recombination pathway.....	9
Figure 1.4: Schematic representation of crossover interference.....	14
Figure 1.5: Mechanical stress model of CO interference.....	15
Figure 1.6: Structure of the synaptonemal complex and its formation through prophase I.	22
Figure 1.7: Structure of SMC proteins and SMC hetero-dimers..	33
Figure 1.8: Subunit arrangement of condensin I, condensin II and cohesin complexes	35
Figure 1.9: Structural organisation of the chromosomes..	38
Figure 3.1: ClustalW2 alignment of the C-terminus of <i>Arabidopsis</i> SMC proteins....	95
Figure 3.2: Expression of SMC4 C-terminal recombinant protein.....	96
Figure 3.3: Soluble and insoluble fractions of cell extracts.....	97
Figure 3.4: Purification of <i>AtSMC4</i> recombinant protein using Ni-NTA beads.....	99
Figure 3.5: Confirming the concentration of <i>AtSMC4</i> -recombinant protein.....	100
Figure 3.6: Concentration of <i>AtSMC4</i> recombinant protein pre- and post- dialysis.	100
Figure 3.7: Western blot analysis of anti- <i>AtSMC4</i> specificity.....	102
Figure 3.8: Immunolocalisation of <i>AtSMC4</i> -Ab on wild-type PMC.	104
Figure 3.9: Western blot analysis of affinity purified <i>AtSMC4</i> -Ab:.....	106
Figure 3.10: Western blot analysis of <i>E.coli</i> column purified <i>AtSMC4</i> -Ab.....	107
Figure 3.11: Immunolocalisation of <i>AtSMC4</i> -Ab on wild-type PMC stages zygotene to late diakinesis/early metaphase I.	110

Figure 3.12: Immunolocalisation of <i>AtSMC4</i> -Ab on wild-type PMC stages metaphase I to dyad/prophase II.....	111
Figure 3.13: Immunolocalisation of <i>AtSMC4</i> -Ab on wild-type metaphase I..	111
Figure 3.14: Immunolocalisation of <i>AtSMC4</i> -Ab on wild-type PMCs stages metaphase II to tetrad.	112
Figure 3.15: Immunolocalisation of pre-immune (PI) serum on wild-type PMCs. ...	113
Figure 3.16: Immunolocalisation of <i>AtSMC4</i> -Ab on wild-type mitotic cells.	115
Figure 3.17: Immunolocalisation of <i>AtSMC4</i> pre-immune (PI) serum on wild-type mitotic cells.....	116
Figure 3.18: Western blot analysis of <i>AtSMC4</i> -Ab on plant protein extracts.	118
Figure 4.1: Schematic representation of the condensin I and II complexes.....	128
Figure 4.2: Position of the T-DNA insert in the Salk_86_D2 line.	130
Figure 4.3: Mean seed set in <i>AtSMC4</i> ^{+/-} plants compared to wild-type.....	131
Figure 4.4: Meiotic phenotypes of <i>AtSMC4</i> ^{+/-} and wild-type plants.	133
Figure 4.5: Immunolocalization of <i>AtASY1</i> and <i>AtZYP1</i> on <i>AtSMC4</i> ^{+/-} and wild-type PMCs.	135
Figure 4.6: Simplified mechanism of RNA interference	137
Figure 4.7: Schematic representation of the <i>RNAi</i> construct designed to deplete mRNA levels in meiotic cells..	139
Figure 4.8: Mean seed set in pPF408 empty vector plants which showed signs of reduced fertility.	141
Figure 4.9: Meiotic phenotypes of pPF408 empty vector transformed plants.	142
Figure 4.10: <i>AtSMC4</i> ^{RNAi} plants showing developmental defects..	144

Figure 4.11: Sequence of PCR product obtained from <i>AtSMC4^{RNAi}</i> plants using insert specific primers..	146
Figure 4.12: Meiotic phenotypes of <i>AtSMC4</i> -pPF408 transformed plants.	149
Figure 4.13: Mitotic anaphase stained with DAPI.	150
Figure 4.14: Western blot analysis of bud and anther protein extract probed with <i>AtSMC4</i> -Ab..	154
Figure 4.15: Western blot showing relative intensities of <i>AtSMC4</i> protein band in anthers from wild-type and <i>AtSMC4^{RNAi}</i> plants.	154
Figure 4.16: Analysis of the relative levels of <i>AtSMC4</i> in anthers from wild-type and <i>AtSMC4^{RNAi}</i> lines.	155
Figure 4.17: Immunolocalisation of <i>AtSMC4</i> -Ab on <i>AtSMC4^{RNAi}</i> line 2.10 and wild-type PMCs at metaphase I.	157
Figure 4.18: Mean seed set in wild-type and <i>AtSMC4^{RNAi}</i> lines.	159
Figure 4.19: Meiotic phenotypes of <i>AtSMC4^{RNAi}</i> lines..	160
Figure 4.20: Immunolocalization of <i>AtASY1</i> and <i>AtZYP1</i> on <i>AtSMC4^{RNAi}</i> and wild-type PMCs.....	164
Figure 4.21: Pachytene axes length data for wild-type, and an <i>AtSMC4^{RNAi}</i> line....	166
Figure 4.22: Schematic representation of the position and size of the 45S and 5S rDNA probes on <i>Arabidopsis</i> chromosomes 1-5.	168
Figure 4.23: Mean total chiasmata counts for wild-type and <i>AtSMC4^{RNAi}</i> lines	171
Figure 4.24: Mean chiasmata counts for individual chromosomes..	171
Figure 4.25: Analysis of the rDNA regions in wild-type and <i>AtSMC4^{RNAi}</i> lines.....	173
Figure 4.26: Analysis of the centromere DNA in <i>wild-type</i>	176
Figure 4.27: Analysis of the centromere DNA in <i>AtSMC4^{RNAi}</i> line 2.10.....	177

Figure 4.28: Analysis of the centromere DNA in <i>AtSMC4^{RNAi}</i> line 6.2.....	178
Figure 4.29: Meiotic phenotypes of <i>AtSMC4^{RNAi}</i> X <i>Atspo11</i> plants.....	181
Figure 5.1: Schematic representation of the condensin I complex..	198
Figure 5.2: Sequence of PCR product obtained from <i>AtCAPD2^{RNAi}</i> plants using insert specific primers.	201
Figure 5.3: Mean seed set in <i>AtCAPD2^{RNAi}</i> lines	204
Figure 5.4: Meiotic prophase II cells in <i>AtCAPD2^{RNAi}</i> lines.....	204
Figure 5.5: Meiotic phenotypes observed in the <i>AtCAPD2^{RNAi}</i> lines in the cytological screen..	205
Figure 5.6: Analysis of the rDNA regions in <i>AtCAPD2^{RNAi}</i> lines and wild-type	207
Figure 5.7: Analysis of centromere regions in <i>AtCAPD2^{RNAi}</i> lines at pachytene..	209
Figure 5.8: Analysis of centromere regions in <i>AtCAPD2^{RNAi}</i> lines at metaphase I. .	210
Figure 6.1: Schematic representation of the condensin II complex..	219
Figure 6.2: Position of the T-DNA insert in the Sail_826_B06 line.....	220
Figure 6.3: Sequence obtained from cloning the PCR band of the insert reaction of <i>Atcapd3</i> T-DNA line Sail-826_B06.	221
Figure 6.4: Pachytene cell from a homozygous plant of the <i>Atcapd3</i> T-DNA knock out line Sail-826_B06	222
Figure 6.5: RT-PCR analysis of <i>AtCAPD3</i> transcript in <i>Atcapd3</i> homozygous and wild-type plants:.....	224
Figure 6.6: Vegetative defects in <i>Atcapd3</i> plants.....	225
Figure 6.7: Mean seed set in <i>AtCAPD3^{+/-}</i> and <i>Atcapd3</i> compared to wild-type.	227
Figure 6.8: Germination assay.....	228
Figure 6.9: Wild-type and <i>AtCAPD3^{+/-}</i> meiosis.....	232

Figure 6.10: <i>Atcapd3</i> meiosis.	233
Figure 6.11: Mitotic cells of wild-type, <i>Atcapd3</i> and <i>AtCAPD3^{+/-}</i> plants.	235
Figure 6.12: Sequence of PCR product obtained from <i>AtCAPD3^{RNAi}</i> plants using insert specific primers.....	237
Figure 6.13: Mean seed set in <i>AtCAPD3^{RNAi}</i> transformants showing signs of reduced fertility.....	239
Figure 6.14: Meiotic phenotypes of <i>AtCAPD3^{RNAi}</i> lines and wild-type plants.	240
Figure 6.15: Analysis of the rDNA regions in <i>Atcapd3</i> mutants	242
Figure 6.16: Analysis of the centromere regions in <i>Atcapd3</i> and wild-type PMCs..	244
Figure 6.17: Immunolocalization of <i>AtASY1</i> and <i>AtZYP1</i> on <i>Atcapd3</i> and wild-type PMCs.	246
Figure 6.18: Expression of the <i>AtCAPD3</i> recombinant protein.....	250
Figure 7.1: Summary of condensin phenotypes in <i>Arabidopsis thaliana</i> compared to wild-type.	265

TABLES

Table 1: Condensin I and II subunit nomenclature for the main organisms discussed.	31
Table 2: Standard PCR cycle.....	74
Table 3: Solutions, concentrations and volumes required for SDS-PAGE electrophoresis.....	84
Table 4: Summary of condensin phenotypes in <i>Arabidopsis thaliana</i> compared to wild-type	264
Table 5: Table of primers. Restriction sites are highlighted in red.....	298
Table 6: Table of T-DNA lines.....	300

LIST OF ABBREVIATIONS:

3D-SIM	Three-dimensional structural illumination microscopy
AE	Axial elements
Ab	Antibody
AESP	<i>Arabidopsis</i> separase homologue
ASY1	Asynaptic 1
<i>At</i>	<i>Arabidopsis thaliana</i>
ATP	Adenosine tri-phosphate
BIO	Biotin
BLAP75	BLM-associated polypeptide
BLM	Bloom syndrome protein
BrdU	Bromodeoxyuridine
Brn1	Yeast Barren homologue
BSA	Bovine serum albumin
CAP	Chromosome associated protein
Cdc	Cell-division-cycle protein
cDNA	Copy DNA
CENP	Centromere protein
CID	Centromere identifier
Cnd	Condensin subunit
CO	Crossover
Col-0	<i>Arabidopsis</i> Columbia ecotype
DAPI	4, 6-diaminido-2-phenylindole
DEPC	diethyl procarbonate
dHj	Double Holliday junction
DIG	Digoxigenin
D-loop	Displacement loop
DMC1	Disruption of meiotic control 1
DNA	Deoxyribonucleic acid
DYP	Dumpy chromosomes
DSB	Double strand break
ECL	Enhanced chemiluminescence
EdU	5-ethynyl-2'-deoxyuridine
EM	Electron microscope
EME1	Essential meiotic endonuclease I
FISH	Fluorescent <i>in situ</i> hybridisation
FITC	Fluorescein isothiocyanate
FRAP	Fluorescent recovery after photobleaching
GAPD	Glyceraldehyde-3-phosphate dehydrogenase
G-C	Guanine-Cytosine
GFP	Green fluorescent protein
HCP-6	Holocentric protein 6
HEAT	Huntington, Elongation factor 3, a subunit of protein phosphatase A and TOR
HIM	High incidence of males
HIS	Histidine
HOP1	Homologue Pairing 1

HORMA	Domain common in: Hop1p, Rev7p and MAD2
HRP	Horseradish peroxidase
H2AX	Histone 2AX
IPTG	Isopropylthio- β -D-galactosidase
KLE2	Kleisin protein 2
LE	Lateral elements
Mam1	Monopolar microtubule attachment during meiosis 1
MEK1	Meiotic kinase 1
Mer	Meiotic recombination defective
MEI2	Meiosis gene 2
MIX-1	Mitosis and X-associated protein 1
MLH	MutL homologue 1
MLH3	MutL homologue 3
MMS4	Methyl methanesulfonate sensitive 4
MND1	Meiotic nuclear division 1
MRE11	Meiotic recombination 11
mRNA	Messenger RNA
MS	Murashige and Skoog
MSH	MutS homologue
MUS81	MMS and UV sensitive 81
NASC	National <i>Arabidopsis</i> stock centre
NBS1	Nijmegen breakage syndrome 1
NEBD	Nuclear envelope breakdown
NCO	Non crossover
Ni-NTA	nickel-nitrilotriacetic acid
NOS	Nopaline synthase
O/N	Overnight
PBS	Phosphate buffered saline
PCH2	Pachytene checkpoint 2
PCR	Polymerase chain reaction
PCS1	<i>Pombe</i> chromosome segregation
PMC	Pollen mother cell
PRD	Putative recombination defect
RAD	Radiation sensitive protein
RCA	Regulation of chromosome architecture
rDNA	Ribosomal DNA
REC	Abnormal recombination
RED1	Reduction division defective 1
RICS	RNA-induced silencing complex
RMI1	RecQ mediated genome instability 1
RNA	Ribonucleic acid
RNAi	RNA interference
RPA	Replication protein A
RT	Room temperature
RT-PCR	Reverse-transcription polymerase chain reaction
SEI	Single-end invasion
SC	Synaptonemal complex
SCC	Sister chromatid cohesion protein

SDS-PAGE	Sodium-dodecyl-sulfate polyacrylamide gel electrophoresis
SDSA	Synthesis-dependant strand annealing
SDW	Sterile distilled water
SMC	Structural maintenance of chromosomes
SPO11	Sporulation specific protein 11
ssDNA	Single-stranded DNA
SYCP	Synaptonemal complex protein
SYN1	Synapsis 1
T2	Second generation transformed plants
T-DNA	Transfer DNA
TF	Transverse filament
TOP3 α	Topoisomerase 3 alpha
Topo	Topoisomerase
Trip13	Thyroid hormone receptor interactor 13
WT	Wild-type
YCG1	Yeast CAP G protein 1
YCS	Yeast condensin subunit
XRCC	X-ray repair complementing defective repair in Chinese hamster cells
XRS2	X-ray sensitive 2

CHAPTER 1

1 INTRODUCTION

1.1 The significance of meiosis

Meiosis is a specialized cell division essential to all sexually reproducing organisms. Meiosis takes a diploid cell containing homologous maternal and paternal copies of each chromosome and halves the chromosome number to produce haploid cells such as gametes and spores. During this halving process the maternal and paternal homologous chromosomes are shuffled and recombined with each other to produce unique mixtures of genes. Upon fertilisation two haploid gametes fuse and a new, genetically distinct organism is produced. The production of genetically unique offspring helps to ensure the survival of species and facilitates species evolution via natural selection. Despite the advantages, meiosis is still a costly and potentially disastrous process in which mistakes can lead to infertility and birth defects. In humans, incorrect segregation of chromosomes can lead to spontaneous abortions and trisomy such as Down's syndrome. In plants understanding the processes of meiosis, in particular meiotic recombination, could lead to improved crop breeding. An example of this comes from the monocot *Hordeum vulgare*, or brewer's barley. Barley only undergoes meiotic recombination in the sub-telomeric regions of the chromosomes which contain relatively few of the organism's genes (James Higgins personal communication). Altering the distribution of crossovers (COs) in Barley and other such crops may lead to the production of novel genetic combinations to increase advantageous traits.

1.2 An overview of meiosis

In order to achieve the halving of chromosome number unique to meiosis, a single round of chromosome replication is followed by two rounds of chromosome segregation (Roeder, 1997). Ploidy is then restored upon fertilisation (Hamant *et al.*, 2006). The halving of chromosome number in meiosis contrasts with a mitotic cell division where a single round of replication is followed by a single chromosome division, thus maintaining chromosome number (Figure 1.1). In the first meiotic division, meiosis I, the maternal and paternal copies of each chromosome, known as the homologous chromosomes, are separated to opposite poles of the cell (Figure 1.2). It is during meiosis I that meiotic recombination occurs. Recombination is the reciprocal exchange of chromosome arms between the homologous chromosomes. The sister chromatids, which are near-identical copies of each chromosome produced during pre-meiotic DNA replication, remain attached at their centromeres and move together to the same pole of the dividing cell. The sister chromatids are then segregated to opposite poles in the second meiotic division, meiosis II (see Figure 1.2).

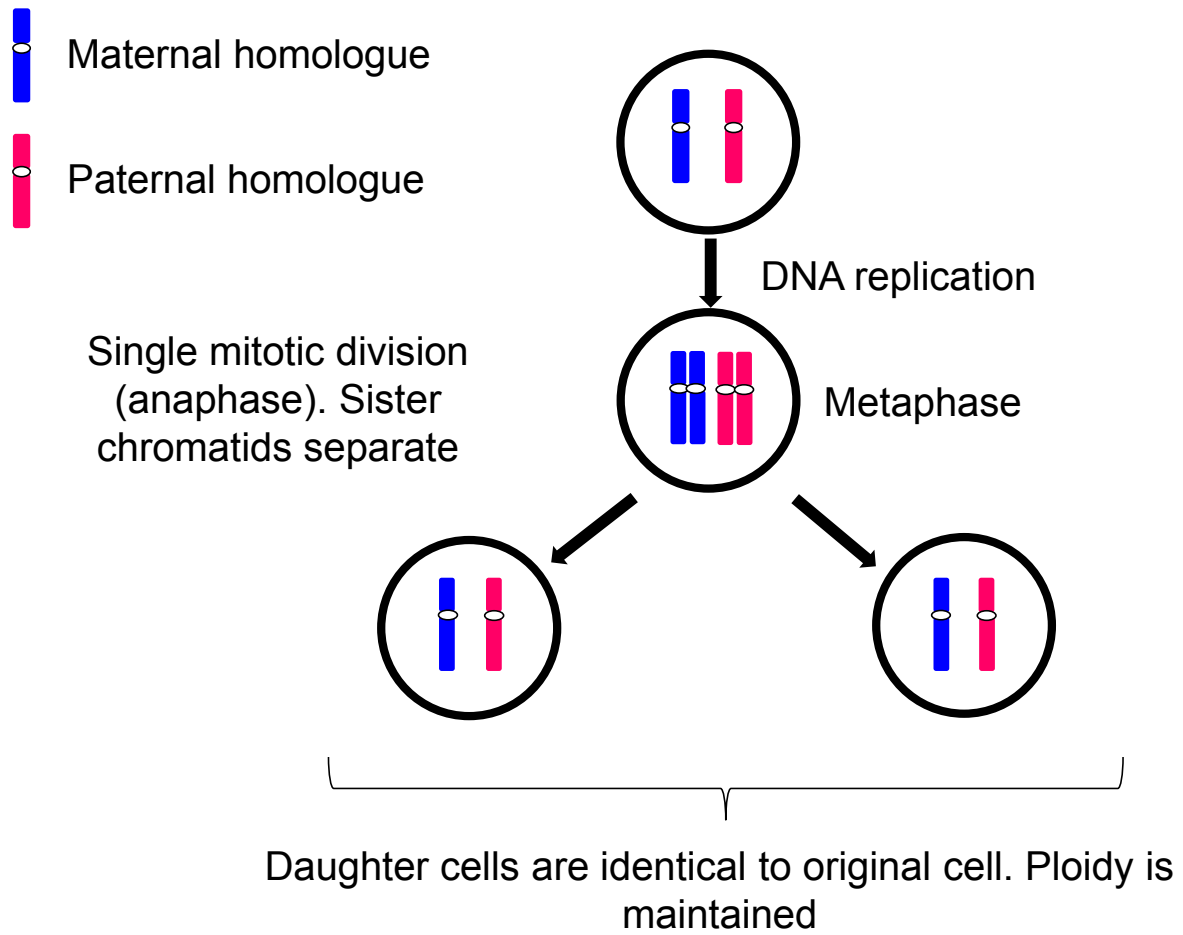


Figure 1.1: Schematic representation of a mitotic cell division. One round of chromosome replication is followed by a single chromosome segregation (anaphase) when the sister chromatids are separated. Ploidy is maintained in daughter cells.

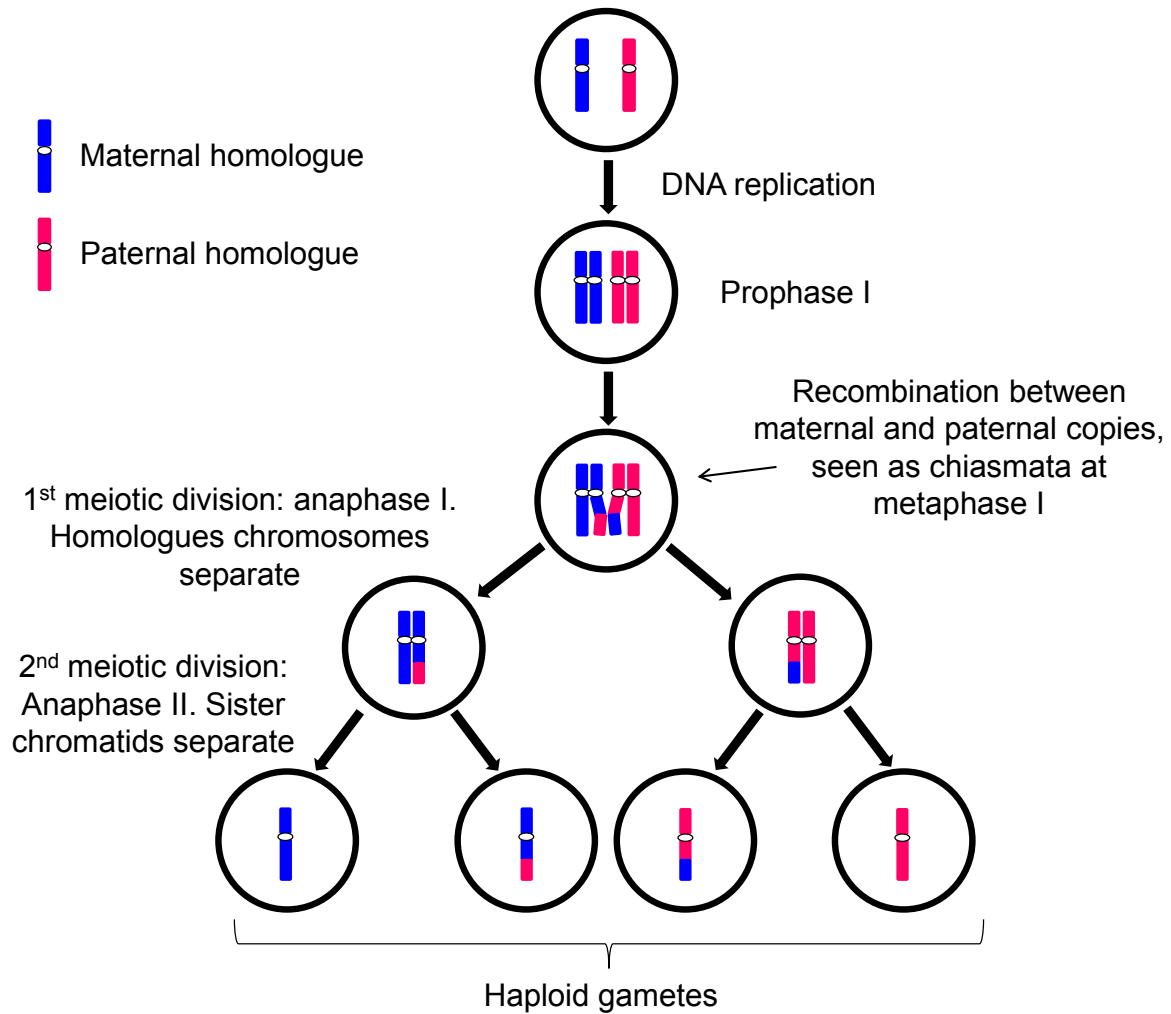


Figure 1.2: Schematic representation of a meiotic cell division (details of recombination not shown). One round of chromosome replication is followed by two rounds of chromosome segregation to produce haploid gametes. In the first meiotic division (anaphase I) homologous chromosomes are segregated, in the second meiotic division (anaphase II) sister chromatids are separated. Recombination occurs between maternal and paternal homologues.

During the first and longest stage of meiosis, prophase I, the homologous chromosomes condense into thread-like structures which first align and pair before becoming closely associated along their length by the polymerisation of a tripartite proteinaceous structure known as the synaptonemal complex (SC). This process is known as synapsis. The stages of prophase I are distinguished based on the progression of synapsis. In leptotene the homologous chromosomes pair along their length before synapsis is initiated. The SC starts to form between paired homologous chromosomes at zygotene; this process is complete at pachytene and the SC starts to disassemble at diplotene. By the final stage of prophase I, diakinesis, the chromosomes begin to condense towards metaphase I. Meiotic recombination also occurs during prophase I and the progression of synapsis and the recombination pathway are closely linked (see below) (Lichten, 2001). Each pair of homologous chromosomes undergoes at least one meiotic recombination event or crossover (CO). As well as increasing genetic diversity as mentioned above, meiotic recombination also creates an essential connection between dividing bivalents. Without such a connection bivalents cannot align and be correctly segregated at anaphase I and missegregation occurs (reviewed by Bishop 2006).

After prophase I the chromosomes condense considerably to form metaphase I bivalents. It is at this stage that the products of the meiotic recombination events which occurred during prophase I can be seen cytologically: these are known as chiasmata. The metaphase I bivalents align along the cell equator and attach to the spindle apparatus at the point of their centromeres via a large protein structure known as the kinetochore (reviewed by Schueler and Sullivan 2006). During anaphase I the homologous chromosomes are pulled to opposite poles of the cell by

the spindle. At telophase the chromosomes have reached the cell poles. In meiosis II the sister chromatids align at the cell equator and become separated to opposite poles of the cell in metaphase II and anaphase II respectively. Dramatic chromosome condensation occurs throughout meiosis: this condensation is essential to allow chromosomes to segregate without damage to the DNA. Correct chromosome organisation is also required to allow meiotic recombination to progress accurately (reviewed by Kleckner, 2006).

Meiosis, and in particular meiotic recombination, has been extensively studied at the molecular level in the budding yeast *Saccharomyces cerevisiae*. At the same time meiotic proteins have been investigated in a large number of species including fission yeast (*Schizosaccharomyces pombe*), mouse (*Mus musculus*) human (*Homo sapiens*), fruit fly (*Drosophila melanogaster*), nematode worm (*Caenorhabditis elegans*) model plants such as Thale cress (*Arabidopsis thaliana*) and crops such as maize (*Zea mays*), rice (*Oryza sativa*) and now barley (*Hordeum vulgare*). Here, for simplicity, recombination will mainly be discussed in the model organisms budding yeast and *Arabidopsis*.

1.3 Meiosis in Arabidopsis

Food security is increasingly becoming a challenge for our expanding population; therefore a drive towards improving our crop species is essential. Understanding meiotic processes in plants could lead to improved breeding programmes in plants such as cereals and foraging grasses. Knowledge of meiosis can also help towards the production of apomixes, a situation where some plants produce seeds asexually,

in sexually reproducing plants (d'Erfurth *et al.*, 2009; Ravi and Chan, 2010). Studies in many crop species are limited by un-sequenced genomes, long regeneration times and large space requirements. *Arabidopsis thaliana* is a valuable plant model, as it has a short generation time, usually around eight weeks, allowing quick analysis of generations, and also requires little growing space (Jones *et al.*, 2003). The small and fully sequenced genome of *Arabidopsis* has facilitated the identification of interesting genes based on homology searches with other organisms (The *Arabidopsis* Genome Initiative, 2000). A large collection of transfer-DNA (T-DNA) mutant lines are available in *Arabidopsis* making the acquisition of desired knock-outs more straightforward. Efficient *Agrobacterium* transformation also allows for, among other things, the generation of RNAi lines, GFP tagged protein lines and complementation analysis (An *et al.*, 1986). *Arabidopsis* has only five chromosomes and its meiosis occurs almost synchronously in meiocytes from the same anther. Both of these traits have advantages for the study of meiosis as they make cytological analysis more straightforward. Of particular importance to the study of meiosis is also the lack of meiotic arrest in many *Arabidopsis* meiotic mutants. In other species, such as budding yeast, cells in meiotic mutants are often arrested before the completion of meiosis, therefore downstream effects of the mutation is not seen (reviewed by Roeder, 1997; Roeder and Bailis, 2000). The absence of this in most meiotic mutants in *Arabidopsis* allows more phenotypes caused by mutations in meiotic genes to be revealed.

1.4 Meiotic recombination

Recombination is initiated in leptotene by the formation of double strand breaks (DSBs) (Sun *et al.*, 1989). DSBs are initiated by the type II topoisomerase SPO11 (Keeney *et al.*, 1997)(Figure 1.3.1). Three homologues of SPO11 are present in *Arabidopsis* *AtSPO11-1*, *AtSPO11-2* and *AtSPO11-3* (Hartung and Puchta, 2000; Grelon *et al.*, 2001; Hartung and Puchta, 2001; Stacey *et al.*, 2006). *Atspo11-1* mutant alleles are completely defective in recombination as no bivalents were present in over 300 metaphase I cells tested in this line. This lack of chiasmata was shown to be due to a failure to form DSBs. The plants were also completely asynaptic (Sanchez-Moran *et al.*, 2007). *Atspo11-2* mutants had normal vegetative growth but a severe reduction in fertility (only 0.13 seeds/silique (seed pod)). These plants were also defective in synapsis and recombination: no bivalents were detected at metaphase I in these alleles (Stacey *et al.*, 2006). Therefore both *AtSPO11-1* and *AtSPO11-2* are required for initiation of recombination. This suggests that *AtSPO11-1* and *AtSPO11-2* may act as a heterodimer in the same pathway of recombination (Stacey *et al.*, 2006; Hartung *et al.*, 2007; Sanchez-Moran *et al.*, 2007).

SPO11 is not sufficient to activate DSBs on its own. In budding yeast, at least 9 other proteins are required: these include Mre11, Rad50, Xrs2, Mer2, Mei2, Rec102, Rec104 and Rec114 (Grelon *et al.*, 2001; Keeney, 2001). AtPRD1 is a protein which interacts with *AtSPO11-1* and is required for DSB formation in *Arabidopsis* (De Muyt *et al.*, 2007). Two related proteins, *AtPRD2* and *AtPRD3* are also required for DSB formation (De Muyt *et al.*, 2009).

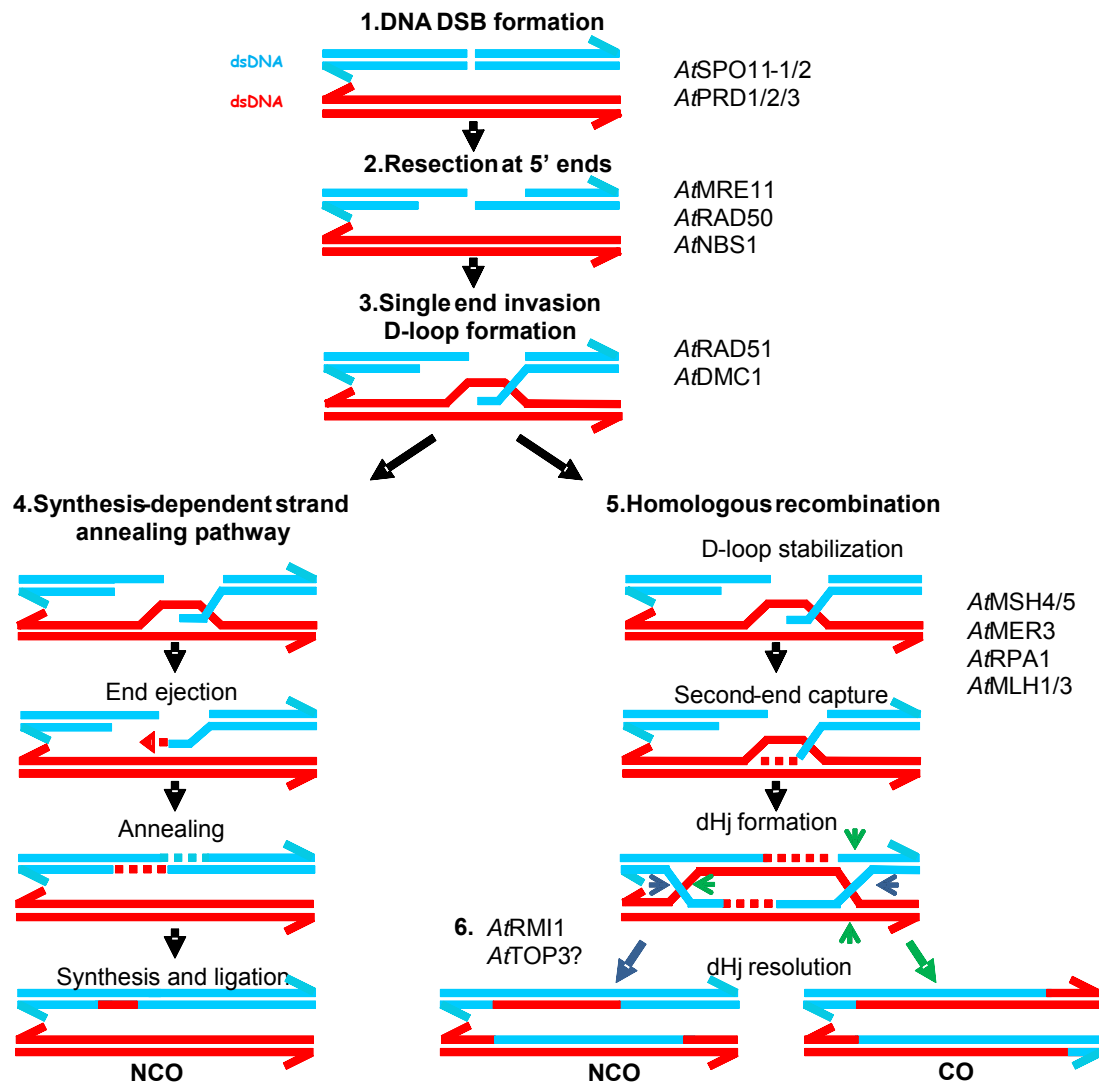


Figure 1.3: Schematic representation of the meiotic recombination pathway. **1.** DNA Double Strand Breaks (DSBs) are formed. **2.** The 5' ends of the DSBs are resected to give 3' overhangs. **3.** The 3' ssDNA invades the homologous strand and forms a D-Loop structure. **4.** Synthesis dependant strand annealing pathway results in the formation of non crossover recombinants (NCOs). **5.** dHj formation lead to crossovers (COs). **6.** dHj resolved as a NCO

1.4.1 Processing of DSBs in the CO pathway

After DSB formation the 5' ends of the break are resected to produce 3' single-stranded overhangs. Resection is carried out by the MRX/N complex which comprises MRE11 (Puizina *et al.*, 2004), RAD50 (Bleuyard *et al.*, 2004) and XRS2/NBS1 (Waterworth *et al.*, 2007) (See Figure 1.3.2). In budding and fission yeast the MRX/N complex is required for the formation of DSBs: removal of SPO11 from the break sites and the resection of the DSB 5' ends to produce a 3' ssDNA overhang (Nairz and Klein, 1997; Usui *et al.*, 1998; Hartsuiker *et al.*, 2009a; Hartsuiker *et al.*, 2009b; Nicolette *et al.*, 2010). Homologues of these proteins have been identified in *Arabidopsis*, (referred to as the MRN complex) (Bundock and Hooykaas, 2002; Gallego and White, 2005; Uanschou *et al.*, 2007). The MRN complex is not required for DSB formation in *Arabidopsis* (Puizina *et al.*, 2004). A striking phenotype of *Atmre11* and *Atrad50* null mutants in *Arabidopsis* is extensive fragmentation at the end of prophase resulting from an inability to repair DSBs (Bleuyard *et al.*, 2004; Puizina *et al.*, 2004; Uanschou *et al.*, 2007).

1.4.2 Single end invasion (SEI)

The ssDNA overhangs produced by resection of the DSBs by the MRX/N complex are then coated with the strand exchange proteins, RAD51 and DMC1, to produce a nucleoprotein filament. Eukaryotic RAD51 and DMC1 are homologues of the bacterial recombinase RecA (Bishop *et al.*, 1992; Shinohara *et al.*, 1992). *Arabidopsis* has one DMC1 homologue and six paralogues of RAD51 (*AtRAD51*, *AtRAD51B*, *AtRAD51C*, *AtRAD51D*, *AtXRCC2*, *AtXRCC3*) (Klimyuk and Jones, 1997; Doutriaux *et al.*, 1998; Osakabe *et al.*, 2002; Bleuyard *et al.*, 2005). Three of these (*AtRAD51*, *AtRAD51C*, and *AtXRCC3*) are required for meiosis (Bleuyard and

White, 2004; Li *et al.*, 2004; Bleuyard *et al.*, 2005; Li *et al.*, 2005). RAD51 and DMC1 work together to catalyse the single end invasion of the homologous chromosome by the 3' overhang by mediating homology searches, the invading strand then base-pairs to complementary single stranded DNA in the homologous chromosome and forms heteroduplex DNA. This results in the displacement of the complementary sequence on the donor homologous chromosome forming the displacement loop (D-Loop) structure (reviewed by Bishop, 2006) (Figure 1.3.3). RAD51 is involved in mitotic processes but DMC1 is meiosis specific (Neale and Keeney, 2006). In *Arabidopsis*, *AtRAD51* defective plants are asynaptic and exhibit chromosome fragmentation due to unrepaired DSBs (Li *et al.*, 2004). *Arabidopsis dmc1* mutants are also asynaptic and fail to form COs, however no fragmentation is present in these plants (Couteau *et al.*, 1999). This is presumably because the DSBs are repaired from the sister chromatid (Siaud *et al.*, 2004). In budding yeast, RAD51 is loaded and polymerized along ssDNA bound by RPA. RPA is thought to remove secondary structures in ssDNA (Alani *et al.*, 1992) and to modulate the loading of RAD51 and stabilise ssDNA (Wang and Haber, 2004). *Arabidopsis* has five RPA homologues, one of which, RPA1a, has been shown to have a role in recombination (Osman *et al.*, 2009).

When a CO event is going to form, the second single end of the DSB or “the partner end” is captured by the invading 3' end which has been extended by the adding of sequence from the donor homologous chromosome. This stage is known as second-end capture. This new sequence replaces that lost from the 5' resection. DNA synthesis and ligation occurs to produce a double Holliday junction (dHj) (see Figure

1.3.5). This structure is then resolved to form a CO event where each chromatid has exchanged flanking regions (Reviewed by (Bishop, 2006).

1.4.3 There is an excess of DSBs compared to COs formed

Not all DSBs will form COs. The number of DSBs generated is significantly more than the number of COs produced in the majority of species. In *Arabidopsis* it is thought that approximately 140 DSBs are formed, as seen from the immunolocalisation of early recombination proteins such as DMC1 (Sanchez-Moran *et al.*, 2007). Immunolocalisation with an antibody specific to *AtSPO11* shows there are approximately 100 foci, corresponding to DSBs. However *AtSPO11* is thought to only load transiently on the chromatin and therefore it is likely that this number is an underestimation, so DMC1 foci may be a closer estimation of the actual DSB number (Sanchez-Moran *et al.*, 2007). Of these ~140 DSBs per cell less than 10% become COs (Estimated by (Sanchez-Moran *et al.*, 2002)), therefore the large majority of DSBs are resolved as non crossovers (NCOs).

Many NCO events are thought to form via the synthesis dependent strand-annealing pathway (SDSA). When a NCO event is going to form, the SEI and D-Loop is not stabilised and instead the nucleoprotein filament is removed from the structure and re-anneals with the other end of the DSB. SDSA is accompanied by a gene conversion event as part of the resected invading ssDNA is repaired from the homologue. The decision as to whether a DSB will become a CO or NCO event is thought to be made around the time of SEI (Borner *et al.*, 2004). This suggestion was based on analysis of ZMM mutants in budding yeast. These mutants formed

DSBs and NCOs at normal levels but were defective in SEI (Borner *et al.*, 2004). However, direct evidence for this is lacking in *Arabidopsis*. A pathway involving AtRMI1/BLAP75 and AtTOP3a may be involved in resolving dHj as NCOs, via a hemicatenane intermediate containing pathway (Figure 1.3.6). To date, this pathway has only been found in plants (Chelysheva *et al.*, 2008; Hartung *et al.*, 2008). In *Arabidopsis* there are approximately three times more recombination-protein containing foci at zygotene than CO's (Osman *et al.*, 2011). It is thought that this excess in foci is to allow timely synapsis, since sites of recombination are thought to mark sites of synapsis initiation (see below). Therefore it is possible that AtRMI1/BLAP75 and AtTOP3a are required to convert some of these CO intermediates to NCOs. Alternatively AtRMI1/BLAP75 and AtTOP3a may form a backup pathway for failed dHjs (Hartung *et al.*, 2008).

1.4.4 CO interference

COs are not randomly placed on the chromosomes. If random CO placement was to occur, not every pair of homologues would necessarily get a CO event. However 0-CO on a bivalent is very rare in normal meiosis: this is known as the CO obligation (Jones and Franklin, 2006). It has also been observed that when one CO is formed the likelihood of a second forming near-by is reduced; this phenomenon becomes weaker the further away you get from the original CO site. This trend is referred to as CO interference (Jones and Franklin, 2006) (Figure 1.4). Evidence of interference has been shown using tetrad analysis in the *Arabidopsis quartet* mutant (Copenhaver *et al.*, 1998). In this mutant the four pollen grains from a meiotic event remain physically attached (Preuss *et al.*, 1994). These results showed that the

majority (85%) of COs showed interference based on their fit to a chi-square distribution (Copenhaver *et al.*, 1998). The remaining COs were “sprinkled, at random, among those distributed as per chi square” (Copenhaver *et al.*, 2002).

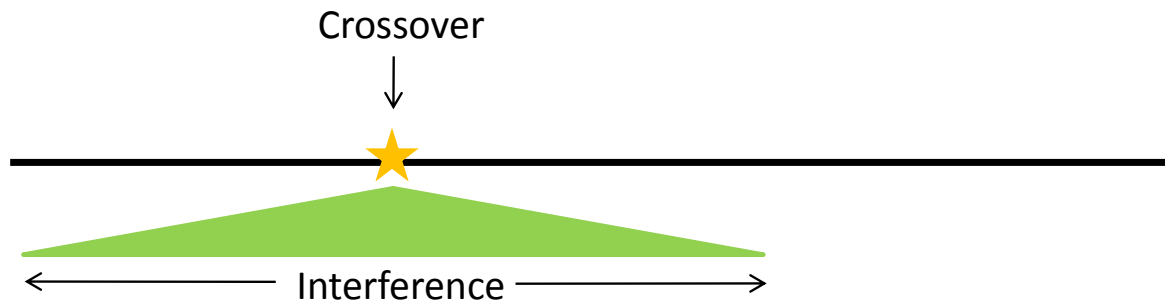


Figure 1.4: Schematic representation of crossover interference. When a CO occurs on a chromosome (star) the likelihood of another occurring nearby is reduced. The chance of another CO occurring is higher further away from the CO site. Green triangle represents the interference signal, decreasing with increased distance from the CO site.

The mechanism responsible for this interference signal remains elusive, however; many models have been put forward to explain how interference may occur. Perhaps the most well known of these theories is that suggested by Kleckner, (2004). This theory, known as the ‘mechanical stress model’ for CO interference suggests that global DNA expansion during prophase I cause stress along the chromosomes and this mechanical stress is required to produce COs. The production of a CO event is thought to locally relieve stress and thus prevent COs occurring in the area surrounding this site. Kleckner, (2004) likens the mechanism behind CO formation and interference to having a metal beam with a fragile ceramic layer on top (see Figure 1.5). This ceramic layer has many flaws (CO intermediates), if the system is then heated the metal beam would expand, however the fragile ceramic layer would not expand to the same extent. The resistance of the ceramic layer would create

stress until one of the flaws would crack (producing a CO). This crack (or CO) would then cause a local relief of stress in the vicinity of the break, preventing near-by flaws from becoming cracks (Kleckner *et al.*, 2004) (see Figure 1.5).

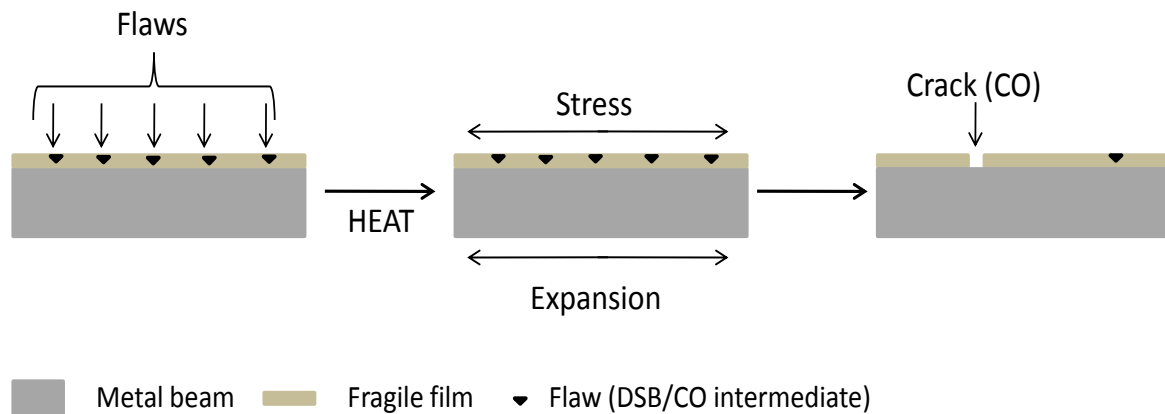


Figure 1.5: Mechanical stress model of CO interference. Interference can be explained by having a metal beam with a fragile ceramic layer on top. This ceramic layer is covered with flaws (CO intermediates), when heat is added to the system metal beam expands, but the ceramic layer cannot expand to the same extent. This results in stress and subsequent crack formation and one of the flaws (COs). This crack (or CO) would then cause a local relief of stress in the vicinity of the break, preventing near-by flaws from becoming cracks. Adapted from Kleckner, (2004).

Other theories have also been suggested including the counting model (Stahl *et al.*, 2004) and more recently the chromosome oscillatory movements or COM model has been put forward (Hulten, 2011).

1.4.5 Two recombination pathways exist in many species

It has been observed that in some organisms not all COs are subject to interference. Only 85% of COs in *Arabidopsis* are subject to interference (Copenhaver *et al.*, 1998). A similar result is seen in budding yeast (de los Santos *et al.*, 2003). Inconsistencies in CO distribution can be explained by the existence of two classes

of COs; class I and class II. Class I COs are sensitive to interference, and class II COs are insensitive to interference and thus are distributed randomly on the chromosomes (de Los Santos *et al.*, 2003). Class I COs are thought to be mediated via the ZMM proteins (Zip1, Zip2, Zip3 Zip4, Mer3, Msh4 and Msh5)(Borner *et al.*, 2004), whereas class II pathways involves MUS81 and MMS4/EME1 (de los Santos *et al.*, 2003; Berchowitz *et al.*, 2007; Higgins *et al.*, 2008b).

1.4.6 The class I pathway of CO formation

The ZMM proteins are essential for class 1 COs and for formation of the SC. Homologues of many of the ZMM proteins have been identified in *Arabidopsis*. The hMSH4/5 complex is thought to initially stabilise the SEI by a 'sliding clamp' mechanism, which helps enable the conversion of SEIs into mature dHjs and subsequent resolution into COs (or NCOs) (Snowden *et al.*, 2004). *At*MSH4/5 is first seen to localise to the chromosomes at leptotene as approximately 30 foci (Higgins *et al.*, 2004; Higgins *et al.*, 2008a), and this localisation is dependent on DSBs. The foci number decrease progressively until pachytene when only around eight foci are seen; consistent with the number of CO events per cell. Synapsis is completed in these mutants, however pachytene is severely delayed (Higgins *et al.*, 2004; Higgins *et al.*, 2008a).

Other proteins essential for the class I pathway of recombination include MLH1 and MLH3, homologues of the bacteria MutL involved in prokaryotic mis-match repair. Both *At*MLH1 and 3 have roles during meiosis however, *At*MLH1, also has a role in mitotic DNA repair (Dion *et al.*, 2007). *At*MLH1 and *At*MLH3 localise to around 9-10 foci on pachytene cells, marking the sites of recombination (Jackson *et al.*, 2006).

SC formation is unaffected in *Atmlh1* and *Atmlh3* mutants, and localisation of AtMSH5 is normal. These results are consistent with MLH1 and MLH3 having a role in the final steps of meiotic recombination. MutL complexes have been suggested to enforce a dHj conformation which encourages their resolution as CO as opposed to NCOs (Franklin *et al.*, 2006).

1.4.7 The class II pathway of CO formation

The second pathway of recombination is interference insensitive and involves MUS81 and EME1 (de los Santos *et al.*, 2003). AtMUS81 and AtEME1 are thought to form a heterodimer that can cleave Hjs. AtMUS81 is seen to localise to the chromosomes at the same time as RAD51 in a DSB dependent manner. AtMUS81 foci decrease throughout prophase I until around 4-5 remain (Higgins *et al.*, 2008b). *Atmus81* mutants appear normal, but when crossed to *Atmsh4*, there is a further reduction in COs from ~1.25 in the *Atmsh4* single mutant to ~0.8 in the double mutant, suggesting AtMUS81 functions in the class II pathway of recombination (Berchowitz and Copenhaver, 2008; Higgins *et al.*, 2008b). In budding yeast it is thought that the MUS81-dependant pathway is a back-up for failed class I recombination events (Oh *et al.*, 2008). There is currently no evidence for this in *Arabidopsis* (Osman *et al.*, 2011).

1.4.8 Relative contribution of the two pathways

The relative contribution of these two CO pathways to the overall number of CO varies between species. Knocking out the recombination protein AtMSH4 resulted in an 85% reduction of COs (Higgins *et al.*, 2004). The remaining chiasmata were

randomly distributed suggesting they belonged to a MSH4/MSH5 independent pathway which was insensitive to interference. A similar result is seen in plants deficient in MER3 (Mercier *et al.*, 2005). These results are consistent with those from pollen tetrad analysis (Copenhaver *et al.*, 1998) and suggest that in *Arabidopsis* class I COs account for the majority (Higgins *et al.*, 2004). Class II MUS81 dependent COs are thought to be responsible for the remaining 15% of COs in MSH4 and MER3 mutants, however in a *msh4/mus81* double mutant some residual COs still remain suggesting the presence of a third pathway of CO formation (Higgins *et al.*, 2008b). In budding yeast class I COs also account for approximately 85% of the COs (de los Santos *et al.*, 2003). *C. elegans* on the other hand has complete interference such that each chromosome only gets one CO, via the class I pathway (Meneely *et al.*, 2002). In contrast fission yeast appears to follow a majority MUS81-EME1 dependent class II, interference free, pathway (Osman *et al.*, 2003).

1.4.9 Double Holliday junction resolution

Despite huge progress in identifying the players important for most stages of the recombination pathways, a dHj resolvase has proved more difficult to identify. Many proteins have been put-forward as potential resolvases; indeed many proteins have *in vitro* resolvase activity. MUS81 has been suggested as a resolvase since the bacterial resolvase, RuvC, rescues the *mus81* phenotype. However MUS81 is not required for most COs in budding yeast or *Arabidopsis*. In mammals and budding yeast GEN1 and Yen1 respectively have recently been identified as dHj resolvases (Ip *et al.*, 2008). In budding yeast Yen1 has been shown to act with MUS81 in a redundant manner (Tay and Wu, 2010), and in fission yeast GEN1 rescued *mus81*

mutants resulting in CO formation (Lorenz *et al.*, 2010) (fission yeast only has the MUS81-dependant class II recombination pathway). Two *At*GEN1 homologues have been identified; however knocking both out produces no meiotic phenotype (Higgins, unpublished data).

1.4.10 Factors influencing CO distribution

It has been observed that COs tend to occur in “hot” and “cold” spots throughout the genome (Gerton *et al.*, 2000). It has been shown using *Arabidopsis* chromosome 4 that COs rarely occur near the centromere (Drouaud *et al.*, 2006) and are also less common at the telomeres (Chen *et al.*, 2008). COs occur less frequently in areas of high G-C content and within genes, pseudogenes, transposable elements and dispersed repeats, but occur more frequently in areas of high GpC ratio and single repeats (Drouaud *et al.*, 2006).

Sites in which COs occur more frequently in the genome are known as CO hotspots (Jeffreys *et al.*, 2001; Myers *et al.*, 2008; McVean and Myers, 2010). The ability of SPO11 to access the DNA is thought to be a major contributor to CO position. Consistent with this, COs are often found in regions of open chromatin in budding yeast (Ohta *et al.*, 1994; Wu and Lichten, 1994; Berchowitz *et al.*, 2009). Some evidence exists that DNA sequence is partly responsible for DSB location. A degenerate 13-nucleotide sequence has been identified, which is found at ~40% of recombination hotspots (Myers *et al.*, 2008). PR-domain-containing 9 (PRDM9) is a protein with histone methyltransferase activity and has been implicated in marking future DSB sites: indeed PRDM9 has been shown to bind the same 13-nucleotide

sequence identified at recombination hotspots (Baudat, 2010). In budding yeast histone (H3) lysine 4 (K4) tri-methylation was increased near DSBs preceding the onset of meiosis (Borde *et al.*, 2009). Knocking-out H3K4-methyltransferase leads to a reduction in DSBs (Borde *et al.*, 2009). Histone H2A lysine 5 acetylation has been shown to determine DSB distribution in *C. elegans* (Wagner *et al.*, 2010). Also required for correct DSB formation in *C. elegans* is HIM-17, a putative chromatin modifying protein required for histone 3 lysine 9 di-methylation in meiosis (Reddy and Villeneuve, 2004).

As well as the epigenetic state of the chromatin, certain chromosomal structural proteins have also been shown to have a role in DSB distribution. The Structural Maintenance of Chromosome (SMC) containing complexes; namely cohesin and condensin, have both been implicated in DSB distribution. In a budding yeast mutant of the meiotic specific cohesin Rec8, the binding of Spo11 to DSB sites was impaired (Kugou *et al.*, 2009). In *C. elegans* the condensin subunit CAP-D2 has been implicated in controlling the number and distribution of DSBs by altering the chromatin axis length (Tsai *et al.*, 2008; Mets and Meyer, 2009) (See below).

1.5 The chromosome axes are highly organised

During prophase I of meiosis the chromatin of each sister chromatid is arranged in a highly organized structure comprising a series of loops which are attached at their bases to a proteinaceous axis (Figure 1.6). Chromatin loops of each sister chromatid are thought to be arranged “in register” in many organisms due to the striated appearance of chromosome axes on electron micrographs (Kleckner, 2006). An

interesting feature of axis organisation is that the density of loops along chromosome axis is conserved between organisms, being approximately 20 loops per micron of axis length (Kleckner, 2006). A result of this conserved loop-density is that organisms with larger genomes have either larger loop size or longer axes as opposed to more compact loops. This conserved loop density is also observed within species. For example human female meiotic axes are twice as long as males and have chromatin loops which are half the length of males (Tease and Hulten, 2004). In addition to this, mice lacking the meiosis specific cohesion SMC1 β have shortened axis length and increased loop size in a subset of loops, but the loop density remains constant. However mutants in the mouse axis associated protein SYCP3 have longer axis and shorter loop size (Revenkova *et al.*, 2004; Novak *et al.*, 2008). Extending 'outwards and upwards' from the base of these loops is a "meshwork" of proteins. The base of these loops and associated proteins form the chromosome axis (Kleckner, 2006). This highly organised structure and presence of a meshwork suggests that several proteins play a role in organising the chromosome axes.

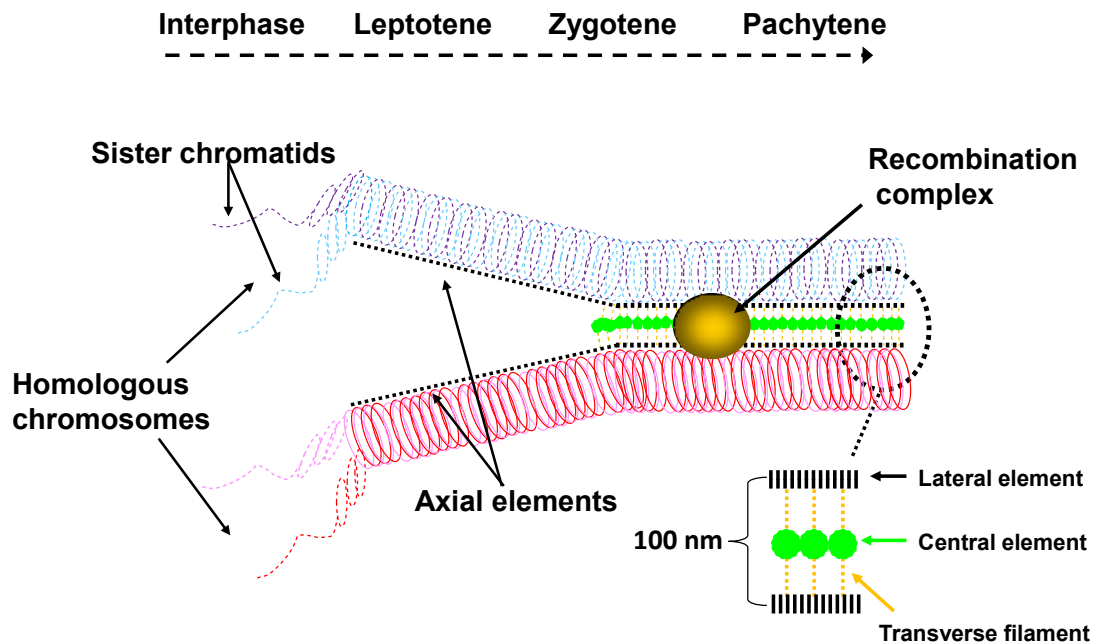


Figure 1.6: Structure of the synaptonemal complex (SC) and its formation through prophase I. At interphase no chromosome axes have formed. At leptotene the chromosome axes form and are known as axial elements (AEs). The AEs of the homologous chromosomes then become aligned at a distance of ~400 nm. At zygotene the SC starts to polymerise along the homologous AEs (now referred to as lateral elements (LEs)). At pachytene the SC is fully polymerised and the homologues are at a distance of 100 nm apart. The SC comprises two LE, a transverse filament (TF) and a central element (CE). Recombination nodules are seen to localise with the SC.

The exact protein composition of the axes is not known, however several proteins which associate with the axes have been identified. Cohesin is a protein complex which is required to hold the sister chromatids together during meiosis and mitosis. Cohesin localises to the meiotic axis in many species (Klein *et al.*, 1999; Cai *et al.*, 2003; Eijpe *et al.*, 2003; Page and Hawley, 2003; Severson *et al.*, 2009) where it may be required for chromatin loop organisation (Novak *et al.*, 2008). Mutants in yeast cohesin subunits are defective in meiotic chromosome axis formation (Klein *et al.*, 1999). However cohesin mutants are often able to form a rudimentary

chromosome axis in higher eukaryotes (Bhatt *et al.*, 1999; Bannister *et al.*, 2004; Xu *et al.*, 2005; Novak *et al.*, 2008). This suggests that a layer of axis organisation appears to exist on which the cohesin complex loads. It has been suggested that this axis may be comprised of proteins involved in the development of mitotic chromosome axes such as Topoisomerase II (Topo II) (Saitoh and Laemmli, 1994; Novak *et al.*, 2008). Axis associated proteins such as SYCP3 in mammals, Red1/Hop1 in budding yeast and *AtASY3/AtASY1* in *Arabidopsis* may represent a third layer to the 'meshwork' of proteins (Saitoh and Laemmli, 1994; Kleckner, 2006; Novak *et al.*, 2008). After their formation these chromosome axis or axial elements (AEs) of the homologous chromosomes are connected along their length by the polymerisation of the transverse filament (TF) of the SC. When polymerisation of the TF initiates the AEs are referred to as lateral elements (LEs) (reviewed by (Zickler and Kleckner, 1999) (figure 1.6). It is seen that in many species when the SC polymerises the axis associated HORMA-domain containing proteins such as *AtASY1* in *Arabidopsis* (unpublished observations) Hop1 in yeast (Borner *et al.*, 2008) and HORMAD1 and 2 in mammals (Wojtasz *et al.*, 2009; Daniel *et al.*, 2011) are depleted from the chromosomes. The mammalian AAA+ ATPase Trip13 has been implicated in the removal of HORMAD1 and HORMAD2 proteins from synapsed chromosomes (Wojtasz *et al.*, 2009). A similar relationship is seen with the yeast Trip13 homologue Pch2 and axis protein Hop1 (Borner *et al.*, 2008). Trip13 and Pch2 are also both required for correct recombination and synapsis and correct axis length (although the two proteins appear to have divergent roles in these processes) (Wojtasz *et al.*, 2009; Borner *et al.*, 2008; Roig *et al.*, 2010). It has been suggested in mammals that the axis protein HORMAD1 and the TF protein SYPC1 are in a negative feedback loop: HORMAD1 promotes presynaptic alignment and

synapsis and the SC removes HORMAD1 from the chromosomes. This is required, at least in mammals, to allow meiotic progression (as HORMAD1 is involved positively in the meiotic silencing of unsynapsed chromosomes: MSUC) (Daniel *et al.*, 2011). Axis proteins such as HORMAD1/2, *AtASY1* and Red1/Hop1 are also required for correct meiotic recombination (see below).

1.6 Recombination and Chromosome organisation

A link between axis formation and recombination and vice versa is seen in many systems (reviewed by Kleckner, 2006). Evidence that these processes are linked can be seen by the observation that recombination complexes are axis associated (Carpenter, 1975; Blat *et al.*, 2002; Tesse *et al.*, 2003; Moens *et al.*, 2007). This physical association is thought to allow the chromosome recombination events to be coordinated with recombination at the axes (Kleckner, 2006). DSB sites are thought to occur in the chromatin loop regions, however whether DSBs occur at the axis, or occur away from the axis in the chromatin loop and then become tethered to the axis shortly after DSB formation, is currently unknown (Blat *et al.*, 2002; Storlazzi *et al.*, 2003; Kim *et al.*, 2010). Either way the recombination complexes remain associated with the axes throughout the rest of the CO recombination pathway. As prophase I progresses from early to mid pachytene CO complexes retain SC association whereas NCO complexes are released from the SC (Moens *et al.*, 2007; Terasawa *et al.*, 2007). In *Arabidopsis* DSB formation (monitored by H2AX phosphorylation which occurs when DSBs are formed (Shroff *et al.*, 2004)) takes place only when the axes are formed, suggesting a temporal link between these two processes (Sanchez-Moran *et al.*, 2007).

1.6.1 SC proteins mediate meiotic recombination

Budding yeast strains mutated in the meiosis specific axis components Red1, Hop1 or the cohesin Rec8 shown an altered distribution of DSBs implying the axes have a role in the initiation and positioning of DSBs (Blat *et al.*, 2002; Glynn *et al.*, 2004). In yeast *red1* mutants AEs are not detectable (Rockmill and Roeder, 1990) and recombination is severely defective. DSBs are formed but only at ~25% of the wild-type level (Xu *et al.*, 1997). The recombination which does occur in these mutants is biased towards the sister chromatid, implying that Red1 mediates homologue bias in recombination (Xu *et al.*, 1997). The Mek1 kinase localises to the binding sites of Red1 and Hop1 and phosphorylates Red1 (Bailis and Roeder, 1998). It has recently been proposed that the role of Red1/Mek1 (and presumably Hop1) in establishing inter-homologue bias maybe to counteract the inter-sister bias imposed by Rec8 and its role in sister chromatid cohesion (Kim *et al.*, 2010). However the authors suggest that the role of Red1/Mek1 in inter-homologue bias may not extend any further than this. Instead this removal of the inter-sister bias imposed by Rec8 locally at CO sites may allow the recombinases DMC1 and RAD51 (and the RAD51 inhibitor Hed1) to mediate homologue bias (Kim *et al.*, 2010).

A role in ensuring inter-homologue bias is also seen in other axis proteins. *AtASY1* is a HORMA domain-containing protein identified in *Arabidopsis* with limited homology to Hop1 in budding yeast (Caryl *et al.*, 2000). *AtASY1* has been shown to associate with the AEs by immunolocalisation and immunogold electron microscopical (EM) localisation (Armstrong *et al.*, 2002). EM analysis of *Atasy1* null mutants reveals that they do not form a proper axis structure. Inter-homologue recombination is severely

compromised in *Atasy1* as shown by an abrupt decline in *AtDMC1* foci on the mutant chromosomes compared to wild-type and a severe reduction in chiasmata (Ross *et al.*, 1997; Sanchez-Moran *et al.*, 2001). These results suggest that *AtASY1* is involved in promoting inter-homologue recombination (Sanchez-Moran *et al.*, 2007). Whether *AtASY1* has a similar role to Red1/Mek1 in counteracting sister chromatid cohesion is currently unknown.

The TF protein *AtZYP1* in *Arabidopsis* has been shown to be required for correct recombination control. When *AtZYP1* levels are depleted in *Arabidopsis*, chromosomes do not synapse and COs are reduced to ~80% of wild-type. Moreover, COs in this mutant are observed between non-homologous chromosomes suggesting that *AtZYP1* plays a role in preventing non-homologous recombination (Higgins *et al.*, 2005). However the role of the TF does not appear to be conserved between species. In rice the TF homologue ZEP1 has recently been identified and investigated for its role in meiosis (Wang *et al.*, 2010). ZEP1 mutants are asynaptic however the number of COs was slightly elevated compared to wild-type. The authors suggest that this may be due to ZEP1 having a role in interference (Wang *et al.*, 2010). A role of the SC in interference was suggested previously in budding yeast, since *zip1* mutants had no interference (Sym and Roeder, 1994). However it is thought that the CO interference acts before the SC in polymerised (Borner *et al.*, 2004) and the COs in *AtZYP1^{RNAi}* plants do exhibit interference (Higgins *et al.*, 2005). Therefore it is generally accepted that the SC does not play a role in interference, however these contrasting results call for further work into this issue.

1.6.2 Recombination initiates pairing and synapsis

The link between recombination and chromosomes axes works both ways. The process of recombination initiates pairing of homologous chromosomes and synapsis. Before the initiation of synapsis the homologues are first loosely aligned at a distance of approximately 400 nm. A link between DSB formation and pairing has been seen in many organisms including *Arabidopsis* (Grelon *et al.*, 2001), budding yeast (Rockmill *et al.*, 1995; Peoples *et al.*, 2002; Henderson and Keeney, 2004) and *Sordaria* (Tesse *et al.*, 2003). In *Sordaria* DSBs were shown to be required for presynaptic co-alignment of homologous chromosomes. Rad51 foci were often seen to form bridges between homologues at sites of close homologue alignment. It has been proposed that early recombination events, namely the homology searching by RAD51 around the stage of SEI, are required for the pairing of homologous chromosomes (Rockmill *et al.*, 1995; Franklin *et al.*, 1999; Moens *et al.*, 2002; Tesse *et al.*, 2003; Clavente *et al.*, 2005). It has been suggested that these homology searches create an association between the DSB site and the homologous sequence in the loop of the homologous chromosome. Pairing may be achieved by the 'reeling in' of this homologous sequence (Tesse *et al.*, 2003). Further evidence for the role of recombination proteins in chromosome spatial arrangements has also been shown recently in *Sordaria* (Storlazzi *et al.*, 2010). In this study the recombination proteins Mer3, Msh4, and Mlh1 were all shown to have distinct roles in pairing and chromosome organisation. The Mer3 helicase was shown to be important in preventing 'entanglements' between chromosomes during homologue alignment. Msh4 was required to maintain the correct distance between aligned homologues since the alignment distance between homologues in *msh4* mutants was ~600-800 nm compared to ~400 nm in wild-type. Mlh1 was shown to be

required to the resolution of interlocks between chromosomes at zygotene/pachytene (Storlazzi *et al.*, 2010).

As well as homologue pairing, meiotic recombination is also required for correct synapsis in many species. Indeed synapsis is initiated at eventual CO sites (Zickler *et al.*, 1992; Lichten, 2001; Mahadevaiah *et al.*, 2001; Fung *et al.*, 2004; Henderson and Keeney, 2004). If Spo11 is mutated in budding and fission yeast then the SC does not polymerize correctly (Keeney *et al.*, 1997). It has been shown in yeast that formation of DSBs, and not Spo11 itself, are required for synapsis since SC defects in *spo11* mutants can be rescued by radiation induced DSBs (Celerin *et al.*, 2000). A similar situation has been observed in *Arabidopsis Atspo11* mutants (Grelon *et al.*, 2001; Sanchez-Moran *et al.*, 2007). The later stages of recombination are also required for complete synapsis and the correct timing of synapsis. For example; *Arabidopsis Atmsh4* mutants have reduced chiasmata frequency and delayed synapsis (Higgins *et al.*, 2004). The coupling of DSBs to synapsis is not present in all organisms. In *Drosophila* females and *C. elegans*, synapsis occurs without DSB formation (Dernburg *et al.*, 1998; McKim *et al.*, 1998).

In mouse, as in many species, an excess of Rad51 foci is seen in early prophase I compared to the number of eventual COs formed (Moens *et al.*, 2002). Therefore, the majority of the Rad51 foci are resolved as NCOs. The purpose of the excess Rad51 foci is thought to be to mediate sufficient pre-synaptic alignment of homologous chromosomes (Moens *et al.*, 2002). A similar situation is seen in plants. In plant species with greatly varying genome sizes a correlation between Rad51 foci

and SC length was observed. This led to the conclusion that excess Rad51 foci were required to allow full synapsis of these larger chromosomes, the remainder were resolved as NCOs (Anderson *et al.*, 2001).

The structure of the chromosomes in early prophase I, as mediated by architectural proteins, appears to be essential for both the formation of DSBs and the subsequent processing of the recombination intermediates. The structure of the chromosome is also required for accurate segregation. Condensin is a complex known to have a role in the organisation of chromosomes (Hirano and Mitchison, 1994).

1.7 Condensin is involved in chromosome organisation during meiosis and mitosis

1.7.1 The condensin complexes

During mitotic and meiotic cell divisions the chromosomes have to condense dramatically from interphase, when chromosomes are not visible under standard microscopy techniques, to metaphase when chromosomes are seen as discrete highly-condensed structures. This compaction of the chromosomes is essential for the accurate segregation of chromosomes at anaphase in both meiosis and mitosis and for the correct regulation of recombination between homologous chromosomes during meiosis. The mechanism behind this progressively increasing condensation is largely unknown and in particular the structural arrangement of the metaphase chromosomes remains elusive. One protein complex which has been identified as a primary player in chromosome organisation is condensin. Condensin is a pentameric complex which comprises two members of the Structural Maintenance of

Chromosomes (SMC) family, SMC2 and SMC4, as well as three non-SMC regulatory subunits. In higher eukaryotes two condensin complexes exist. Both contain the SMC2 and SMC4 backbone but have different regulatory proteins. Condensin I comprises CAP-H/Barren, CAP-D2 and CAP-G whereas condensin II comprises CAP-H2, CAP-D3 and CAP-G2 (Ono *et al.*, 2003; Yeong *et al.*, 2003; Hirano, 2005). Table 1 summarises the names of the subunits in various organisms.

Condensin I and II are both present in metazoans, however fungi have only the condensin I complex. It has been suggested that the second condensin complex has evolved in higher eukaryotes that have larger genomes in order to cope with the extra organisation required to deal with the additional DNA (Hirano, 2005). However this genome size theory does not entirely hold true as *Cyanidioschyzon merolae*, a unicellular red alga, which has a similar size genome to *S. cerevisiae*, has both condensin I and condensin II complexes (Hirano, 2005). Nevertheless it is worth noting that organisms such as *S. cerevisiae*, *S. pombe*, *Aspergillus nidulans* and *Neurospora crassa* which all only have the canonical condensin I complex do not compact their DNA as dramatically as metazoans at the onset of mitosis (Guacci *et al.*, 1994).

Condensin I

<i>A. thaliana</i>	AtSMC2-1/2 AtCAP-E1/E2	AtSMC4 AtCAP-C	AtCAP-D2	AtCAP-G	AtCAP-H
<i>S. cerevisiae</i>	SMC2	SMC4	ycs4	ycs5/ycg1	Brn
<i>S. pombe</i>	Cut14	Cut3	Cnd1	Cnd3	Cnd2
<i>C. elegans</i>	Mix-1	SMC-4	DPY-28	CAP-G	DPY-26
<i>D. melanogaster</i>	DmSMC2	DmSMC4/ Gluon	dCAP-D2	dCAP-G	Barren
<i>X. laevis</i>	XCAP-E	XCAP-C	XCAP-D2	XCAP-G	XCAP-H
<i>H. sapiens</i>	hCAP-E	hCAP-C	hCAP-D2	hCAP-G	hCAP-H

Condensin II

<i>A. thaliana</i>	AtSMC2-1/2 AtCAP-E	AtSMC4 AtCAP-C	AtCAP-D3	AtCAP-G2	AtCAP-H2
<i>C. elegans</i>	Mix-1	SMC-4	HCP-6	CAP-G2	KLE2
<i>D. melanogaster</i>	DmSMC2	DmSMC4/ Gluon	dCAP-D3	–	dCAP-H2
<i>X. laevis</i>	XCAP-E	XCAP-C	XCAP-D3	XCAP-G2	XCAP-H2
<i>H. sapiens</i>	hCAP-E	hCAP-C	hCAP-D3	hCAP-G2	hCAP-H2

Table 1: Condensin I and II subunit nomenclature for the main organisms discussed.

1.7.2 Identification of the condensin complexes

The condensin subunit SMC2 was first identified as a component of the chromosome scaffold along with Topo II (Earnshaw *et al.*, 1985). SMC2 was later further confirmed as a scaffold component when it was knocked out in chicken DT40 cells causing the chromosome scaffold to dissolve (Hudson *et al.*, 2003). The condensin complex was first identified in *Xenopus* egg extracts where it was shown to have an essential role in chromosome condensation (Hirano and Mitchison, 1994; Hirano *et al.*, 1997). When components of the condensin I complex were depleted in *Xenopus* the chromosomes became poorly condensed or ‘fuzzy’. This led to the suggestion that condensin plays a role in chromosome condensation during meiosis and mitosis (Hirano *et al.*, 1997). Condensin subunits were also identified around the same time in budding yeast (Strunnikov *et al.*, 1995; Koshland and Strunnikov, 1996) and

fission yeast (Saka *et al.*, 1994) where they were shown to be required for chromosome segregation.

Condensin II was discovered relatively recently in vertebrates (Ono *et al.*, 2003). Database searches using the hCAP-D2 sequence identified hCAP-D3. Immunoprecipitation experiments revealed that hCAP-D3 associated with SMC2 and SMC4, as well as two uncharacterised proteins which they named hCAP-H2 and hCAP-G2. The authors estimated that condensin I was five times more abundant in *Xenopus* egg extracts than condensin II, which they suggest may have prevented its discovery in the early characterisation experiments in *Xenopus* (Hirano *et al.*, 1997). Consistent with this, condensin I depletion in *Xenopus* leads to a more severe phenotype than condensin II depletion (Ono *et al.*, 2003). Condensin I and II were however equally abundant in HeLa cells (Ono *et al.*, 2003). This suggests that the contribution of the two complexes to chromosome organisation may differ between species and/or cell types.

1.7.3 Structural Maintenance of Chromosome proteins

SMC proteins are a family of large coiled-coil proteins which are conserved across the 3 domains of life, prokaryotes, eukaryotes and archaea. In all eukaryotes 6 major SMC proteins can be found, SMC1-SMC6. These proteins form hetero-dimers with other SMC proteins and form the backbone of larger protein complexes. SMC1 and SMC3 form the heterodimer which is part of the cohesin complex involved in sister chromatid cohesion and SMC5 and SMC6 form a complex involved in DNA repair

(Lehmann *et al.*, 1995; Verkade *et al.*, 1999). SMC proteins have a unique structure shown in Figure 1.7.

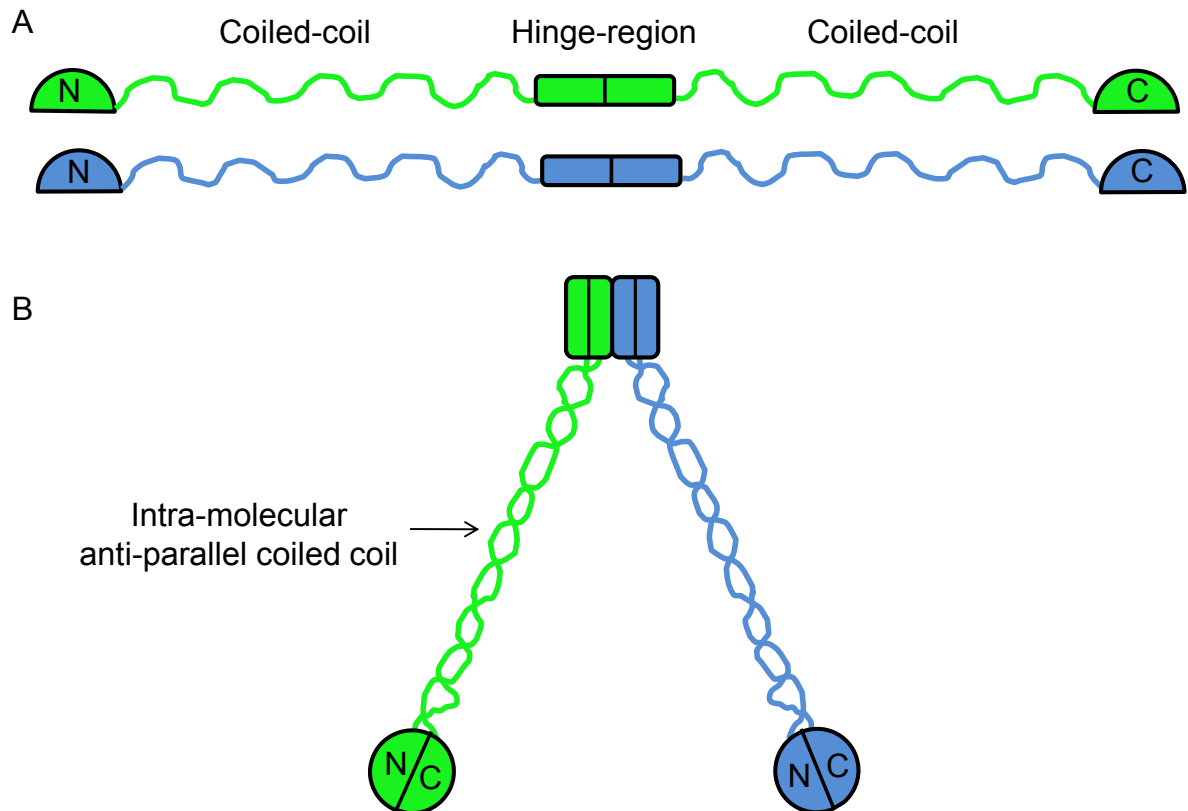


Figure 1.7: Structure of SMC proteins and SMC hetero-dimers. **A:** SMC proteins consist of a central hinge region, two coiled-coil regions a N-terminal Walker A motif and a C-terminal Walker B motif. **B:** The Walker A and Walker B motifs come together to form an ATPase domain. Each arm of the SMC dimer is made up of an intra-molecular anti-parallel coiled coil.

Each SMC protein is comprised of two large coiled-coil domains separated by a hinge domain. The N and C termini of the coiled-coils contain globular domains which have nucleotide binding motifs known as Walker A and Walker B motifs respectively. Each SMC protein folds in half at the hinge domain producing an intra-molecular anti-parallel coil interaction (Melby *et al.*, 1998; Hirano, 2001; Haering *et*

al., 2002; Losada and Hirano, 2005). This conformation brings together the Walker A and B motifs to create a region with ATPase activity (Hirano *et al.*, 2001; Haering *et al.*, 2002).

Electron micrograph images of human cohesin and condensin SMC dimers show that they form structures with distinct morphologies (Anderson *et al.*, 2002). Both structures had the characteristic two-armed structure of SMC proteins. However the coiled-coil arms of condensin are placed close together resembling a 'lollipop' whereas the coiled-coil regions in cohesin are spread into a ring-like structure (Anderson *et al.*, 2002).

Cohesin has been the complex most extensively studied biochemically. However, more recently, studies into the geometry of the condensin subunits have been carried out. In human the N-terminus of hCAP-H has been shown to interact with hSMC2 and hCAP-D2, whereas the C-terminus has been shown to interact with hSMC4 and hCAPG. The same geometry was also found for the condensin II complex (Onn *et al.*, 2007). ATP binding or hydrolysis has little effect on the assembly of condensin complexes. However, the authors report that a conformational change may occur in the hSMC4 subunit upon ATP binding (Onn *et al.*, 2007), which may alter *in vivo* function. Condensin binds DNA *in vitro* by wrapping 190 bp of DNA in an ATP hydrolysis-dependent manner (Bazett-Jones *et al.*, 2002). This ATP activity of condensin is stimulated in the presence of DNA (Kimura and Hirano, 1997, 2000).

It was suggested that both the condensin complexes have a ‘pseudosymmetrical’ subunit arrangement with a number of similarities, but also some differences to that of cohesin (Onn *et al.*, 2007). Figure 1.8 shows the predicted subunit arrangements of each complex. However it is unknown if condensin forms single complexes as shown in figure 8; other possibilities exist. Examples of SMC proteins forming multimers, such as rosette-like structure of 4-8 complexes, have been reported (Matoba *et al.*, 2005). Chromosomes assembled *in vitro* had an excess of the SMC2/4 dimer compared to non-SMC subunits, therefore additional SMC2/4 may bind in the presence of the condensin holocomplex (Hirano *et al.*, 1997). SMC2/SMC4 has been seen to form aggregates with DNA in *S. pombe* (Yoshimura *et al.*, 2002) and *S. cerevisiae* (Sakai *et al.*, 2003).

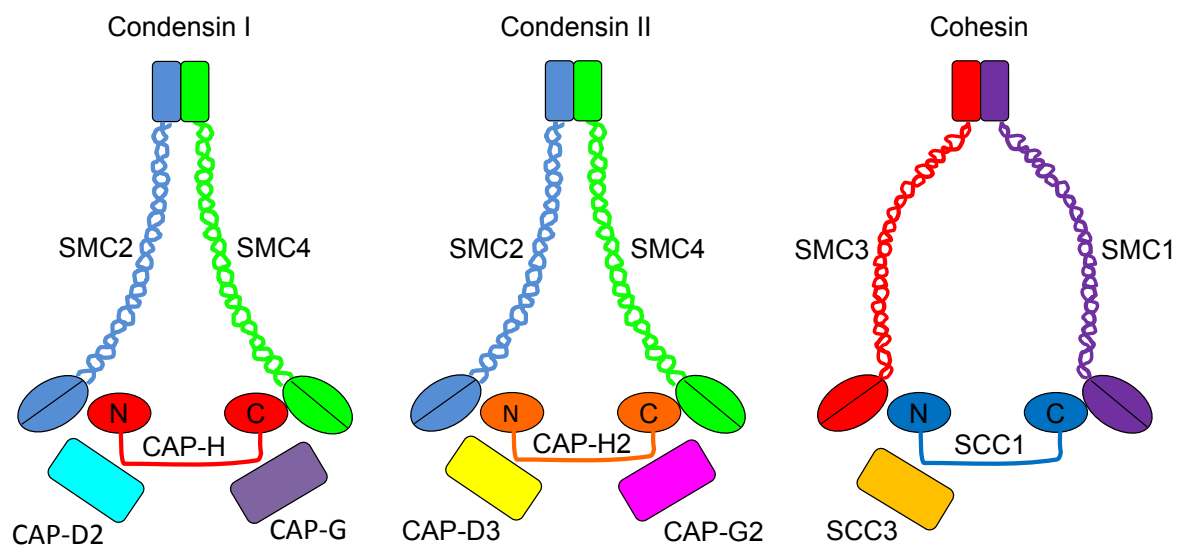


Figure 1.8: Subunit arrangement of condensin I, condensin II and cohesin complexes

The SMC arms of the cohesin complex are thought to bind DNA by 'embracing' it (Anderson *et al.*, 2002; Haering *et al.*, 2002; Haering *et al.*, 2008). When a cleavable form of SMC2 was introduced into the condensin complex and cleaved, condensin remained on the DNA (unlike cleavage of cohesin SMC3 which removed the complex from DNA (Ivanov and Nasmyth, 2005) therefore condensin may not bind DNA in the same way as cohesin does (Hudson *et al.*, 2008). Indeed, atomic force microscopy has shown that the condensin hinge sits on DNA and does not topologically 'embrace' it like that of cohesin (Yoshimura *et al.*, 2002). However recent studies have challenged this idea and shown evidence of condensin rings embracing DNA in a similar way to cohesin. This embracing of DNA by condensin was shown to be essential for the functions of condensin in chromosome segregation (Cuylen *et al.*, 2011).

The non-SMC subunits in condensin I, II and cohesin have very limited sequence homology. However detailed sequence analyses by the Nasmyth Lab identified conserved domains, which were used to group some of the non-SMC proteins into the kleisin family (from the Greek meaning 'closure'). SCC1/REC8 of cohesin, CAP-H of condensin I and CAP-H2 of condensin II are all part of the kleisin family which bind the two SMC head domains to 'close' the structures. SCC1 and REC8 are α -kleisin proteins, CAP-H2 is a β -kleisin and CAP-H a γ -kleisin (Schleiffer *et al.*, 2003).

The remaining non-SMC proteins of condensin and cohesin are grouped as HEAT-repeat containing proteins. HEAT repeats (named after where they were first identified: Huntington, Elongation factor 3, a subunit of protein phosphatase A and

TOR) are involved in protein-protein scaffold interactions and may therefore be involved in complex assembly (Neuwald and Hirano, 2000).

1.7.4 Condensin and chromosome condensation

Chromatin is highly organised in cells, in particular during cell divisions as seen by the highly condensed metaphase chromosomes. At the first level of organisation the chromosomes are wrapped around histone proteins to form the 'beads on a string' 10 nm fibre (see Figure 1.9). This structure is then further folded to form a 30 nm fibre. The exact organisation of this fibre, and indeed its existence in some experimental conditions, is highly debated (reviewed by Tremethick, 2007; Woodcock and Ghosh, 2010). How the chromosomes are further organised into metaphase chromosomes is largely unknown. Figure 1.9 shows a possible model for further folding. A model involving 'hierarchical folding' and an 'axial glue' corresponding to condensin has been suggested (Kireeva *et al.*, 2004).

Condensin and Topo II have been implicated in organisation of the metaphase chromosomes however their precise role remains unknown. Condensin is seen to localise to the chromosome axes (Hirano and Mitchison, 1994; Steen *et al.*, 2000; Steffensen *et al.*, 2001; Beenders *et al.*, 2003; Savvidou *et al.*, 2005) (see below) and Topo II has also been suggested to bind to the chromosome core (Sumner *et al.*, 1996). These proteins may collaborate, along with cohesin, and other proteins to help condense/maintain the metaphase chromosomes.

This section discusses the recent papers investigating the role of condensin in chromosome organisation.

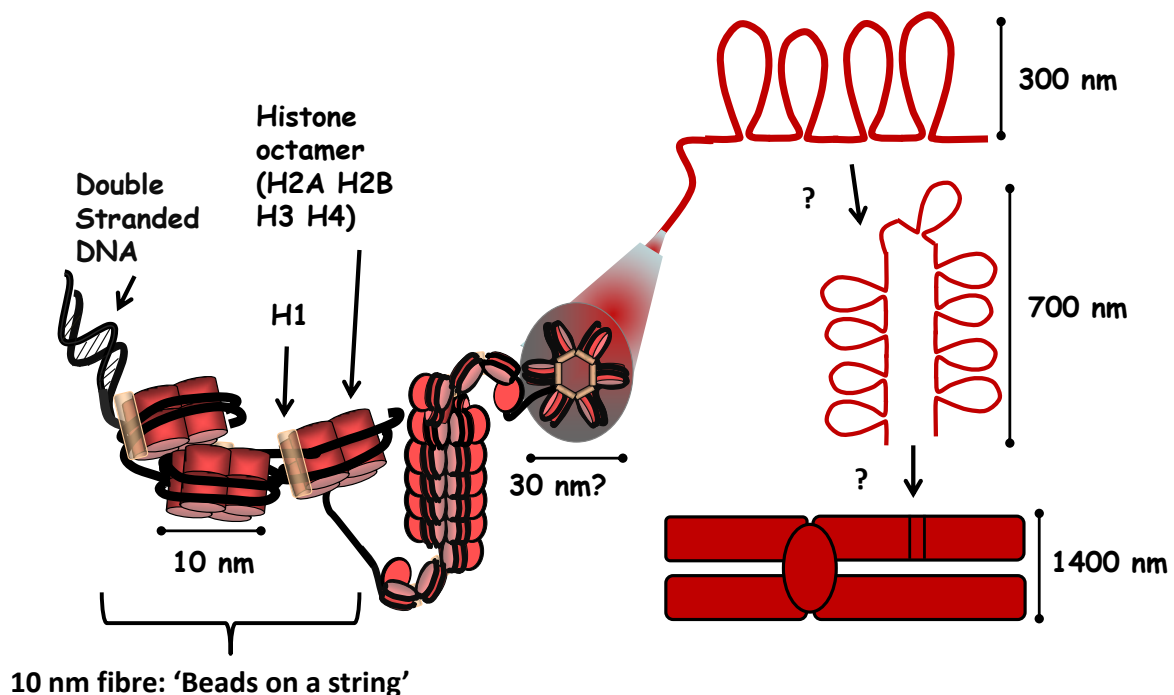


Figure 1.9: Structural organisation of the chromosomes. DNA wraps around histone octamers to form the 10 nm fibre, this is then thought to fold into a 30 nm fibre, the organisation of this is unknown, here it is shown as a 'solenoid' organisation fibre. This 30 nm fibre is then thought to fold in to a looped structure and eventually into metaphase chromosomes. The approximate size of each level of folding is shown as well as the 'typical' histone proteins. Courtesy of /adapted from, Eugenio Sanchez-Moran.

In *Xenopus* egg extracts condensin I depletion results in chromosomes which appear fuzzy and disorganised (Hirano *et al.*, 1997). This same phenotype of 'fuzzy' chromatin is also found in both budding and fission yeast lacking components of the condensin I complex (Saka *et al.*, 1994; Strunnikov *et al.*, 1995; Sutani *et al.*, 1999; Freeman *et al.*, 2000; Ouspenski *et al.*, 2000; Lavoie *et al.*, 2002; Yu and Koshland, 2003). However, condensin does not appear to have a role in chromosome condensation *per se* in all systems: indeed many more recent studies have implicated condensin in maintaining chromosome architecture rather than in

compaction itself. Dramatically decondensed chromosomes at metaphase were not observed in *C. elegans* SMC4 deficient cells (Hagstrom *et al.*, 2002; Chan *et al.*, 2004), although CAP-G condensin II depletion results in a failure to fully condense and individualise mitotic prophase cells in *C. elegans* (Csankovszki *et al.*, 2009). Conditional mutants of condensin SMC subunits in chicken DT40 cells show delays in reaching wild-type levels of metaphase condensation (Hudson *et al.*, 2003) or minor reductions in metaphase I compaction levels (Vagnarelli *et al.*, 2006).

HeLa cells deficient in both condensin complexes were still able to condense at wild-type levels, however in chicken this condensation was severely delayed, leading to the suggestion that condensin is not essential for condensation but instead confers chromosome rigidity (Hirota *et al.*, 2004; Gerlich *et al.*, 2006). Consistent with this, in human HeLa cells, chromosome condensation defects were observed in SMC2 or SMC4 deficient cells only after hypotonic treatment (Ono *et al.*, 2003).

In *Drosophila smc4* mutants only mild defects in condensation were observed. The chromosomes in these flies appeared disorganised at prophase and remained diffuse through to anaphase. Chromosome axial length at metaphase was unaffected by the mutation, however the chromosomes were wider than wild-type (Steffensen *et al.*, 2001). More severe phenotypes were observed in *Drosophila* CAP-D2 RNAi cells after treatment with hypotonic solutions (Savidou *et al.*, 2005). Depleting condensin in different cell types appears to produce vastly distinct phenotypes. For example, when *barren* was knocked-down by RNAi in *Drosophila* S2 cells, chromosomes appeared to have severe problems in condensation. By

metaphase chromatin appeared “fuzzy”, “loose”, and individual chromosomes could not be distinguished. Chromosomes from these cells remained decondensed through anaphase and telophase (Somma *et al.*, 2003). These phenotypes appeared more reminiscent of those seen in condensin deficient cells of yeast or *Xenopus*. The discrepancy between condensin phenotypes in regards to chromosome compaction was partly answered by Dej *et al.*, (2004). In this study *Drosophila dcap-g* mutants showed mild condensation defects in normal cycling cells, however, when replication was blocked, by mutation in the replication inhibitor *dup*, condensin mutants showed severe chromosome condensation defects. The authors suggest that the inconsistencies between the phenotypes for condensin in different experimental systems may be due to the use of replicated versus unreplicated chromosomes. Many factors which differ between replicated and unreplicated chromosome were suggested as possible reasons for the different requirement of condensin on replicated and unreplicated chromosomes. Cohesin is active on replicated chromosomes and not on unreplicated chromosomes, and Topo II has been shown to be activated during DNA replication and required to form a functional chromosome axis (Cuvier and Hirano, 2003; Dej *et al.*, 2004). However, this does not fully explain the different phenotypes in different organisms since a recent study using the *Xenopus* cell free extract system has shown that depletion of condensin from replicated chromosomes also produces dramatic loss of chromosome structure (Shintomi and Hirano, 2011).

Taken together results from condensin knock-down in vertebrates and *C. elegans* have led to the suggestion that other condensin-independent factors are involved in

chromosome condensation. Recently an unknown factor named RCA (Regulator of Chromosome Architecture) has been investigated for its role in chromosome condensation up until anaphase (Vagnarelli *et al.*, 2006). The authors proposed that condensin and RCA act together to maintain chromosome architecture up to anaphase, at which time RCA is inactivated by the PP1 phosphatase (which is targeted by Repo-Man), and condensin becomes essential to maintain chromosome architecture (Vagnarelli *et al.*, 2006).

Topo II has also been implicated in chromosome condensation (Earnshaw and Migeon, 1985; Uemura *et al.*, 1987) as it is required for chromosome assembly (Adachi *et al.*, 1991; Hirano and Mitchison, 1993). However its exact role in this process remains controversial. Many studies suggest that Topo II and condensin may work together to organise chromosomes. When CAP-D2 and Topo II are both knocked out in *Drosophila* the phenotype resembles that of condensin single knock-out (Savvidou *et al.*, 2005). The ability of condensin to organise chromosomes depends on prior axis formation by Topo II (Cuvier and Hirano, 2003). In chicken DT40 cells depleted of SMC2, Topo II is mislocalized (Hudson *et al.*, 2003). Topo II activity was also reduced when SMC4 levels were reduced by RNAi in *Drosophila* S2 cells (Coelho *et al.*, 2003) and mislocalized in *Drosophila* CAP-D2 depleted cells (Savvidou *et al.*, 2005). However Topo II and condensin were shown to localise independently on *Xenopus* mitotic egg extracts (Hirano *et al.*, 1997).

H3S10 phosphorylation has also been implicated in chromosome condensation in some species since histone H3 phosphorylation temporally correlates with the onset

of condensation (Wei *et al.*, 1999); however its exact role remains unknown. Some studies suggest H3S10 phosphorylation may be required to recruit condensin to chromosomes (Schmiesing *et al.*, 2000).

1.7.5 Condensin I and II play different roles during mitotic cell divisions

Condensin I and II appear to play distinct roles in chromosome organisation. Reducing condensin I subunits in HeLa cells resulted in 'swollen' chromosomes, which were distinct from the 'curly' chromosomes seen after depletion of condensin II subunits. This suggests that the two complexes play distinct roles in meiotic chromosome organisation (Ono *et al.*, 2003). Studies have shown condensin II to have an earlier role in mitotic chromosome condensation than condensin I (Ono *et al.*, 2003). The condensin I subunit CAPD3 was shown to stably associate with mammalian chromosomes in prophase of mitosis and depletion of this subunit disrupted prophase chromosome condensation. CAPD2 on the other hand was shown to only localise to the chromosome after nuclear envelope break down (NEBD) and to be dispensable for condensation in prophase (Hirota *et al.*, 2004; Ono *et al.*, 2004; Gerlich *et al.*, 2006). Condensin I has been shown to be highly dynamic in its localisation to HeLa mitotic chromosomes (Gerlich *et al.*, 2006). In this system condensin I was shown to have an architectural role in maintaining chromosome stability instead of in chromosome compaction itself. Using FRAP (fluorescent recovery after photobleaching) condensin II was shown to load to the chromosomes stably at prophase (Gerlich *et al.*, 2006).

Recently a paper which looked at the importance of the ratio of condensin I to condensin II in regulating chromosome shape has suggested that condensin II is involved in chromosome shortening. When the ratio of condensin I to condensin II was reduced from 5:1 to 1:1 on replicated chromosomes in *Xenopus* embryos chromosomes became shorter and fatter, resembling somatic chromosomes. The loading of condensin II on chromosomes also appeared to be inversely proportional to the amount of cohesin remaining (Shintomi and Hirano, 2011).

1.7.6 Condensin is specifically required for rDNA organisation in yeast

The rDNA is a large region of repetitive DNA which encodes for the ribosomal RNA subunits. Due to the highly repetitive nature of this DNA region and high transcription rates it is prone to homologous recombination (HR) between its repeats. Unstable rDNA can result in the creation of extrachromosomal rDNA circles (ERC) (Sinclair and Guarente, 1997; Park *et al.*, 1999). In order to control for rDNA lost by HR, a gene amplification system is present in most eukaryotes. This system involved unequal repair of the rDNA repeats from the sister chromatin and re-replication of some repeats after a DSB has been induced at the replication fork barriers (Kobayashi *et al.*, 1998). The rDNA needs to be carefully regulated and maintained in order to prevent damage occurring.

In *S. cerevisiae* condensin I (the only condensin complex present in yeast) has been shown to have a specific role in the condensation, maintenance and segregation of the rDNA regions (Freeman *et al.*, 2000; Bhalla *et al.*, 2002; Lavoie *et al.*, 2002;

D'Amours *et al.*, 2004; Machin *et al.*, 2004; Sullivan *et al.*, 2004; Wang *et al.*, 2004; Wang *et al.*, 2005b; Nakazawa *et al.*, 2008).

A recent paper has suggested that cohesion between the rDNA repeats, induced by condensin, is required to help stabilize the rDNA regions. In this study budding yeast strains with reduced numbers of rDNA repeats were used to investigate the rDNA regions. Strains with reduced copies of the rDNA repeats had higher transcription in the rDNA region to compensate for fewer repeats. This high transcription resulted in increased sensitivity to DNA damage inducing agents due to an inability to repair damage. This was thought to be due to a reduced loading on condensin in the low copy number strains (Ide *et al.*, 2010).

The SMC5/6 complex has been implicated in the maintenance of the rDNA repeats by preventing hyperrecombination at the rDNA by excluding the Rad52 recombination protein (Torres-Rosell *et al.*, 2007). Cohesin has also been shown to be required for the correct folding of the rDNA and to help in the repair of DSBs in the rDNA regions (Lavoie *et al.*, 2002; Kobayashi *et al.*, 2004; Lavoie *et al.*, 2004). Therefore rDNA organisation appears to be a role of all SMC complexes.

Condensin is enriched at the rDNA in budding yeast throughout mitosis, becoming further enriched onto the rDNA at the start of anaphase, where it is required to properly compact and segregate the rDNA (Freeman *et al.*, 2000; Bhalla *et al.*, 2002; Yu and Koshland, 2003; Sullivan *et al.*, 2004; Yu and Koshland 2005). The

recruitment of condensin to the rDNA at anaphase occurs in a Cdc14-dependant manner: Cdc14 is a phosphatase which works in the FEAR (Cdc-Fourteen Early Anaphase Release) pathway during cell divisions (Wang *et al.*, 2004). Condensin and cohesin have both been shown to be required for the correct folding of the rDNA (Lavoie *et al.*, 2002; Lavoie *et al.*, 2004). Localisation of condensin to the rDNA is thought to be inversely proportional to the level of rDNA transcription (Wang *et al.*, 2006; Johzuka *et al.*, 2007; Wang and Strunnikov, 2008).

The rDNA segregates later than other DNA regions, in fact the rDNA in yeast only reaches its full compaction during anaphase in wild-type cell divisions (Sullivan *et al.*, 2004). In budding yeast condensin mutants, segregation of chromosomes, especially the rDNA region, is impaired at anaphase. The origin of these bridges has been suggested to be due to recombination between rDNA repeats, as recombination in this region is elevated in Ycs4 mutant (Bhalla *et al.*, 2002). However catenations in the rDNA which prevent segregation are also a possible cause. A study by D'Ambrosio *et al.*, (2008a) has addressed the function of condensin in segregation of the rDNA. To this end, the authors arrested cells at metaphase, when much of the genome had condensed (but not the rDNA), then inactivated condensin before allowing cells to continue into anaphase. This study showed that ectopic expression of foreign Topo II from *Chlorella* virus, but not endogenous Topo II, was able to resolve rDNA anaphase bridges seen in the condensin inactivated cells. The authors conclude that catenation is responsible for the bridges but that endogenous Topo II requires condensin to function whereas; Topo II from *Chlorella* represents an

evolutionally distinct form of Topo II which does not require condensin to function (D'Ambrosio *et al.*, 2008a).

Condensin also accumulates at the rDNA in fission yeast: in this system the peak of condensin loading is at metaphase where it is bound to the non-coding regions of the rDNA. Accumulation was shown to require Nuc1 (a subunit of DNA polymerase 1) as well as Acr1 (Accumulation of Condensin at rDNA) which the authors suggest are required to alter the architecture of the rDNA to produce condensin docking sites. In condensin mutants, like in budding yeast mutants, the rDNA was not correctly condensed or segregated (Nakazawa *et al.*, 2008).

Condensin does not appear to play a specific role in rDNA organisation in other species, for example, in chicken DT40 cell no selective defects in the rDNA were observed (Vagnarelli *et al.*, 2006). However, condensin is seen to localise to the nucleolus in many species, suggesting it may have a subtle role in rDNA organisation. Accumulation of condensin I subunits in the nucleolus has been described in human cells (Cabello *et al.*, 2001). Condensin I and the SMC subunits have also been shown to accumulate in the nucleolus in interphase cells in *Xenopus*; however, this signal did not co-localise with the DNA which suggests it may not be reflecting a role for condensin in rDNA maintenance (Beenders *et al.*, 2003; Uzbekov *et al.*, 2003). During interphase, *Drosophila* CAP-G and SMC4 have been shown to alter position-effect variegation in regions close to the rDNA, suggesting that these regions may be more sensitive to defects in condensin (Cobbe *et al.*, 2006). An

investigation into the localisation of condensin in mitosis in *Arabidopsis* has also shown AtCAP-H2 to localise to the nucleolus (Fujimoto *et al.*, 2005).

1.7.7 Condensin is required for correct centromere and kinetochore function

In many eukaryotes, including plants, the centromeres are large regions of repetitive DNA including centromere satellite repeats and centromere retro-transposons. The *Arabidopsis* centromere consists of 180 bp tandem repeats or satellites. These repeats cover a region of 0.4-1.4 Mb, depending on the chromosome analysed. This central repetitive region is flanked by the pericentromeric heterochromatin. The centromere specific histone variant CENH3 (or CENP-A) localises to the centromeres and is required for the assembly of the kinetochores (reviewed by Ma *et al.*, 2007). The kinetochores are large protein structures which are required to attach the chromosomes to the spindle microtubules at the centromere DNA and orchestrate anaphase segregation. The kinetochore is composed to two domains; the inner kinetochore which is comprised of proteins which tightly associate with the centromeric DNA and the outer kinetochore which contains proteins involved in attachment to the microtubules (reviewed by Ma *et al.*, 2007). The kinetochore is required to gauge tension from the spindle and only when enough microtubules have attached to the kinetochore creating enough tension will anaphase be initiated by the anaphase promoting complex (APC) (reviewed by Yu *et al.*, 2000). Centromere stiffness is required to counter the force of the spindle. Defects at the centromere/kinetochore can result in inappropriate microtubule attachment such as merotelic attachment. The stiffness of the pericentromeric heterochromatin is also

thought to be important in accurate segregation and preventing merotelic microtubule attachment (Gregan *et al.*, 2007).

Condensin has been implicated in centromere organisation. Condensin complexes localise to the centromeric DNA in *C. elegans* (Hagstrom *et al.*, 2002; Chan *et al.*, 2004), *Xenopus* (Hirano and Mitchison 1994), human (Schmiesing *et al.*, 1998; Gerlich *et al.*, 2006) and *Drosophila* (Steffensen *et al.*, 2001; Savvidou *et al.*, 2005). The Aurora kinase may be required for the targeting of condensin to centromeres in human (Lipp *et al.*, 2007), *C. elegans* (Maddox *et al.*, 2006) and *Xenopus* (Takemoto *et al.*, 2007)

Attachment of the kinetochores to the spindle is disrupted in condensin I deficient cells in *S. cerevisiae* (Lavoie *et al.*, 2000; Ouspenski *et al.*, 2000) and *Xenopus* (Wignall *et al.*, 2003). Spindle attachment defects were observed in both condensin I and II deficient cells in human, although depletion of each complex produced distinct phenotypes (Ono *et al.*, 2004; Watrin and Legagneux, 2005). In *C. elegans* RNAi depletion of the condensin SMC4 subunit resulted in defects in orientation of centromere towards the spindle but centromere formation and spindle attachment were not affected (Hagstrom *et al.*, 2002).

In addition to defects in spindle attachment and centromere orientation, condensin has also been shown to be important for the structural integrity of the chromosomes (Oliveira *et al.*, 2005; Yong-Gonzalez *et al.*, 2007). In budding yeast, condensin-

deficient cells show defects in centromere structure (Yong-Gonzalez *et al.*, 2007). Centromeres in Barren depleted flies became stretched after they attached to the spindle, suggesting that the elastic properties of the centromeres were defective in these flies (Oliveira *et al.*, 2005). A similar phenotype was seen in *Drosophila* CAP-D2 RNAi lines (Savvidou *et al.*, 2005).

The ATPase activity of SMC2 is required for normal levels of centromere stiffness in chicken DT40 cells (Ribeiro *et al.*, 2009). Centromeres appeared to condense normally in these cells but became distorted when pulling force was applied to the kinetochores. In human, condensin I but not condensin II depletion impairs mechanical stability of centromeres. Condensin was not required for initial compaction but to withstand the forces of the spindle created by bi-polar attachment. If the spindle tension was removed centromeres returned to normal suggesting this stretching is reversible (Ribeiro *et al.*, 2009). This same phenomenon was seen in human (Gerlich *et al.*, 2006). This contrasts condensin I depletion in *Drosophila* which causes irreversible stretching of the centromeres (Oliveira *et al.*, 2005).

A recent study also in human cells argues against bi-polar attachment of kinetochores to the spindle and normal spindle forces as the cause of stretched centromeres (Samoshkin *et al.*, 2009). The authors suggest that merotelic attachment is responsible for the stretching of the centromeres seen in SMC2 depleted cells. Merotelic attachment is the attachment of spindles from both poles to one kinetochore. An increase in merotelic attachment was seen in condensin depleted cells. The authors suggest that merotelic attachments fail to be resolved

due to the mis-localisation of the aurora B kinase in condensin deficient cells (Aurora B is required for the severing and reattachment of microtubules from the incorrect pole to the correct pole) (Samoshkin *et al.*, 2009). Alternatively, condensin may be required to clamp microtubule binding sites during metaphase to prevent merotelic attachment, and role of Aurora B may be to recruit condensin (Tada *et al.*, 2011). Thus in this context Aurora B may indirectly stabilise correct microtubule attachments. The condensin II subunit HCP-6 in *C. elegans* is also required to prevent merotelic attachment (Stear and Roth, 2002).

Many studies have suggested that the mis-localisation of a centromere histone variant as a cause for the centromere defects. The centromere specific histone Cse4p is partially lost from the centromeres in budding yeast condensin mutants (Yong-Gonzalez *et al.*, 2007). In human, centromere protein A and E (CENP-A and CENP-E) targeting to and maintenance at the centromeres is deficient in condensin I and II depleted cells (Ono *et al.*, 2004; Samoshkin *et al.*, 2009). In *Xenopus* CENP-E localisation was abnormal in egg extracts deficient in CAP-G and SMC2 (Wignall *et al.*, 2003) and CENP-A localisation to and retention at the centromeres requires condensin II but not condensin I (Bernad *et al.*, 2011). The authors suggested condensin localises CENP-A by promoting correct order of the centromere chromatin. Condensin I has also been implicated in correct localisation of the CENP-A homologue CID in *Drosophila* (Jager *et al.*, 2005).

1.7.8 Condensin and chromosome segregation

During cell divisions chromosome must condense in order to accurately segregate their chromosome to the daughter cells. Segregation defects can lead DNA damage and aneuploidy. In mammals it is thought that maximal chromatin compaction occurs during late anaphase when the chromosomes are segregating (Mora-Bermudez *et al.*, 2007). In yeast maximal chromosome compaction of the rDNA region also occurs during anaphase (Sullivan *et al.*, 2004). In mammals it is thought that compaction at anaphase may be a mechanism to resolve aberrant chromosome connections at anaphase, such as those found in condensin deficient cells (Mora-Bermudez *et al.*, 2007). Anaphase bridges can arise during defective cell divisions. There are many possibly causes including unresolved recombination or replication intermediates as well as catenations, for example in PICH (Plk1-interacting checkpoint “helicase”) and BLM defective cells (for review see Chan and Hickson, 2011).

One of the most striking phenotypes of condensin mutants is the presence of anaphase bridges between segregating chromosomes in both meiosis and mitosis (Saka *et al.*, 1994; Bhat *et al.*, 1996; Freeman *et al.*, 2000; Lavoie *et al.*, 2000; Ouspenski *et al.*, 2000; Steffensen *et al.*, 2001; Hagstrom *et al.*, 2002; Lavoie *et al.*, 2002; Coelho *et al.*, 2003). The origin of these bridges has often been attributed to an inability to remove catenations between segregating chromosomes. It is thought that condensin and Topo II cooperate to ensure resolution of sister chromatids at anaphase (or homologous chromosomes at anaphase I of meiosis) (Koshland and Strunnikov, 1996; Hirano, 2000; Holmes and Cozzarelli, 2000). In support of this, an

interaction has been shown between the bacterial SMC MukB and bacterial TopoIV (Hirano, 2010).

A direct interaction has also been shown between *Drosophila* Barren and Topo II (Bhat *et al.*, 1996) and Ycs4 is required to load Topo II to chromatin in *S. cerevisiae* (Bhalla *et al.*, 2002). However, in other systems a direct interaction has not been shown and condensin and Topo II are seen to load independently onto chromosomes (Hirano *et al.*, 1997; Lavoie *et al.*, 2000). Therefore, alternative suggestions for the origin of the anaphase bridges have been proposed. A study using conditional knock-out of SMC2 in chicken DT40 cells suggests that anaphase bridges arose due to a loss of chromosome condensation during anaphase and were not only a result of catenations between chromosomes (Vagnarelli *et al.*, 2006). The authors suggested that an unknown factor, which they called RCA (Regulation of Chromosome Architecture), is required for condensation up until anaphase when it is inactivated and condensin becomes essential to maintain chromosome structure. Therefore when RCA is inactivated at anaphase onset in condensin mutants a 'catastrophic loss of individual chromosome architecture' occurs. It is this loss of chromosome structure that was suggested as the cause of the anaphase bridges seen in condensin mutants. Although it is possible that Topo II may still have a role in decatenation at anaphase (Vagnarelli *et al.*, 2006). A role for condensin in maintaining chromosome integrity at anaphase has also been suggested in budding yeast (Cuylen and Haering, 2011; Cuylen *et al.*, 2011).

Incomplete cohesin removal before anaphase has also been suggested as a cause of the anaphase bridges in condensin mutants. Condensin I but not condensin II was shown to be required for complete removal of cohesin from chromosome arms in mammals (Hirota *et al.*, 2004). Consistent with this, condensin has been implicated in the removal of arm cohesin between segregating chromosomes in budding yeast. In wild-type cells chromosomes were seen to stretch and recoil when segregating at anaphase, this stretching was due to residual cohesin on chromosome arms. It was shown that condensin is required for cohesin removal indirectly by promoting recoiling, (recoiling may increase accessibility of the site to separase- the enzyme responsible for cleaving cohesin (Ciosk *et al.*, 1998; Uhlmann *et al.*, 1999; Uhlmann *et al.*, 2000). The authors argue that condensin does not play a role in resolution of catenanes between sisters and instead suggests it is involved in cohesin removal via arm recoiling (Renshaw *et al.*, 2010).

1.7.9 Condensin recruitment onto DNA

Scc2 and Scc4 are known to load the cohesin complex onto the chromosomes (Lengronne *et al.*, 2004). Recently Scc2/4 has also been implicated in condensin recruitment to DNA in budding yeast (D'Ambrosio *et al.*, 2008b). In this study Scc2 and Scc4 could not account for all of condensin loading since *scc2* mutants had significantly reduced, but not a total removal, of condensin loading (D'Ambrosio *et al.*, 2008b). The DNA Pol III transcription factor TFIIIC was also implicated in condensin loading in this study: condensin loading sites corresponded to tRNA genes and other loading sites of TFIIIC. Further experiments showed that an ectopic B-box element (the DNA sequence recognised by TFIIIC) was capable of creating a

condensin binding site. The loading pattern of condensin is different to that of cohesin. Cohesin is thought to translocate along the chromosomes from the sites of loading to sites of convergent transcription, whereas condensin remains at the site of loading where it may bridge distant sites together throughout the genome (D'Ambrosio *et al.*, 2008b).

Some evidence suggests that histones may be involved in the recruitment of condensin to chromosomes. Condensin proteins load on to the chromosomes at the same time that H3S10 phosphorylation is first seen, condensin subunits and H3S10 phosphorylation are also seen to co-localise (Schmiesing *et al.*, 2000). The mitotic kinase Aurora B is required for the localisation of condensin I to chromosomes in *Xenopus* (Lipp *et al.*, 2007; Takemoto *et al.*, 2007). However, localisation of condensin II appears to be Aurora-B independent (Lipp *et al.*, 2007). Aurora B is the kinase responsible for phosphorylating histone H3 at serine 10 (Hsu *et al.*, 2000). When Aurora B kinase is depleted from *Drosophila* cells, levels of Barren on the chromatin were also reduced (Giet and Glover, 2001); a similar phenotype is also seen in *C. elegans* (Hagstrom *et al.*, 2002) and fission yeast (Petersen and Hagan, 2003). However the link to H3S10 phosphorylation and condensin binding is not seen in all systems (de la Barre *et al.*, 2000; Kimura and Hirano, 2000). *In vitro* experiments show that human CAP-D2 binds histones H1 and H3, independently of S10 phosphorylation, the interaction with histone H3 was also confirmed *in vivo* (Ball *et al.*, 2002). Recently histone H2A and its variant H2A.Z have been shown to be required to load condensin complexes on to chromosomes in *S. pombe*. The association of condensin Cnd2 with H2A and H2A.Z depends on its prior

phosphorylation by Aurora B kinase. The authors showed that the specific localisation of condensin to the kinetochores depends on the monopolin homologues Pcs1 and Mde1 (Tada *et al.*, 2011).

Other proteins implicated in condensin loading to chromosomes include; cAMP-dependent protein kinase A anchoring protein (AKAP95) which targets condensin I to the chromatin after NEBD in HeLa cells (Collas *et al.*, 1999; Steen *et al.*, 2000). Vasa is a DEAD-box RNA helicase which is required to correctly localise condensin subunits to chromosomes, possibly via a physical interaction with CAP-D2 and Barren (Pek and Kai, 2011). Protein Phosphatase 2a (PP2A) has been shown to target condensin II but not condensin I to chromosomes in vertebrate cells (Takemoto *et al.*, 2009).

1.7.10 Regulation of condensin during mitotic divisions

It has been shown that phosphorylation of the condensin subunits is required for the full functionality of the complex in *Xenopus* (Hirano *et al.*, 1997; Kimura *et al.*, 1998) human (Takemoto *et al.*, 2003) and fission yeast (Sakai *et al.*, 2003). Condensin I non-SMC subunit phosphorylation by Cdk1 (cyclin-dependant kinase 1) or Cdc2-cyclin B in *Xenopus* or human, respectively, was shown to be required for the DNA supercoiling activity of the complex (Kimura *et al.*, 1998; Kimura and Hirano, 2000; Kimura *et al.*, 2001). Mitotic phosphorylation of the SMC subunits of condensin increases supercoiling activity of the complex in *S. pombe* (Sakai *et al.*, 2003). In budding yeast mitotic cells, the polo-like-kinase, Cdc5, has been shown to hyperphosphorylate all three non-SMC condensin subunits at the onset of anaphase (St-Pierre *et al.*, 2009). Cdk1-mediated phosphorylation may 'prime' condensin earlier in

the cell cycle, allowing Cdc5 to hyper-phosphorylate the complex and fully activate it (St-Pierre *et al.*, 2009). A similar situation has recently been shown in human cells (Abe *et al.*, 2011). However in this study it is the condensin II subunit hCAPD3 which is initially phosphorylated by Cdk1, this results in the binding of Polo-like kinase to hCAPD3 and subsequent hyperphosphorylation of all of the non-SMC condensin II subunits. Hyperphosphorylation of condensin II is required for correct chromosome condensation in prophase (Abe *et al.*, 2011).

In *S. pombe* the Aurora-B-like kinase, Ark, was shown to phosphorylate Cnd2 throughout mitosis: this phosphorylation was required for the correct function of condensin (Nakazawa *et al.*, 2011). Phosphorylation of Cut3 in *S. pombe* by Cdk1-cyclin B was required to localise condensin to the nucleus (Sutani *et al.*, 1999; Nakazawa *et al.*, 2008). Human SMC4, CAP-D2, CAP-H, and CAP-G are all phosphorylated in interphase in mitotic cells but different sites are used at different stages of the cell cycle (Takemoto *et al.*, 2004; Takemoto *et al.*, 2006).

1.7.11 Condensin and gene regulation

In addition to its role in chromosome organisation condensin is also involved in gene regulation. In budding yeast, condensin Ycs4 is involved in silencing mating type loci (Bhalla *et al.*, 2002). In *C. elegans* condensin subunits working in the dosage compensation complex (DCC) are responsible for reducing expression of both X chromosomes by half in hermaphrodite (XX) worms. In *Drosophila* the Barren subunit of condensin I has been shown to be involved in gene silencing in the Bithorax gene complex (Lupo *et al.*, 2001). It is possible that the condensin complex

affects all of these processes by its influence on higher order chromosome structure (Legagneux *et al.*, 2004).

1.7.12 Condensin in meiosis

Correct condensation, structural maintenance and segregation of chromosomes, are essential to meiotic as well as to mitotic cell divisions. In addition to this, a meiotic cell division has special events such as meiotic recombination, which is required for successful meiosis. The success of this recombination is linked to the meiotic structural organisation of the chromosome and vice versa. It is therefore conceivable that the condensin complex may have a role in such processes. During meiosis the SMC containing cohesin complex exchanges certain subunits (for example Scc1 is replaced with Rec8 in yeast (Kitajima *et al.*, 2003) to perform meiosis specific functions (Lin *et al.*, 1992; Molnar *et al.*, 1995). No such cell specific subunit exchange has been seen in condensin complexes to date, however altered post-translational modifications of condensin may occur between meiosis and mitosis. Different loading requirements between meiosis and mitosis have been suggested for condensin in *C. elegans*. HCP-6 and MIX-1 can localise independently of each other on mitotic chromosomes however MIX-1 is dependent on HCP-6 for association with meiotic chromosomes (Chan *et al.*, 2004). HCP-6 localisation to mitotic chromosomes also required CENP-A, however the meiotic association of HCP-6 and MIX-1 did not (Chan *et al.*, 2004).

The role of the condensin complexes in meiosis has been investigated in a variety of species revealing interesting similarities and differences. In *S. cerevisiae*, which only

has the canonical condensin I complex, a role for condensin in mediating meiotic axial length compaction and individualisation of homologous chromosome at pachytene has been suggested (Yu and Koshland, 2003). Loading of the axis proteins Red1 and Hop1 was deficient in condensin depleted cells. These results suggest that condensin is a component of the axial core on which other proteins, such as those of the SC, are loaded. Ycs4 co-localised with the SC TF protein Zip1, and *ycs4* and *ycg1* mutants cells did not assemble the SC properly, as was evident from the occurrence of many Zip1 polycomplexes (present when Zip1 cannot polymerise on the axis)(Yu and Koshland, 2003). Condensin deficient cells also have defects in the pairing of homologous chromosomes and in the correct processing of DSBs. In the absence of condensin, DSBs were formed at wild-type levels (although with a slight delay) but were processed independently of DMC1 (Yu and Koshland, 2003). Budding yeast condensin is also required for the correct co-orientation of the sister chromatids during meiosis I, a process required to ensure segregation of both sisters to the same pole. The loading of Maml, a subunit of the monopolin complex involved in co-orientation of the sister chromatids, is decreased in the absence of condensin (Brito *et al.*, 2010).

In *Drosophila* condensin I *dcap-g* mutants, SC assembly is unaffected however there is a delay in SC disassembly (Resnick *et al.*, 2009). This study also showed that in *dcap-g* mutants, metaphase I homologous chromosomes often separated and migrated towards the poles prematurely, resulting in aneuploidy. This could be a result of a defect in COs: recombination may be absent, or chiasmata may not form properly or may be lost prematurely due to a premature loss of arm cohesion (Resnick *et al.*, 2009). Condensin II has also been investigated in *Drosophila*

meiosis. Condensin II mutants in this system show prophase I defects in the form of defects in chromosome territory formation and chromosome individualisation. In addition to this, segregation defects at anaphase I were seen, which may have been due to the previous problems in territory formation (Hartl *et al.*, 2008a).

A few studies have looked into the role of condensin in *C. elegans* meiotic divisions. The condensin SMC subunits SMC-4 and MIX-1 were seen to localise to centromeres at metaphase I and II (Hagstrom *et al.*, 2002). RNAi depletion of either SMC-4 or MIX-1 failed to show any morphological defects in meiosis I chromosomes. Segregation defects were seen in these knock-down cells in meiosis II but not meiosis I (Hagstrom *et al.*, 2002). Later studies focusing on non-SMC condensin II subunits, using mutant alleles combined with RNAi, revealed that condensin II HCP-6 is required for chromosome segregation at both anaphase I and II (Chan *et al.*, 2004). Results from these studies and previous RNAi experiments (Hagstrom *et al.*, 2002) revealed that anaphase I appears to be less sensitive to condensin depletion than anaphase II, thus explaining the lack of meiosis I segregation defects in the original study (Hagstrom *et al.*, 2002). Condensin II depleted worms show no defects in SC assembly or disassembly or homologue compaction in pachytene. These worms did however show defects in diplotene and diakinesis chromosome condensation (Chan *et al.*, 2004). Later studies detected a defect in axial length shortening and CO distribution in condensin II deficient worms (Mets and Meyer, 2009). Condensin II was seen to partially associate with the DNA in pachytene I and localise fully to the DNA at diplotene and diakinesis, where it persisted on the chromatin throughout the rest of meiosis (Chan *et al.*, 2004; Mets and Meyer, 2009).

CO distribution was also affected in condensin I deficient worms. DPY-28 (later to be found to be the CAPD2 homologue) accumulates on meiotic staged cells and partially overlaps with meiotic chromosomes during pachytene. DPY-28 was shown to restrict COs by limiting the number of DSBs formed and thus altering CO distribution. In *dpy-28* mutants CO interference was reduced. There was an increase of 2-CO and even 3-CO bivalents and CO often occurred in adjacent intervals (Tsai *et al.*, 2008). The increase in DSBs seen in *dpy-28* cells was dependent on the axis component HIM-3 which suggests a link between DPY-28 and the chromosome axes. HIM-17 is required for histone modification and is thought to influence CO number by influencing chromosome structure. *dpy-28* mutants were able to partially restore CO number in *him-17* mutants, suggesting that DPY-28 may influence DSB number by affecting chromosome structure in an opposing way to HIM-17 (Tsai *et al.*, 2008). Budding yeast DSBs occur at sites of high C-G content. *C. elegans* has a constant G-C content, however despite this the COs are still distributed in a similar pattern to those in yeast. Therefore the authors suggested that chromosome structural components, such as DPY-28, may be compensating for the constant G-C content by altering higher order chromatin structure (Tsai *et al.*, 2008). Indeed, DSB formation is thought to occur in more open chromatin (Wu and Lichten, 1994). SC formation occurred as in wild-type in *dpy-28* mutants (Tsai *et al.*, 2008), however pachytene axis length was increased (Mets and Meyer, 2009). The authors went on to show that all subunits of the condensin I complex are required to restrict DSB formation and therefore CO number and distribution. Both condensin I and condensin II mutants have an increase in axis length and increased DSBs and COs. However the two complexes appeared to exert their effects on axis length independently, this was demonstrated by depleting both complexes which resulted in

an additive effect on axis length. CO distribution was altered in condensin II mutants but in the opposite way to mutants in condensin I subunits. Condensin I mutants had less COs on the left of the X and more on the right, whereas condensin II mutants had an increase on the left of the X and less on the right (Mets and Meyer, 2009). The authors concluded that the increase in axis length was responsible for the increase in DSBs and COs.

In mouse the two condensin complexes have been recently investigated (Lee *et al.*, 2011). In this study condensin II was seen to localise to the nucleus first during prophase I and after germinal vesicle break-down (GVBD; the equivalent to NEBD in mitosis) and was associated with the chromosome axis on metaphase I chromosomes. Condensin I was shown to localise mainly around the centromeres at metaphase I and only localised to the arms after anaphase I. Comparing this loading pattern to mitosis where condensin II loads during prophase it is clear that there appears to be a delay in condensin loading in meiosis, although the order of association of the two complexes remains conserved. The authors suggest that this delay may be due to the presence of large amounts of cohesin along prophase chromosome arms (Lee *et al.*, 2011). The two complexes were reduced by immunoinjection of antibodies specific to condensin I and condensin II subunits, revealing distinct roles for the two complexes. The results suggested that condensin I may be required for monopolar attachment of the kinetochores, possibly by a role in the underlying centromere structure. Bivalents in condensin I depleted mice also appeared 'bumpy' suggesting that condensin I is required for structural organisation of the metaphase I chromosomes to some extent. Condensin II may be required for chromosome individualisation. In condensin II depleted mice the chromosomes also

seemed to lose compactness appearing 'extended' when attached to the spindle (Lee et al., 2011).

As in mitotic divisions, bridges at anaphase are seen between segregating chromosomes at both meiotic divisions in condensin deficient cells in all species tested. Condensin I was shown to be required for MI and MII segregation in the budding yeast *Saccharomyces cerevisiae* (Yu and Koshland, 2003), whereas studies in *Xenopus* have suggested that condensin I is required for anaphase II segregation and not anaphase I (Watrin et al., 2003). However, in light of the RNAi depletion experiments in *C. elegans*, which suggested that meiosis II is more sensitive to condensin depletion than meiosis I (Hagstrom et al., 2002; Chan et al., 2004), it is possible that in the *Xenopus* study incomplete knock-down by RNAi may mask anaphase I segregation defects. The cause of these bridges is still unclear, although several studies have suggested possible origins. In *S. cerevisiae* Ycs4 and Ycg1 were shown to be important in the resolution of recombination-dependent linkages between segregating chromosomes. When condensin was mutated in a *spo11-Y13F* background (an allele which only affects DSBs and has no effect on pairing), anaphase bridges were reduced. Remaining bridges were associated with the rDNA loci where the bridges are recombination independent. The role of condensin in resolving recombination-dependent linkages was suggested to be promoting cohesion release, possibly by enhancing association of Cdc5 with chromatin (Yu and Koshland, 2005). Condensin II deficient meiocytes also have anaphase bridges. In *C. elegans*, HCP-6 is thought to help resolve cohesin-independent linkages which are thought to be responsible for the segregation defects seen in both meiotic

divisions. The authors suggest that condensin may work with Topo II to remove/prevent the formation of linkages between chromosomes (Chan *et al.*, 2004).

In *Arabidopsis*, condensin I and II homologues exist. *AtSMC4* has been shown previously to be an essential protein in plants as homozygous T-DNA knock-out mutants are lethal (Siddiqui *et al.*, 2003). *AtSMC2* has a role in homologous chromosome segregation during meiosis as reduced *AtSMC2* levels resulted in chromosome connections at anaphase I. Anaphase II was not analysed in these lines (Siddiqui *et al.*, 2006).

1.8 Project aims

The structure of the chromosomes is essential for correct segregation at anaphase and meiotic recombination in prophase I. This project will focus on the role of the two condensin complexes during meiosis in *Arabidopsis*. This is the first in-depth analysis of the condensin complexes in this system. Condensin in other organisms affects the structure of the chromosome axes and in some cases the process of meiotic recombination. However comparative analysis in plants is lacking. This project aims to address this gap in the condensin literature to shed further light onto the complex role of these complexes in higher eukaryotes.

The aims of this project are to:

1. Produce an antibody against a condensin subunit in order to assess the localisation of the complex during meiotic cell divisions.
2. Obtain condensin mutants either by T-DNA lines or meiosis-specific knock-down lines of condensin subunits in order to investigate their role during a meiotic division.
 - a. One protein from the SMC backbone of condensin, present in both condensin I and condensin II complexes, will be chosen in order to see the effect of knocking-down the whole of condensin during meiosis.
 - b. Non-SMC proteins unique to each of condensin I and condensin II complexes will also be knocked down in order to investigate whether condensin I and II have different roles during a meiotic division.

CHAPTER 2

2 MATERIALS AND METHODS

2.1 Plant cultivation

Stock plants were obtained from the European *Arabidopsis* Stock Centre (NASC). Seeds were grown in John Innes No. 1 potting compost, which were then covered with a thin layer of vermiculite (perlite) to retain moisture. Seeds were grown at 18-25°C, with 16 hours white light per day, and watered twice daily by immersion. The Columbia 0 (Col-0) ecotype was used as a control in all experiments.

2.1.1 Sterilisation of seeds for plating on MS media

Seeds were sterilised in 20% Parazone™ for 15 minutes followed by three 15 minute washes in sterile distilled water (SDW) prior to plating on to MS plates (for recipe see appendix).

2.2 Cytological procedures

All slides were viewed on a Nikon Eclipse E400 microscope using Cell P Soft Imaging System software (an Olympus company). A Hamamatsu ORCA-ER Digital camera was used to capture images.

2.2.1 Preparation of slides

Microscope slides (SuperFrost VWR) were pre-cleaned in acetone for 10 minutes followed by ethanol for 10 minutes before they were used for cytological procedures.

2.2.2 Cytology: chromosome spreading

Buds were collected from young plants and immediately fixed in ice cold Carnoy's solution (3:1 ethanol: acetic acid). The fixing solution was changed after 1-2 hours and again after 14-16 hours. Buds were stored at 4 °C for at least 24 hours, or until required. Fixed buds were placed in a black cuvette with 2-3 ml of ice cold Carnoy's solution and dissected using 5.s watchmaker's tweezers (ideal-tek Switzerland). Buds with visible yellow coloured anthers or a pointed shape were discarded as meiosis in these buds will have passed. Buds were washed 3 times for 2 minutes in 10 mM citrate buffer pH 4.5 (445 µl 0.1 M citric acid and 555 µl 0.1 M Na citrate and made up to 10 ml with SDW). Buds were then incubated in enzyme mix (0.3% w/v, cellulase (C1794 Sigma) and 0.3% pectolysase (P5936) in 0.01 M citrate buffer) for 1 hour 15 minutes- 1 hour 30 minutes at 37 °C in a moist environment in order to digest cell walls.

After digestion, a drop of water was added to a microscope slide to which 1-4 buds were added. A small brass rod was then used in break up the tissue of the bud. A 10 µl drop of 60% acetic acid was added to the slide, which was placed on a hot plate at 45 °C. The slide was left on the hot plate for 1 minute while the tissue was mixed with a needle in a circular motion, causing the cells to form an even spread-out layer. The

cells were then fixed with 200-500 μ l of ice cold Carnoy solution applied in a circle around the tissue. The excess was poured off and the slide was dried from the back with a hair dryer. For basic cytology the slides were stained with DAPI 4',6-diamidino-2-phenylindole (10 μ l); Stock 1 mgml⁻¹, in Vectorshield mounting medium (Vector Laboratories). A small cover slip was then added to the slide and pressed with a tissue to remove bubbles.

2.2.3 Nick translation of Fluorescence *in situ* hybridisation FISH probes

For production of T-DNA FISH probes, 1-3 μ g of mini-prep plasmid DNA and 4 μ l of nick translation mix (Roche); BIO (Biotin) or DIG (Digoxigenin), made up to 20 μ l with BPC water was incubated at 15 °C for 90 minutes. After which 1 μ l of 0.5 M EDTA (pH 8.0) was added and the reaction heated for 10 minutes in a water bath at 65 °C.

For the 45S, 5S and centromere probes the following constructs were used:

45S: Clone pTa71 (Gerlach and Bedbrook 1979) consisting of a 9 Kb *Eco*RI fragment of *Triticum aestivum* containing the 18S-5.8S-25S rRNA genes and spacer regions.

5S: (Campell *et al.*, 1992) Plasmid pCT4.2 containing the 5S rDNA gene from *A. thaliana* as a 500-bp insert cloned in pBlu.

pAL38: containing the 180 bp pAL1 centromeric repeat (Martinez-Zapater *et al.*, 1986).

2.2.4 Fluorescence *in situ* hybridisation

Spread chromosome preparations were made as previously described. Slides were washed in 2x SSC for 10 minutes at room temperature and then digested with 0.01 % pepsin in 0.01 M hydrochloric acid, for 90 seconds, and washed in 2xSSC (see appendix for recipe) for another 10 minutes. Slides were then fixed in 4% paraformaldehyde for 10 minutes, rinsed in SDW and then dehydrated in an alcohol series of 70% ethanol, 85% ethanol and 100% ethanol respectively for 2 minutes per concentration. Hybridization of probes was then carried out. The following solution was added to each slide: 14 μ l of hybridization mix (5 ml deionized formaldehyde, 1 ml 20 x SSC, 1 g dextran sulphate, pH 7) and 2 μ l of each desired probe (approximately 100-300 ng), made up to 20 μ l with water. A cover slip was added to each slide and sealed with rubber solution. Slides were placed in a hot block at 75 °C for 4 minutes to denature the DNA and probes and then incubated at 37 °C in a moist box overnight. Slides were then washed 3 times in 50% formaldehyde in 2xSSC for 5 minutes, once in 2xSSC for 5 minutes and once in 4xSSC and 0.05% Tween 20 for 5 minutes, each wash being carried out at 45 °C. These were followed by a wash in 4xSSC and 0.05% Tween 20 for 5 minutes at room temperature. Probes were detected with fluorescent labeled secondary antibodies. A 50 μ l solution of secondary antibodies either labeled with BIO (used at 1:200 Milk block) or DIG (1 in 50 DIG block) (see appendix for recipes) were added to each slide and incubated at 37 °C for 30 minutes in a moist box. When more than one probe was used, each secondary antibody was added separately and separate 30 minute incubations carried out for each, slides were washed in 2xSSC twice for 5 minutes between applications of secondary antibodies. Final 3 x 5 minutes washes in 4x SSC and 0.05% Tween 20

were carried out; slides were then dehydrated in an ethanol series as before and stained with 10 μ l DAPI/Vectorshield.

2.2.5 Immunolocalisation by spreading

Anthers from buds which were approximately 0.2-0.7 mm in length were dissected out on damp filter paper. The anthers from 10-20 buds were used for each slide. Anthers were transferred to a slide with 5 μ l EM digestion medium (originally used for electron microscope preparations) containing, 0.4 % Cytohelicase (C8274), 1.5% sucrose, and 1% polyvinylpyrrolidone in SDW. Anthers were gently taped with a brass rod to release meiocytes after which a further 5 μ l of enzyme mix was added to prevent the slides drying out. Slide were then placed in a moist box on a hot plate at 37 °C for 4 min. 1% lipsol (Bibby Sterilin Ltd.) (10 μ l) was then added to each slide and the mixture spread with a needle to separate the cells. Slides were then fixed with 20 μ l 4% paraformaldehyde, to make a final concentration of 2% paraformaldehyde, after which slides were left to dry. When slides were dry a 50 μ l solution of primary antibodies in EM block (1% Bovine Serum Albumin in 1% PBS, 0.1% Triton X100) (anti-AtASY1 1:5000 (Armstrong *et al.*, 2002); anti-AtZYP1 1:1000 (Higgins *et al.*, 2005)) was applied and the slides incubated overnight at 4 °C in a moist box. After primary antibody incubation slides were washed 2 x for 5min in PBS with 0.1% Triton X100. 50 μ l of the secondary antibody diluted in EM block (1:200 Texas red (anti-rat and -rabbit both from: Sigma) or 1:50 FITC (anti -rat and rabbit both from: Vector laboratories) was then applied to the slides which were then incubated in a moist box at 37 °C for 30 min. Slides were then washed twice in 1%

PBS and 0.1% triton before 10 µl of DAPI/Vectashield was added to the slides to label chromatin and reduce fading of fluorescent conjugates.

2.2.6 Immunolocalisation on fixed bud material

Buds which had been fixed in 3:1 Carnoy's solution were washed 3 times for 2 minutes in citrate buffer pH 4.5 and incubated in enzyme mix (0.3 % w/v, cellulase (C1794 Sigma) and 0.3% pectolysase (P5936) in 0.01 M citrate buffer) for 3 hours in a moist chamber at 37 °C. Buds were washed with SDW to stop the reaction. 3 buds between 2 and 5 mm long were selected for each slide. Anthers were dissected from the buds and placed in 3 µl of water on a slide. Anthers were broken apart thoroughly using a blunt needle or hook to release meiocytes. 10 µl of 60% acetic acid was added to the suspension of cells and the slides were placed in a hot block at 45 °C stirring continually for 2 minutes, another 10 µl of 60% acetic acid was added after the first minute. Slides were then removed from the hot block and ice cold Carnoy's fixative was applied around the drop of solution and slides were left to dry. Slides were then transferred to a plastic coplin jar containing 10 mM citrate buffer pH 7 and microwaved at 800W for 40 seconds before being transferred to 1% PBS and 0.1% Triton for 5 minutes. Slides were then incubated with primary and secondary antibodies as for the standard immunolocalisation procedure (section 2.3.5).

2.2.7 Alexander staining of pollen

Buds were fixed overnight in 10% ethanol. Anthers were dissected from the buds and placed on a slide in a drop of water; anthers were then squashed with a needle to release the pollen. A few drops (2-3) of Alexander stain were added to the slide and

covered with a coverslip. The coverslip was pressed down gently before sealing with rubber solution. Slides were incubated on a hot block at 50 °C for 1 hour, and then viewed under a light microscope. The pollen wall stains green and the pollen cytoplasm stains dark red.

2.3 DNA and RNA manipulations

2.3.1 Plant DNA extractions

Extract'n'Amp Plant PCR kit (Sigma) was used to isolate leaf DNA.

A small disc from new leaf was taken using the cap of a 0.5 ml microfuge tube. To this 40 µl of extraction buffer was added, the leaf was then broken up with the tip of a pipette. The samples were placed in a PCR machine for 10 minutes at 95 °C after which 40 µl of dilution buffer was then added and the tube flicked in order to further break up the tissue. The samples were then centrifuged for 15 seconds at full speed. DNA was stored at -20 °C. For genotyping 1 µl of supernatant containing extracted DNA was used in a 25 µl reaction.

2.3.2 RNA extraction

All 1.5 and 0.5 ml tubes and plastic rods used to break up plant tissue were treated with diethyl pyrocarbonate (DEPC) prior to use with RNA. Equipment was immersed in DEPC (1:1000 with SDW) overnight and subsequently autoclaved to inactivate the DEPC. RNA was extracted from plant tissue (< 100mg per sample) using the method described in the manufactures handbook using buffer RLT RNeasy mini kit (Qiagen). Plant tissue was snap frozen in liquid nitrogen upon collection and ground-up in a 1.5

ml tube using a pestle grinding rod before adding RLT buffer and vortexing. RLT buffer contains guanidine thiocyanate and β -mercaptoethanol which denature proteins and RNase. The tissue was then passed through a QIAshredder spin column to remove cell debris, followed by a binding to a silica membrane containing RNeasy mini column. The column was then washed with RW1 buffer containing ethanol. The sample was eluted in RNase free (DEPC treated) water. Eluted RNA was stored at -70°C .

2.3.3 cDNA synthesis

cDNA was synthesised using the 1st strand cDNA synthesis Superscript[®] II reverse transcriptase kit (Invitrogen) according to the manufacturer's protocol. 1.5 μl of Oligo (dt) primer was added together with 1 μg of RNA and 1 μl of dNTP mix, and made up to 12 μl with RNase free water. The RNase inhibitor used was RNasin (Promega). cDNA stored at -20°C .

2.3.4 Agarose Gel electrophoresis for DNA

Agarose gels were made by dissolving agarose powder in 0.5 x TBE (5 x TBE: 0.45 M Tris, 0.45 M Orthoboric acid, and 12.5 mM EDTA). 1% agarose gels were used in most cases unless otherwise stated. 0.5 μgml^{-1} of ethidium bromide was added to the molten gel before being left to set. Size comparison was achieved by electrophoresis of 10 μl of 1 Kb ladder (15 μl 1Kb Ladder (Invitrogen), 50 μl DNA Loading Buffer, (40% (v/v) glycerol, 0.25% (w/v) Bromophenol blue, 0.25% (w/v) xylene cyanol), 135 μl , SDW). Loading buffer was added to DNA if not already included in the sample (Bromophenol blue runs at ~ 400 bp; xylene cyanol runs at ~ 4000 bp). Gels were run

using Hybaid or Biorad electrophoresis kits. Images of gels were captured using a FlourS Max multi-imager or a Gel-Doc XR imager using QuantityOne Software.

2.3.5 Agarose Gel electrophoresis for RNA

Gels were prepared, ran and visualised as for DNA gels however RNA loading dye (Invitrogen) at a ratio of 1:1 was added to each RNA sample and samples were incubated at 65 °C before loading on the gel.

2.3.6 Primer design

All PCR primers were designed and supplied by Eurofins MWG operon. See Appendix 9.2 for the table of all primers used.

2.3.7 Polymerase Chain Reactions (PCR)

PCR reactions were used to amplify gDNA, cDNA and plasmid DNA. For amplifying DNA for experiments such as plant genotyping Reddymix Taq polymerase (Invitrogen) was used in accordance with the manufacturer's guidelines. For reactions requiring more accurate proof reading Taq polymerises PfuUltratm II fusion HS DNA polymerase was used (Agilent Technologies) in accordance with the manufacturer's guidelines. The annealing temperature depended upon the melting temperature of the primers being used, generally being 5 °C below the T_m of the primers. The length of time allowed for the annealing stage to complete was 1 minute per kb of sequence to be amplified. Primers were used at a final concentration of 10 μ M. Reaction mixes

were undertaken in a ThermoHybaid Omnigene, Techne TC-412 or ThermoHybaid PCR Sprint thermo-cycler.

Standard PCR cycle:

Temperature (°C)	Time (minutes)	Number of cycles
94	2	1
94	1	35
5 °C below T_m of primers	1	
72	1 minute/kb	
72	10	1

Table 2: Standard PCR cycle

2.4 Cloning procedures

2.4.1 Amplification of sequence specifically for cloning

PCRs were carried out as described above (2.4.7). If the fragment was to be cloned for use in recombinant protein or RNAi construct production, primers were designed with specific restriction sites at the end. PCR products were run on an agarose gel (see 2.4.5).

2.4.2 Extraction of amplified DNA from agarose gels

Gels were visualised under weak UV light in order to extract DNA fragments. Gel extraction was carried out using QIAquick Gel Extraction Kit Protocol (QIAGEN), following the manufacturer's guidelines. Briefly DNA was extracted from the gel using a razor blade and transferred to a 1.5 ml microcentrifuge tube. The gel fragment was dissolved in three volumes (w/v) of buffer QG at 50°C for 10 minutes. After which the

solution was transferred to a QIAquick spin column. The sample was washed with PE buffer and eluted in nuclease free water.

2.4.3 Quantification of nucleic acids

Nucleic acid concentrations were estimated either by comparison with DNA of known concentration (Bioline HyperLadder I), or by measuring absorbency of 100-fold diluted samples at 260 nm. Absorbency readings were converted to concentrations, given that a solution of nucleic acid, with concentration 40 mgml^{-1} , has an OD_{260} of 1 unit.

2.4.4 Cloning Vectors

pDRIVE (Qiagen) is a 3.8 Kb vector used for cloning PCR fragment amplified with Reddymix Taq polymerase. This plasmid has multiple cloning sites within the *lacZ* and permits blue/white selection of colonies (X-gal). This plasmid has ampicillin and kanamycin resistance.

pZErO background Kan (Invitrogen) is a 3.3 Kb plasmid with multiple cloning sites within the *lacZ* gene). Downstream of the cloning site is *ccdB* a gene encoding a lethal protein that acts by inhibiting the action of topoisomerase II. Cloning into the multiple cloning sites disrupts *ccdB* expression so only recombinants grow. The plasmid also contains the kanamycin resistance gene.

pET21b (Novagen) is a 5.4 Kb plasmid with multiple cloning sites. The vector contains a T7 promoter, expression of which is under the control of the Lac operator

(*lacI*) which allows for isopropylthio- β -D-galactosidase (IPTG) inducible expression. The plasmid also contains 6 repeats of the CAC codon, which codes for histidine, downstream of the insert site. This hexahistidine tag is attached to the C-terminus of the recombinant protein and allows for easier protein purification. The vector also contains an ampicillin resistance gene

pHANNIBAL is a 5.8 Kb binary vector which contains two cloning sites separated by an intron sequence. This vector has the CaMV 35S promoter and OCS terminator as well as ampicillin resistance.

pPF408 is an ~11.5 Kb binary plasmid which contains the meiosis specific plant DMC1-promotor (Kilmyuk and Jones, 1997). This construct also contains chloramphenicol and BASTA resistance cassettes.

2.4.5 Ligation into pZErO cloning vector

Ligations were carried out at 14 °C for no longer than 1 hour, as recommended for pZErO (Invitrogen). A molecular ratio of 10:1 insert: vector was used for each ligation.

Molecular ratios were calculated as follows:

$$X \text{ ng insert} = (10)(\text{bp insert})(6 \text{ ng linearized pZErO-2}) / 3297 \text{ bp pZErO-2}$$

'No insert', 'no vector' and ligase controls were also included. Reaction volumes were used according to manufactures guidelines.

2.4.6 Ligation into pET-21b, pHANNIBAL and pPF404

Ligations of insert into vectors were performed over night at 14 °C. A molecular ratio of 3:1 insert: vector was used and made up to 15 µl in Biological performance certified (BPC) water. 3 µl of 5x ligation buffer and 0.5 µl T4 ligase (Invitrogen) were added to each reaction.

2.4.7 Preparation of competent *E. coli* cells

To make competent cells the required *E. coli* strain (DH5α) was streaked on a Lysogeny broth (LB) agar plate (see appendix for recipe) from a glycerol stock and incubated overnight at 37 °C. The following day 5 ml of LB was inoculated with a single colony and grown for ~16 hours at 37 °C shaking at 200-225 rpm. 100 ml of LB in a 2 litre flask was then inoculated with 200 µl of culture and grown under the same conditions until the optimal density at OD₅₅₀ was between 0.3-0.4. Flasks were cooled on ice for 10 minutes then transferred to pre-cooled 250 ml buckets and centrifuged for 5 minutes at 3000 rpm at 4 °C (SORVALL® RC26). As much supernatant as possible was discarded by pipetting. Cells were then re-suspended by swirling in 20 ml of ice-cold TFB1 (30 mM potassium acetate, 100 mM rubidium chloride, 10 mM calcium chloride, 50 mM magnesium chloride, 15% (v/v) glycerol pH 5.8 filter sterilised). Cells were left on ice for 2 hours then centrifuged for 5 minutes at 2000 rpm at 4 °C and the supernatant carefully removed with a pipette. The cells were then re-suspended in 4 ml ice-cold TFBII (10 mM MOPS, 75 mM calcium chloride, 10 mM rubidium chloride, 15% (v/v) glycerol, pH 6.5, filter sterilised) by swirling. Cells were left overnight on ice at 4 °C and then aliquoted (40-50 µl) with a

sterile cut blue tip into microcentrifuge tubes, snap frozen in liquid nitrogen and stored at -80 °C.

2.4.8 Transformation of *E. coli* competent cells by heat-shock

4-6 µl of ligation reaction was added to 50 µl of chemically competent DH5α (*E. coli* DH5α: supE44ΔlacU169(φ80LacZΔM15)hsdR17 RecA1 gyrA96 thi-1 recA1) or BL21 (DE3) (F⁻ ompT gal dcm lon hsdS_B(r_B⁻ m_B⁻) λ(DE3 [lacI lacUV5-T7 gene 1 ind1 sam7 nin5]) cells and incubated for 30 minutes on ice. Cells were then heat shocked at 42 °C for 45 seconds and incubated on ice for a further 5 minutes. 500 µl of LB were added to the cells which were then transferred to 15 ml tubes using sterile pipettes with cut tips. The cells were incubated at 37 °C shaking at 200 rpm, for 40-45 minutes. Cells were plated on agar plates containing the specific antibiotic required for selection. For blue/white selection, 40 µl of 40 mgml⁻¹ 5-bromo-4-chloro-3-indolyl-β-D-galactosidase (X-gal) was added to plates. Plates were incubated at 37 °C overnight.

2.4.9 Production of electro-competent *A. tumefaciens* cells

A 5 µl culture of *Agrobacterium* was grown for 48 hours at 28 °C in LB containing rifampicin. This was then used to inoculate a fresh 200 ml of LB plus rifampicin. This culture was grown until it reached an OD₆₀₀ of 0.5-0.8 (typically overnight). Cells were then cooled on ice and harvested by centrifugation at 500 rpm for 5 minutes at 4 °C. The cell pellet was then washed once with each of 1.0, 0.5, 0.2 and 0.02 culture volumes of 10% glycerol by repeated resuspension and centrifugation of cells. Cells

were then aliquoted into 100 μ l aliquots, snap frozen in liquid nitrogen and stored at -80 °C.

2.4.10 Transformation of electro-competent *A. tumefaciens* cells

A 100 μ l aliquot of electro-competent *A. tumefaciens* GV3101 cells was thawed on ice. To this the pPF408 plasmid (either with or without an inverted repeat insert) was added and the cells were left on ice for 20 minutes. The cells were then transferred to a 0.2 cm electroporation cuvette (BioRad) and electroporated using a BioRad micropulser set to EC2 (2.5 KV, 5-6 ms). After electroporation 1 ml of LB was added to the cuvette containing the cells and this was incubated at 28 °C for 3-4 hours rotating at 200 rpm. Aliquots of cells were then plated onto LB agar supplemented with rifampicin and chloramphenicol and grown for 2-3 days at 28 °C.

2.4.11 Bacterial Growth media

All media was prepared in distilled water and sterilised by autoclave at 15 psi and 121 °C for 20 minutes. See appendix for LB medium and LB agar recipes. Liquid cultures were grown for ~16h at 37 °C on a rotary shaker at ~200 rpm. Agar plates were poured to a depth of ~2.5 mm and stored at 4 °C inverted. Inoculations of liquid culture and agar plates were carried out under aseptic conditions.

For selective media ampicillin was used at a final concentration of 100 μ gml⁻¹; kanamycin at a final concentration of 50 μ gml⁻¹ and chloramphenicol at a final concentration of 12.5 μ gml⁻¹ for *E. coli* and 100 μ gml⁻¹ for *A. tumefaciens*.

2.4.12 Colony PCR

Colonies were tested for the presence of an insert by colony PCR using one primer specific to the construct and one primer specific to the insert. Colonies were tapped with a sterile stick and again on to an agar plate with antibiotic. Sticks were then mixed in the PCR reaction mixture. PCR was performed as in 2.4.7.

2.4.13 Purification of plasmid DNA

Plasmid DNA was purified from bacterial cultures using Wizard plus SV Minipreps DNA purification system (Promega). Purification was carried out using manufacturer's guidelines for the Microcentrifuge protocol. Briefly, bacteria cells are split, treated with protease and spun-down to remove cell debris. This solution containing the plasmid DNA is then passed through a spin column to which the plasmid DNA is trapped in the presence of high salt. The column is then washed with ethanol and eluted in BPC water.

2.4.14 Sequencing of plasmid DNA

Sequencing was carried out by the Functional Genomics Laboratory in the University of Birmingham. Typically 4 µl Primer (0.8 µM), 200-600 ng of DNA (purified using the Wizard prep kit) was used and made up to a 10 µl volume with Biological BPC grade water (Sigma).

2.4.15 Sequence analysis

The sequence obtained was analysed using Chromas software. Homology searches were undertaken using the website provided by the National Centre for Biotechnology Information at www.ncbi.nlm.nih.gov using the Entrez and BLAST functions of the site. Reverse complementation was carried out using www.bioinformatics.org/sms/rev_comp.html. *In silico* translation of DNA into protein sequence was carried out using ExPASy translation tool: www.web.expasy.org/translate.

2.4.16 Restriction digests

Digests were carried out in appropriate buffers supplied with the enzymes. Digestions were carried out at 37 °C from 1 hour to overnight. Restriction enzymes were removed by heat denaturation (incubating reaction at 65 °C for 30 minutes), phenol/chloroform extraction or using QIAquick PCR purification Kit (Qiagen). Restriction enzymes were obtained from New England Biolabs, or Fermentas.

2.4.17 Phenol chloroform extraction

Digested samples were made to a volume of 50 µl with BPC grade water. 50 µl of Phenol was added, solution mixed thoroughly and centrifuged for 2-3 minutes at high speed. The top layer was removed with a pipette in to a clean tube to which 50 µl Phenol: chloroform (1:1) was added, mixed and centrifuged for 2-3 minutes. The top layer was again taken into a new tube and 50 µl of chloroform was added and the solution mixed and centrifuges for 2-3 minutes. The top layer was taken and washed

twice with ether, centrifuging and removing bottom layer into a clean tube. 100 μ l of 100% ethanol and 1 μ l glycogen were then added and reaction incubated at -20 for 30-60 minutes. The solution was centrifuged for 10 minutes at 4 °C and the supernatant removed. The pellet was then washed with two times the volume of 70% ethanol and centrifuged for 5 minutes. The supernatant was removed and the pellet resuspended in 20-100 μ l BPC grade water (Sigma) depending on the downstream applications of the product.

2.5 Protein manipulations

2.5.1 Induction of recombinant protein from *E. coli* cells

Cultures of BL21 *E. coli* containing the pET-21b vector with the desired insert and selective antibiotic were grown in 500 ml conical flasks on an orbital shaker at 200-225 rpm at 37 °C for 17 hours. Two lots of 5 ml of culture were then transferred to two 50 ml volumes of L-broth containing antibiotic. Cultures were incubated at 37 °C shaking at 200-225 rpm for 3 hours. The optimal density at was checked to ensure it was between 0.6-1.0. IPTG (final concentration 1 mM) was added to one of the two 50 ml cultures and the cultures were incubated for a further 4 hours. Cultures harvested in various aliquots by centrifugation.

2.5.2 Recombinant protein extraction from bacteria cells

All volumes stated are applicable for the extraction of protein from a pellet from 1 ml of bacterial culture. Larger extractions were carried out by scaling up these volumes. Bacterial pellets were resuspended in 75 μ l BugBuster Master Mix (Novagen) and

incubated for 30 minutes at room temperature on a rotor. Solutions were then centrifuged for 10 minutes at high speed. The soluble supernatant was transferred into a new tube and stored on ice. The insoluble pellet was resuspended 75 μ l of Biological performance certified (BPC) grade water (Sigma) by pipetting. 5x final suspension buffer was added to each sample and samples were boiled in a water bath for 5-10 minutes. After boiling samples were loaded on to an SDS-page protein gel.

2.5.3 SDS-PAGE gel electrophoresis

Proteins were analysed on sodium-dodecyl-sulfate polyacrylamide (SDS-PAGE) protein gels using the BioRad 3rd generation self-assembly kit. The resolving gels were made first, the percentage of which depended on the size of the protein to be resolved (Table 3). Typically for full length *AtSMC4* ~150 kDa protein was resolved on a 10% gel and the ~ 30 and ~ 27 kDa recombinant protein were resolved on 15% gels. Approximately 7 ml of resolving gel was poured in-between the glass plates immediately after the addition of TEMED to the gel solution. A layer of butanol was then added to remove air-bubbles and the gel was left to set. The butanol was then washed off and approximately 2.5 ml of stacking buffer added. A gel comb was placed in the stacking buffer and the gel left to set. The gel tank was assembled as described in the manufacturer's instructions. Protein to be loaded on the gels was mixed with 5X protein loading buffer and boiled for 10 minutes prior to loading. Sea Blue (Invitrogen), PageRuler and PageRuler Plus (Fermentas) protein weight markers were used to assess the size of the proteins on the gel. Gels were run in 1 x

ELFO buffer at 80 V to allow proteins to enter the gel, and 150 V subsequent to this until the dye front had reached the bottom of the gel.

	Resolving gel		Stacking gel
	10%	15%	-
SDW	6.1 ml	3.6 ml	3.0 ml
Resolving buffer (1.5 M tris, pH 8.8)	3.75 ml	3.75 ml	
Stacking buffer (1.0 M Tris, pH 6.6)			1.25 ml
Acrylamide (Protogel)	5.0 ml	7.5 ml	625 μ l
10% (w/v) Sodium dodecyl sulphate (SDS)	150 μ l	150 μ l	50 μ l
15% (w/v) APS	75 μ l	75 μ l	25 μ l
TEMED (Sigma)	15 μ l	15 μ l	5 μ l
Final volume	15 ml	15 ml	5 ml

Table 3: Solutions, concentrations and volumes required for SDS-PAGE electrophoresis. Amounts of each solution for 10% and 15% SDS-PAGE resolving gels and stacking gels are shown.

2.5.4 Coomassie staining

Gels were stained for 1 hour in Coomassie blue stain (0.1% Coomassie R250, 45% methanol, 45% Glacial Acetic acid, 9.9% MilliQ water). Gels were then de-stained with 20% methanol and 7% acetic acid de-staining solution until products were visible. Gels were dried between cellophane sheets.

2.5.5 Isolation of HIS-tagged proteins using Ni-NTA resin (QIAGEN)

Pellets of 10 ml or 50 ml colonies were resuspended in 600 μ l or 1500 μ l respectively of lysis buffer (50 mM Tris, 300 mM NaCl pH 8). The solution was transferred to a new 2 ml tube and lysozyme at 1.0-1.5 mgml⁻¹ final solution was added. Samples were thoroughly mixed and placed on ice. After 30 minutes samples were sonicated 6 times at 10,000 amplitude for 10 seconds, cooling on ice between each sonication. Samples were centrifuged for 10-15 minutes at full speed and the supernatant

transferred to a new tube and this step repeated. Ni-NTA agarose beads were prepared by centrifuging for one minute at full speed, removing supernatant and replacing with an equal volume of lysis buffer. Beads were added to the sample and incubated at 4 °C on a rotor for 2 hours. Samples were then centrifuged for 2 minutes and the supernatant transferred to a new tube, being carefully not to disturb the beads. 500- 1000 µl of 0 mM imidazole solution (200 µl lysis buffer/ml SDW) was added and the beads incubated on a rotor for 5-15 minutes at 4 °C. Samples were then centrifuged for 2 minutes and supernatant transferred to a new tube. This wash was repeated twice followed by a wash with 50 mM imidazole solution (100 mM, 150 mM, and 200 mM imidazole concentrations were also used when required). Samples were eluted in 2X 50-200 µl 250 mM imidazole and incubated on a rotor at 4 °C for 15 minutes then centrifuged for 2 minutes to separate beads and supernatant. When all samples were collected they were centrifuged for 1 minute at full speed and the supernatant transferred to a new tube. This step removes any Ni-NTA residue which may have been transferred with the washes.

2.5.6 Dialysis of purified recombinant proteins

Protein was dialysed in dialysis membrane suitable for 12 to 14000 Dalton proteins (Medicell International Ltd). Approximately 6 inches of tube was used/ ml of protein solution. 1 L of pre-cooled buffer was used for 1 ml of protein. Protein was first dialyzed against 50 mM tris and 300 mM NaCl solution for 4 hours at 4 °C. The buffer was then changed to 50 mM tris and 100 mM NaCl and left at 4 °C overnight. Protein was removed from tubing by pipetting. Recovered protein was then centrifuged for 1 minute and the supernatant transferred to a fresh tube.

2.5.7 Protein quantification

Proteins were quantified using BIO-RAD Protein Assay and a Jenway 6305 UV/Vis spectrophotometer at 595 nm. Samples were compared to a known concentration of BSA (NEB).

2.5.8 Protein extraction from plant material:

2.5.8.1 Large-scale extraction protocol

Plant tissue (approximately 500 μ l) was collected and frozen in liquid nitrogen. Plant tissues were then ground up using a sterile plastic rod and frozen in liquid nitrogen if the sample started to thaw. 500 μ l of IP- buffer (20 mM Tris-HCL, pH 7.7, 150 mM NaCl, 10 % glycerol, 2 mM EDTA) plus protease inhibitor (Complete mini EDTA-free tablets; Roche) was added to each sample and the tissue ground further. Samples were then vortexed for a few seconds and spun for 10 minutes at 4 °C. The supernatant was removed being careful not to disturb the pellet and either used immediately or snap frozen in liquid nitrogen and stored at -20 °C.

2.5.8.2 Protein extraction from anthers

Anthers were collected into IP-buffer containing protease inhibitor (Complete mini EDTA-free tablets; Roche) and snap-frozen in liquid nitrogen. Samples were then frozen at -20 °C and thawed 2-3 times and ground with a pipette tip to help break up tissues. 5 x final suspension buffer (FSB) was added to each sample and the sample was boiled for 10 minutes before loading on to an SDS-PAGE gel.

2.5.9 Western transfer analysis

An SDS-PAGE gel with the desired protein was run as previously described and transferred to Hybond-C Extra membrane (Amersham Biosciences) using a BioRad western transfer kit following manufacture guidelines for assembling the apparatus. Transfers were run in 1x transfer buffer (14.4 g Glycine; 3.03 g Tris; 200 ml methanol in one litre MiliQ water). An ice pack was added to the apparatus to help prevent the transfer buffer from getting too hot. BioRad power packs were used to transfer the protein: 400 mA for 1 hour. After transfer membranes were blocked in milk block (5% milk, 0.1% Tween in 1X TBS) shaking over night at 4 °C.

2.5.10 Antibody labelling

After blocking the western membrane in milk block overnight the membranes were incubated with the primary antibody for 2 hours at room temperature. The primary antibody was at a titre of 1:1000 in milk block. The membranes were then washed 3 times in 10 ml of milk block for 10 minutes. A secondary antibody, either alkaline phosphatase (AP) or horse radish peroxidase (HRP) was then added (1:5000 in milk block) after which a 10 minute wash in milk block was carried out followed by 3 x 10 minute washes in 1X TBS.

2.5.10.1 Alkaline phosphatase detection

Membranes were then incubated in Alkaline phosphatase detection buffer (100 mM NaCl, 5 mM MgCl₂ and 100 mM Tris) with 66 µl 0.5% X- Phos(BCIP) Disodium

(Melford) and 33 μ l 0.5% NBT Nitro blue tetrazolium (Melford). The reaction was left to develop in the dark and stopped by adding 1 x TBS.

2.5.10.2 Enhanced chemiluminescence (ECL) detection

The membrane was treated with ECL reagents A and B according to manufacturer's guidelines (GE Healthcare). Blots were exposed to photographic film (Amersham Hyperfilm ECL: GE Healthcare) using an AGFA CURIX 60 Xograph.

2.5.11 Affinity purification of antibody

Approximately 0.4 mg of *AtSMC4* recombinant protein was loaded into a 12.5% SDS-PAGE gel and run as previously stated. The protein was transferred to PVDF membrane (Hybond-P Amersham) by western blot, as previously stated and stained with Ponceau stain to label to protein. The band corresponding to the *AtSMC4* recombinant protein was cut out incubated in block (10 mM Tris-HCl, 150 mM NaCl pH 7.4, 0.1% Tween, and 5% milk) for 2 times 30 minutes at room temperature. The block was then removed and the strip was incubated with 1 ml antiserum diluted 1:1 in milk block overnight at 4 °C gently rotating. The serum was then removed and the strips washed 4x 5 minutes (1 x TBS, 0.1% TWEEN 20). To elute the bound antiserum the strips were incubated with (50 mM Glycine, 150 mM NaCl, 100 μ gml⁻¹ BSA pH 2.4) for 30 seconds, the eluate was then transferred to a tube containing 1.5 M Tris base in order to restore the antiserum solution to ~pH 8. Elution was repeated 3 times. The purified antiserum then only contains antibodies to the protein of

interest, removing all background proteins. This was then aliquoted and stored at -20 °C.

2.5.12 Purification of antibody using Immobilized *E. coli* Lysate Kit (Thermo scientific)

1 ml of final bleed *AtSMC4* antibody, animal 3107 was cleaned using the Immobilized *E. coli* Lysate Kit (Thermo scientific) using the manufactures guidelines.

2.5.13 Plant transformation

Agrobacterium tumefaciens (GV3101) containing the binary plasmid pPF408 was introduced into wild-type *Arabidopsis* plants by the floral dip method. *A. tumefaciens* cultures were grown overnight at 28 °C and 200 rpm in media containing 100 µgml⁻¹ chloramphenicol and 50 µgml⁻¹ rifampicin. 125 µl of culture was then re-cultured into 500 ml LB and grown to an OD₆₀₀ of 1.5-2.0. Cultures were spun down for 10 minutes at 3000 rpm. The LB was then removed and the pellet re-suspended in with 5% sucrose medium to make a final OD₆₀₀ of ~ 0.8. Silwet (50 µlml⁻¹ of bacteria/sucrose solution) was added to and plants dipped in the solution for 2-5 seconds whilst gently agitating. After dipping plants were grown for 24 hours covered in cling-film to retain moisture and placed under the bench away from direct light. Plants were left to grow to maturity and seeds were collected. Seeds from these plants were then grown under selection conditions either on BASTA containing MS plates (25 µgml⁻¹) or by spraying with BASTA (DL-Phosphinothricin) (Duchefa Biochemie) 3 times at 8–10 day intervals. PCR was performed on the selected plants

for presence of the construct with primers pHanF (5_-TCCCAACTGTAATCAATCC-3_) and pHanR (5_-GACAAGTGATGTGTAAGACG-3_).

2.6 Statistical procedures

Statistical procedures were carried out using Microsoft Office Excel software.

2.7 List of websites:

ExpASY bioinformatics resource portal: <http://www.expasy.org/>

Eurofins MWG: <http://www.eurofinsdna.com/products-services/oligonucleotides0.html>

NCBI: <http://www.ncbi.nlm.nih.gov/guide/>

NCBI, BLAST: <http://blast.ncbi.nlm.nih.gov/Blast.cgi>

NASC: <http://arabidopsis.info/>

SALK institute T-DNA express: <http://signal.salk.edu/cgi-bin/tdnaexpress>

Sequence alignment: <http://www.ebi.ac.uk/Tools/msa/clustalw2/>

Tm calculator: <http://www6.appliedbiosystems.com/support/techtools/calc/>

CHAPTER 3

3 PRODUCTION AND ANALYSIS OF AN ANTI-ATSMC4 ANTIBODY

3.1 INTRODUCTION

Investigating the localisation of a protein *in vivo* can provide valuable insight into its function. Condensin is a structural organiser of chromosomes important in both mitotic and meiotic cell divisions. There are two condensin complexes present in higher eucaryotes, condensin I and condensin II. Both condensin complexes are thought to contain the same SMC backbone, consisting of SMC2 and SMC4 proteins and are distinguished by their regulatory non-SMC subunits.

During a mitotic cell division condensin localises to the chromosome axis in many species where it is thought to form a structural component of the chromosomes (Hirano and Mitchison, 1994; Steen *et al.*, 2000; Steffensen *et al.*, 2001; Beenders *et al.*, 2003; Savvidou *et al.*, 2005). Condensin is also seen to accumulate at certain chromosome locations. In budding yeast condensin is concentrated at rDNA throughout mitosis, becoming further enriched onto the rDNA at the start of anaphase where it has a role in the organisation and segregation of the rDNA (Freeman *et al.*, 2000; Bhalla *et al.*, 2002; Yu and Koshland, 2003; Sullivan *et al.*, 2004; Yu and Koshland, 2005). A specific rDNA localisation has not been observed in other species, however condensin does localise to the nucleolus in human (Cabello *et al.*, 1999, 2001) and *Arabidopsis* (Fijimoto *et al.*, 2005), suggesting a possible rDNA role. Condensin complexes are also enriched at the centromeres in *C. elegans* (Hagstrom

et al., 2002; Chan *et al.*, 2004), *Xenopus* (Hirano and Mitchison 1994), human (Schmiesing *et al.*, 1998; Gerlich *et al.*, 2006), *Drosophila* (Steffensen *et al.*, 2001; Savvidou *et al.*, 2005), and *S. cerevisiae* (Bachelier-Bassi *et al.*, 2008), where they play a role in centromere organisation.

The localisation of condensin during meiosis has also been investigated in a few species. In budding yeast, Ycs4 co-localises with the SC TF protein Zip1 and is involved in the polymerisation of the SC (Yu and Koshland, 2005). In *C. elegans* the condensin SMC subunits SMC-4 and MIX-1 localised with centromere proteins at metaphase I and II (Hagstrom *et al.*, 2002). The condensin II specific subunit, HCP-6 was first detected after pachytene where it partially localised with DNA. At diplotene and diakinesis HCP-6 fully localised to the chromatin and persisted on the chromatin throughout meiosis (Chan *et al.*, 2004). In mouse all condensin I subunits localised to chromosomes in prometaphase as axial structures and accumulated at the telomeres and kinetochores (Viera *et al.*, 2007).

In plants the localisation of condensin has only been briefly investigated. The localisation of *Arabidopsis* AtCAP-H and AtCAP-H2 has been observed in tobacco mitotically dividing cells. In this experiment GFP tagged AtCAP-H and AtCAP-H2 were transformed into tobacco transgenic cell suspension cultures (Fujimoto *et al.*, 2005). Both proteins localised to mitotic chromosomes from prometaphase until telophase. During interphase AtCAP-H was located in the cytoplasm whereas AtCAP-H2 was seen in the nucleolus (Fujimoto *et al.*, 2005). The localisation of

condensin has not been investigated in *Arabidopsis* cells, and in particular the localisation of any condensin subunits during meiosis has not been investigated in any plant species to date. This chapter describes the production of a recombinant protein corresponding to part of the C-terminus of AtSMC4 which was used to raise an antibody specific to AtSMC4 as well as subsequent analysis of antiserum by immunolocalisation and western blot analysis. Immunolocalisation analysis allows insight into the role of AtSMC4, and therefore both condensin I and condensin II complexes, during meiosis based on the distribution of the protein within the cell.

3.2 RESULTS

3.2.1 Cloning AtSMC4 C-terminus for antibody production

To make an AtSMC4 specific antibody a 241 amino acid sequence at the C-terminus of AtSMC4 corresponding to residues 780 and 1021 was chosen for recombinant protein production. This sequence was selected due to its low level of homology to other SMC proteins. Figure 3.1 shows an alignment of the C-terminal amino acid sequence of all 6 SMC proteins in *Arabidopsis* using ClustalW2. The region used to make the AtSMC4 antibody is highlighted. A construct containing the desired AtSMC4 recombinant protein sequence was designed and cloned by a previous member of the group; however sequence analysis revealed that this construct contained a single base mutation which resulted in the sequence being out of frame. Due to this, a primer (SMC4Ab-g_F) was designed in order to remove the error. The correct sequence was amplified from the original vector using SMC4Ab-g_F in conjunction with the original SMC4Ab_R primer. This fragment was cloned into pET21b (Invitrogen). NheI and NotI restriction sites were incorporated into the forward and reverse primers respectively to allow cloning into pET21b. pET21b contains a 6-residue histidine tag downstream of the insert. The HIS-tag is attached to the N-terminus of the expressed recombinant protein and allows for efficient protein purification. To confirm that no sequence errors had occurred during cloning and that the original error was removed, the construct was sequenced. The sequence was translated *in silico* using the ExPASy translation tool. This confirmed that the construct would produce the correct AtSMC4 C-terminal polypeptide in-frame with the HIS-Tag attached.

```

SMC2-1      AQLLELKMYDMSLFLKRAEQNEH--HKLGDVAVKKLEEEVEEMRS--QIKE--KEGLYKSCA 765
SMC2-2      AQLLELKTYDLSLFLKRAEQNEH--HKLGEAVKKLEEELEEAKS--QIKE--KELAYKNCF 768
SMC3        QRLEADWTLCKLQVEQLKQEIANANKQKHAIHKAIEYKEKLLG--DIRTR-IDQVRSSMS 765
SMC1        KKIQYAEIEKKS IKDKLPQLEQEERN IEEIDRIKPELSKAIA--RTEVDKRKTEMNKLE 792
SMC4        RAAENEVSGLEMELAKSQREIESLNSEHNYLEKQLASLEAASQPKTDEIDRLKELKKIIS 809
SMC6        ASFDDQIKDLEIEASREQSEIQECRGQKREAEMNLEGLESTMRRLLKQRTQLEKDLTRKE 694
SMC5        ASVDSVYQSRLLLCGVDVGELEKLRSRKEELEDSEILFMEETHKSLQTEQRRLEEEAAKLH 659
          :
SMC2-1      DTVSTLEKSIKDHDKNREG-RLKDLEKNIKT LKARIQASSKDLKGHENVRERLVMEQEAV 824
SMC2-2      DAVSKLENSIKDHDKNREG-RLKDLEKNIKT IKAQMQAASKDLKSHENEKEKLVMEEEAM 827
SMC3        MKEAEMGTELVDHLTPPEEREQLSKLNPEIKDLKEKKFAYQADRIERETRAELEANIATN 825
SMC1        KRMNEIVDRIYKDFSQSVGVPNIRVYEETQLKTAEKEAEERLELSNQLAKLKYQLEYEQN 852
SMC4        KEEKEIENLEKGSKQLKDKLQTNIENAGGEKLGQKAKVEKIQT D I D K N N T E I N R C N V Q I 869
SMC6        LEMQDLKNSVASETKASPTSSVNLHLEIMKFQKEIEEK----- 733
SMC5        KEREIVNVSYLEKKKRRELESRYQQRKTKLESLEQEED----- 698
          :
SMC2-1      T---QEQSYLKSQLTSLRTQISTLASDVGNQRAKVD AI QKDHDQSLSELKLIHAKMKECD 881
SMC2-2      K---QEQSLESHTSLETQISTLTSEVDEQRAKVDALQKIHD ESLAEKLIHAKMKECD 884
SMC3        ----LKRRI TELQATIASIDDDSLPSSAGTKEQELDDAKLSVNEAAKELKSVCD S IDEKT 881
SMC1        RDVGSRI R K I E S S I S S L E T D L E G I Q K T M S E R K E T A V K I T N E I N N W K K E M E E C K Q K S E E Y E 912
SMC4        ETNQKLIK K L T K G I E E A T R E K E R L E G E K E N L H V T F K D I T Q K A F E I Q E T Y K K T Q Q L I D E H K 929
SMC6        -----ESLLEK L Q D S L K E A E L K A N E L K A S Y E N L Y E S A K G E I E A L E K A E D E L K E K E 783
SMC5        -----MDASVAKLIDQASRANADRYTYAINLKKLLVEAVAHKWSYAEKHMASIELE 749
          :
SMC2-1      TQISGSIAEQEKCLQKISDMKLD R K K L E N E V T R M E M E H K N C S V K V D K L V E K H T W I T S E K R 941
SMC2-2      TQISGFVTDQEKCLQKLSDMKLERK K L E N E V V R M E T D H K D C S V K V D K L V E K H T W I A S E K Q 944
SMC3        KQIKKIKDEKAKLKTLEDDCKGTLQDLDKKLEELFSLRNTLLAKQDEYTKKIRGLP--- 938
SMC1        KEILDWKKQASQATTSITKLN R Q I H S K E T Q I E Q L I S Q K Q E I T E K C E L E H I T L P V L S D A M E 972
SMC4        D V L T G A K S D Y E N L K K S V D E L K A S R V D A E F K V Q D M K K K Y N E L E M R E K G Y K K K L N D L Q I A F T 989
SMC6        DELHSAETEKNHYEDIMKDKVLP-----EIKQAETIYKELEMKRQESNKKASIIICPESE 837
SMC5        RKIRESEINIKQYEKTAQQLSLAVEYCKKEVEGKQQR----LATAKRDAESVATITPELK 805
          :
SMC2-1      LFGNGGTDYDFESR-----DPHKAREELERLQTDQSS-----LEKRVNKKVTAMFEK 988
SMC2-2      LFGKGGTDYDFESC-----DPYVAREKLEKLQSDQSG-----LEKRVNKKVMAMFEK 991
SMC3        ---LSSDAFDTYKR-----KNIKELQKMLHRCSEQLQ-----QFSHVNKKALDQYVN 982
SMC1        EDDSDGPQDFDFSELGRAYLQERRPSAREKVEAEFRQKIESKTSEIERTAPNLRALDQYEA 1032
SMC4        KHMEQIQKDLVDPDKLQATLMDNNLN E A C D L K R A L E M V A L L E A Q L K E L N P N L D S I A E Y R S 1049
SMC6        IKALGPWDG-----PTPLQLSAQINKINHRLK-----RENENYSESIDDLRI 879
SMC5        KEFMEMPTT-----VEELEAAIQDNLSQAN-----SILFINENILQEYEH 845

```

Figure 3.1: ClustaW2 alignment of the C-terminus of *Arabidopsis* SMC proteins 1-6. The region highlighted in red was used for recombinant protein production *= identical residues, :=highly similar residues, .= similar residues

3.2.2 Production of AtSMC4 C-terminal recombinant protein

The pET21b vector containing the AtSMC4 fragment was transformed into *E. coli* expression cells, BL21 DE3. The expression of the protein was assayed in a test-induction experiment. Expression of the recombinant protein was induced with non-metabolisable Isopropyl β -D-1-thiogalactopyranoside (IPTG). The soluble protein fraction was extracted from induced and un-induced cultures and resolved on a 15% SDS-PAGE denaturing gel. Non-recombinant pET21b was used as a control. The SDS-PAGE gel was stained with Coomassie blue (R-250) to visualise the protein. A strong band of protein was present in the induced colonies and absent from the un-induced. This band migrated at around 36 KDa, close to the predicted size of the AtSMC4 C-terminal protein (30 KDa) (Figure 3.2).

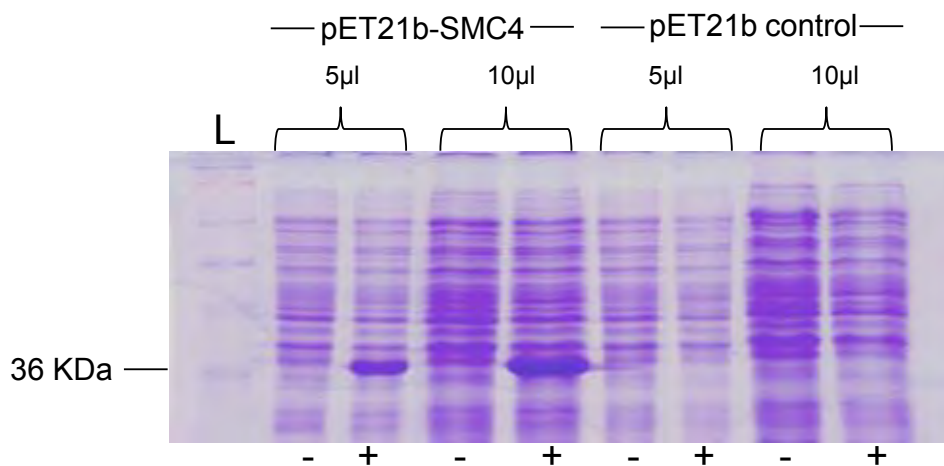


Figure 3.2: Expression of SMC4 C-terminal recombinant protein. Uninduced (-) and induced (+) extracts are shown. Non-recombinant pET21b was used as a control. 5 µl and 10 µl of each sample was loaded. A band at 36 kDa can be seen, which is close to the predicted size of the SMC4 C-terminal recombinant protein. L= SeeBlue plus 2 protein ladder (Invitrogen).

3.2.3 Determining the cellular localisation of the expressed AtSMC4 recombinant protein

Once it had been established that the *AtSMC4* C-terminal recombinant protein was expressed at a level detectable by Coomassie staining, an experiment was carried out to determine if the recombinant protein was present within the bacteria predominantly in the soluble fraction of proteins or if it was present at higher levels within inclusion bodies. Soluble and insoluble fractions of IPTG-induced cultures were separated by centrifugation and extracts resolved on a 15% SDS-PAGE gel (Figure 3.3). Soluble and insoluble un-induced extracts were used as controls. The SDS-PAGE gel was stained with Coomassie blue which showed that the recombinant protein was expressed in the soluble fraction.

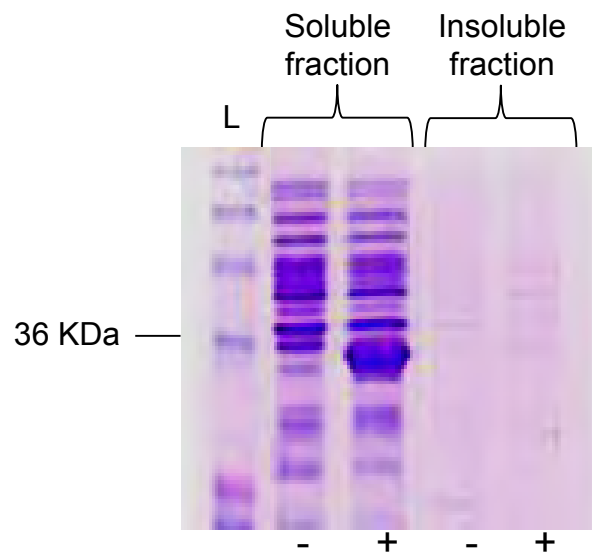


Figure 3.3: Soluble and insoluble fractions of cell extracts. Extracts from induced (+) and un-induced (-) cultures are shown. 5 μ l of each sample were loaded. L= SeeBlue plus 2 protein ladder (Invitrogen).

3.2.4 Large scale purification of AtSMC4 recombinant protein

AtSMC4 recombinant protein was purified using its C-terminal HIS-tag. Purification was carried out in order to minimise the presence of *E. coli* proteins in the sample before it was sent for antiserum production. A preliminary protein purification using Ni-NTA beads (Qiagen) was carried out on extracted protein. Ni-NTA beads bind to histidine with high affinity and are therefore able to selectively purify the hexahistamine tagged recombinant protein. The initial purification procedure confirmed the process was working efficiently.

Protein purification was then carried out on a large scale. Figure 3.4 shows protein extract before and after incubation with Ni-NTA beads. Some AtSMC4 recombinant protein remains in the sample after binding to the Ni-NTA beads was carried out; however a large proportion of the AtSMC4 recombinant protein has been successfully bound to the beads. The Ni-NTA beads with AtSMC4-recombinant protein bound were subjected to a series of washes with 50 mM imidazole in order to remove any non-target *E. coli* proteins which may have affinity for the beads. The target protein was eluted in 250 mM imidazole and quantified on a spectrophotometer using BioRad protein assay solution. A concentration of 1.8 $\mu\text{g}/\mu\text{l}$ was obtained from the purification procedure; this concentration was confirmed by Coomassie staining of an SDS-PAGE gel loaded with known concentrations of BSA (Figure 3.5). After purification on Ni-NTA agarose beads the protein was dialyzed to remove the imidazole. The concentration was compared pre- and post-dialysis to ensure no protein was lost during the process (Figure 3.6). The AtSMC4 recombinant

protein (2.88 mg, 1.6 ml) was sent to BIOGENES (Germany) for anti-serum production in two rabbits.

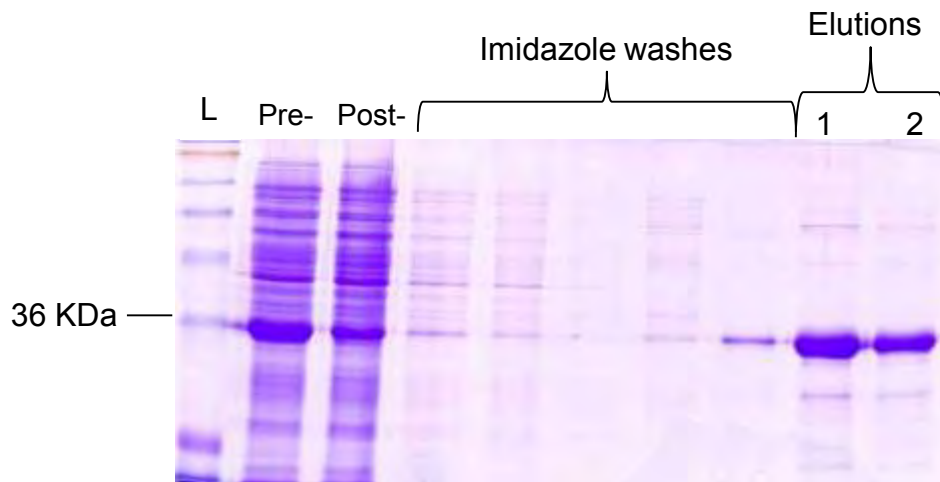


Figure 3.4: Purification of AtSMC4 recombinant protein using Ni-NTA beads. Pre = AtSMC4 recombinant protein sample before binding to the Ni-NTA beads. Post = AtSMC4 recombinant protein after binding to the Ni-NTA beads. A series of washes with imidazole (50 mM) were carried out in order to remove any non-target proteins bound to the beads. Imidazole (250 mM) was used to elute recombinant protein. The AtSMC4 recombinant protein was eluted from the beads twice. Un-purified and purified AtSMC4 recombinant protein can be seen as a band at approximately 36 KDa. L=SeeBlue Plus2 pre-stained protein ladder (Invitrogen).

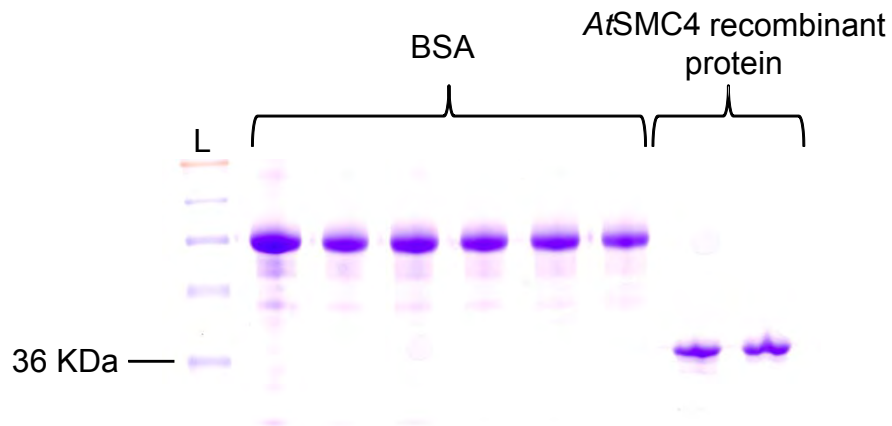


Figure 3.5: Confirming the concentration of *AtSMC4*-recombinant protein. BSA at varying concentrations (left to right: 10.0 μ g, 6.0 μ g, 5.5 μ g, 5.0 μ g, 4.5 μ g, 4.0 μ g) was loaded on an SDS-PAGE gel and compared to 2 x 5.4 μ g of *AtSMC4* recombinant protein. L=SeeBlue Plus2 pre-stained protein ladder (Invitrogen).

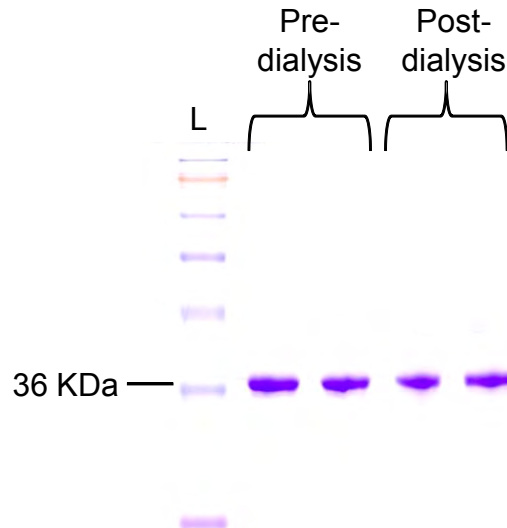


Figure 3.6: Concentration of *AtSMC4* recombinant protein pre- and post- dialysis. Each sample was loaded twice as a control against loading error. L=SeeBlue Plus2 pre-stained protein ladder (Invitrogen).

3.2.5 Testing the specificity of the AtSMC4 antibody

The specificity of the AtSMC4 test bleed antiserum was tested by western blot analysis. A range of different quantities of AtSMC4 recombinant protein were loaded on two replica SDS-PAGE gels. The protein was then transferred by western blot to a nitrocellulose membrane for antibody probing. AtSMC4 antiserum (1:1000) was used to probe one blot; pre-immune serum (1:1000) was used as a control. The presence of the AtSMC4 antibody was detected using an alkaline phosphatase conjugated secondary anti-rabbit antibody (1:5000). This analysis revealed that the AtSMC4 antiserum recognises the AtSMC4 recombinant protein at amounts as low as 10 ng (see Figure 3.7). This result was obtained after a 30 seconds exposure of the blot. The blot which was probed with the pre-immune serum did not detect the recombinant protein (Figure 3.7). Similar results were obtained with antiserum and pre-immune bleeds from both rabbits. The AtSMC4 antiserum recognises additional bands with lower intensity to the band corresponding to the AtSMC4 recombinant protein. Many of the bands with a lower molecular weight than the AtSMC4 recombinant protein may be break-down products of the AtSMC4 recombinant protein. The antiserum may also contain antibodies raised against contaminating *E. coli* proteins which were present in the protein sample sent for antiserum production.

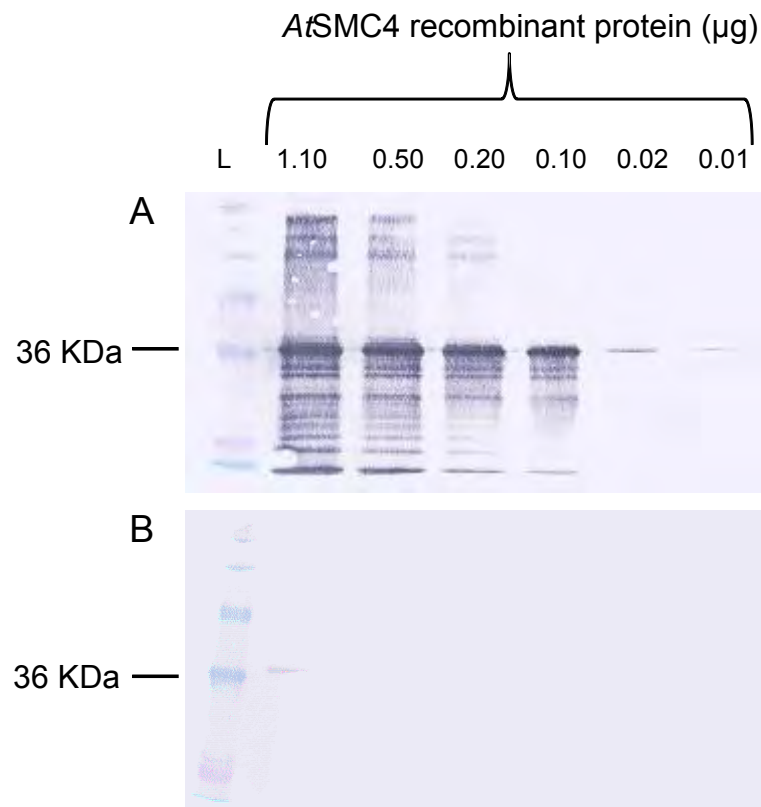


Figure 3.7: Western blot analysis of anti-*AtSMC4* specificity. Varying concentrations (1.1, 0.5, .02, 0.1, 0.02 and 0.01 µg) of *AtSMC4* recombinant protein were run on two replica SDS-PAGE gels and transferred to nitrocellulose membrane. **A** = Western blot probed with the *AtSMC4*-anti serum (1:1000), **B** = Western blot probed with the *AtSMC4*-pre-immune serum (1:1000). *AtSMC4*-Ab was detected with anti-rabbit alkaline phosphatase conjugated secondary antibody (1:5000). Blots exposed for ~30 seconds. L=SeeBlue Plus2 pre-stained protein ladder (Invitrogen).

3.2.6 Immunolocalisation of AtSMC4 on pollen mother cells (PMCs)

Western blot analysis revealed that the AtSMC4 antiserum successfully recognised the AtSMC4 recombinant protein. To investigate whether the antibody recognises AtSMC4 on wild-type chromosome spreads, immunolocalisation studies were carried out. Meiotic stage PMCs were immobilized on a slide and probed with either the anti-AtSMC4-Ab or the pre-immune serum as a control. Meocytes throughout prophase I were analysed in this assay. AtSMC4 antibody was detected on late prophase I cells and appeared to localise to the central region of the SC. However this signal was also detected in the pre-immune serum of rabbits, suggesting that it is a non-specific signal (Figure 3.8). The SC-associated signal of the pre-immune serum was a similar intensity as the signal from the AtSMC4 antibody. A variety of different modifications to the immunolocalisation procedure were tested with the hope of finding possible conditions in which the pre-immune serum gave no signal and the antibody did. Varying the antibody and pre-immune concentrations (from 1:100 to 1:5000), increased blocking times (10 minutes to overnight), varying the length of antibody incubation (1, 2, 4 and 6 nights) altering the temperature at which the antibody is incubated (4 °C and 37 °C) and modifications such as mechanical agitation during PBS washes and additional washes were all tried. No suitable modifications were found in which the antibody serum gave a signal which was not present in the pre-immune control.

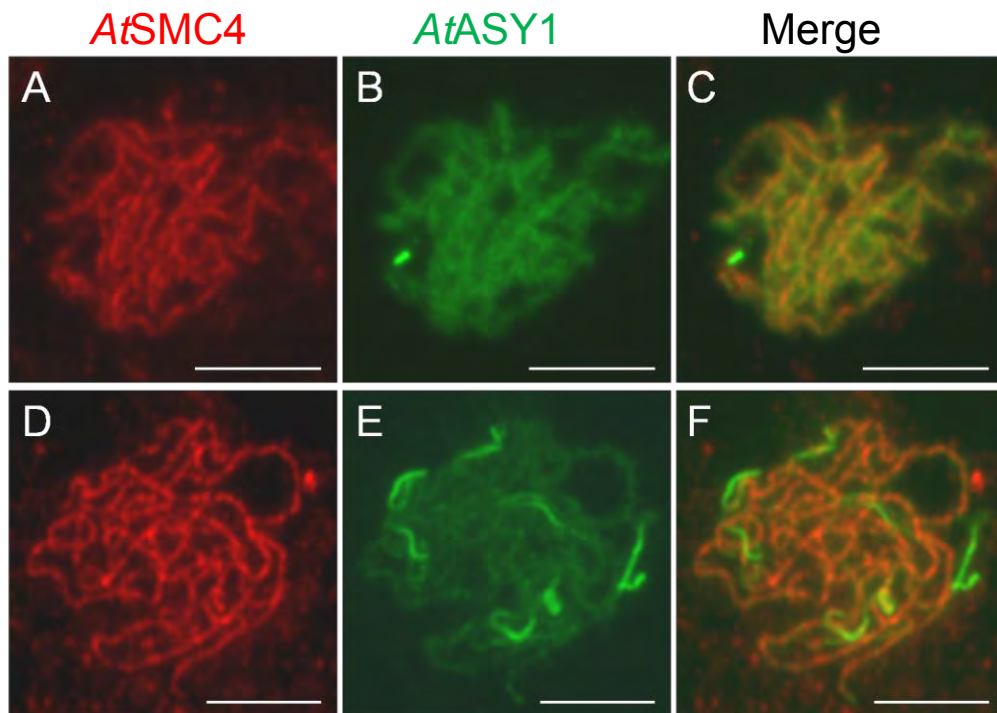


Figure 3.8: Immunolocalisation of *AtSMC4*-Ab on wild-type PMC. **A-C** = *AtSMC4*-Ab (first bleed) **D-F** = *AtSMC4* pre-immune serum. *AtSMC4*-Ab/pre-immune = red. *AtASY1* = green. Scale bar = 5 μ m.

3.2.7 Purification of AtSMC4-Ab

Due to the axis-associated pre-immune signal seen in immunolocalisation experiments the AtSMC4 antiserum was purified. Two antibody purification methods were tested. The first method involved antibody purification based on affinity of the AtSMC4 antibody for the recombinant protein. An SDS-PAGE protein gel was loaded with approximately 330 µg of AtSMC4 recombinant protein and transferred to a nitrocellulose membrane. The membrane containing the recombinant protein was then stained with Ponceau stain and the band corresponding to the recombinant protein was excised. This was then incubated overnight with the AtSMC4 antiserum. The following morning the non-bound serum was removed, the membrane washed and then the antibody bound to the recombinant protein eluted from the membrane. The elution (1:1000), along with the unpurified antibody (1:1000), was then tested by western blot analysis using AtSMC4 recombinant protein. Varying amounts of AtSMC4 recombinant protein were loaded in order to assess whether the titre of the antibody had reduced after the purification procedure. AtSMC4 antibody was detected using alkaline phosphatase secondary antibody (1:5000). Western blot analysis revealed that the purification of the antibody was not completely successful. Many of the non-specific bands present in the uncleaned antiserum were still present in the affinity purified antiserum (Figure 3.9).

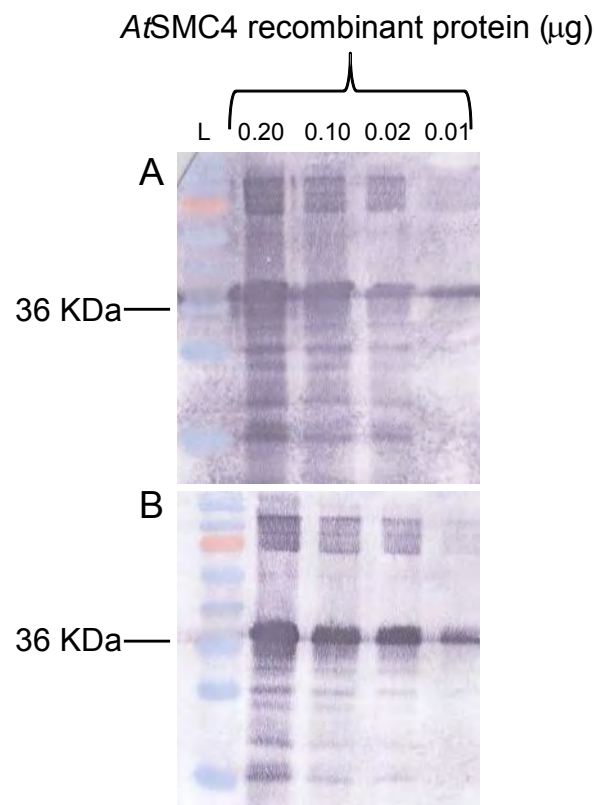


Figure 3.9: Western blot analysis of affinity purified *AtSMC4*-Ab: **A** = Crude *AtSMC4*-Ab (1:1000) and **B** = affinity purified *AtSMC4*-Ab (1:1000) on *AtSMC4* recombinant protein. Different amounts of *AtSMC4* recombinant protein were loaded (0.2, 0.1, 0.02, and 0.01 µg). *AtSMC4*-Ab was detected with anti-rabbit alkaline phosphatase conjugated secondary antibody (1:5000). L= SeeBlue plus2 pre-stained Protein ladder (Invitrogen).

The *AtSMC4*-antiserum and pre-immune serum were also purified using an *E. coli* immobilized lysate column. This column contains lysate from *E. coli* cells covalently linked to agarose beads. Purifying an antibody using one of these columns will remove any antibodies which have been raised against *E. coli* proteins from the antibody of interest. After *E. coli* column purification, the specificity of the antibody was re-tested by western blot; both cleaned and uncleaned antiserum and pre-immune serum were used at a dilution of 1:1000. As with the affinity purification method, varying amounts of recombinant protein were used to test if the activity of the antibody had reduced after the cleaning process.

Western blot experiments revealed that the *E. coli* immobilised lysate column removed many of the non-specific bands which the unclean AtSMC4 antibody recognises (Figure 3.10: compare A and C). Overall the antibody appeared much cleaner after the *E. coli* column purification. Both cleaned and non-purified pre-immune serums do not recognise the AtSMC4 recombinant protein. It was concluded that the *E. coli* purification was the most successful and AtSMC4 antibody purified with this method was used in subsequent experiments.

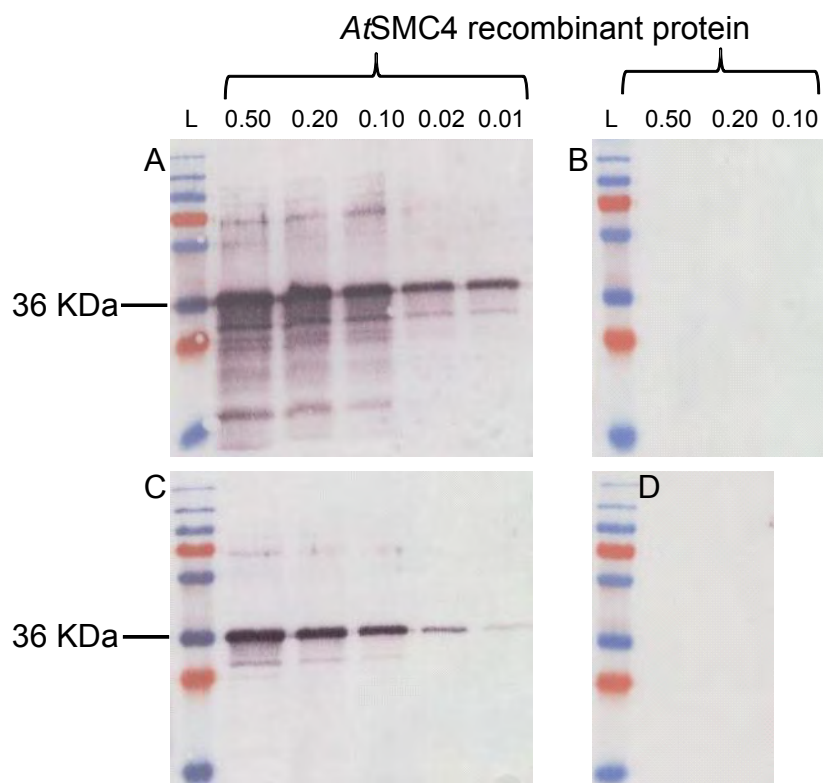


Figure 3.10: Western blot analysis of *E.coli* column purified AtSMC4-Ab: **A** = uncleaned AtSMC4-Ab (1:1000); **B** = uncleaned pre-immune (1:1000); **C**= *E. Coli* lysate column cleaned AtSMC4-Ab (1:1000) and **D** = *E. Coli* lysate column cleaned pre-immune serum (1:1000) on AtSMC4 recombinant protein. Different amounts of AtSMC4 recombinant protein were loaded (0.5, 0.2, 0.1, 0.02, and 0.01 µg). AtSMC4-Ab was detected with anti-rabbit alkaline phosphatase conjugated secondary antibody (1:5000). L= SeeBlue plus2 pre-stained Protein ladder (Invitrogen).

3.2.8 Immunolocalisation of AtSMC4 during meiosis using fixed bud material

Purified AtSMC4 antiserum was tested at a range of concentrations and conditions on wild-type PMC chromosomes, using the unpurified serum as a positive control. The axis-associated signal which was seen in the unpurified serum and pre-immune serum was not detected in the purified antibody during this analysis. However, no other signal was detected during prophase I using the purified AtSMC4 antibody. It is difficult to detect later stages of meiosis (after prophase I) using this technique. Therefore a new immunolocalisation technique from M. Grelon's group (Chelysheva *et al.*, 2010) was used to see if AtSMC4 could be detected on post-prophase chromosomes. The technique involves applying antibodies to slides made from material fixed in 3:1 ethanol: acetic acid (Carnoy's solution). As well as being useful to detect later stages of meiosis, this technique can unmask antigens which may be masked in alternative immunolocalisation techniques (Chelysheva *et al.*, 2010). Purified AtSMC4 antiserum and AtSMC4 pre-immune serum were tested in wild-type chromosome spreads from fixed bud material. Chromosomes were counter-stained with DAPI (4',6-diamidino-2-phenylindole).

AtSMC4 antiserum was not detected on the chromosome axis at any stage in early prophase I. However, AtSMC4 was occasionally detected on the paired centromeres during prophase I (Figure 3.11 E +H) which was absent from the pre-immune serum (Figure 3.15). However, this signal was weak and therefore the significance of this signal is unknown. As the chromosomes began to resemble metaphase I bivalents the entire chromosome was seen to be decorated with AtSMC4 (Figure 3.11). At metaphase I, in approximately 50% of cells, AtSMC4 was seen to stain the

centromeric regions of the chromosomes more intensely than other chromosome regions (Figure 3.13). *AtSMC4* signal remained on the chromosomes during chromosome segregation at anaphase I. At prophase II, when the chromosomes decondense slightly before re-condensing at metaphase II, *AtSMC4* was seen to localise to the diffuse chromatin (Figure 3.12 F and I). At metaphase II and anaphase II *AtSMC4* decorated all of the condensed chromatin (Figure 3.14, F and I). At the tetrad stage, *AtSMC4* was seen as a weak signal surrounding the chromatin. Pre-immune serum did not localise to the chromosomes at any stage of meiosis (Figure 3.15) indicating that the signals observed with the *AtSMC4* antiserum are specific to the *AtSMC4* antiserum.

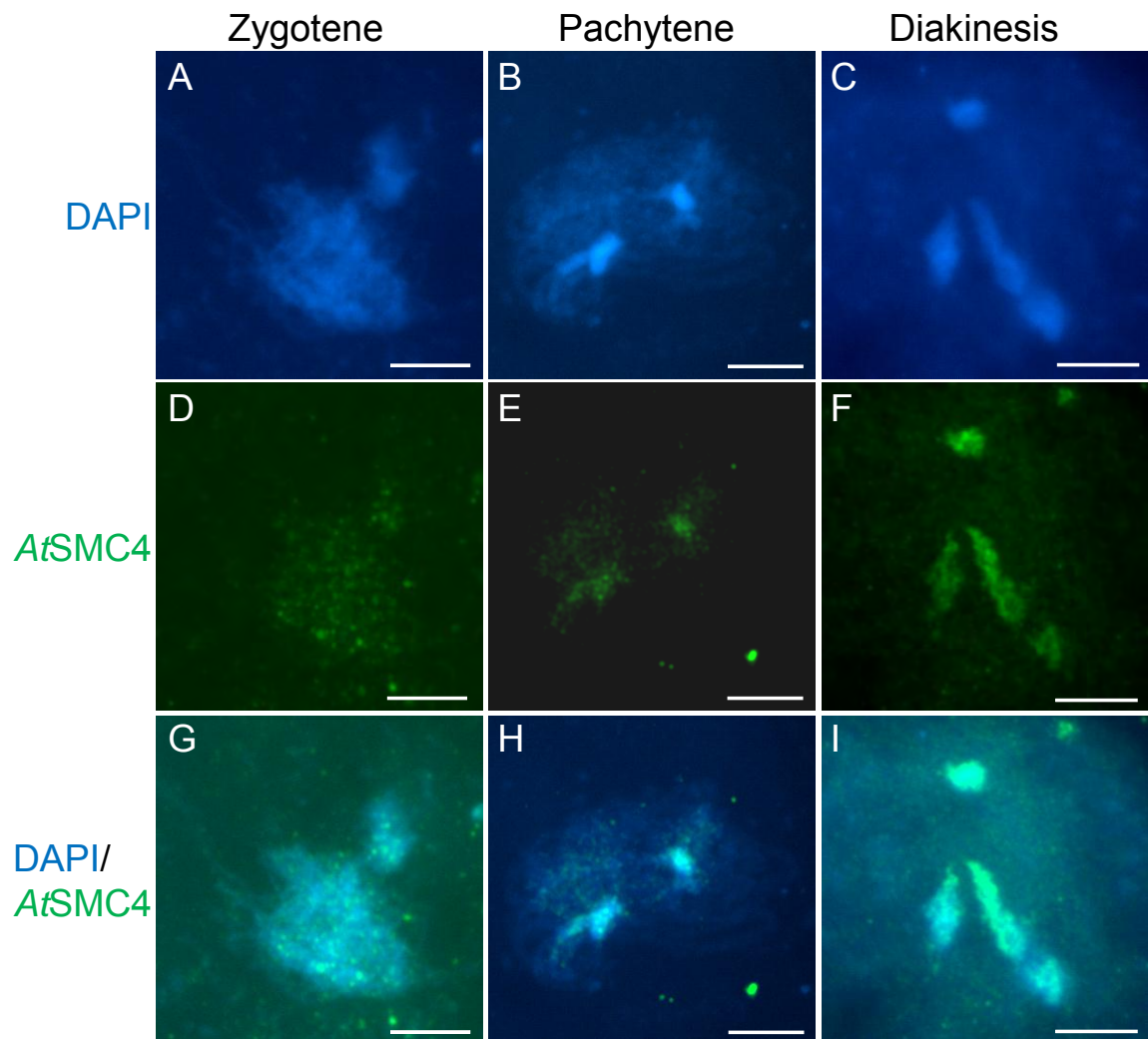


Figure 3.11: Immunolocalisation of *AtSMC4*-Ab on wild-type PMC stages zygotene to late diakinesis/early metaphase I. **A, D, G** = zygotene; **B, E, H** = pachytene; **C, F, I** = late diakinesis/early metaphase I). **A-C** =DAPI; **D-F** = *AtSMC4* antiserum (FITC); **G-I** = DAPI (blue)/*AtSMC4* (green) merge. Scale bar = 5 μ m.

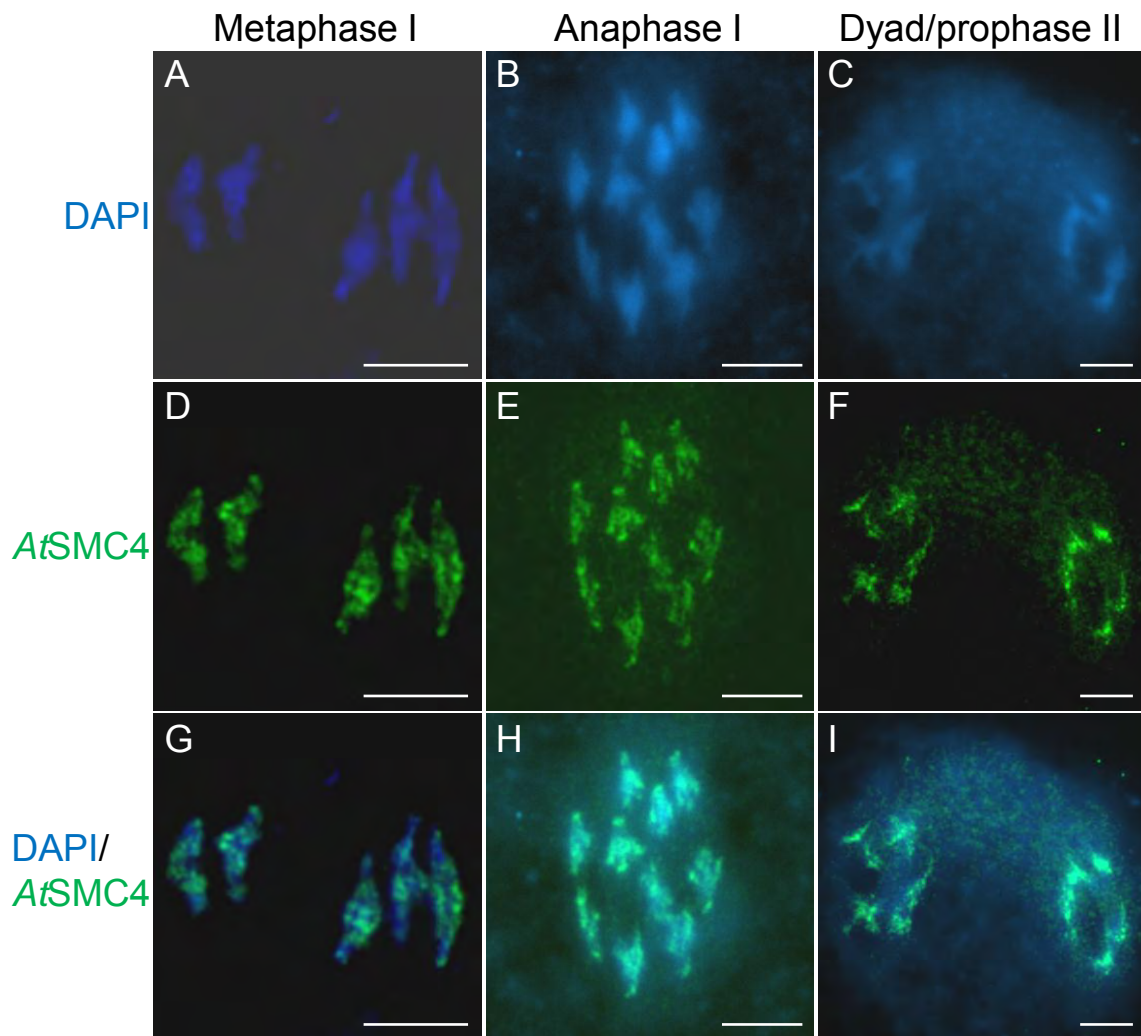


Figure 3.12: Immunolocalisation of AtSMC4-Ab on wild-type PMC stages metaphase I to dyad/prophase II. (A, D, G = metaphase I; B, E, H = anaphase I; C, F, I = dyad/prophase II). A-C = DAPI; D-F = AtSMC4 antiserum (FITC); G-I = DAPI/AtSMC4 merge. Scale bar = 5 μ m.

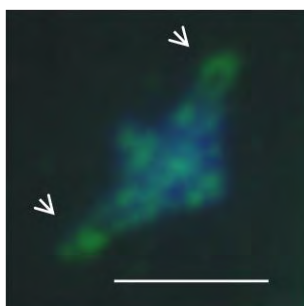


Figure 3.13: Immunolocalisation of AtSMC4-Ab on wild-type metaphase I. Image = DAPI/AtSMC4 merge. Arrow-heads are indicating centromere regions with more intense AtSMC4 staining (Green). Scale bar = 5 μ m.

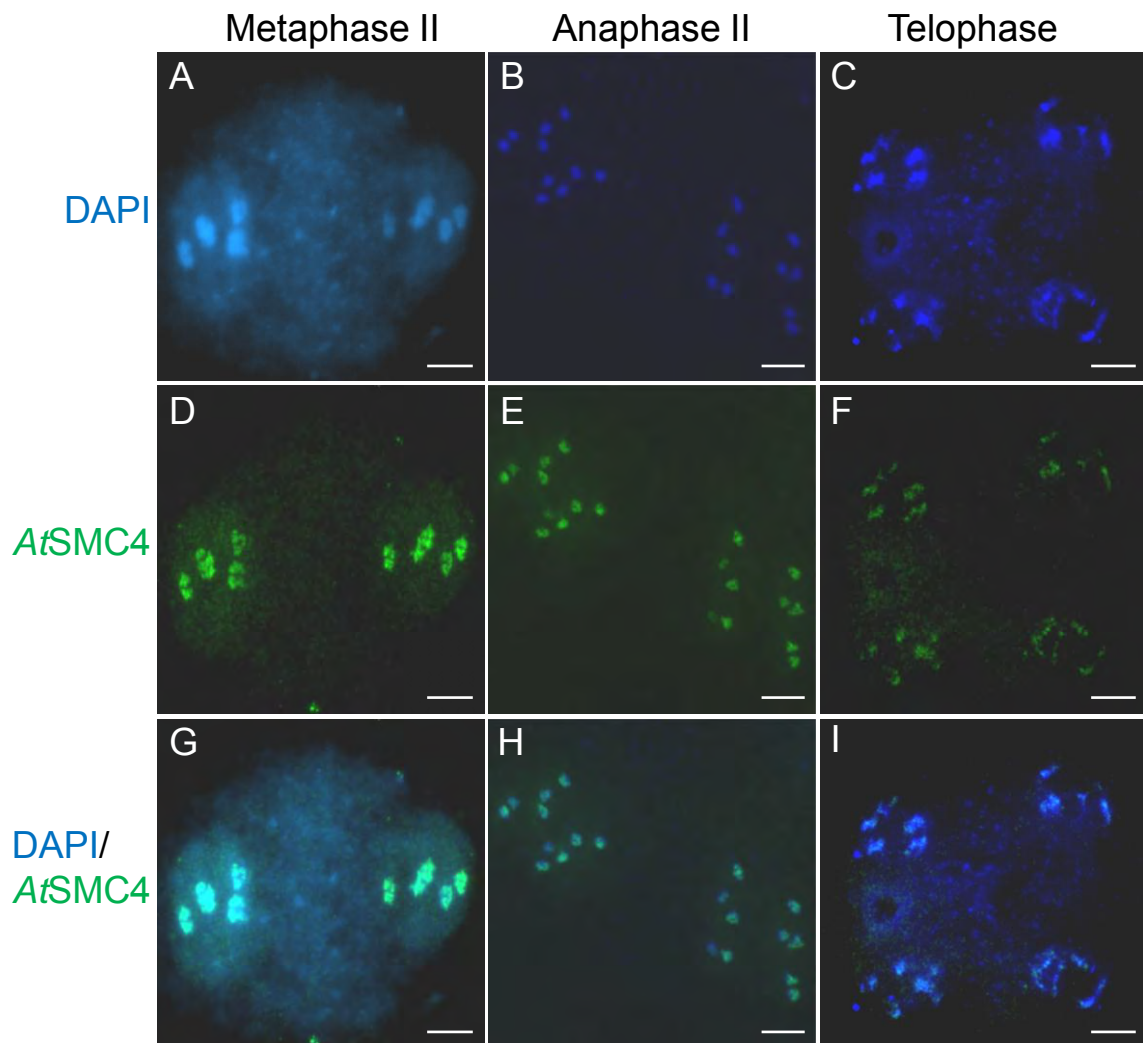


Figure 3.14: Immunolocalisation of *AtSMC4*-Ab on wild-type PMCs stages metaphase II to tetrad. **A, D, G** = metaphase II; **B, E, H** = anaphase II; **C, F, I** = tetrad. **A-C** = DAPI; **D-F** = *AtSMC4* antiserum (FITC); **G-I** = DAPI/*AtSMC4* merge. Scale bar = 5 μ m.

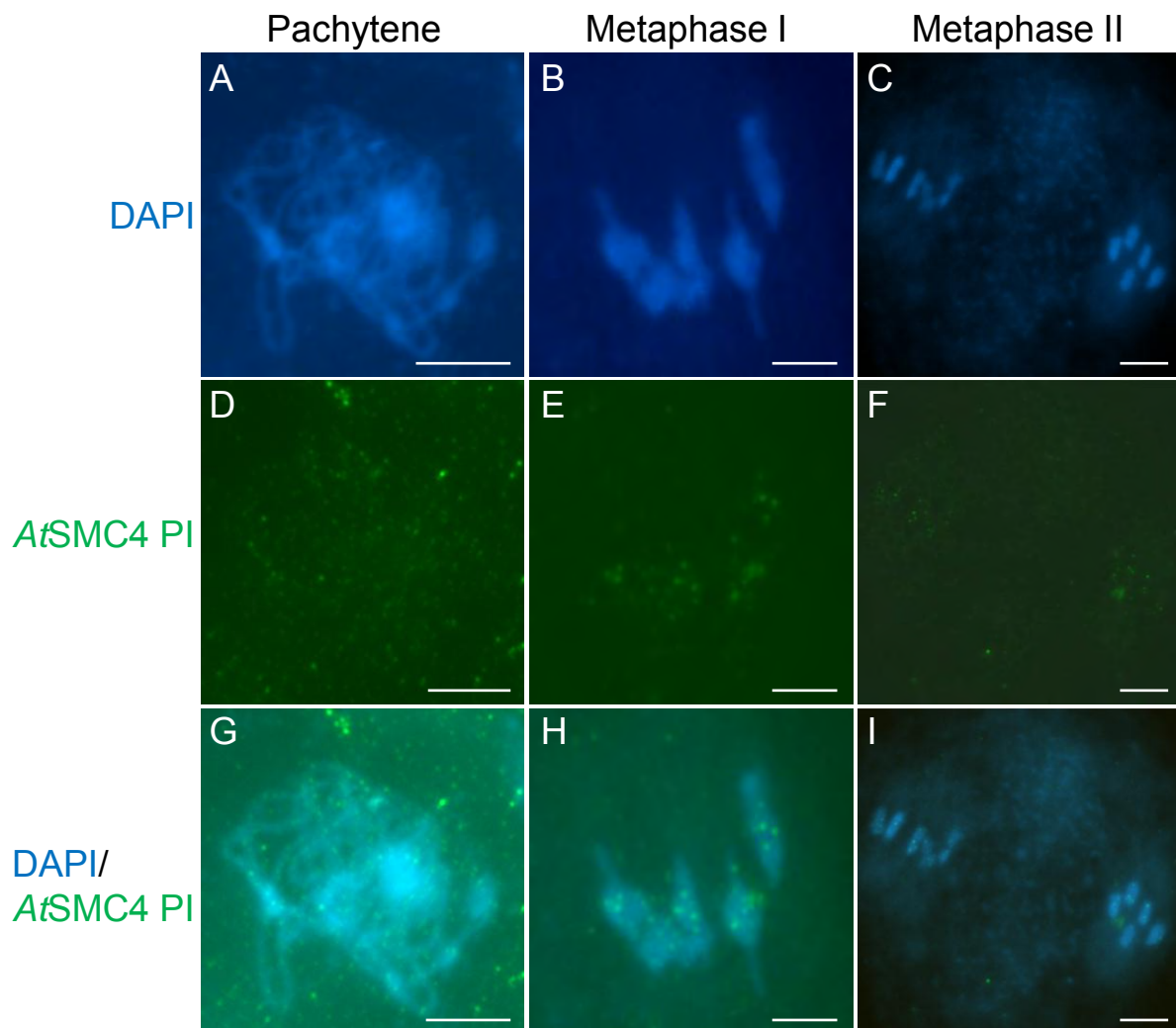


Figure 3.15: Immunolocalisation of pre-immune (PI) serum on wild-type PMCs. **A, D, G** = pachytene; **B, E, H** = metaphase I; **C, F, I** = metaphase II. **A-C** =DAPI; **D-F** = *AtSMC4* pre-immune serum (FITC); **G-I** = DAPI/*AtSMC4* Pre-immune merge. Scale bar = 5 μ m.

3.2.9 *AtSMC4* localisation to mitotic cells

AtSMC4 functions in both mitotic and meiotic cell divisions; therefore the localisation of *AtSMC4* was also tested in mitotic cells present in the bud tissue using the *AtSMC4*-antiserum. *AtSMC4* antibody was detected in mitotic prophase cells where it was seen to be enriched at the centromeres and gave a faint coating on the rest of the chromatin (Figure 3.16, E and I). At mitotic metaphase *AtSMC4* could be seen to coat the entire chromosomes; this staining remained throughout anaphase and telophase (See Figure 3.16, F and J). The pre-immune serum did not localise to the chromosomes at any stage of mitosis (Figure 3.17).

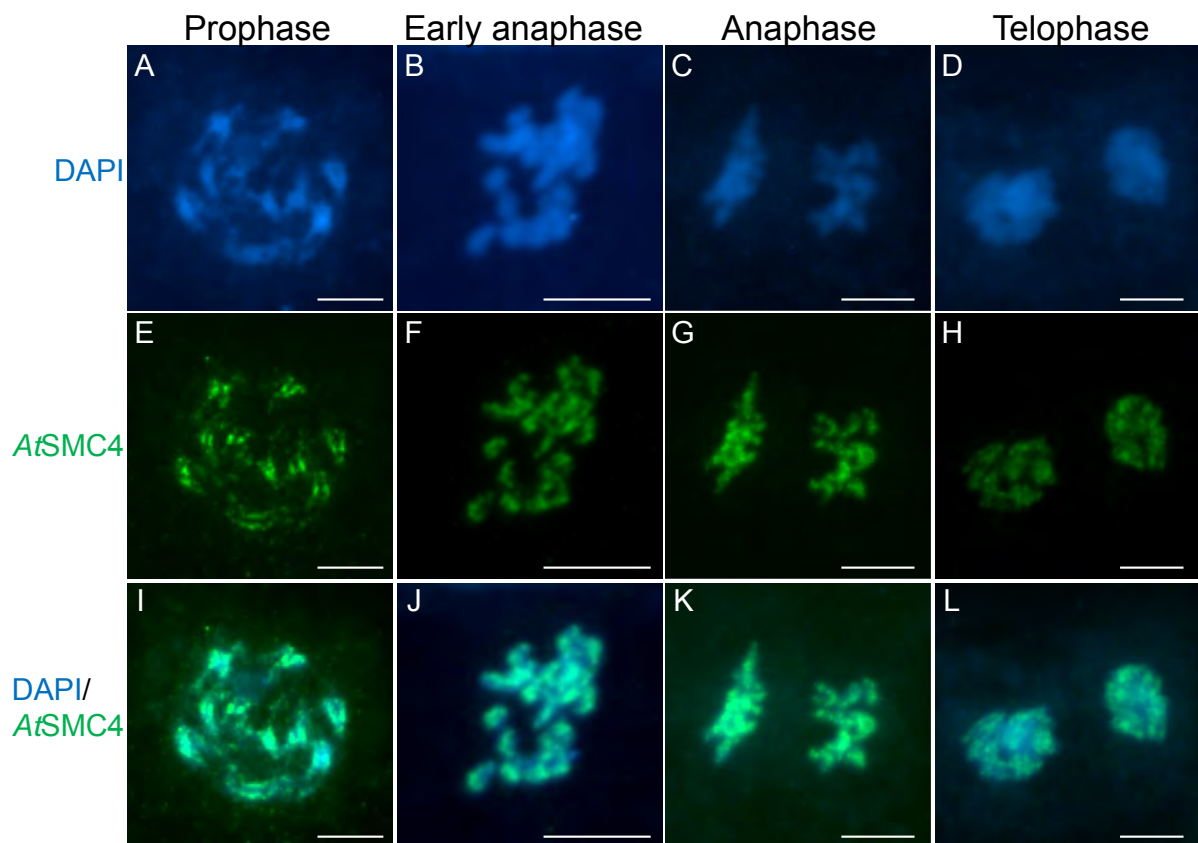


Figure 3.16; Immunolocalisation of AtSMC4-Ab on wild-type mitotic cells. **A, E, I** = prophase; **B, F, J** = metaphase; **C, G, K** = anaphase; **D, H, L** = telophase. **A- D** = DAPI; **E-H** = AtSMC4 antiserum (FITC); **I-L**= DAPI/AtSMC4 merge. Cell stage indicated above column. Scale bar = 5 μ m

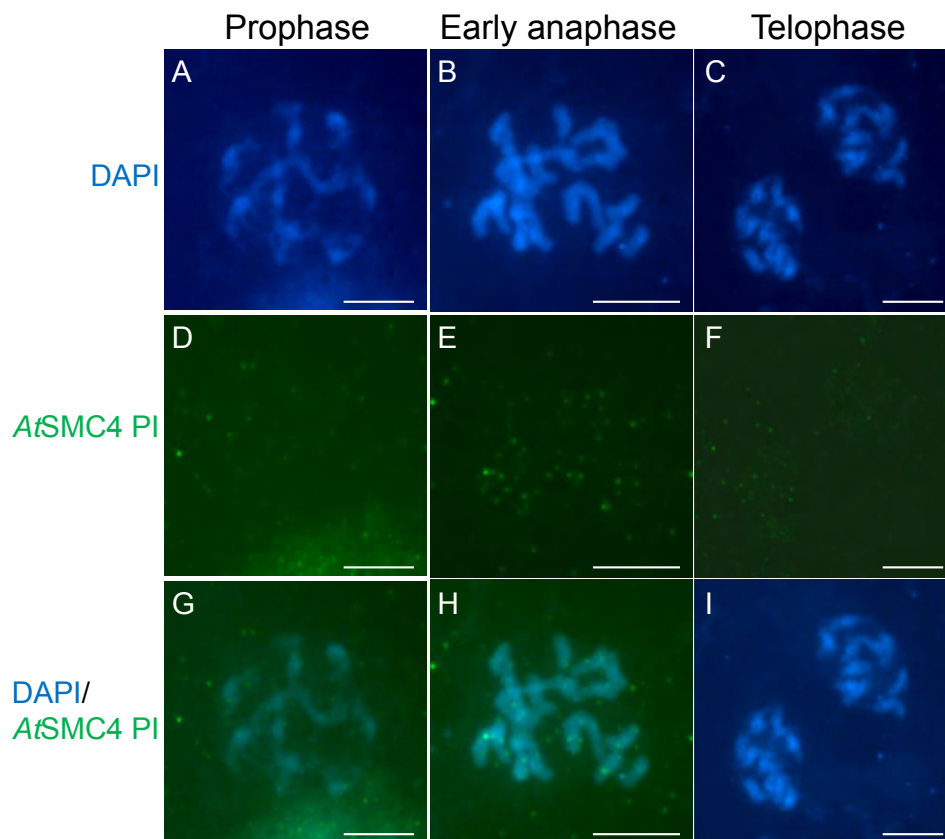


Figure 3.17: Immunolocalisation of *AtSMC4* pre-immune (PI) serum on wild-type mitotic cells. **A, D, G** = prophase; **B, E, H** = Early anaphase; **C, F, I** = telophase. **A-C** =DAPI; **D-F** = *AtSMC4* pre immune serum (FITC). **G-I** = DAPI/*AtSMC4* pre-immune merge. Cell stage indicated above column. Scale bar = 5 μ m.

3.2.10 Western blot analysis on plant protein extract

Immunolocalisation experiments on wild-type PMCs have shown that the AtSMC4 antibody is able to recognise AtSMC4 on meiotic and mitotic chromosomes. In order to investigate whether the AtSMC4 antibody is able to detect AtSMC4 protein in plant extracts, a western blot analysis was carried out. Protein was extracted from buds, leaves and seedlings of wild-type plants. AtSMC4 is expected to be present in mitotic tissue as well as meiotic cells. Seedling tissue is more actively dividing than cells in fully grown leaves, therefore it may be expected that more AtSMC4 protein is detected in seedlings than leaf. 4 replica western blots containing ~25 µg of bud, seedling and leaf protein were probed with unpurified AtSMC4-Ab, purified AtSMC4-Ab, unpurified pre-immune and purified pre-immune. A loading control was also run on another SDS-PAGE gel and stained with Coomassie blue. In this assay a band at ~150 KDa, the predicted size of AtSMC4 protein, was detected in the blots probed with AtSMC4 immune serum and is absent from the pre-immune serum probed blots (Figure 3.18). AtSMC4 appears to be more concentrated in bud tissue than seedling or leaf. Comparing the purified samples to the un-purified, it can be seen that several nonspecific bands present in the unclean samples are absent from, or reduced in intensity in the purified antiserum indicating that the *E. coli* antibody purification column has reduced non-specific background in the AtSMC4 antiserum.

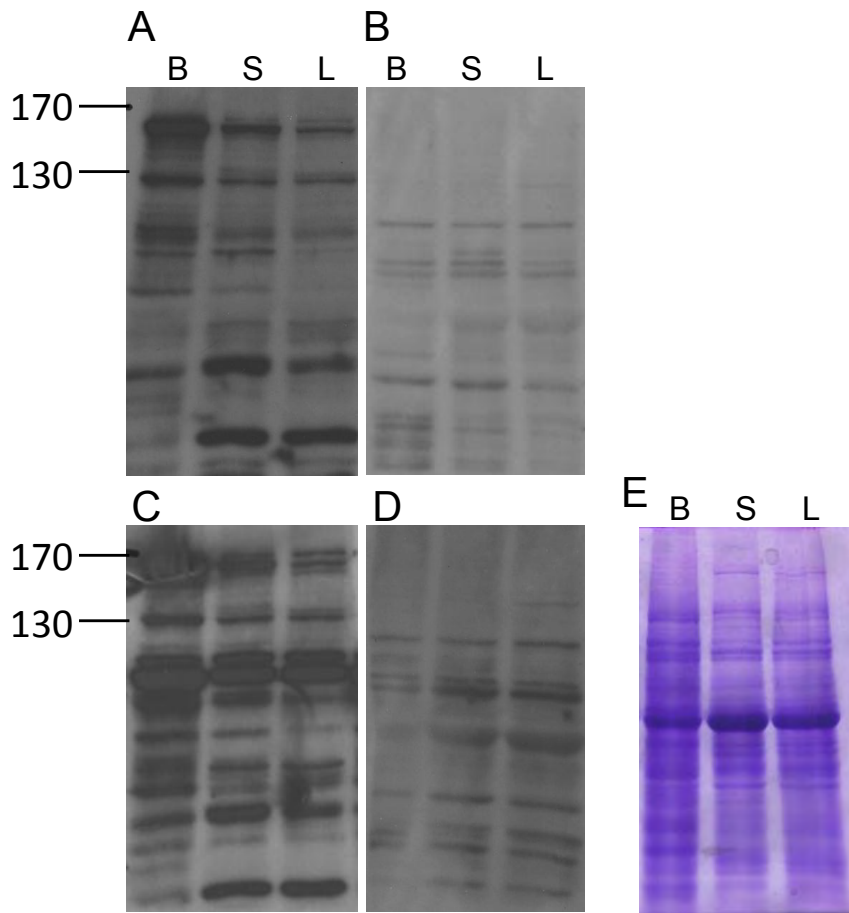


Figure 3.18: Western blot analysis of AtSMC4-Ab on plant protein extracts. Protein was extracted from wild-type bud (B), seedling (S) and leaf (L). (**A,C**) = AtSMC4-Ab and (**B,D**) = pre-immune serum. **A** and **B** are probed with antiserum and pre-immune serum which has been purified using an *E. coli* immobilised lysate kit. **C** and **D** have been probed with crude serum. AtSMC4-Ab was detected with anti-rabbit HRP conjugated secondary antibody (1:5000). Blots were exposed for 10 minutes. **E** = Coomassie stained loading control ~25 μ g of each sample was loaded. Ladder = PageRuler (fermentas), 170 and 130 kDa markers are indicated.

3.3 DISCUSSION

3.3.1 Origin of non-specific axis-associated signal in the pre-immune serum

The un-purified pre-immune serums from both animals gave a non-specific axis-associated signal. The prophase I chromosome axis contain a large meshwork of proteins (Kleckner, 2006) therefore since an epitope need only be a few amino acids, it is possible that antibodies can bind non-specifically to this meshwork. After the AtSMC4-Ab and the pre-immune serum were purified on an *E. coli* lysate column the axis associated signal no longer seemed to be detected in immunolocalisation experiments. Therefore it is assumed that the *E. coli* column removed the immunoglobulin which was giving this non-specific signal from the AtSMC4-Ab and pre-immune samples. The *E. coli* lysate column is designed to remove antibodies from anti-serum samples which have been raised against *E. coli* protein present in the recombinant protein preparation. However in this case it appears that the *E. coli* lysate column has removed an immunoglobulin present in the rabbits before immunisation which was recognising a component of the meiotic chromosome axis.

3.3.2 *E. coli* column antibody purification was more successful than affinity purification

E. coli cell lysate column purification of the AtSMC4 antibody resulted in fewer non-specific bands being detected on western blot analysis of AtSMC4 recombinant protein. However, the affinity-based purification method was largely unsuccessful. This may have been due to non-specific antibodies binding to the membrane and not being washed sufficiently from the membrane. The excised band of AtSMC4

recombinant protein may also contain bands corresponding to *E. coli* proteins which run at the same position, therefore these may limit the stringency of the purification procedure. In order to improve purification by this method the antiserum can also be incubated with the area of the membrane which contains the non-specific bands (i.e the membrane left after the recombinant protein band has been excised). This may help to remove non-specific antibodies. Additional and more stringent washes of the membrane would also help to remove non-specific immunoglobulins. Such adjustments to the protocol were not tested here due to the successful purification of the antiserum using the *E. coli* column.

3.3.3 AtSMC4-Ab recognises recombinant AtSMC4 protein and a protein corresponding to the size of AtSMC4 from plant extracts.

To test the specificity of the AtSMC4 antibody, western blot analysis was carried out on the AtSMC4 recombinant protein as well as on protein extracted from wild-type leaf, bud and seedling. Results showed that the AtSMC4 antiserum successfully recognises the AtSMC4 recombinant protein before and after antibody purification. Western blot analysis on plant protein extracts showed that the AtSMC4 antiserum recognises a protein which runs at the predicted molecular weight of the AtSMC4 protein. This band is absent from the pre-immune control. Additional bands are present in all tissue types, although many are reduced in intensity in the purified antibody. Equal amounts of protein from bud, leaf and seedling were loaded on the gel. The signal in the bud extract is more intense than that of the leaf or seedling samples. This indicates that more AtSMC4 protein is present in the bud protein extract than those which only contain somatic material (leaf and seedling). This may

be due to the large proportion of dividing cells (both meiotic and mitotic) present in bud tissue. Indeed more AtSMC4 is present in the highly dividing seedling tissue than in fully grown leaf. The increased AtSMC4 in bud tissue may also indicate that a higher proportion of total cellular AtSMC4 is required for meiotic cell divisions.

3.3.4 Condensin localisation during meiosis in *Arabidopsis*

In this chapter an antibody specific to the AtSMC4 subunit of condensin I and II has been produced in rabbit. Immunolocalisation experiments on fixed *Arabidopsis* meiocytes reveal that AtSMC4 is first detected as a weak signal at the centromeres on prophase I cells. At late diakinesis AtSMC4 is detected over the entire chromatin. This signal remains throughout metaphase I, where it appears to be enriched at the centromeres, and anaphase I. AtSMC4 is also detected on metaphase II and anaphase II meiocytes. AtSMC4 signal becomes diffuse at telophase. AtSMC4 appeared to coat all of the chromatin during the condensed stages of meiosis. This contrasts with other studies which show condensin to be either enriched at the rDNA (Yu and Koshland, 2005), the centromeric regions (Hagstrom *et al.*, 2002; Yu and Koshland, 2006; Viera *et al.*, 2007) or occasionally the telomeric regions (Viera *et al.*, 2007) during meiosis.

AtSMC4 was not detected along prophase I chromosomes axes in this study. In budding yeast, Ycs4 co-localised with the SC TF protein Zip1 forming semi-continuous foci (Yu and Koshland, 2005). In *C. elegans* condensin II specific subunits are detected at pachytene, partially localising with DNA and fully localising to the

DNA at diplotene and diakinesis (Chan *et al.*, 2004). It is possible that condensin in *Arabidopsis* does not have a role in chromosome organisation during prophase I of meiosis, as suggested by immunolocalisation results. However it is also possible that AtSMC4 localisation during prophase I is undetectable due to antigen masking. The structural differences between chromosomes in prophase I and metaphase I may result in the former structure masking the AtSMC4 epitope. Fixation methods can also affect antigen masking (Uzbekov *et al.*, 2003), therefore further studies testing different methods may reveal prophase I localisation of AtSMC4. Condensin II may be the primary condensin complex involved in prophase chromosome organisation during meiosis in *Arabidopsis* as in mitotic cell divisions in mammals (Ono *et al.*, 2003; Hirota *et al.*, 2004; Ono *et al.*, 2004; Gerlich *et al.*, 2006). In *Xenopus* the relative amounts of condensin I and condensin II complexes seen on mitotic chromosomes is 5:1, therefore it is possible that the concentration of condensin II to *Arabidopsis* meiotic chromosomes may be less than that of condensin I. Detection of the condensin II complex may therefore be difficult due to low epitope concentration.

During both prophase I and metaphase I an AtSMC4 signal is detected at the centromeres. This signal may reflect a role of condensin in centromere organisation. Condensin has been shown to localise to the centromeres during mitosis in *C. elegans* (Hagstrom *et al.*, 2002; Chan *et al.*, 2004) *Xenopus* (Hirano and Mitchison 1994), human (Schmiesing *et al.*, 1998; Gerlich *et al.*, 2006) and *Drosophila* (Steffensen *et al.*, 2001; Savvidou *et al.*, 2005), where it plays a role in centromere organisation (Oliveira *et al.*, 2005; Savvidou *et al.*, 2005; Gerlich *et al.*, 2006; Yong-Gonzalez *et al.*, 2007; Ribeiro *et al.*, 2009; Samoshkin *et al.*, 2009). Condensin has

been implicated in maintaining the stiffness of the centromeres so that they can withstand the force of the spindles (Oliveira *et al.*, 2005; Savvidou *et al.*, 2005; Gerlich *et al.*, 2006; Yong-Gonzalez *et al.*, 2007; Ribeiro *et al.*, 2009) and in the prevention of merotelic spindle attachment (Stear and Roth, 2002; Samoshkin *et al.*, 2009; Tada *et al.*, 2011).

AtSMC4 antibody is first detected on the chromosomes when they are already starting to resemble fully condensed metaphase I bivalents. This suggests that condensin may not be required for the compaction of the chromosomes but more the maintenance of chromosome structure. A similar conclusion has been suggested for condensin in *C. elegans* (Hagstrom, *et al.*, 2002; Chan *et al.*, 2004), chicken (Hudson *et al.*, 2003), human (Ono *et al.*, 2003; Hirota *et al.*, 2004; Gerlich *et al.*, 2006) and *Drosophila* (Savvidou *et al.*, 2005).

3.3.5 Condensin localisation during mitotic cell divisions

The localisation of condensin was also investigated in mitotic cell divisions. During prophase AtSMC4 was seen to be enriched at the centromeres; at metaphase AtSMC4 coated the entire chromosomes and remained during anaphase and telophase. These results resemble the localisation of condensin I and SMC subunits during mitotic cell divisions in *Drosophila* (Steffensen *et al.*, 2001), human (Steen *et al.*, 2000) and *Xenopus* (Hirano and Mitchison, 1994; Beenders *et al.*, 2003) where condensin subunits are first seen to localise to the chromatin at prophase/prometaphase and remain on the chromatin throughout mitosis before

becoming diffuse at telophase. Condensin complexes have also been shown to be enriched at the centromeres in *C. elegans* (Hagstrom *et al.*, 2002; Chan *et al.*, 2004), *Xenopus* (Hirano and Mitchison 1994), human (Schmiesing *et al.*, 1998; Gerlich *et al.*, 2006), *Drosophila* (Savvidou *et al.*, 2005; Steffensen *et al.*, 2001), and *cerevisiae* (Bachelier-Bassi *et al.*, 2008), where they are required for centromere organisation. Taken together these results suggest that condensin may be involved in the organisation of the centromeric DNA, at least during a mitotic cell division, and possibly also during a meiotic cell division. No specific localisation of condensin subunits to the rDNA was observed in this study, unlike yeast (Freeman *et al.*, 2000; Bhalla *et al.*, 2002; Yu and Koshland, 2003; Sullivan *et al.*, 2004; Yu and Koshland, 2005). However *Arabidopsis* condensin II does localise to the nucleolus in tobacco mitotic cells (Fijimoto *et al.*, 2005).

3.3.6 Future perspectives

The AtSMC4-Ab produced and assessed here can be used for many more downstream applications. The AtSMC4-Ab recognises a protein corresponding to the size of AtSMC4 on a western blot of plant protein extracts. This band is clear and intense, and absent from the pre-immune control and relatively few other bands are detected by the AtSMC4-Ab, especially after *E. coli* lysate column clean up. These results show that the AtSMC4-Ab would be useful for assessing the levels of AtSMC4 in plants deficient in AtSMC4 (See chapter 4), and for experiments such as immunoprecipitation, where a highly specific antibody which is able to recognise its target protein with high affinity, is desired. Immunoprecipitation experiments would provide interesting insights into possible proteins which interact with condensin.

It would be interesting to know how the distribution of the two condensin complexes differs during both meiotic and mitotic cell divisions in *Arabidopsis*. Using GFP-tagged *Arabidopsis* AtCAP-H and AtCAP-H2 expressed in tobacco transgenic cell suspension cultures it has been suggested that the two condensin complexes do have distinct distributions. Both proteins were seen to localise on mitotic chromosomes from prometaphase until telophase. However this distribution differed during interphase when AtCAP-H was located in the cytoplasm and AtCAP-H2 was seen in the nucleolus (Fujimoto *et al.*, 2005). Research into the specific condensin I and condensin II loading patterns in *Arabidopsis* is an interesting area for further study, therefore the production of antibodies specific to condensin I and condensin II subunits would be a valuable area of further study.

3.3.7 Conclusions

This chapter examines the localisation of both condensin complexes during a meiotic and mitotic cell division in *Arabidopsis*. This is the first time the localisation of condensin has been investigated in *Arabidopsis* cells, and the first time condensin localisation has been investigated during meiosis in any plant species. AtSMC4 localisation suggests that condensin may have a role in maintaining chromosome structure instead of in compaction itself. Possible centromere enrichment also suggests a role for condensin in centromere organisation in plants.

CHAPTER 4

4 THE CONDENSIN SUBUNIT ATSMC4 IS ESSENTIAL FOR MEIOTIC CHROMOSOME ORGANISATION IN *ARABIDOPSIS* *THALIANA*

4.1 INTRODUCTION

The role of condensin has been well studied during mitosis in many species where it has been shown to have a role in chromosome compaction, maintenance of chromosome structure, chromosome segregation, centromere organisation and rDNA organisation in yeast (as discussed in sections 1.7.4-1.7.8).

A few papers have also looked into the role of condensin in meiosis (Hagstrom *et al.*, 2002; Beenders *et al.*, 2003; Watrin *et al.*, 2003; Wignall *et al.*, 2003; Yu and Koshland, 2003; Chan *et al.*, 2004; Yu and Koshland, 2005; Tsai *et al.*, 2008; Resnick *et al.*, 2009; Brito *et al.*, 2010). In *C. elegans* condensin mutants disrupt CO interference possibly by increasing the length of the chromosome axes (Tsai *et al.*, 2006). In budding yeast condensin is also required for axis length compaction, as well as SC assembly, the proper processing of DSBs, and anaphase chromosome segregation (Yu and Koshland 2003, 2005). In *Drosophila* a delay in SC disassembly has been seen in condensin deficient flies, but no defects in SC assembly or prophase axis length were reported (Resnick *et al.*, 2009). The role of condensin in *Arabidopsis* meiosis has only been briefly covered. Disrupting one of the two partially redundant SMC2 homologues in *Arabidopsis* resulted in segregation defects during a meiotic cell division (Siddiqui *et al.*, 2003).

This chapter describes the phenotypes observed from reducing the amount of cellular condensin by targeting the *AtSMC4* mRNA by RNAi. This approach should result in the knock-down of total cellular condensin as *AtSMC4* is a component of both condensin complexes. The meiosis specific DMC1 promoter (Klimyuk and Jones, 1997) was used to drive the expression of the RNAi construct specifically in meiotic tissue. The aim of this work was to investigate the role of condensin during meiosis in *Arabidopsis* as this has not been previously studied in detail. The role of condensin during meiosis in other species is not entirely functionally conserved, therefore further analysis, in a different organism, will shed more light on to the complex role of these proteins. Figure 4.1 shows the predicted subunit arrangement of condensin I and II complexes.

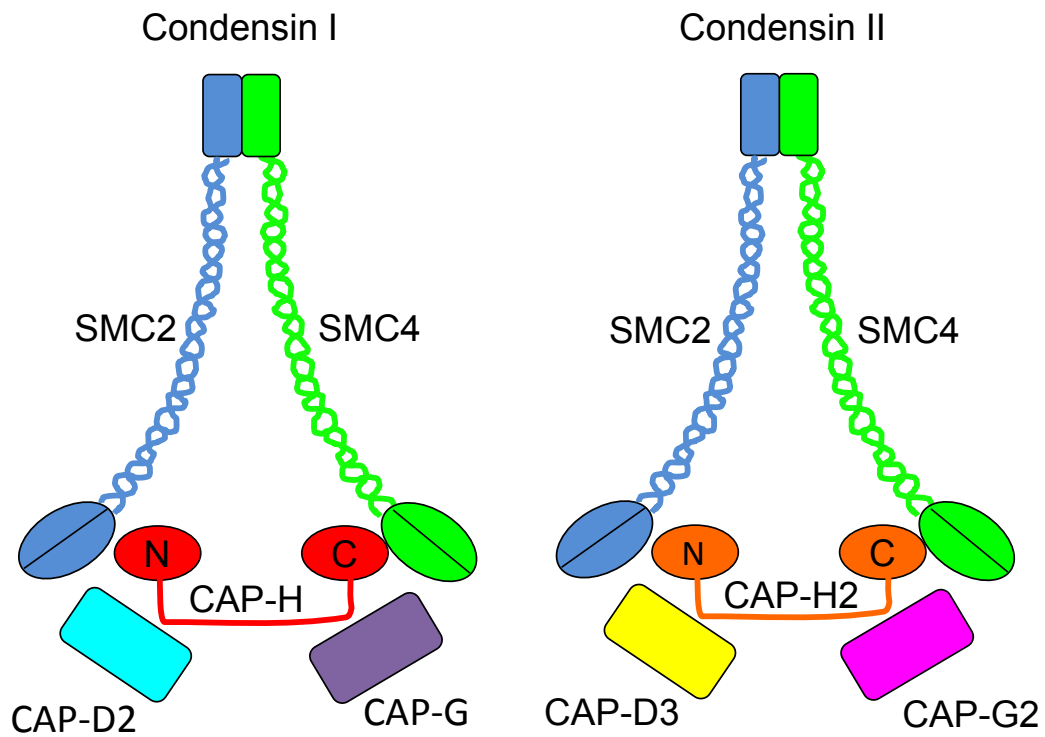


Figure 4.1: Schematic representation of the condensin I and II complexes. Both condensin I and condensin II complexes share the same SMC2/SMC4 backbone but differ in their regulatory subunits. Condensin I comprises CAP-H, CAP-D2 and CAP-G; condensin II comprises CAP-H2, CAP-D3 and CAP-G2.

4.2 RESULTS

4.2.1 Isolation and Characterisation of an AtSMC4 T-DNA insertion line

To investigate the function of *AtSMC4* in meiosis a T-DNA insertion mutant of *AtSMC4* was sought. The NASC (European *Arabidopsis* Stock Centre) database was screened for plants containing an insert in the *AtSMC4* gene (At5g48600). Seeds containing a T-DNA insertion in the 7th intron of the *AtSMC4* gene were ordered for analysis (Salk_86_D2). These plants had already been worked on by Siddiqui *et al.*, (2006) who were unable to obtain any homozygous plants. To further confirm this result, 124 plants were screened for the presence of a T-DNA insert by PCR, out of which 19 contained a single insert and the remaining 105 plants contained no insert. No homozygous plants were obtained. These findings along with previously published work suggest that *Atsmc4* homozygous mutants are lethal. Heterozygous plants were recovered with a much lower frequency (19/124) than would be predicted from Mendelian genetics. This finding was shown to be significant with chi-squared analysis ($\chi^2=237.4$ 2df >0.001). *AtSMC4* heterozygous mutants (*AtSMC4*^{+/-}) grew normally and had no obvious somatic abnormalities. However, the plants did have short siliques (seed pods) compared to wild-type controls (19.4%) suggesting a reduction in fertility. The band obtained in PCR reactions used to identify the presence of the T-DNA insert was cloned and sequenced to confirm the insert was in the *AtSMC4* gene. Figure 4.2 shows the sequence obtained, and the position of the insert site relative to the intron/exon composition of the gene.

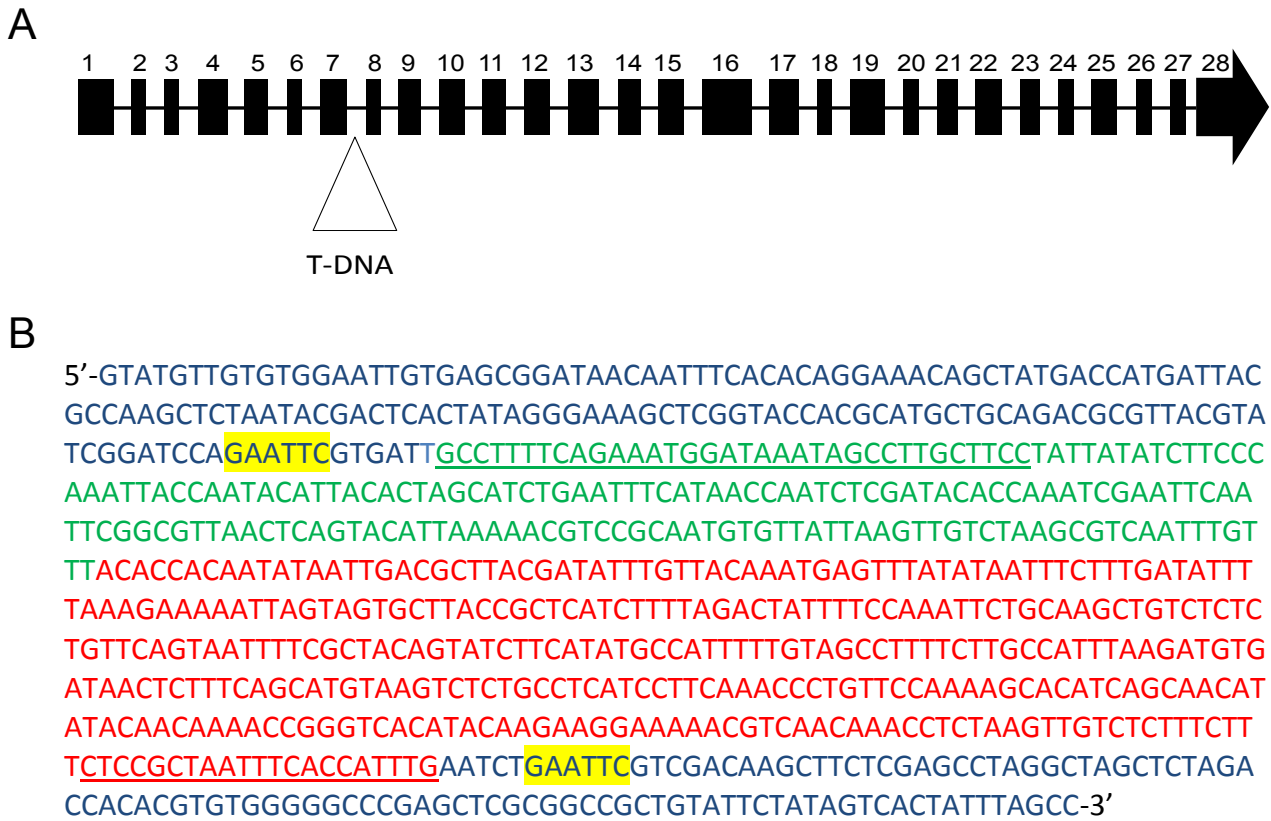


Figure 4.2: Position of the T-DNA insert in the Salk_86_D2 line. **A** = Insert is in the 7th intron of the *AtSMC4* gene (At5g48600). Exons are numbered. **B** = Sequence obtained from cloning the insert band from genotyping PCR reactions. Blue sequence is pDrive cloning vector, green sequence is the T-DNA insert sequence, red sequence is the At5g48600 7th intron sequence. EcoRI cloning sites present in the pDrive cloning vector are highlighted in yellow.

4.2.2 Fertility of *AtSMC4*^{+/-} plants

To assess the level of fertility in these lines, silique length and seed number were scored from *AtSMC4*^{+/-} plants as well as wild-type approximately 60 days after planting when the seed pods had dried out. The results showed the *AtSMC4*^{+/-} plants had a 64% reduction in seed set compared to wild-type ($p < 0.005$, student's *t*-test). Siliques were 11% shorter in the *AtSMC4*^{+/-} plants compared to wild-type ($p < 0.005$, student's *t*-test). Figure 4.3 shows the average seed set for wild-type and *AtSMC4*^{+/-}

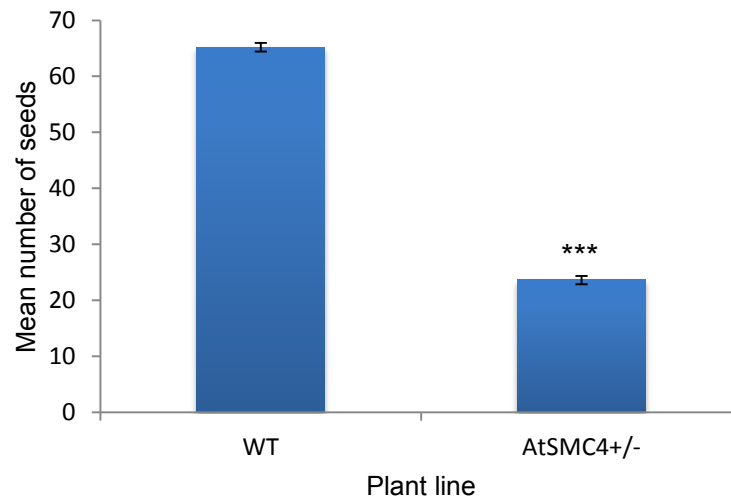


Figure 4.3: Mean seed set in *AtSMC4*^{+/-} plants (n=2) compared to wild-type (WT) (n=4). 10 siliques from each plant were scored. *** = $p < 0.005$. Error bars = Standard error of the mean.

4.2.3 Meiosis in *AtSMC4*^{+/-} plants

The reduction in fertility seen in the *AtSMC4*^{+/-} plants may reflect a meiotic defect. In order to investigate this, meiosis was assessed in *AtSMC4*^{+/-} plants as well as wild-type by DAPI (4',6-diamidino-2-phenylindole) stained chromosome spreads of *Arabidopsis* PMCs. DAPI is a fluorescent dye which binds to DNA allowing the chromosomes to be visualised. In wild-type meiosis chromosomes are seen in leptotene as thread-like structures which align and join along their length at the onset of zygotene. At pachytene the homologous chromosomes are fully synapsed (Figure 4.4: A). After pachytene the chromosomes de-synapse at diplotene and begin to condense into discrete bivalents during diakinesis (Figure 4.4: B). Bivalents are fully condensed and become aligned along the cell equator by the spindle at metaphase I (Figure 4.4: C). Homologous chromosomes segregate at anaphase I to opposite poles of the cell (Figure 4.4: D) and sister chromatids separate at anaphase II. In *AtSMC4*^{+/-}, chromosomes appeared normal during prophase I (Figure 4.4: G) but at metaphase I univalents were observed in 10% of cells (n=20) (Figure 4.4: I). These may be due to a lack of recombination between homologous or an early segregation of homologous chromosomes. No missegregation was observed in MII or tetrad cells in these plants (Figure 4.4: K and L). All other stages of meiosis appeared normal in these lines. Figure 4.4 shows the phenotypes observed in the *AtSMC4*^{+/-} plants.

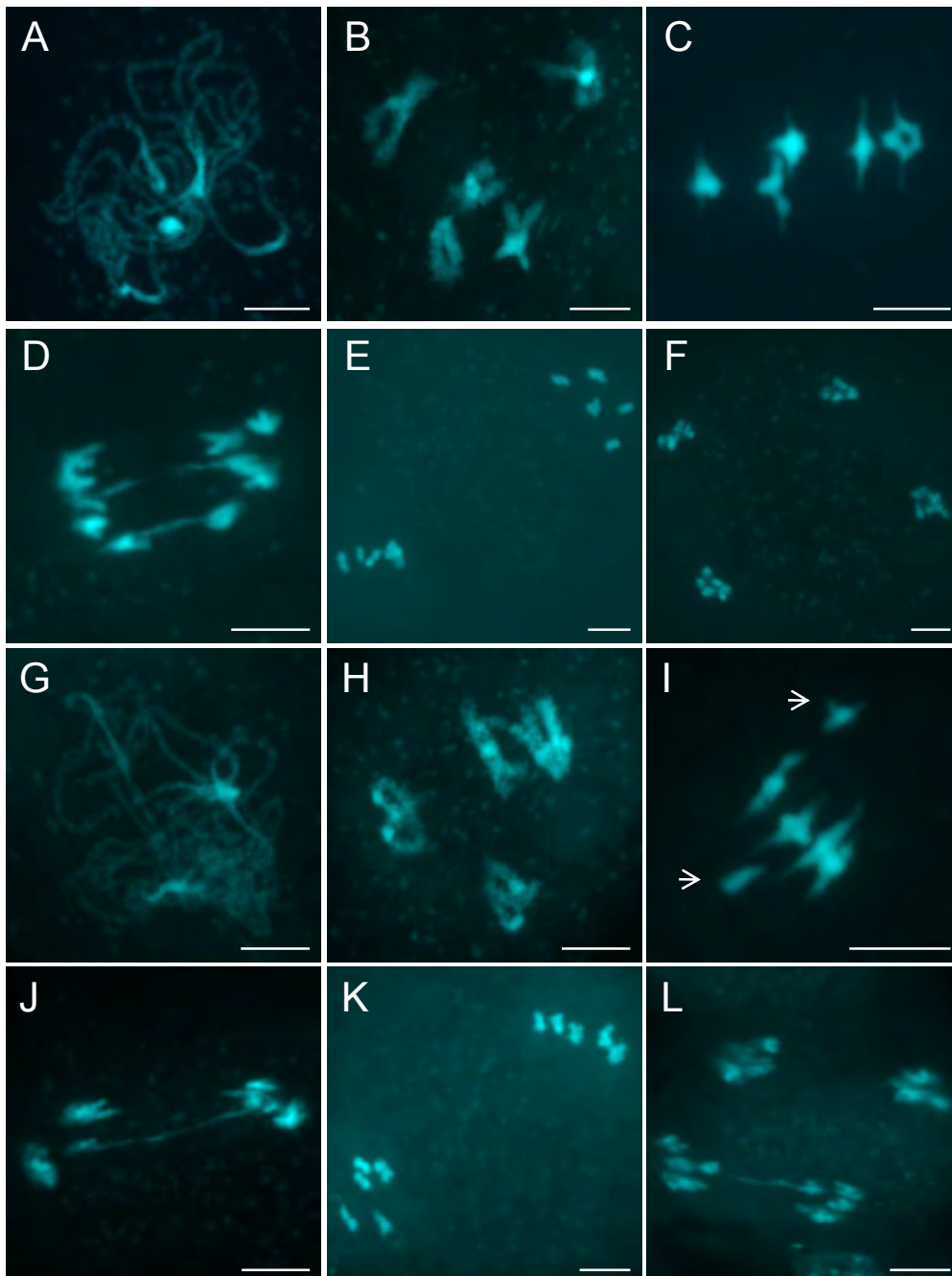


Figure 4.4: Meiotic phenotypes of *AtSMC4*^{+/-} and wild-type plants. DAPI stained chromosome spreads. **A-F** = wild-type; **G-L** = *AtSMC4*^{+/-}. **A** and **G** = pachytene; **B** and **H** = diakinesis; **C** and **I** = metaphase I; **D** and **J** = anaphase I; **E** and **K** = metaphase II; **F** and **L** = anaphase II. Arrowheads indicate univalents. Scale bar = 5 μ m.

4.2.4 Synapsis and the chromosome axis appear normal in *AtSMC4^{+/-}*

Subtle axis defects in prophase I are not always easy to indentify in DAPI stained chromosome spreads, therefore further investigation of the chromosome axes in the *AtSMC4^{+/-}* plants was carried out using immunolocalisation experiments on spread chromosome preparations. Experiments were carried out on wild-type and *AtSMC4^{+/-}* plants using antibodies specific to the axis associated protein *AtASY1* (Caryl *et al.*, 2000) as well as the SC TF protein *AtZYP1* (Higgins *et al.*, 2005). In wild-type meiosis *AtASY1* is first seen on the chromatin at leptotene as a continual signal along the axes and remains associated with the axis from leptotene until late pachytene. *AtZYP1* is first detected at leptotene as numerous foci marking the sites of DSBs. *AtZYP1* polymerises throughout zygotene until it is fully polymerized between the homologous chromosomes at pachytene (Figure 4.5: A-F). In *AtSMC4^{+/-}* *AtASY1* appears on the axis in leptotene as in wild-type and *AtZYP1* appears to polymerise along the axis forming the SC in a manner indistinguishable from wild-type (Figure 4.5: G-L).

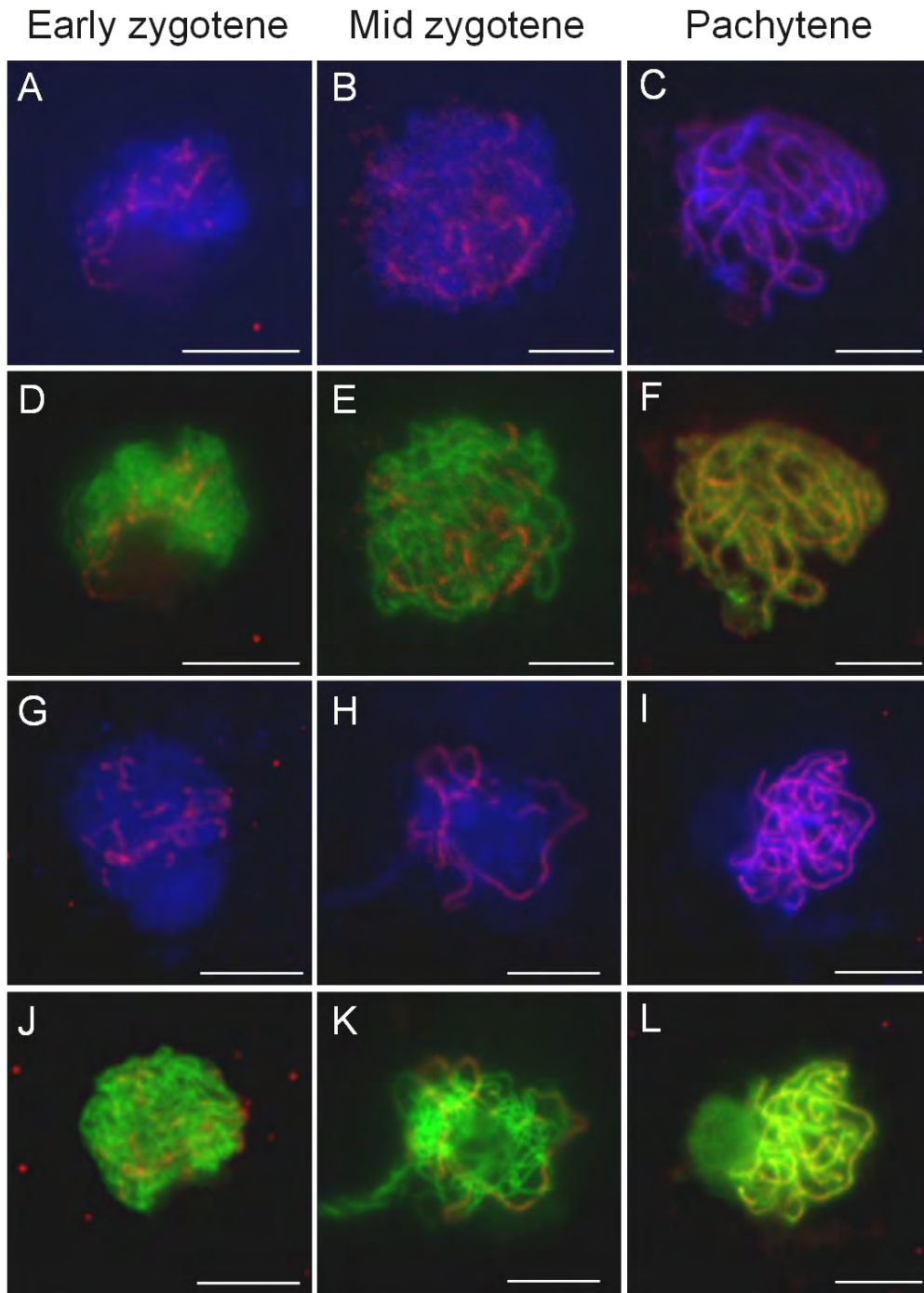


Figure 4.5: Immunolocalization of *AtASY1* (FITC green) and *AtZYP1* (Texas red) on *AtSMC4*^{+/+} and wild-type PMCs. Chromosomes were counter-stained with DAPI. **A-F** = wild-type; **G-L** = *AtSMC4*^{+/+}. **A-C** and **G-I** = DAPI/*AtZYP1* merge; **D-F** and **J-L** = *AtASY1*/*AtZYP1* merge. Cell stages are indicated above column. Scale bar 5 μ m.

4.2.5 RNA interference: a form of post-transcriptional gene silencing

Due to the apparent lethality of homozygote *Atsmc4* mutants an RNAi approach was adopted in order to reduce the level of *AtSMC4*. RNA interference (RNAi) is a form of post-transcriptional gene silencing used to knock-down the amount of a target protein by acting on its mRNA (Fire *et al.*, 1998). RNAi knock-down can be achieved by different approaches. In the method adopted here a construct containing sense and antisense fragments of the target gene is introduced into the plant genome. When expressed the sense and antisense sequences base-pair to form a double-stranded RNA structure known as hairpin RNA (see Figure 4.6). This double stranded RNA is recognised by the cell and broken down into 21-25 nt fragments by the DICER enzyme (Hamilton and Baulcombe, 1999). The sense strands of the 21-25 nt fragments are then targeted to the mRNA of the target gene by the RISC protein complex in a sequence dependent manner. This leads to destruction of the target mRNA and therefore a reduction of the target protein (Fire *et al.*, 1998) (Figure 4.6). RNAi can result in a reduction of target protein in the plant often to mimic null phenotypes as well as hypomorphic phenotypes which can provide valuable insight into the function of a particular gene (for review see (Ketting, 2011)). RNAi is a valuable technique when the protein of interest is essential for the viability of the organism so null mutants cannot be analysed. Tissue specific knock-down can also be achieved in many organisms using promoters which are specific to certain tissue types (reviewed by (Mansoor *et al.*, 2006). However the robustness of tissue-specific knock down in plants is debated due to small RNA molecules being transported through the phloem via plasmodesmata (Dunoyer, 2010) and reviewed by (Baulcombe, 2004; Voinnet, 2005). Inducible promoters are also available which allow the investigator to turn the expression of the RNAi construct on and off as

required, this can allow greater flexibility in experimental design (Masclaux *et al.*, 2004).

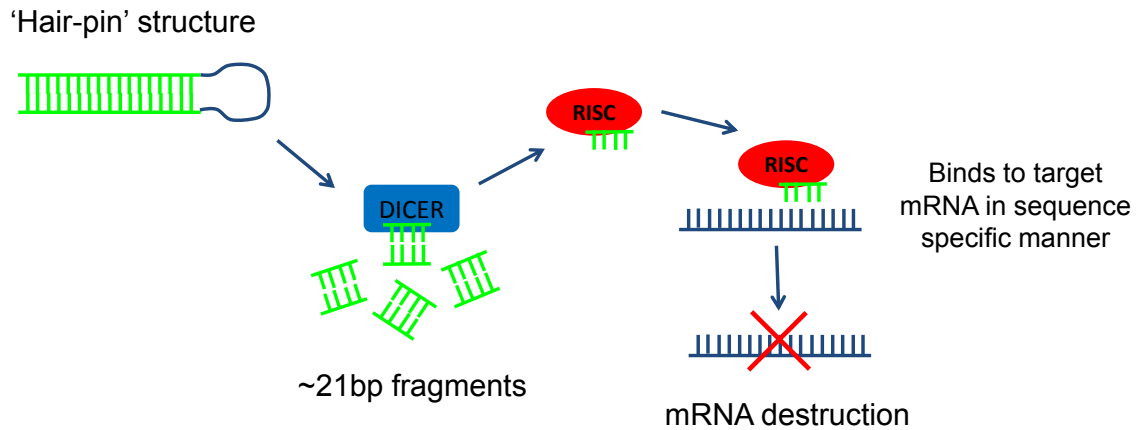


Figure 4.6: Simplified mechanism of RNA interference: double stranded RNA in a 'hair-pin' structure is digested into ~21 bp fragments by the endogenous DICER protein. The fragments are then recognised by the RISC complex which targets them in a sequence-specific manner to the target mRNA. This double-stranded RNA structure is then destroyed by the cell, preventing it from being translated into protein.

4.2.6 Choosing and cloning the *AtSMC4* sense and antisense sequence

To produce an RNAi construct against *AtSMC4*, a 387 bp sequence in the middle region of *AtSMC4* mRNA was selected (between base 1633 and 2020). This sequence was checked for its lack of similarity to other sequences in order to reduce the chances of “off-site” effects caused by the RNAi construct. Two copies of this sequence, one in the sense orientation and one in the antisense were amplified from wild-type leaf cDNA by PCR and cloned into the pDrive vector for sequencing. The sense fragment was cloned with *XhoI* and *EcoRI* restriction sites flanking the desired sequence. The antisense fragment contained *HindIII* and *BamHI* sites. When the sequence was confirmed to be the correct fragment and without nucleotide mutations the sense and antisense fragments were separately subcloned into the pHANNIBAL cloning vector in two successive cloning steps. The sense and antisense fragments are cloned in such a way as to have an approximately 800 bp intron between the sequences. The presence of the intron increases the efficiency of the RNAi by facilitating the formation of the hairpin structure (Hirai *et al.*, 2007). A 2400 bp fragment (containing the *AtSMC4* sense and antisense fragments, the 800 bp intron and the terminator) was then subcloned into to the pPF408 binary vector (Siaud *et al.*, 2004). pPF408 contains the meiosis specific DMC1 promoter (Klimyuk and Jones, 1997) allowing investigation of the role of *AtSMC4* more specifically in meiosis. pPF408 also contains chloramphenicol and BASTA (DL-Phosphinothricin) resistance cassettes.

The pPF408 construct containing the sense and antisense fragments of *AtSMC4* (Figure 4.7) was transformed into *Agrobacterium tumefaciens*. Positive colonies were then cultured and used to transform wild-type *Arabidopsis*. The pPF408

plasmid without any insert was also transformed into wild-type *Arabidopsis* as a control for the transformation procedure.

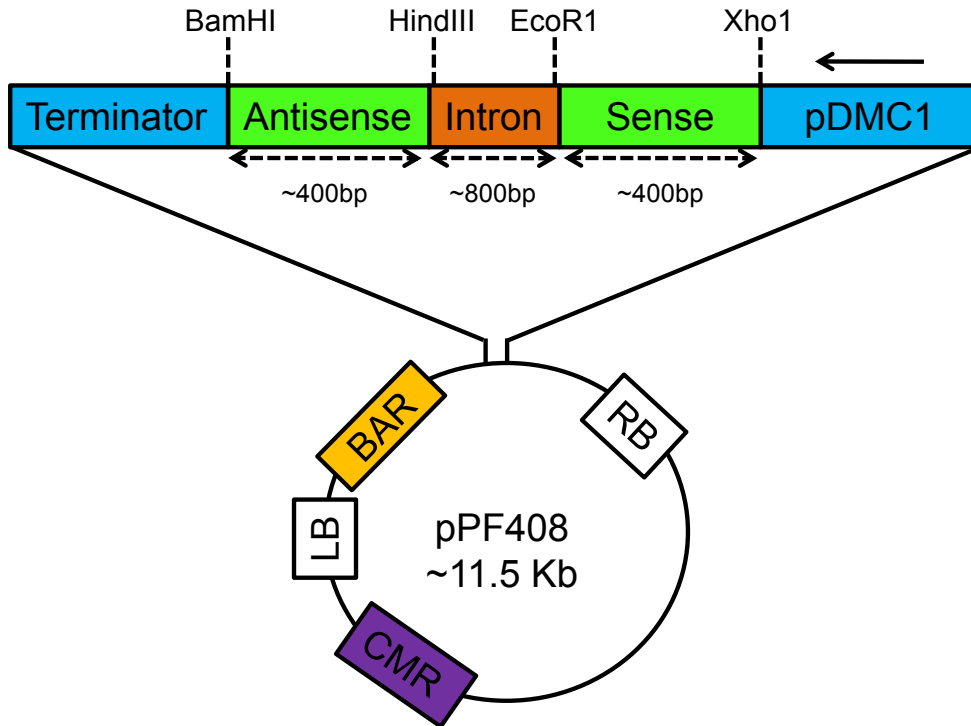


Figure 4.7: Schematic representation of the *RNAi* construct designed to deplete mRNA levels in meiotic cells. BAR= BASTA resistance cassette. CMR = chloramphenicol resistance cassette. LB and RB = left and right borders respectively. All sequence between the LB and RB is inserted into the plant upon transformation. Restriction sites used to close the sense and antisense fragments are indicated.

4.2.7 Screening of pPF408-empty lines

Inserting DNA into the genome of a plant can sometimes cause chromosome rearrangements (Nacry *et al.*, 1998). Therefore in order to control for these artefacts, plants were transformed with the pPF408 plasmid containing no insert. This would allow any phenotype caused by the transformation of the plasmid itself to be distinguished from those caused by the RNAi depletion of condensin subunits. Seeds from plants transformed with the pPF408 empty vector were plated on Murashige and Skoog (MS) agar plates containing BASTA. Plants which survived selection, as ascertained by the growth of true leaves, were transplanted to soil for further analysis. 160 BASTA resistant plants were obtained in this original screen. Buds were collected from all plants after which they were left to set seed. When the siliques had dried all plants were scored by eye for signs of reduced fertility; gaps in their siliques or short siliques compared to wild-type. Although the majority of transformants had normal seed set, 6 plants were identified in this screen which showed signs of reduced fertility. Seed set was measured in these lines. Figure 4.8 shows the fertilities of these 6 lines compared to wild-type.

Since this reduced fertility may indicate a problem in meiosis, a cytological analysis on PMC was carried out on these 6 lines (plants 38, 47, 69, 111, 140, and 142). Lines 140 and 142, both of which had the most severe fertility reduction were found to have defects in meiosis. Prophase I appeared normal in both lines however at diakinesis and later at metaphase I connections were observed between non homologous chromosomes. These multivalents involved 2 chromosomes (Figure 4.9). Line 142 also showed missegregation at the tetrad stage. In addition to these

chromosome defects, line 142 had a fasciated stem, however all other aspects of development appeared normal. Line 140 exhibited no apparent developmental defects.

The remaining 4 lines, (38, 69, 47, 111) did not show any defects in meiosis suggesting that the fertility defect may have been due to other factors. In line 69 several siliques on the main inflorescence were very short containing no seeds, these siliques clustered in the middle section of the main inflorescence. All remaining siliques on the plant had wild-type seed-set. Lines 47, 111 and line 38 appeared normal however these plants appeared to have died before the seed pods had dried, possibly due to poor survival after transplantation to soil. This is likely to have resulted in the reduced seed set observed in these lines.

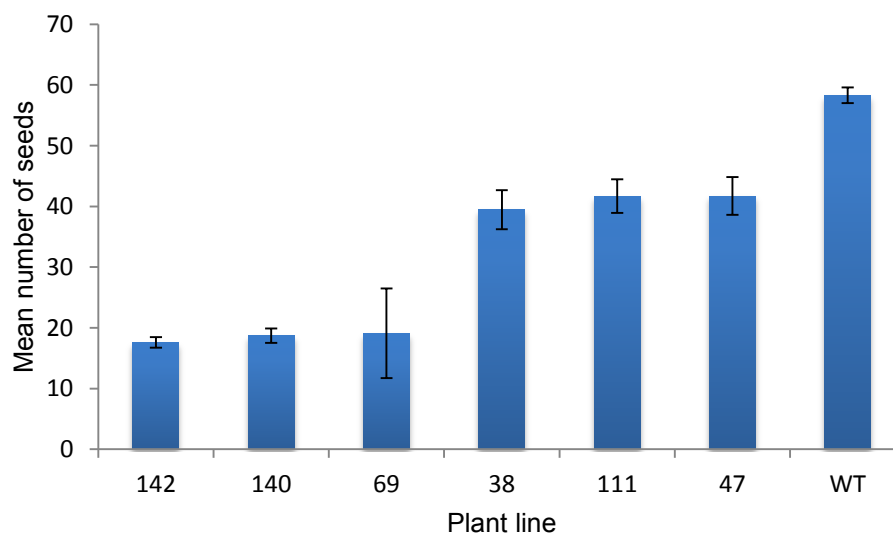


Figure 4.8: Mean seed set in pPF408 empty vector plants which showed signs of reduced fertility. 10 siliques from each plant were scored. Error bars = Standard error of the mean.

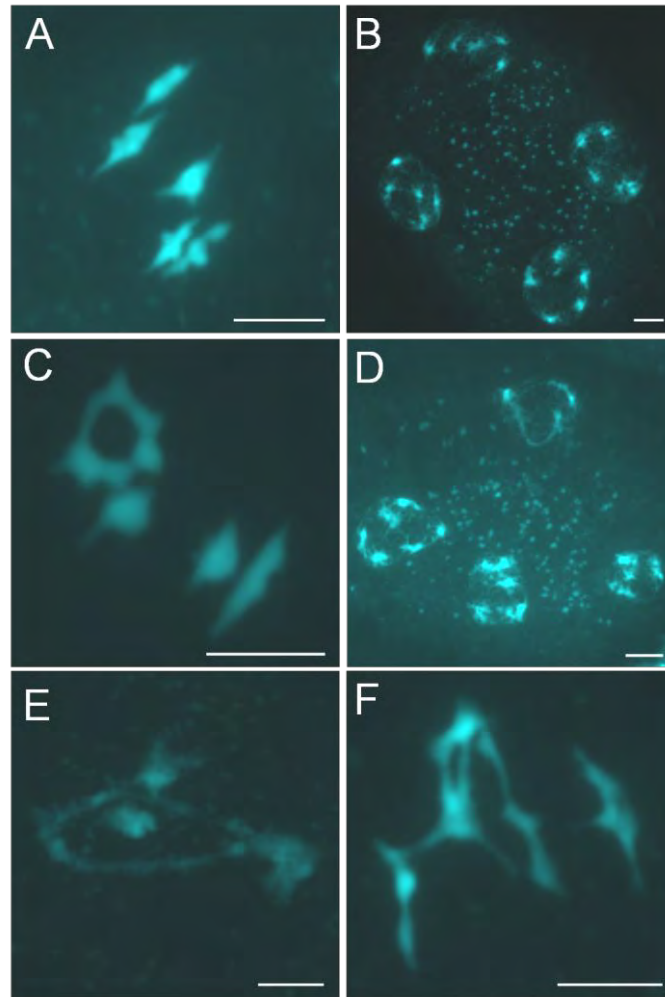


Figure 4.9: Meiotic phenotypes of pPF408 empty vector transformed plants. Chromosome PMC spreads stained with DAPI. **A - B** = wild-type; metaphase I and tetrad stage respectively. **C - D** = empty vector control line 142; metaphase I and tetrad respectively. **E** and **F** = empty vector control line 142; diakinesis and metaphase I respectively. Scale bar 5 μ m.

4.2.8 Initial screening of AtSMC4^{RNAi} lines

Seeds from plants dipped with *Agrobacterium* containing the pPF408-AtSMC4^{RNAi} construct were grown on soil and sprayed with BASTA in order to select for transformed plants. Around 80 BASTA resistant plants were recovered from this selection. Approximately one-third of these plants had a clear somatic phenotype. These plants had small rosette leaves and few secondary inflorescences. Cauline leaves were small and curled and the plants themselves were small in stature (Figure 4.10). Buds from all transformants were collected and fixed in Carnoy's solution for cytological analysis of meiotic defects. The AtSMC4^{RNAi} lines were then left to set seed so that fertility could be assessed at 60 days after planting. Fertility was screened visually and any plant with gaps in its siliques was analysed for meiotic phenotypes. 14 plants had signs of reduced fertility. These plants could be divided into 2 groups: group 1 contained 6 plants which had reduced fertility and no somatic phenotype, group 2 contained 8 plants which had reduced fertility and had the vegetative defects previously described.



Figure 4.10: *AtSMC4^{RNAi}* plants showing developmental defects. **A** = wild-type Columbia (Col-0) ecotype; **B-D** = *AtSMC4^{RNAi}* plants varying in vegetative phenotype; **E** = wild-type rosette leaves; **F** = *AtSMC4^{RNAi}* plant showing small rosette leaves.

4.2.9 Checking for the presence of the RNAi insert by PCR and cloning of the PCR band

The presence of the RNAi construct in the BASTA resistant plants was confirmed by PCR using 2 sets of primers specific to the RNAi construct. The first set of primers amplified the sense fragment from the DMC1 promoter to the intron (using DMC pro primer- and pHan seq rev: see appendix, table 8.2) and the second reaction amplified the antisense fragment from the intron to the terminator (using primers pHan seq for and pHan seq rev 2: see appendix, table 8.2). PCR bands obtained from each set of primers were cloned into pDrive and sequenced to confirm they corresponded to the RNAi construct. Figure 4.11 shows the sequences obtained from cloning the sense and antisense bands.

A

5'-TTGTTTCGGATTCATAGAGCTGAAGAAACGAGATCTCTCGAGAAGAGTCAGAATGAGGTTTTGAA
 GGCAGTTTTAAGAGCGAAGGAGAACAATCAAATTGAAGGAATATATGGAAGGATGGGGGACTTAG
 GTGCCATTGATGCAAATACGATGTCGCCATATCAACTGCGTGCGCCGGCCTTGATTACATTGTTGTT
 GAAACAACCTTCTTCAGCACAAGCATGTGTTGAGCTGCTGCGGAAGGAAATCTTGGCTTTGCAACAT
 TTATGATATTGGAAAAACAAACAGATCATATACATAAACTGAAGGAGAAAGTGAAAACACAGAGG
 ATGTACCACGCCTCTTTGATCTTGTGAGAGTTAAGGATGAAAGGATGAAACTTGCATTCTATGCAGC
 CTTGGGAAACACTGTTGTGGCAAAGGAATTCGGTACCCCAGCTTGGTAAGGAAATAATTATTTTCTT
 TTTTCCTTTTAGTATAAAATAGTTAAGTGATGTTAATTAGTATGATTATAATAATATAGTTGTTATAAT
 TGTGAAAAAATAATTTATAAATATATTGTTTACATAAAACAACATAGTAAT-3'

B

5'-AAATGGATTGACTATTAATTAATGAATTAGTCGAACATGAATAAACAAGGTAACATGATAGATC
 ATGTCATTGTGTTATCATTGATCTTACATTTGGATTGATTACAGTTGGGAAGCTGGGTTCGAAATCGA
 TAAGCTTGGCCACAACAGTGTTCCTCAAGGCTGCATAGAATGCAAGTTTCATCTTTCATCTTAACCT
 TGACAAGATCAAAGAGGCGTGGTACATCCTCTGGTGTTCCTTCTCCTTCAGTTTATGTATATGA
 TCTGTTTGTTCCTCAATATCATAAATGTTGCAAAGCCAAGATTTCCCTTCCGCAGCAGCTCAACACAT
 GCTTGTGCTGAAGAAGTTGTTTCAACAACAATGTAATCAAGGCCGGCGCACGCAGTTGATATGGCG
 ACATCGTGTTCATCAATGGCACCTAAGTCCCCATCCTTCCATATATTCCTTCAATTTGATTGTTCT
 CCTTCGCTCTTAAACTGCCTTCAAACCTCATTCTGACTCTTCTCGGATCCTCTAGAGTCCTGCTTAA
 ATGAGATATGCGAGACGCCTATGATCGCATGATATTGCTTTCAATTCTGTTGTGCACGTTGTAAAAA
 ACCTGAA-3'

Figure 4.11: Sequence of PCR product obtained from *AtSMC4*^{RNAi} plants using insert specific primers. **A** = DMC1 promoter - intron reaction (sense fragment). **B** = Intron-terminator reaction (antisense fragment). Green = DMC1 promoter sequence. Red = sense and antisense *AtSMC4* sequence. Light blue = intron sequence. Dark blue = terminator sequence. Restriction sites are highlighted in yellow (top to bottom: *XhoI*, *EcoRI*, *HindIII*, *BamHI*).

4.2.10 Screening transformants for meiotic phenotypes

Initially the lines with a normal developmental phenotype and reduced fertility were assessed for meiotic defects (group 1: lines 2.6, 5.3, 5.6, 7.4, 7.5, 9.4). 3 of these lines (5.3, 7.4, and 9.4) showed no meiotic defects; therefore other factors may have resulted in the 30% reduction in fertility compared to wild-type in these plants. 2 of the 6 lines, 2.6 and 5.6, had metaphase connections similar to those observed in the empty vector control, hence it could not be excluded that the defects was unrelated to the *AtSMC4 RNAi* construct. For this reason these plants were excluded from further analysis. These 2 plants had fertilities of ~25 and 30% of wild-type level respectively. In addition to this empty-vector control-like phenotype, line 2.6 also had thin threadlike chromatin between segregating chromosomes at anaphase I and II. Line 7.5 shared this phenotype, albeit weakly, however its fertility was severely affected at only 10% of wild-type that it is likely that other factors may be causing the reduction in fertility. No other meiotic defects were observed in this plant.

The 8 plants which had developmental defects and reduced fertility (group 2: 1.6, 2.9, 2.10, 6.2, 7.2, 7.6, 9.3, 9.6) were also screened for meiotic phenotype. 7 of the lines (1.6, 2.9, 2.10, 6.2, 7.2, 7.6, and 9.3) shared the same phenotype. Prophase I in each line appeared normal (Figure 4.12: G), however at metaphase I the chromosomes appeared elongated compared to wild-type (Figure 4.12: compare B and H). At the anaphase stage of both meiotic divisions the chromosomes appeared diffuse and thin curtains of chromatin were seen to span the space between the segregating chromosomes (Figure 4.12: I). Metaphase II chromosomes also appeared misshapen in several of the lines analysed. Thin bridges at the dyad stage

were observed in some lines which appeared to link the 2 sets of homologous chromosomes, presumably showing anaphase I defects which were not properly resolved (Figure 4.12: J, arrowhead). These phenotypes were distinct from those of the empty vector control plants. A few plants with no clear reduction in fertility were also assessed cytologically. 1 line with no somatic defect (line 6.1) and 1 line with the somatic defect (line 1.3) were identified which had thin anaphase bridges, however the phenotype appeared weaker in these lines.

4.2.11 Mitotic defects in *AtSMC4^{RNAi}* lines

Due to the somatic defect in many of the *AtSMC4^{RNAi}* lines it was thought that this may be due to *AtSMC4* transcript being knock-down in somatic cells as well as meiotic. To investigate this, mitotic cells in these lines were viewed on DAPI stain chromosome spreads. It was found that at mitotic anaphase the chromosomes appeared to have defects in segregation such that chromatin was seen to lag behind the segregating chromosomes (Figure 4.13).

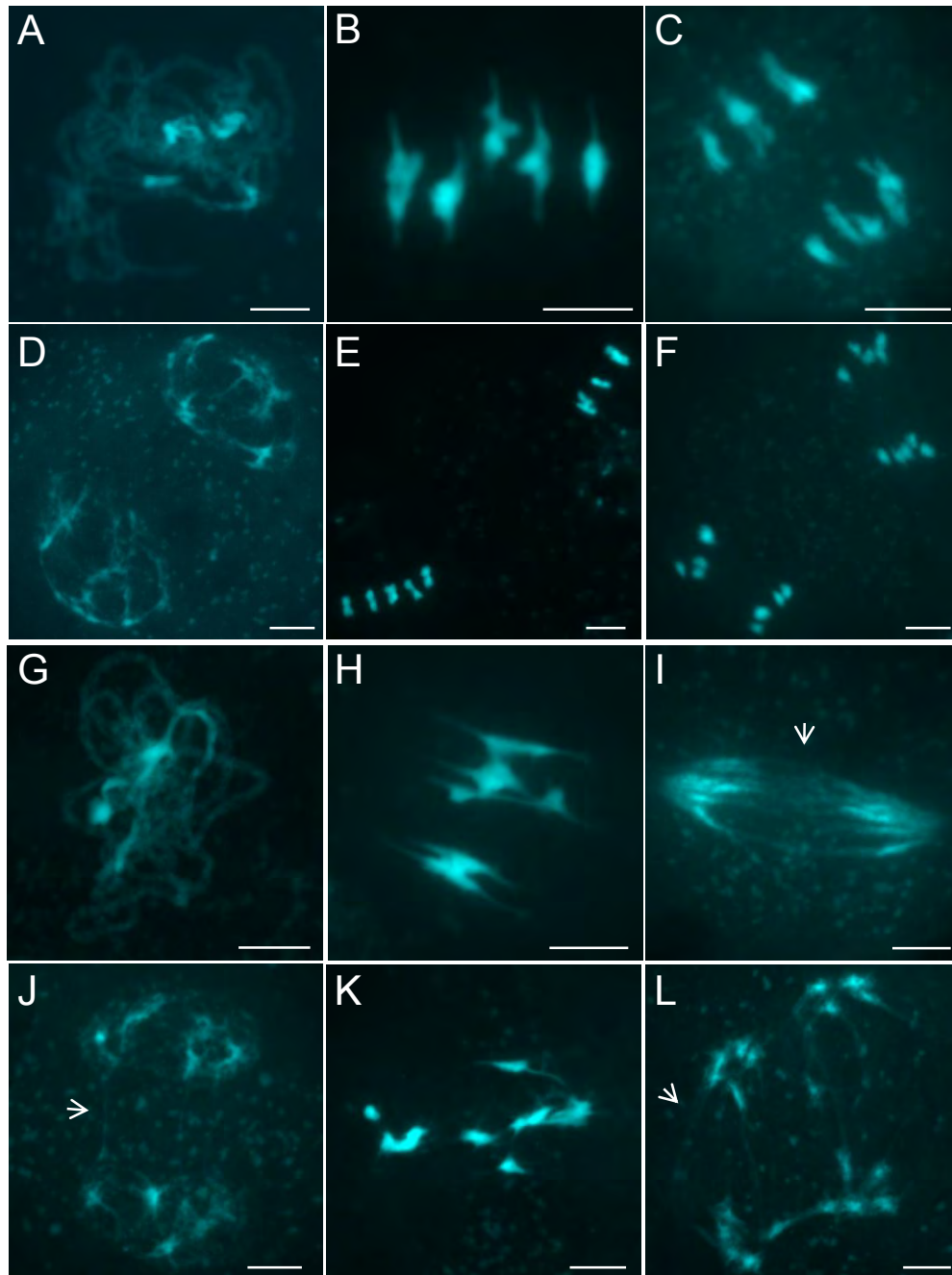


Figure 4.12: Meiotic phenotypes of *AtSMC4*-pPF408 transformed plants. Chromosome spreads PMCs stained with DAPI. **A-F** = wild-type; **G-L** = *AtSMC4*^{RNAi} (**G**= line 2.10; **H - J** = line 1.6; **K -L**= line 2.9). **A** and **G** = pachytene; **B** and **H** = metaphase I; **C** and **I** = anaphase I; **D** and **J** = prophase II (dyad); **E** and **K** = metaphase II; **F** and **L** = anaphase II. Arrowhead = lagging chromatin between segregating chromosomes at anaphase I (**I**), dyad stage (**J**) and anaphase II (**L**). Scale bar 5 μ m.

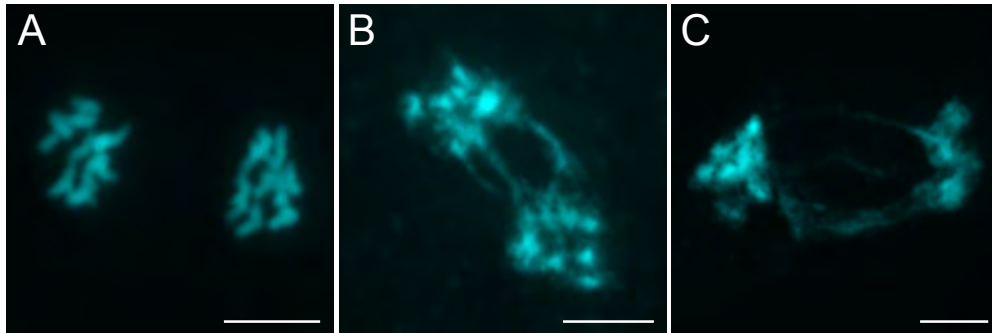


Figure 4.13: Mitotic anaphase stained with DAPI. **A** = wild-type; **B** = *AtSMC4^{RNAi}* line 2.10; **C** = *AtSMC4^{RNAi}* line 6.2. Scale bar 5 μm.

4.2.12 Selection of *AtSMC4^{RNAi}* lines for further analysis

Plant 2.6 was the only plant that was identified that had a normal vegetative phenotype combined with the meiotic phenotype unique to plants containing the *AtSMC4^{RNAi}* construct. Unfortunately its cells also exhibited connections similar to those seen in the empty-vector control, therefore this plant was excluded. Three lines were selected from group 2 (somatic defect and reduced fertility) which had the meiotic phenotype of anaphase defects. These were lines; 2.10, 6.2 and 1.6. All 3 lines were from independent transformation events. Seeds from these lines were grown to T2 from which seed was collected and grown to the third generation on BASTA selective plates in order to find a plant for each line which was homozygous for the construct. Homozygous plants should have 100% survival on MS + BASTA agar. Seeds from 9 plants from line 2.10 were grown, all of which showed an approximately 1:3 segregation of sensitive: resistant plants. For line 6.2 seeds from 8 plants were grown these had a mixture of segregating lines, 4 plants had an approximately 3:1 segregation ratio and one line which had 100% survival on BASTA, the remaining 3 plants had segregation ratios of: 1.9:1, 0.7:1 and 5.5:1, which may suggest multiple inserts or silencing of the resistant cassette. For the line 1.6 seeds from 10 plants were grown on BASTA selective plates, 6 of which appeared to be homozygote and 4 were hemizygotes (all with ~3:1 segregation). A hemizygous plant for line 2.10 and homozygous plants from lines 6.2 and 1.6 were selected for further analysis.

4.2.13 Western blot analysis of extracts from *AtSMC4^{RNAi}* lines

In order to test whether the level of *AtSMC4* protein was knocked-down to a detectable level in the *AtSMC4^{RNAi}* lines, western blot analysis was performed. As mitotic *AtSMC4* should not be knocked-down in the *AtSMC4^{RNAi}* lines, samples needed to be enriched for meiotic cells as much as possible to limit the amount of mitotic *AtSMC4* in each sample. This would increase the likelihood of detecting a difference between *AtSMC4^{RNAi}* lines and wild-type. It was therefore decided that meiotic stage anthers should be used in this assay. First it needed to be established how many anthers would be required to detect an *AtSMC4* signal in wild-type. 250 wild-type anthers at meiotic stages were dissected and transferred into protein extraction buffer. Protein was extracted physically using a pipette tip to break up tissue and freeze thawing samples 2-3 times. After boiling for 10 minutes in SDS-containing loading buffer, final suspension buffer (FSB), the extract was divided in half and half again so that extract from approximately 125, 62, and 31 anthers were loaded on an SDS-PAGE gel and transferred to western blot. Wild-type bud protein (8 µg), in which a 150 KDa protein presumed to correspond to *AtSMC4* was detected in previous experiments (section 3.2.10), was loaded as a positive control. Protein was detected using the purified *AtSMC4* antibody. A clear band which ran at ~150 KDa was seen in the 125 anther extract after a 5 minute exposure. Faint bands at the same position were detected in the 62 and 31 anther lanes (Figure 4.14).

Once it had been established that a clear detectable band could be seen in protein extracted from approximately 125 anthers, analysis into the level of *AtSMC4* protein present in anthers of *AtSMC4^{RNAi}* plants was carried out. Approximately 200 meiotic

stage anthers were dissected from 3rd generation *AtSMC4^{RNAi}* lines 2.10, 6.2 and 1.6 as well as wild-type plants. Anthers from 2 wild-type plants and 3 *AtSMC4^{RNAi}* 2.10 plants were collected as duplicate samples to assess variation in the lines. One *AtSMC4^{RNAi}* 6.2 plant and pooled anthers from 3 *AtSMC4^{RNAi}* 1.6 plants were also tested. Protein was extracted as before. As quantification of the protein was not possible with this extraction procedure, an initial loading test was carried out on the anther protein extracts in which 5 µl of each sample (Colx2, 2.10x3, 6.2 and 1.6) was loaded on to a gel and probed with anti-tubulin antibody. The blot was exposed for ~1 second to prevent overexposing the signal. Densitometry was carried out on each sample in order to calculate the relative amounts of protein in each sample. Another SDS-PAGE gel was then loaded with different proportions of the anther protein extract, standardised using the initial loading test. This was transferred to western blot and cut in half between the 70 and 55 KDa markers. The lower half of the blot was probed with anti-tubulin antibody as a loading control and the upper half was probed with *AtSMC4*-antiserum. Figure 4.15 shows the *AtSMC4* band and tubulin loading control for wild-type and *AtSMC4^{RNAi}* lines. *AtSMC4* protein is clearly weaker in the *AtSMC4^{RNAi}* lines compared to wild-type. All three *AtSMC4^{RNAi}* lines tested show a reduction in *AtSMC4* protein levels compared to wild-type. The three separate plants tested from line 2.10 all showed a similar reduction in protein. The tubulin loading control is almost equal across the samples. In order to obtain a more precise estimate of knock-down in the lines, densitometry was carried out and each sample was standardised using the tubulin loading control band intensity. Figure 4.16: (A) shows the relative amount of protein in each sample. All *AtSMC4^{RNAi}* plants tested showed an ~40 % reduction in the amount of *AtSMC4* protein present. Figure

4.16: (B) shows the data with wild-type and *AtSMC4*^{RNAi} 2.10 samples pooled to obtain an average.

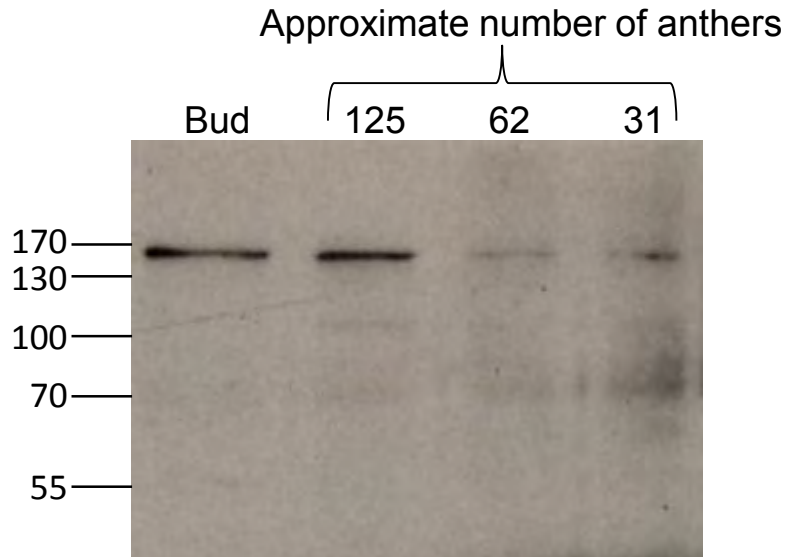


Figure 4.14: Western blot analysis of bud and anther protein extract probed with *AtSMC4*-Ab. Bud protein (8 μ g), and protein from approximately 125, 62 and 31 meiotic stage anthers was loaded on to an SDS-PAGE gel and transferred to western blot. Blot was probed with *AtSMC4*-Ab (1:1000) and detected with anti-rabbit HRP secondary antibody (1:5000). A band at approximately 150 kDa corresponding at *AtSMC4* is detected in all samples.

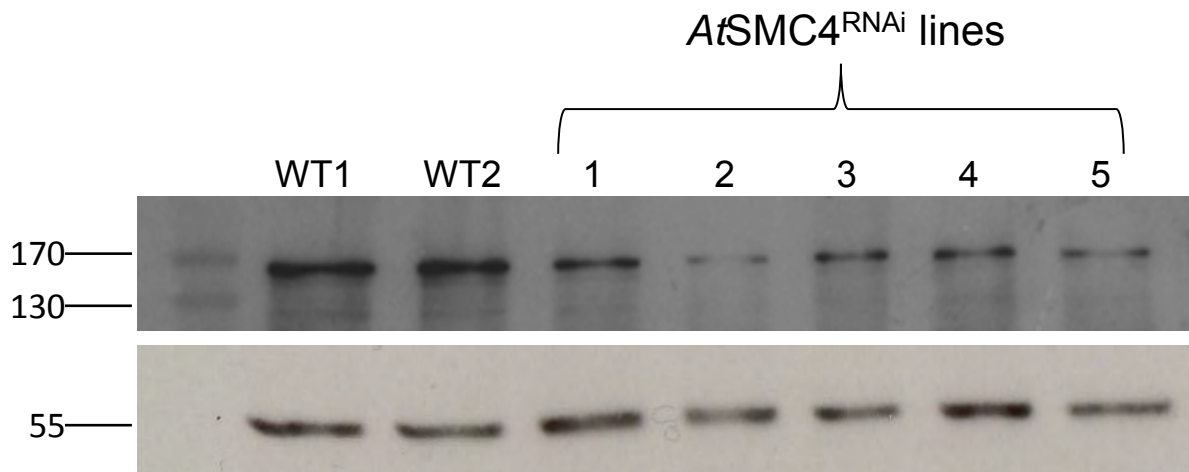


Figure 4.15: Western blot showing relative intensities of *AtSMC4* protein band in anthers from wild-type (WT) and *AtSMC4*^{RNAi} plants (above) with tubulin loading control (below). 1: line 2.10 plant A, 2: line 2.10 plant B, 3: line 2.10 plant C, 4: line 6.2, 5: line 1.6.

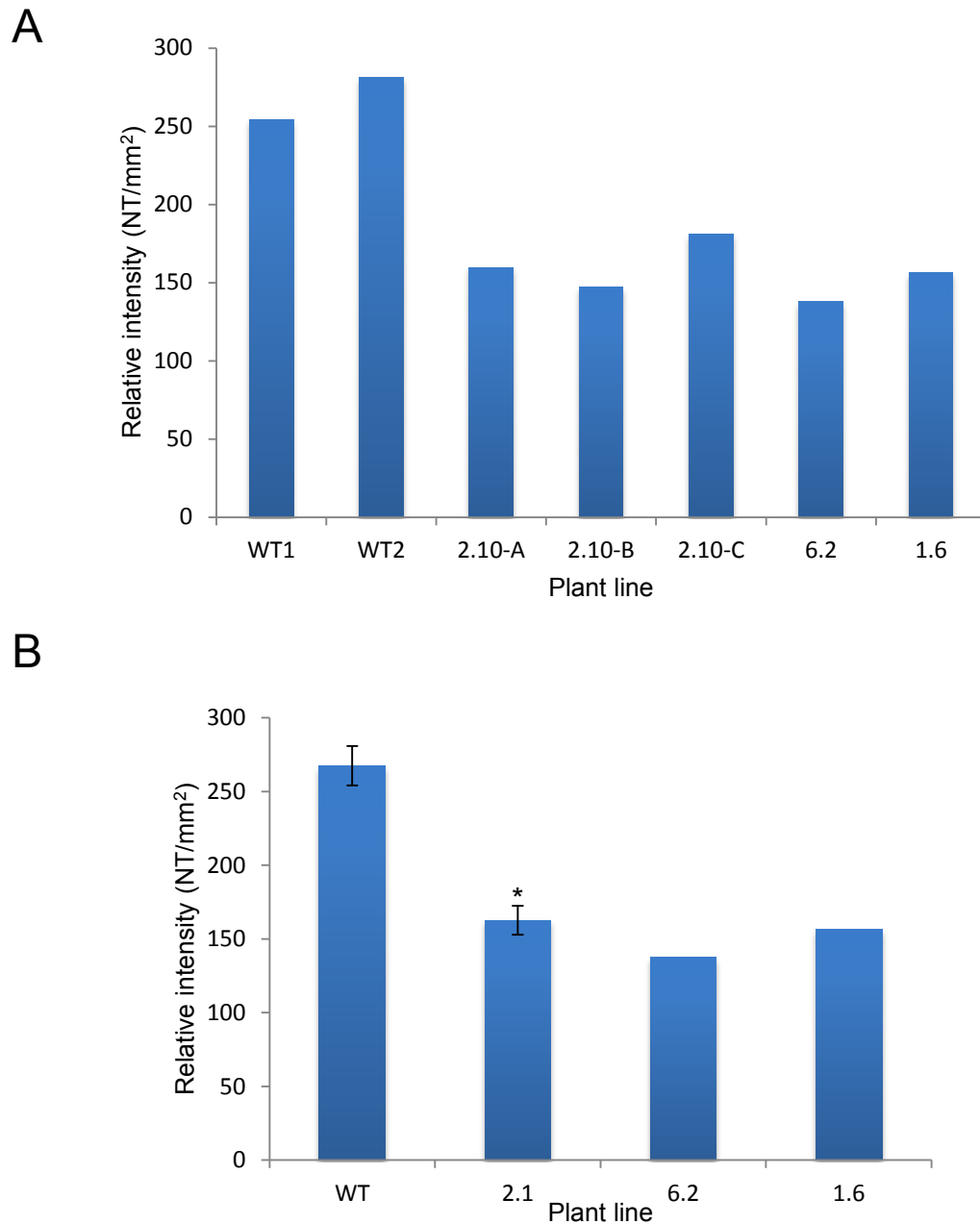


Figure 4.16: Analysis of the relative levels of *AtSMC4* in anthers from wild-type and *AtSMC4*^{RNAi} lines. **A** = Relative intensities of *AtSMC4* protein signal adjusted for tubulin loading control. **B** = Relative intensities of *AtSMC4* protein band adjusted for tubulin loading control showing averages over 2 wild-type and 3 2.10 samples. * = $p < 0.05$. Error bars = Standard error of the mean.

4.2.14 Localisation of AtSMC4-Ab on fixed buds of AtSMC4^{RNAi} lines

Chapter 3 described the production of an antibody specific to AtSMC4 in rabbit. Analysis on wild-type fixed bud material indicated that the antibody strongly stained the chromosomes at metaphase I. The signal remained on the condensed stages throughout meiosis and became faint at telophase. To further confirm that the AtSMC4^{RNAi} lines have reduced levels of AtSMC4, preliminary immunolocalisation analysis was carried out on fixed bud material from wild-type and AtSMC4^{RNAi} lines. This analysis also allows the level of knock down to be assessed purely in meiocytes without AtSMC4 levels in surrounding somatic cells affecting the results (as with the western analysis on anthers).

Analysis was primarily carried out on line 2.10. AtSMC4 antibody does not appear to localise on AtSMC4^{RNAi} lines at metaphase I when in wild-type it localises over the entire chromatin (Figure 4.17). These preliminary results suggest that AtSMC4 does not localise to meiotic cells in AtSMC4^{RNAi} lines. It was observed that the chromosomes in the AtSMC4^{RNAi} lines appear to become more diffuse when using this immunolocalisation technique than under standard cytological techniques. This was not observed for wild-type. This may be due to soaking the buds in water overnight after digestion thus causing them to swell as is seen when hypotonic treatment is applied to condensin mutants in other species (Ono *et al.*, 2003; Savvidou *et al.*, 2005).

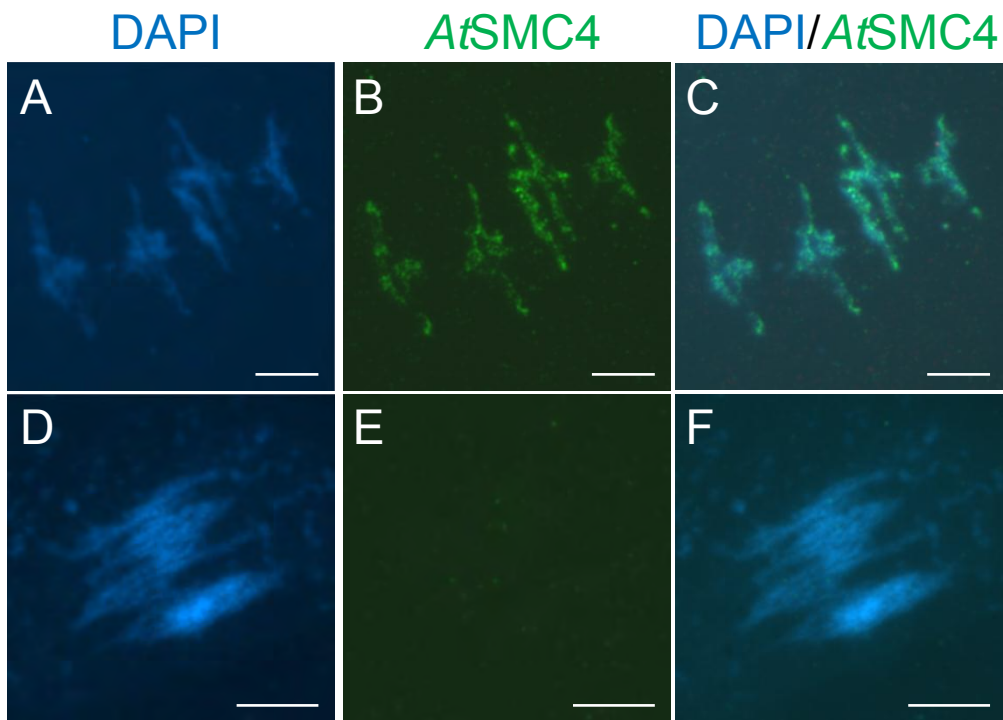


Figure 4.17: Immunolocalisation of *AtSMC4*-Ab on *AtSMC4^{RNAi}* line 2.10 and wild-type PMCs at metaphase I. Chromosomes counter-stained with DAPI. **A-C** = Wild-type; **D-F** = *AtSMC4^{RNAi}* 2.10. Scale bar = 5 μ m

4.2.15 Detailed phenotypic analysis of selected lines

Preliminary cytological analysis revealed chromosome abnormalities in the AtSMC4^{RNAi} lines. These plants also showed a reduction in fertility, resulting in gaps where seeds were absent. During the course of analysing line 1.6 it became apparent that its phenotype often appeared to be silenced. For this reason line 1.6 was not included in all analysis and is therefore not included here.

4.2.15.1 Fertility and pollen viability of AtSMC4^{RNAi} lines

In order to quantify the reduction in fertility observed in the initial screening of the first generation of plants seed silique length and seed number were scored in AtSMC4^{RNAi} plants 2.10 and 6.2 and compared to wild-type plants. Seed set results are shown in Figure 4.18. Both lines 2.10 and 6.2 show a significant reduction in both silique length and seed set compared to wild-type ($p < 0.005$ for both lines, t -test). Line 2.10 had a 11% reduction in silique length compared to wild-type and line 6.2 had a 10% reduction. Line 2.10 had a 29% reduction in seed set compared to wild-type and line 6.2 had a 51% reduction. In this assay line 6.2 had a lower overall fertility compared to line 2.10 ($p < 0.005$, t -test). The pollen viability of the AtSMC4^{RNAi} plants 6.2 and 2.10 was assessed to see if the meiotic defects observed resulted in pollen abortion. Pollen was stained with Alexander stain (Alexander, 1969). Alexander stain contains malachite green which stains cellulose in pollen walls and acid fuchsin which stains pollen protoplasm pink. Pollen which has been aborted early in development (did not develop a protoplasm) appears green and viable pollen stains a deep pink colour. Two plants from each genotype were used in this analysis and the results pooled. Wild-type slides contained a large proportion of

viable pollen at a ratio of viable to not viable of 138.6:1 (n=4927). More pollen in *AtSMC4^{RNAi}* lines 2.10 and 6.2 was non-viable. In line 2.10 the ratio of viable to non-viable pollen was 89:1 (n=5261) and in 6.2 the ratio was 28:1 (n=1546).

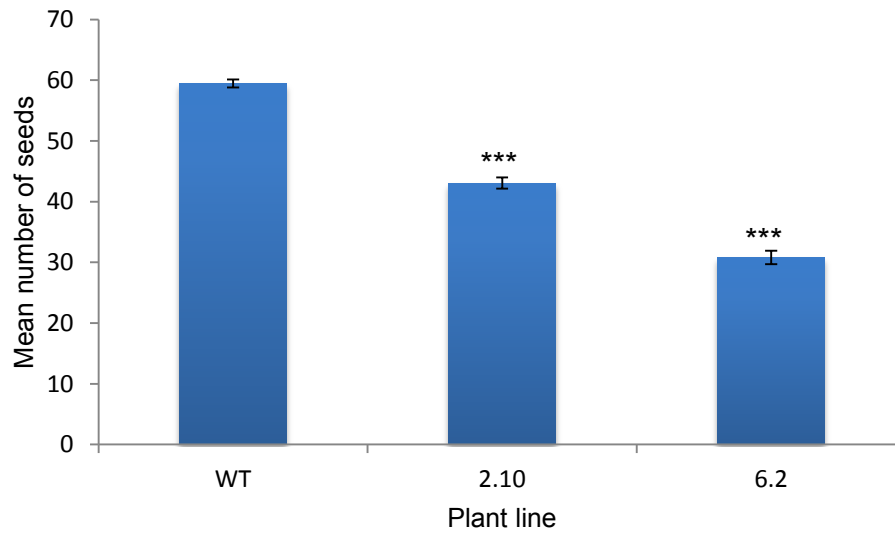
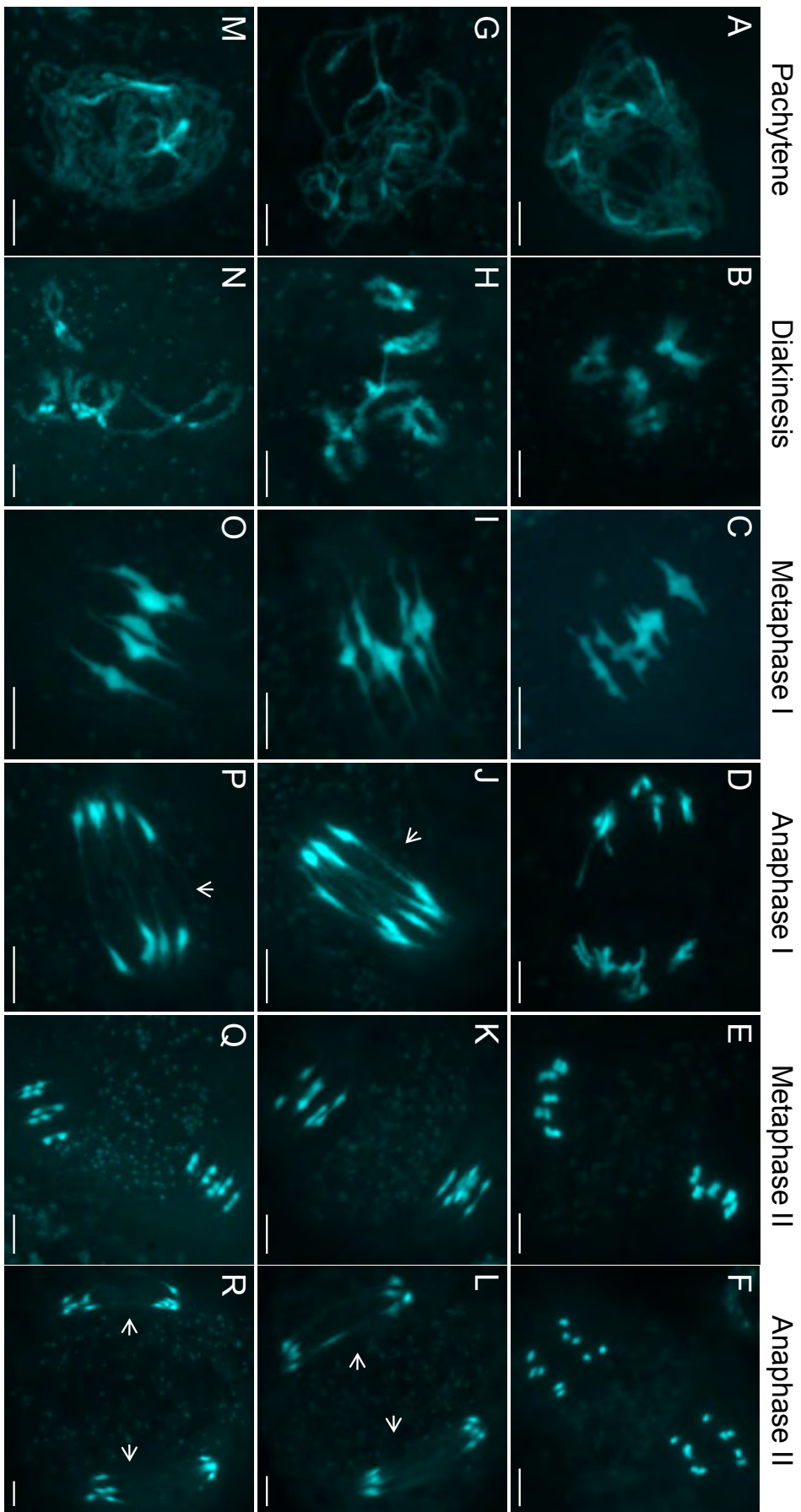


Figure 4.18: Mean seed set in wild-type and *AtSMC4^{RNAi}* lines. WT = wild-type (n=10), *AtSMC4^{RNAi}* lines 2.10 (n=8) and 6.2 (n=13). 10 siliques were counted per plant. *** = p<0.005. Error bars = Standard error of the mean.

4.2.15.2 Full cytological atlas of AtSMC4^{RNAi} lines

Many phenotypes relating to chromosome organisation were observed in the initial screen of AtSMC4^{RNAi} lines. To assess the cytological phenotype of AtSMC4^{RNAi} lines in more detail, a full cytological analysis was carried out on the 3rd generation of lines 2.10 and 6.2. The phenotypes which were observed in the initial screen were confirmed for both AtSMC4^{RNAi} lines. Chromosomes appeared indistinguishable from wild-type throughout prophase I (Figure 4.19: A, G, M). However at metaphase I, when the chromosomes were highly compact in wild-type, the chromosomes in the AtSMC4^{RNAi} lines appeared elongated (Figure 4.19: C, I, O). At anaphase I when the chromosomes segregated to opposite pole in wild-type, multiple thin threads of chromatin were seen between segregating chromosomes in the AtSMC4^{RNAi} lines (Figure 4.19: D, J, and P). These were seen between each pair of chromosomes as they segregated. At metaphase II in wild-type the chromosomes are condensed into discrete units, however in the AtSMC4^{RNAi} lines the chromosomes again appeared elongated and misshapen (Figure 4.19: E, K, and Q). Thin curtains of chromatin were again seen between segregating chromosomes at anaphase II which were not seen in wild-type (Figure 4.19: F, L, and R). At tetrad stage chromosomes decondensed as in wild-type.

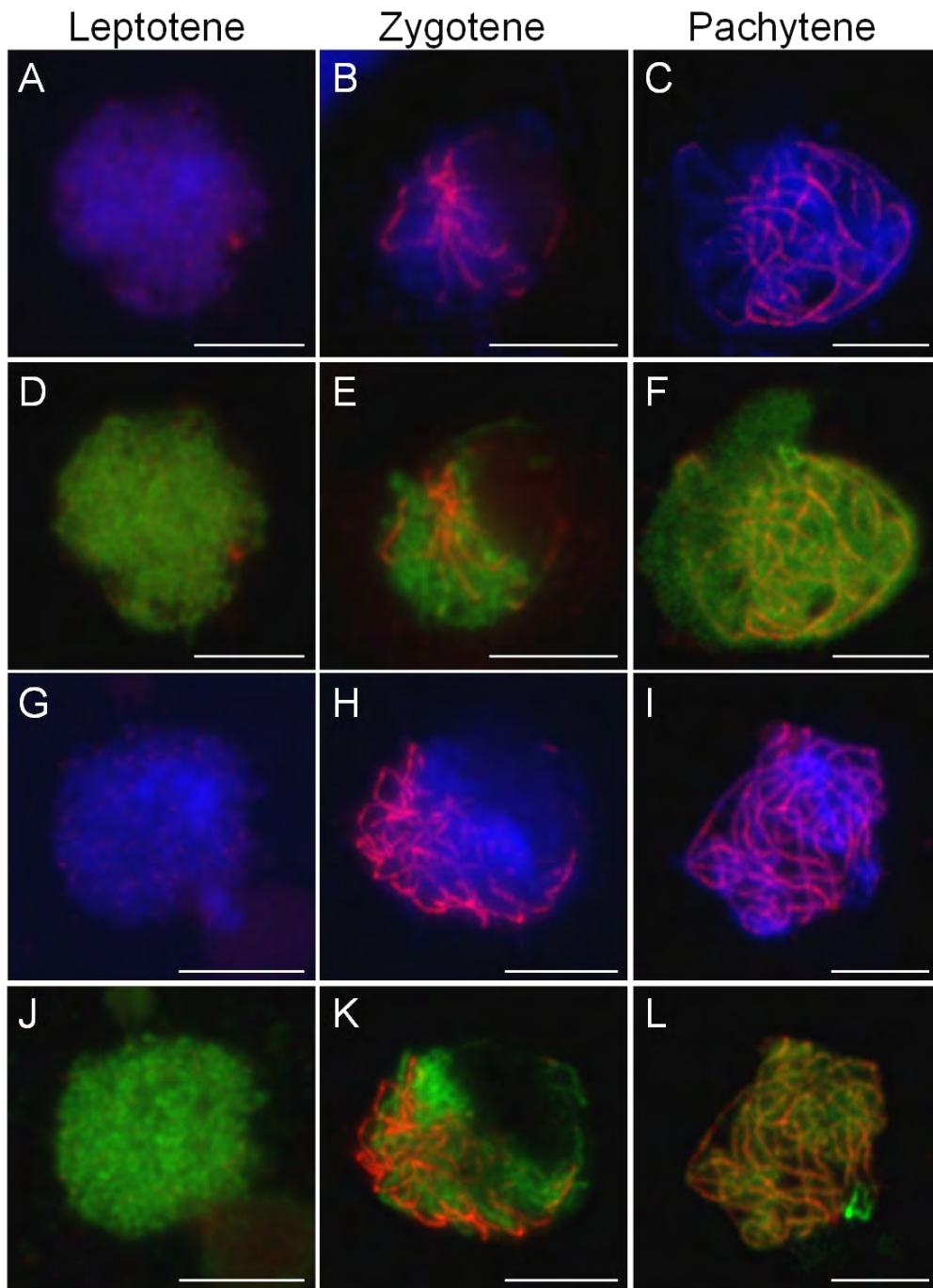
Figure 4.19: Meiotic phenotypes of AtSMC4^{RNAi} lines. Chromosome stained with DAPI. **A-F** = wild-type; **G-L** = AtSMC4^{RNAi} line 2.10; **M-R** = AtSMC4^{RNAi} line 6.2. Cell stages indicated at top of columns. Scale bar = 5 µm.



4.2.15.3 **AtSMC4^{RNAi} lines appeared to have normal prophase I**

chromosome axes

SC assembly is defective in budding yeast condensin deficient strains (Yu and Koshland 2003). In order to assess whether the axes of the *AtSMC4^{RNAi}* lines were aberrant, immunolocalisation was carried out on PMC spread chromosome preparations using antibodies specific to the axis associated *AtASY1* protein (Caryl *et al.*, 2000) and the SC TF protein *AtZYP1* (Higgins *et al.*, 2005). *AtASY1* is seen along the axes in wild-type meiosis and its localisation is aberrant in meiotic mutants such as the meiotic specific cohesin *syn1* mutant (Tiang, unpublished). In wild-type meiosis, at leptotene, *AtASY1* is seen as a continual linear signal along the unpaired chromosomes. As the homologous synapse *AtASY1* signal reduces in areas of synapsis so that by late pachytene the *AtASY1* signal is weaker and more diffuse than in earlier cells. The loading of *AtASY1* on the *AtSMC4^{RNAi}* lines appears indistinguishable from wild-type, suggesting that the underlying axes are not affected severely enough to alter *AtASY1* protein loading in these lines. Synapsis was also investigated in the *AtSMC4^{RNAi}* lines using an antibody specific to the SC TF protein *AtZYP1* on chromosome spreads. In wild-type, *AtZYP1* is seen as numerous foci at the sites of DSBs. Polymerisation occurs along the entire length of the homologous chromosomes so that at pachytene synapsis is complete. Synapsis in the *AtSMC4^{RNAi}* lines also appeared indistinguishable from wild-type suggesting there is no obvious defect in this process.



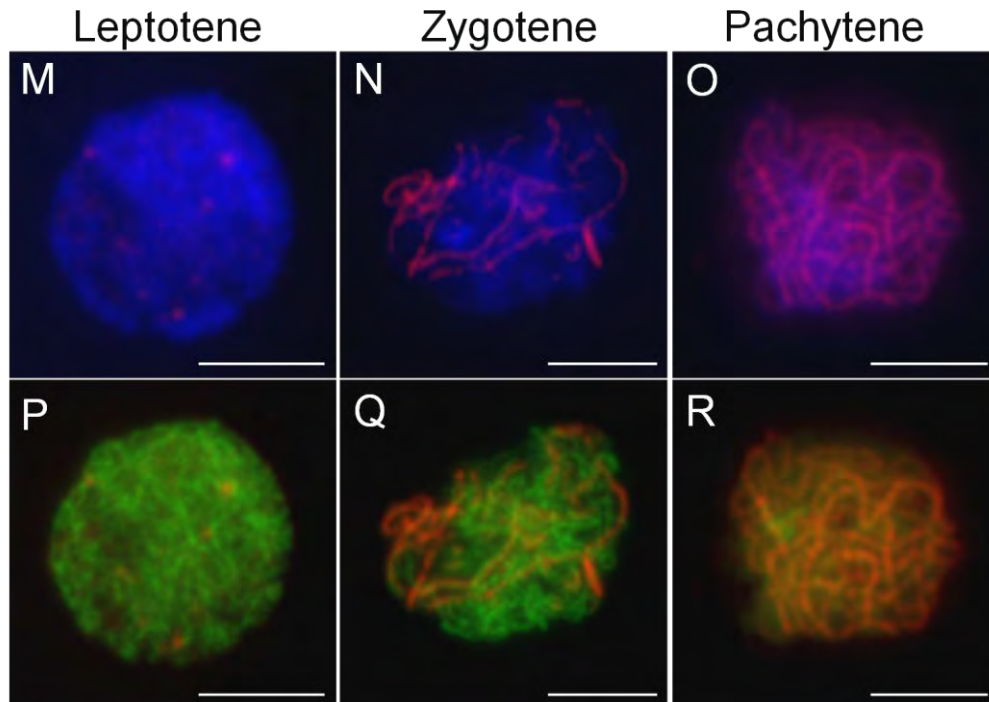


Figure 4.20: Immunolocalization of *AtASY1* (FITC green) and *AtZYP1* (Texas red) on *AtSMC4*^{RNAi} and wild-type PMCs. Chromosomes were counter-stained with DAPI (blue). **A-F** = wild-type; **G-L** = *AtSMC4*^{RNAi} 2.10; **M-R** = *AtSMC4*^{RNAi} 6.2. **A-C**, **G-I** and **M-O** = DAPI /*AtZYP1* merge; **D-F**, **J-L** and **P-R** = *AtASY1*/*AtZYP1* merge. Cell stages are indicated above column. Scale bar 5 μ m.

Condensin knock-down in budding yeast and *C. elegans* leads to an increased axis length during prophase I of meiosis (Yu and Koshland, 2003; Mets and Meyer, 2009). An investigation into the chromosome axes length at pachytene in the *AtSMC4^{RNAi}* lines was carried out. Line 2.10 was selected for this analysis and compared to wild-type axes length. To be able to accurately score the cells and be sure all cells were as close to the same stage as possible an immunolocalisation approach was carried out using the *AtZYP1*-Ab. Only cells in which *AtZYP1* was fully polymerised, as judged by eye, were used for analysis. It was also necessary to only use cells which were sufficiently spread in order to get an unambiguous axis length measurement. Measurements were carried out using the NIS elements.3 software. No significant difference in axes length was seen in *AtSMC4^{RNAi}* line 2.10 (n=27) compared to wild-type (n=33) (p= 0.26 Student's *t*-test) (see Figure 4.21). Taken together these data suggest that the prophase I chromosomes axes are unaffected in the *AtSMC4^{RNAi}* lines.

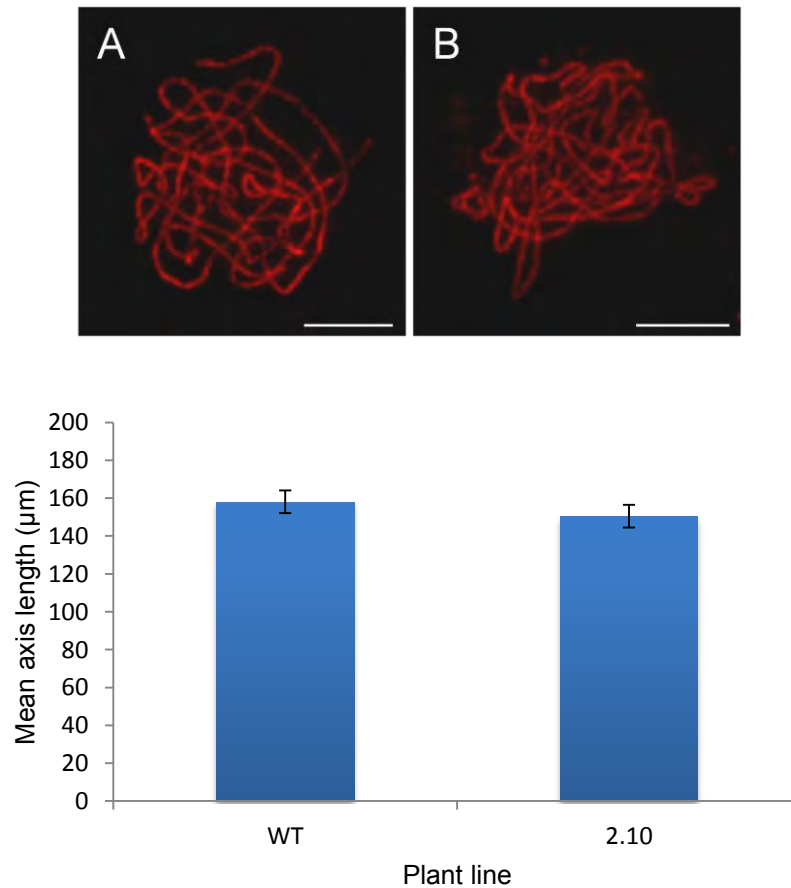


Figure 4.21: Pachytene axes length data for wild-type, and *AtSMC4*^{RNAi} line 2.10. **Top** = Pachytene stage chromosome spread preparations showing continuous loading of *AtZYP1* antibody. **A** = wild-type; **B** = *AtSMC4*^{RNAi} line 2.10. **Bottom** = Mean axis length for wild-type (n=33) and *AtSMC4*^{RNAi} line 2.10 (n=27) pachytene cells. Error bars = Standard error of the mean.

4.2.15.4 **AtSMC4^{RNAi} lines show a slight reduction in chiasmata**

Defects in meiotic recombination have been observed in condensin deficient cells in *C. elegans* (Tsai *et al.*, 2008; Mets and Meyer, 2009), budding yeast (Yu and Koshland, 2003) and possibly *Drosophila* (Resnick *et al.*, 2009). AtSMC4^{+/-} plants also had univalents occurring at a low frequency which suggests a possible recombination defect.

To study if there was an effect on recombination in AtSMC4^{RNAi} lines, metaphase I cells were analysed. At metaphase I, chiasmata are visible allowing the number of COs to be scored. Fluorescent *in situ* hybridisation (FISH) using probes designed against the 45S and 5S ribosomal DNA (rDNA) regions was carried out on slides containing metaphase I cells of wild-type and AtSMC4^{RNAi} lines 2.10 and 6.2. Application of the probes allows the identification of individual chromosomes (Figure 4.22) and facilitates chiasmata scoring. Chiasmata were scored based on bivalent morphology (Sanchez-Moran *et al.*, 2001).

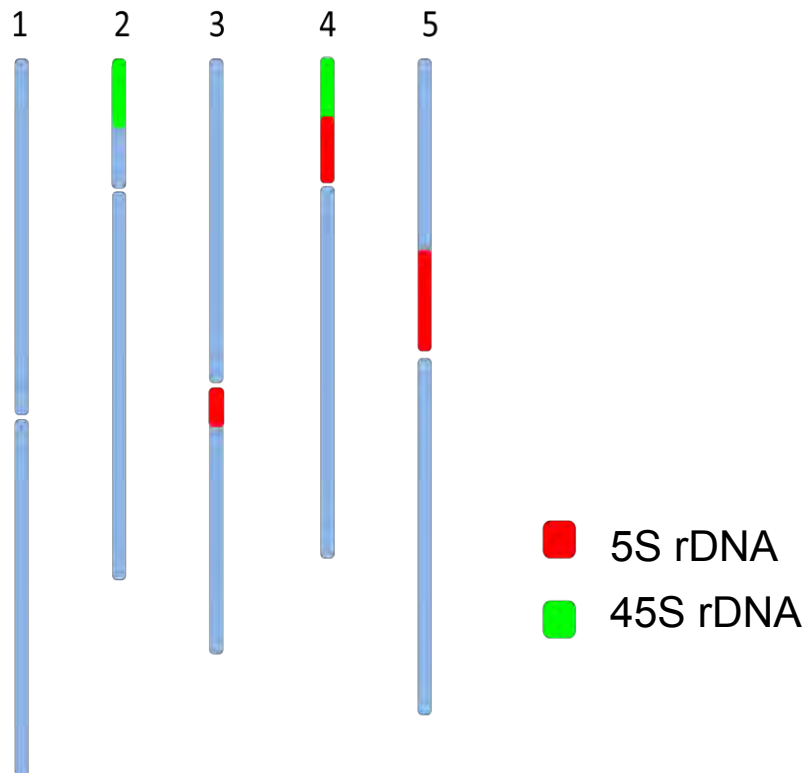


Figure 4.22: Schematic representation of the position and size of the 45S and 5S rDNA probes on *Arabidopsis* chromosomes 1-5.

Chiasmata were scored on metaphase I cells from wild-type, *AtSMC4*^{RNAi} line 2.10 and *AtSMC4*^{RNAi} line 6.2 plants grown at the same time, under the same conditions. This analysis revealed that both *AtSMC4*^{RNAi} lines had a reduction in total chiasmata compared to wild-type. Wild-type had a mean number of chiasmata of 9.05, *AtSMC4*^{RNAi} line 2.10 had a mean of 8.44 and line 6.2 had a mean of 8.15. Both of the means from the *AtSMC4*^{RNAi} lines were shown to be significantly different to wild-type (2.10, $p = 0.043$; 6.2, $p = 0.0057$) (Figure 4.23). In this analysis line 6.2 had a more severe reduction in chiasmata than line 2.10 compared to wild-type. Line 2.10 was only significant to the lowest degree. The two *AtSMC4*^{RNAi} lines were not statistically different from each other when compared in a student's *t*-test. The value for wild-type obtained here is slightly lower than previous published results, for example: 9.86 (Higgins *et al.*, 2005).

The distribution of chiasmata on individual chromosomes was then assessed statistically. Figure 4.24 shows the mean number of chiasmata for wild-type (A), line 2.10 (B) and line 6.2 (C). For both lines a student t-test was carried out on each chromosome compared to wild-type to see if the means were statistically different. This analysis showed that the distribution of the chiasmata between different chromosomes was slightly altered in the *AtSMC4^{RNAi}* lines. Chromosome 1 has the highest number of chiasmata in wild-type. This pattern is maintained in the *AtSMC4^{RNAi}* lines however, in both cases the number of chiasmata on chromosome 1 is reduced in these plants. As with the total number of chiasmata line 6.2 has a more significant reduction than line 2.10 (2.10, $p=0.03$; 6.2, $p=0.0001$).

Chromosome 2 has the fewest chiasmata in wild-type; however this pattern is not maintained in the *AtSMC4^{RNAi}* lines. In line 2.10 chromosome 2 does not have a significant difference in chiasmata compared to wild-type, however in these plants it is chromosome 4 which has the lowest number of chiasmata not chromosome 2 (however this difference was not statistically significant). In line 6.2 chromosome 2 has significantly more chiasmata than wild-type chromosome 2 ($p=0.004$), and again it is chromosome 4 and not chromosome 2 which has the lowest number of chiasmata.

The mean number of chiasmata on chromosome 3 is not statistically different between wild-type and either *AtSMC4^{RNAi}* line. For chromosome 4 however both *AtSMC4^{RNAi}* lines had a statistically significant reduction in chiasmata compared to wild-type (2.10, $p=0.001$; 6.2, $p=0.0004$). Again line 6.2 appeared to have a more

severe reduction, (however there was no statistical difference in chiasmata number on chromosome 4 between the two lines). The number of chiasmata on chromosome 5 was not statistically different in either *AtSMC4^{RNAi}* line compared to wild-type.

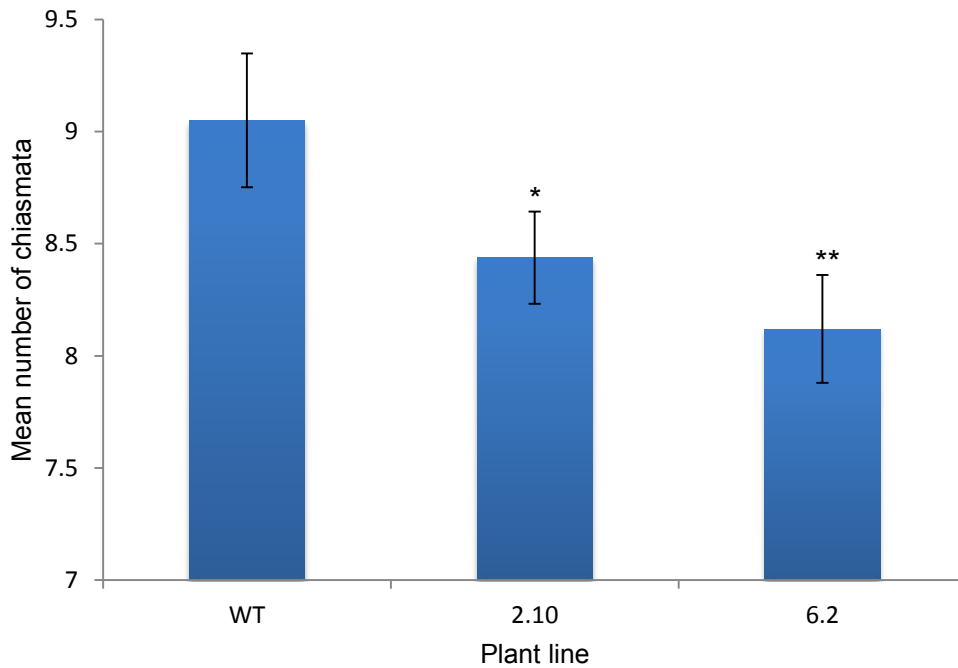


Figure 4.23: Mean total chiasmata counts for wild-type (WT) (n=20) and *AtSMC4*^{RNAi} lines 2.10 (n=32) and 6.2 (n=25). * = p < 0.05; ** = p < 0.01. Student's *t*-test compared to wild-type data. Error bars = Standard error of the mean.

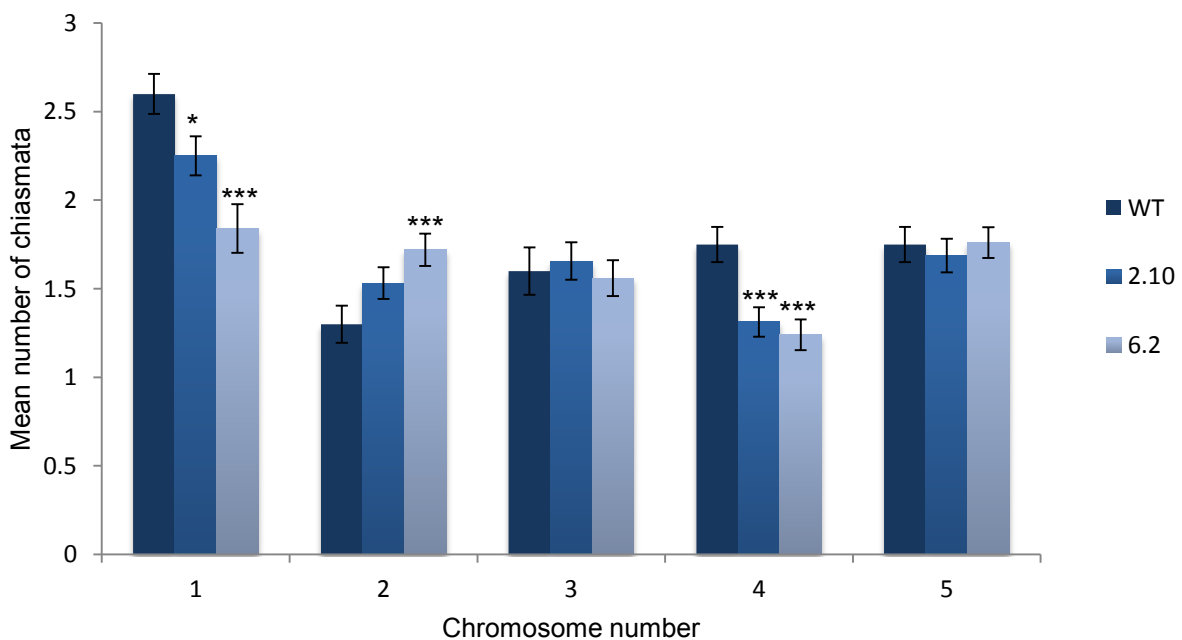


Figure 4.24: Mean chiasmata counts for individual chromosomes. Dark blue (WT) = wild-type. Blue (2.10) = *AtSMC4*^{RNAi} line 2.10, light blue (6.2) = *AtSMC4*^{RNAi} line 6.2. * = p < 0.05; *** = p < 0.005. Student's *t*-test compared to wild-type data. Error bars = Standard error of the mean.

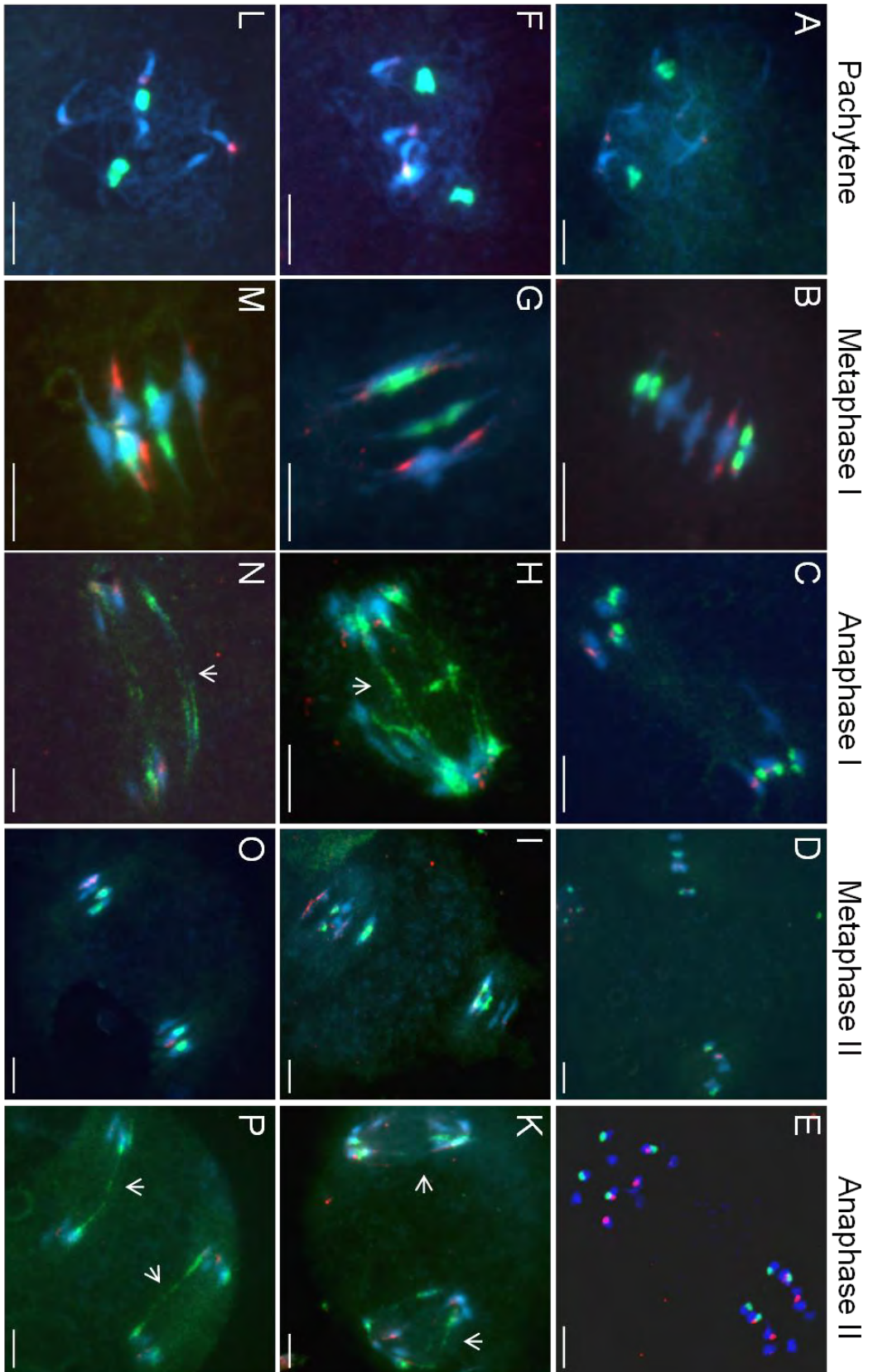
4.2.15.5 The rDNA appears disorganised in the AtSMC4^{RNAi} lines

In budding and fission yeast, condensin subunits have a specific role in the organisation of the rDNA repeats (Freeman *et al.*, 2000; Bhalla *et al.*, 2002; Lavoie *et al.*, 2002; D'Amours *et al.*, 2004; Machin *et al.*, 2004; Sullivan *et al.*, 2004; Wang *et al.*, 2004; Wang *et al.*, 2005b; Nakazawa *et al.*, 2008). Defects in the rDNA are not seen in higher eukaryotes deficient in condensin (Vagnarelli *et al.*, 2006), however there is some evidence of subtle defects in the rDNA regions during interphase in *Drosophila* (Cobbe *et al.*, 2006), and nucleolar localisation of condensin subunits in human (Cabello *et al.*, 2001) and *Arabidopsis* (Fujimoto *et al.*, 2005) suggests a possible role at the rDNA. Investigation into the integrity of the rDNA during meiosis in AtSMC4^{RNAi} lines and wild-type was carried out using the 45S and 5S FISH probes. In wild-type the 45S and 5S signals were seen as discrete organised signals throughout meiosis (Figure 4.25: A-E). In the AtSMC4^{RNAi} lines the 45S and 5S signals appeared normal during prophase I (Figure 4.25: F and L), however at metaphase I the signals often appeared slightly larger than those in wild-type (Figure 4.25: compare B with G and M). The rDNA signals also appeared large at metaphase II in AtSMC4^{RNAi} lines compared to wild-type (Figure 4.25: compare D with I and O). It is not clear whether the enlarged rDNA signals seen in the AtSMC4^{RNAi} lines are due to specific defects in the organisation of the rDNA, or a result of reduced compaction of the entire chromosome. To address this, the rDNA signals in AtSMC4^{RNAi} lines and wild-type were measured using imageJ software and compared as a ratio of the total chromosome size. The 5S signal on chromosome 4 and the 45S signal on chromosome 5 were used for this analysis. This analysis revealed that the ratio of chromosome 4 to 5S rDNA in wild-type was not significantly different from that of AtSMC4^{RNAi} lines (2.10, p= 0.09; 6.2, p= 0.5). This suggests that

the metaphase I 5S regions are not specifically affected by reducing condensin. However the ratio of chromosome 5 to 45S rDNA was significantly different between wild-type and *AtSMC4^{RNAi}* lines (2.10, $p=0.002$; 6.2 $p=0.01$), these results suggest that there may be a specific defect in the compaction of the 45S rDNA regions in *AtSMC4^{RNAi}* lines.

In addition to the defects in the rDNA signals seen at metaphase I and II, the rDNA at anaphase I and II was also abnormal. In the *AtSMC4^{RNAi}* lines the 5S signal was seen to span the gap between the segregating chromosomes at both anaphase I and II in all cells analysed in each line (Total: $n=26$) (see Figure 4.25: H, N, K and P). The 45S signal also appeared to span the segregating chromosomes at anaphase I in 2/17 cells and at anaphase II in all cells ($n=9$), however this signal was often difficult to detect so this may be an underestimation. rDNA anaphase defects were not seen in wild-type cells (Figure 4.25: C and E). These rDNA signals which spanned the space between the segregating chromosomes did not account for all lagging chromatin seen at anaphase, since threads of chromatin were seen between each pair of segregating chromosomes.

Figure 4.25: Analysis of the rDNA regions in wild-type and *AtSMC4^{RNAi}* lines. PMCs hybridised with FISH probes specific to the rDNA. 5S (green) and 45S (red). DNA stained with DAPI. **A-E** = wild-type; **F-K** = *AtSMC4^{RNAi}* line 2.10; **L-P** = *AtSMC4^{RNAi}* line 6.2. Meiotic stages indicated above columns. Scale bar 5 μm .



4.2.16 Centromere organisation in the *AtSMC4*^{RNAi} lines

The centromeres, like the rDNA, are large regions of repetitive DNA. Condensin is involved in centromere organisation in many species (Oliveira *et al.*, 2005; Savvidou *et al.*, 2005; Gerlich *et al.*, 2006; Yong-Gonzalez *et al.*, 2007; Ribeiro *et al.*, 2009; Samoshkin *et al.*, 2009). In the previous chapter *AtSMC4* was seen to localise to the centromeres in mitotic (and possibly meiotic) cells. To investigate whether *Arabidopsis* condensin is also involved in centromere organisation FISH analysis using the centromere probe pAL38, was carried out on chromosome spreads of *AtSMC4*^{RNAi} lines and wild-type. pAL38 localises to the 180 bp satellite repeats in the *Arabidopsis* centromeres (Martinez-Zapater *et al.*, 1986). At prophase I the centromere signal in the *AtSMC4*^{RNAi} lines appeared discrete and was indistinguishable from that of wild-type (compare: Figure 4.26: A-D with Figure 4.27: A-D and Figure 4.28: A-D). However at metaphase I when the chromosomes had aligned along the equator of the cell the centromere signals appeared diffuse and unorganised, unlike the discrete, clear signal seen in wild-type. The signals also often appeared more stretched compared to those of wild-type (compare Figure 4.26: E and F with Figure 4.27: E and F and Figure 4.28: E and F). Metaphase II centromere signals were also more diffuse in the *AtSMC4*^{RNAi} lines than wild-type (compare Figure 4.26: I and J with Figure 4.27: I and J and Figure 4.28: I and J). The stretched centromeres seen in this analysis may explain the elongated chromosomes seen at metaphase I and II in the *AtSMC4*^{RNAi} lines.

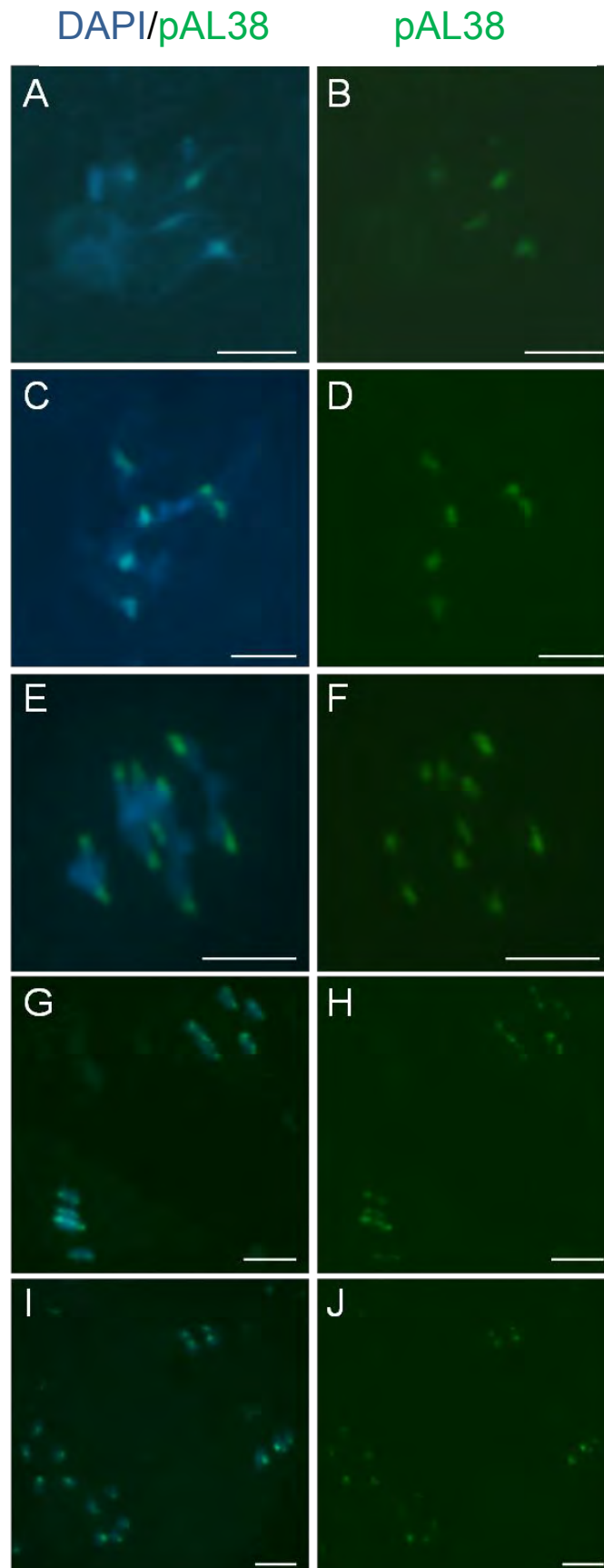


Figure 4.26: Analysis of the centromere DNA in *wild-type*. PMCs hybridised with a FISH on probe specific to the centromeric DNA (green). DNA stained with DAPI. **A - B** = pachytene; **C - D** = diakinesis; **E - F** = metaphase I; **G - H** = metaphase II; **I - J** = anaphase II. **A, C, E, G and I** = DAPI/centromere probe (FITC) merge; **B, D, F, H and J** = centromere probe (FITC). Scale bar 5 μ m.

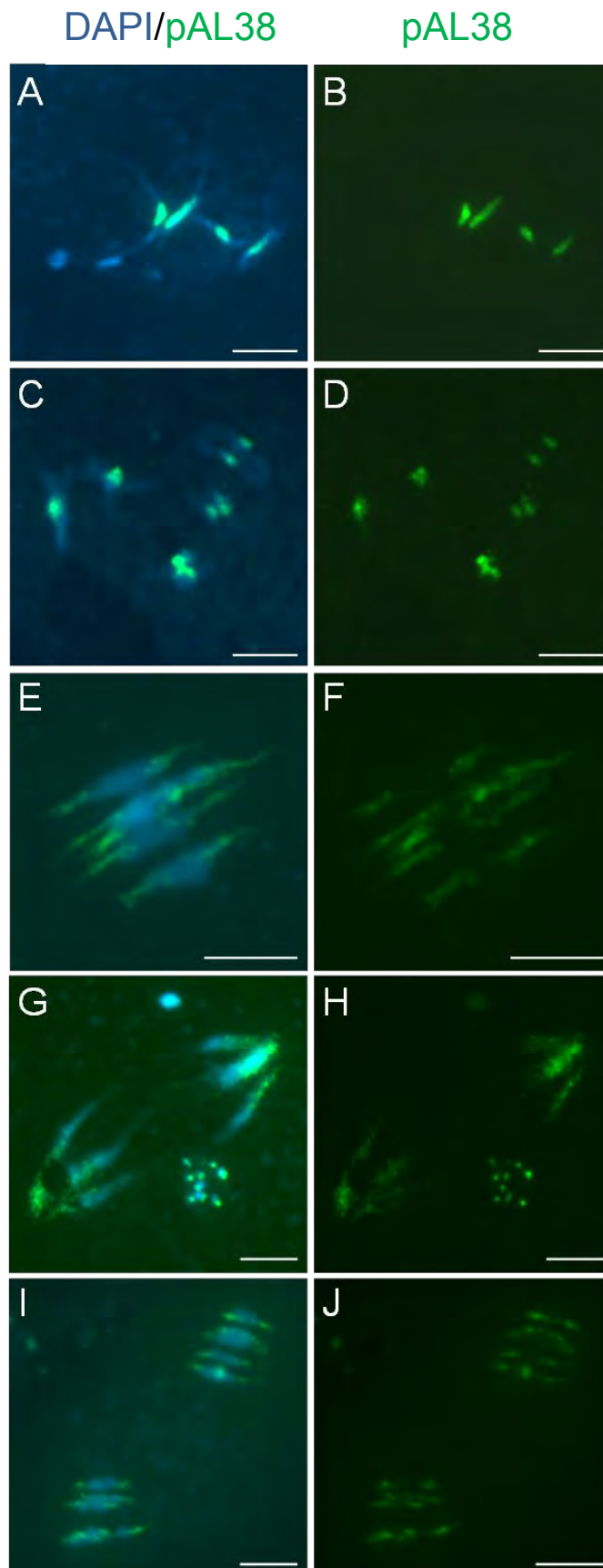


Figure 4.27: Analysis of the centromere DNA in *AtSMC4*^{RNAi} line 2.10. PMCs hybridised with a FISH on probe specific to the centromeric DNA (green). DNA stained with DAPI. **A - B** = pachytene; **C - D** = diakinesis; **E - F** = metaphase I; **G - H** = metaphase II; **I - J** = anaphase II. **A, C, E, G** and **I** = DAPI/centromere probe (FITC) merge; **B, D, F, H** and **J** = centromere probe (FITC). Scale bar 5 μ m.

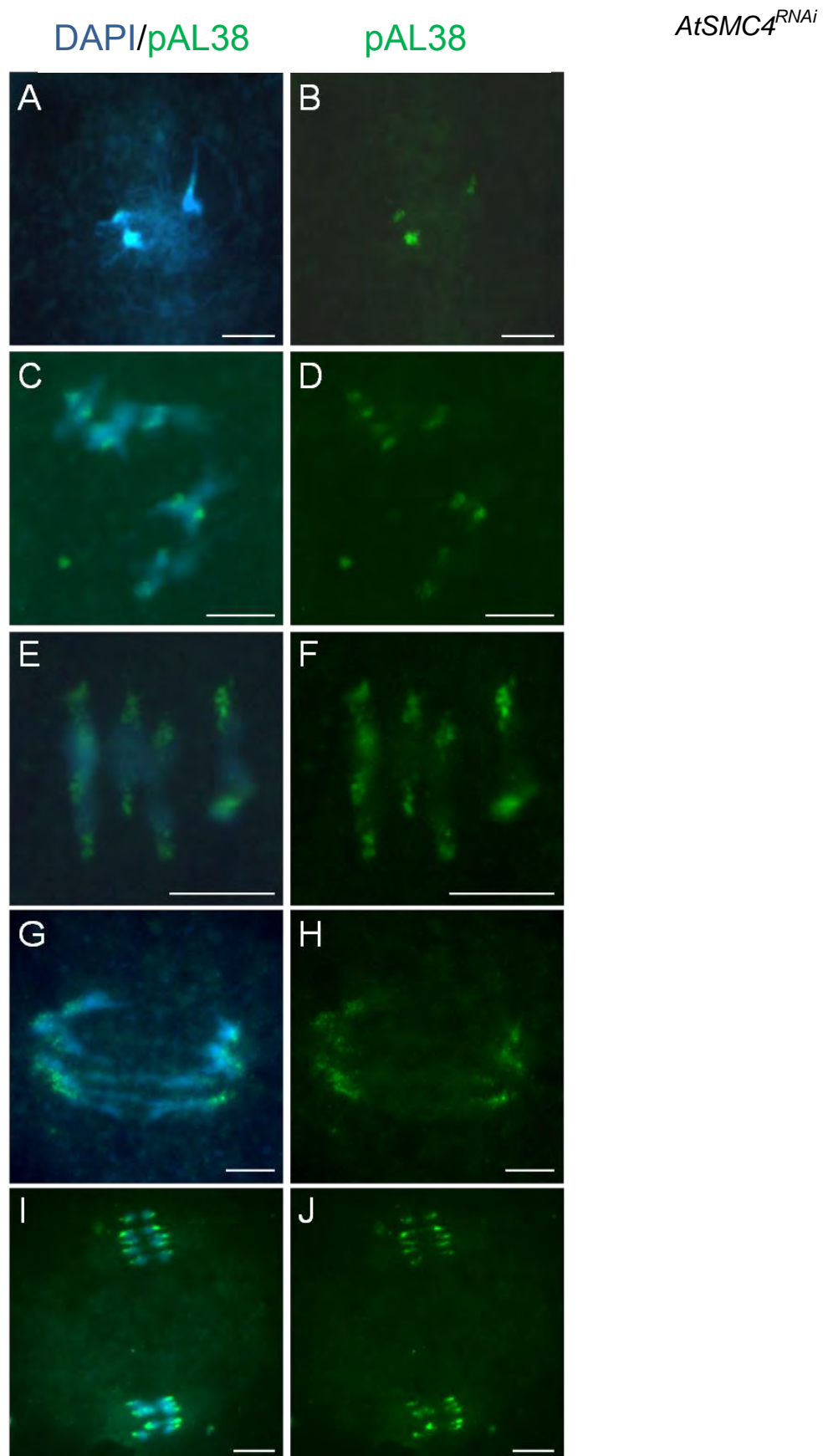


Figure 4.28: Analysis of the centromere DNA in *AtSMC4*^{RNAi} line 6.2. PMCs hybridised with a FISH on probe specific to the centromeric DNA (green). DNA stained with DAPI. **A - B** = pachytene; **C - D** = diakinesis; **E - F** = metaphase I; **G - H** = metaphase II; **I - J** = anaphase II. **A, C, E, G** and **I** = DAPI/centromere probe (FITC) merge; **B, D, F, H** and **J** = centromere probe (FITC). Scale bar 5 μ m.

4.2.17 Investigating the origin of the anaphase defects

At anaphase I and II in the *AtSMC4*^{RNAi} lines segregation problems occur. Thin thread-like pieces of chromatin appear to be lagging behind the chromosomes as they segregate which often appear to connect the two segregating chromosomes. Anaphase defects have been seen in condensin mutants in other species. In budding yeast it has been suggested that bridges occur at anaphase which are recombination dependent, possibly due to the inability to remove cohesin from the recombination sites (Yu and Koshland, 2005). However in *C. elegans*, anaphase bridges occur which are recombination independent and instead are thought to be due to unresolved catenations between chromosomes (Chan *et al.*, 2004). To explore the cause of the anaphase defects in the *AtSMC4*^{RNAi} lines in more detail, line 6.2 was crossed to a *Atspo11-1* mutant plant. *AtSPO11-1* is one of the 2 *AtSPO11* homologues required to initiate recombination. In the *Atspo11-1* mutants, no recombination occurs and only univalents are seen at metaphase I. Therefore the role of recombination in the formation of the anaphase defects could be analysed. The seeds from this cross were grown for 2 generations in order to obtain an *AtSMC4*^{RNAi} positive plant in an *Atspo11* background. 4 such plants were obtained from this cross and 2 were analysed cytologically. An *Atspo11* plant and an *AtSMC4*^{RNAi} plant from the cross were also analysed as controls. In the *AtSMC4*^{RNAi} plant 5, bivalents were seen at metaphase I (Figure 4.29: A), and at anaphase I a veil of chromatin was seen to trail behind the segregating chromosomes, consistent with previous analysis (sections 4.2.10 and 4.2.15.2) (Figure 4.29: B). In the *Atspo11* plant, 10 discrete univalents were seen at metaphase I (Figure 4.29: C) which segregated randomly to each pole at anaphase I (Figure 4.29: D) remaining compact as they segregated; these results were also consistent with previous analysis

(Grelon *et al.*, 2001). In the *AtSMC4^{RNAi}* x *Atspo11* plants, 10 univalents were seen at metaphase I, as in *Atspo11-1* (Figure 4.29: E). However when they came to segregate randomly to each pole at anaphase I many of the chromosomes appeared to lose compactness and large trails of chromatin were left behind the segregating chromosomes (Figure 4.29: F-I). This loss of compactness may be a result of the two sisters of some of the univalents trying to segregate to separate poles (i.e like in mitosis or meiosis II). Other univalents segregated intact (both sisters together) to one pole. Univalents are often seen to segregate their sisters in other meiotic mutants, however usually they remain as discrete, compact chromatids (Gareth Jones personal communication). The cause of this decondensed chromatin may be due to a loss of chromosome architecture, or an inability to remove cohesin from between the sister chromatids which are trying to segregate, or a combination of both. Alternatively catenations or telomere entanglements may be present between the sisters which inhibit the segregation.

In some cells (Figure 4.29), presumably corresponding to the dyad (prophase II) stage in wild-type, thick pieces of chromatin, bridge the gap between the two sets of chromosomes. These are presumably remnants of the univalents attempting to segregate, seen in Figure 4.29: G. At anaphase II the chromosomes are again seen to lose compactness and trail behind the segregating chromosomes.

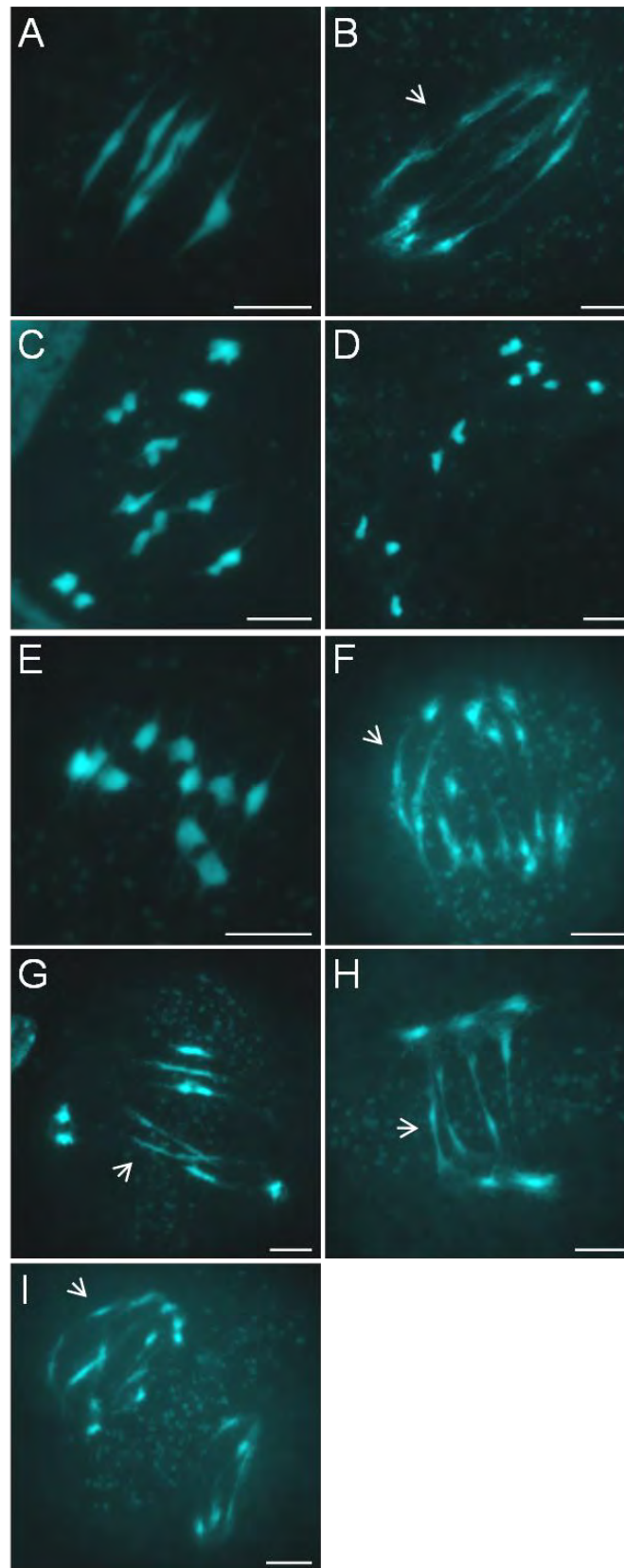


Figure 4.29: Meiotic phenotypes of *AtSMC4*^{RNAi} *X Atspo11* plants. DAPI stained PMCs. **A - B** = *AtSMC4*^{RNAi}; **C - D** = *Atspo11*; **E-I** = *AtSMC4*^{RNAi} *x Atspo11*. **A, C** and **E** = Metaphase I; **B, D** and **F** = anaphase I; **G** and **H** = approximately metaphase II/dyad stage; **I** = anaphase II. Arrowheads indicate chromatin trailing behind segregating chromosomes. Scale bar 5 μ m.

4.3 DISCUSSION

AtSMC4 is an essential protein for plant viability as shown by our inability to acquire homozygote T-DNA insertion mutants of this gene as seen in previous studies (Siddiqui *et al.*, 2006). Consistent with this, condensin subunits are essential for viability in other species for example; *C. elegans* (Lieb *et al.*, 1998; Hagstrom *et al.*, 2002), *Drosophila* (Bhat *et al.*, 1996; Steffensen *et al.*, 2001), fission yeast (Saka *et al.*, 1994) and budding yeast (Strunnikov *et al.*, 1995; Freeman *et al.*, 2000). AtSMC4 heterozygous T-DNA insert mutants are obtained less frequently than expected from Mendelian genetics suggesting a semi-dominant phenotype from the insert. This result is consistent with previous analysis (Siddiqui *et al.*, 2006).

No meiotic defects were observed in *AtSMC4*^{+/-} plants in the previous study, and the reduction in fertility was attributed to embryo lethality (Siddiqui *et al.*, 2006). In order to investigate the possible semi-dominant role of the *AtSMC4*^{+/-} in meiosis in more detail a cytological analysis was carried out as well as an immunolocalisation analysis on the chromosome axis and SC. On the whole, meiosis in these plants appeared as wild-type, however in a small number of cells at metaphase I univalents were observed. This may reflect a reduction in recombination in these lines, or a loss of cohesion between bivalents. Due to the homozygous knock-out lines being lethal an RNAi approach was adopted in order to further analyse the role of *AtSMC4* in meiosis. *AtSMC4*^{RNAi} lines had clear defects in chromosome organisation and segregation during meiosis; however no univalents were seen in the cytological screen. The discrepancy in phenotype between *AtSMC4*^{+/-} plants and *AtSMC4*^{RNAi}

plants may reflect dosage effects and may be revealing a complex role for condensin in chromosome organisation.

4.3.1 The *DMC1* promoter is 'leaky'

Plants with the strongest meiotic phenotypes also had clear developmental defects and a mitotic phenotype at anaphase; we hypothesise that this may be due to leaky expression of the RNAi construct under the *DMC1* promoter. When *DMC1* was cloned, the promoter drove a strong meiosis expression of *GUS*. However a small amount of *DMC1* mRNA was present in the vegetative tissue (Klimyuk and Jones, 1997). This could be enough to explain the leaky phenotype we observe. Alternatively, siRNA molecules have been shown to move around the plants via their plasmodesmata and spread the RNAi signal away from the target tissue (Dunoyer *et al.*, 2010) and reviewed by (Baulcombe, 2004; Voinnet, 2005). Therefore this may also account for the somatic phenotype observed.

4.3.2 *AtSMC4*^{RNAi} lines have reduced *AtSMC4* protein levels as shown by western blot and immunolocalisation

Western blot analysis revealed that the *AtSMC4*^{RNAi} lines were reduced in the levels of *AtSMC4* protein. An approximately 40% reduction in protein was seen in the *AtSMC4*^{RNAi} lines compared to wild-type. Anthers were used in this analysis in order to enrich for meiotic tissue since the knock-down is likely to be most severe in the meiotic tissue due to the use of the meiosis specific *DMC1* promoter. Despite enriching for the meiotic tissue the anthers will still contain many mitotic tissues, as only a small proportion of anthers are made up of meiotic cells. Therefore it is likely

that a significant proportion of the protein detected on the western blot analysis in the *AtSMC4^{RNAi}* lines is from the non-meiotic tissues in the anthers. Thus the 40% reduction of *AtSMC4* protein observed in the *AtSMC4^{RNAi}* lines is likely to be an underrepresentation of the actual level of knock-down. However it is worth noting that these *AtSMC4^{RNAi}* lines had a distinct vegetative phenotype which is assumed to be due to a reduction of *AtSMC4* protein in somatic as well as meiotic cells. Therefore how much the anther somatic cells contribute to the protein levels seen in the *AtSMC4^{RNAi}* lines is unknown. Perhaps a more specific analysis of the *AtSMC4* levels in meiocytes of wild-type compared to *AtSMC4^{RNAi}* lines was carried using immunolocalisation on fixed bud material. Preliminary results suggested that *AtSMC4* was reduced to levels undetectable by the immunolocalisation technique in the *AtSMC4^{RNAi}* lines compared to wild-type. However it should be noted that this immunolocalisation technique using fixed buds is quite temperamental therefore quantification of protein levels using this method is likely to be inaccurate. Nevertheless both these forms of analysis have shown that the level of *AtSMC4* is reduced in the *AtSMC4^{RNAi}* lines. An alternative method to quantify level of knock-down would be to use mRNA levels. Recently it has become more straight-forward to extract mRNA from meiocytes which have been squeezed from anthers. This method would allow for an analysis of meiocyte specific knock-down, and combined with quantitative PCR may allow more accurate quantification of the level of knock-down. However meiocyte extraction is not exempt to contamination from somatic cells; therefore mRNA analysis in the *AtSMC4^{RNAi}* lines also has its drawbacks.

4.3.3 Chromosome axes appear normal in AtSMC4^{RNAi} lines

Condensin is required for correct prophase I axis length compaction in *C. elegans* (Tsai *et al.*, 2006) and budding yeast (Yu and Koshland 2003, 2005), for SC assembly in budding yeast (Yu and Koshland 2003, 2005) and correct timing of SC disassembly in *Drosophila* (Resnick *et al.*, 2009).

To address if a role in prophase I axis and SC organisation is conserved in *Arabidopsis* meiosis, analysis of the axis was carried out using AtASY1-Ab. SC progression was also assayed using AtZYP1 antibody. No abnormalities in axis organisation or the SC were seen in AtSMC4^{RNAi} lines compared to wild-type. Further analysis of the chromosome axis was carried out by measuring the axis length at pachytene in an AtSMC4^{RNAi} line compared to wild-type. Again no difference in axis length was seen in condensin deficient cells compared to wild-type. These results indicate that condensin does not appear to play a role in prophase I axis organisation during meiosis. It is possible that factors other than condensin are required for prophase I axis organisation and that condensin does not play the same role as in other species. Alternatively incomplete RNAi may be responsible for the lack of prophase I axes phenotype. The highly compact chromosomes in later stages of meiosis may be more sensitive to condensin reduction than the comparatively less compact prophase I chromosomes. It is also possible that the chromosome axes are defective in the AtSMC4^{RNAi} lines but that the assays used did not detect the defects; for example, the timing of synapsis was not investigated therefore it is possible that there may be a delay in SC assembly or disassembly in *Arabidopsis* AtSMC4^{RNAi} lines as is seen in *Drosophila* condensin deficient cells (Resnick *et al.*, 2009).

Alternatively a more detailed look at axis organisation using EM or three-dimensional structural illumination microscopy (3D-SIM) (Wang *et al.*, 2009) may reveal axis defects.

4.3.4 AtSMC4^{RNAi} lines have a slight reduction in chiasmata

Defects in meiotic recombination have been observed in condensin deficient *C. elegans* (Tsai *et al.*, 2008; Mets and Meyer, 2009), budding yeast (Yu and Koshland, 2003) and possibly *Drosophila* (Resnick *et al.*, 2009). However the effect of reducing condensin levels on recombination in these species differs. In *C. elegans* mutating either condensin I or condensin II subunits result in an increase in COs and a removal of CO interference. *C. elegans* has “complete” interference such that only one CO occurs per-bivalent. However in condensin mutants there is an increase in 2 and 3 COs bivalents: these COs also do not appear to display interference. The distribution of COs is also altered in these mutants compared to wild-type (Tsai *et al.*, 2008). In *S. cerevisiae* condensin deficient cells, DSBs occur at near wild-type levels but appear to be processed independently of DMC1 (Yu and Koshland, 2003). In *Drosophila* univalents are seen to separate prematurely to each pole, the authors suggest this may be due to a premature loss of cohesin or a reduction in COs (Resnick *et al.*, 2009). Here chiasmata number were analysed in order to see if there was any alternation in the AtSMC4^{RNAi} lines compared to wild-type. A small but statistically significant reduction in the number of chiasmata was seen in the AtSMC4^{RNAi} lines compared to wild-type. This was more pronounced in line 6.2. Chiasmata number on individual chromosomes was also analysed and it appeared that the more COs were lost from chromosomes 1 and 4 than chromosomes 2, 3 and

5. Chromosome 2 appeared to have an increased in chiasmata which was significant for line 6.2. In addition to this, rare univalents were also occurred in the *AtSMC4^{+/-}* plants, which suggests a defect in recombination. No univalents were detected in the *AtSMC4^{RNAi}* plants in this study. The discrepancy between these observations is unclear but may be reflecting a dosage effect of condensin knock-down. Nevertheless taken together these results suggest that condensin appears to have a role in recombination. How condensin may affect recombination rates in this manner is unclear especially since no *AtSMC4*-Ab was detected in prophase I (Section 3.2.8), when recombination is occurring. Scoring *AtMHL1* foci at pachytene can provide an estimation of total crossover numbers. The *AtMHL1* antibody could be used in immunolocalisation experiments to further investigate the recombination phenotype in these plants.

4.3.5 Effect of reducing *AtSMC4* on chromosome organisation

In the *AtSMC4^{RNAi}* lines multiple aspects of chromosome organisation appeared defective. These included elongated chromosome at metaphase (possibly due to defective centromere stiffness), defects at anaphase and disorganised rDNA and centromere regions. Many of these phenotypes suggest condensin may be involved in maintaining chromosome structure as opposed to condensing the chromosomes.

4.3.5.1 Centromere structure is compromised in *AtSMC4^{RNAi}* lines.

In Chapter 3, condensin subunit *AtSMC4* was seen to localise to the centromeres in mitotic cells (section 3.2.9), and possibly also meiotic cells (section 3.2.8). To establish whether this centromeric localisation reflected a specific role at the

centromeres in *Arabidopsis*, FISH analysis was carried out using the centromere specific probe pAL38. FISH analysis revealed that the centromeres in the AtSMC4^{RNAi} lines were abnormal. During prophase I the centromere signals in the AtSMC4^{RNAi} lines were indistinguishable from those in wild-type. However, at metaphase I (and metaphase II) the centromeres appeared elongated compared to wild-type. These results suggest that the centromeres in *Arabidopsis* condensin knock-down lines are defective and that the pulling force of the spindle when the centromeres are aligned along the metaphase plate may be responsible for the distortion of the centromeric DNA. This may be caused either from loss of centromere stiffness after normal spindle attachment or from abnormal merotelic attachment. Condensin may therefore be required to maintain centromere structure. The elongated centromeres seen in AtSMC4^{RNAi} lines at metaphase I may cause the elongated appearance of the metaphase bivalents in these plants.

Condensin has been shown to have a role in the organisation of the centromeres in many species (Oliveira *et al.*, 2005; Savvidou *et al.*, 2005; Yong-Gonzalez *et al.*, 2007). Many studies report that the centromeres lose structural integrity when they become attached to the spindle (Oliveira *et al.*, 2005; Savvidou *et al.*, 2005; Gerlich *et al.*, 2006; Ribeiro *et al.*, 2009). However some studies argue that merotelic attachment of the spindles is responsible for the stretching of the centromeres seen in condensin depleted cells (Samoshkin *et al.*, 2009; Tada *et al.*, 2011). Centromere-specific histone mis-localisation is seen in condensin deficient budding yeast (Yong-Gonzalez *et al.*, 2007), human (Ono *et al.*, 2004; Samoshkin *et al.*, 2009), *Xenopus* (Wignall *et al.*, 2003; Bernad *et al.*, 2011) and *Drosophila* (Jager *et al.*, 2005). These

studies suggest that condensin I is required to organise the centromeric DNA into a structure in which centromere-specific histones are able to be successfully recruited and maintained.

4.3.5.2 The rDNA appears disorganised in the *AtSMC4*^{RNAi} lines

Analysis of the rDNA regions using the FISH probes 45S and 5S showed that the 45S rDNA did not appear as well compacted at metaphase I as it was in wild-type. The anaphase defects seen in the *AtSMC4*^{RNAi} lines were also shown to be least in part due to problems segregating the rDNA. The rDNA signals also appeared larger at metaphase II in the *AtSMC4*^{RNAi} lines compared to wild-type (although this was not analysed by ImageJ). These results suggest that the *AtSMC4*^{RNAi} lines may have trouble organising their rDNA. Condensin has been implicated in rDNA maintenance in yeast (Freeman *et al.*, 2000; Bhalla *et al.*, 2002; Lavoie *et al.*, 2002; D'Amours *et al.*, 2004; Machin *et al.*, 2004; Sullivan *et al.*, 2004; Wang *et al.*, 2004; Wang *et al.*, 2005; Tsang *et al.*, 2007; D'Ambrosio *et al.*, 2008a; Nakazawa *et al.*, 2008). The role of condensin in rDNA segregation has been suggested to be to prevent recombination occurring between rDNA repeats (Bhalla *et al.*, 2002). Alternatively condensin may help prevent or remove catenations in the rDNA regions (D'Ambrosio *et al.*, 2008a).

Condensin may be required more specifically at the rDNA due to the repetitive nature of the DNA sequence and high transcription rates which makes the rDNA unstable and prone to homologous recombination. Nutrient starvation has been shown to promote the loading of condensin to the rDNA locus in budding yeast in

order to protect the locus when it is not being expressed (Tsang *et al.*, 2007). High levels of transcription in the rDNA can lead to topological problems that inhibit chromosome segregation in yeast cell divisions, during which transcription is not silenced. Thus condensin may be required in budding yeast to help remove topological links to allow correct segregation (Bhalla *et al.*, 2002). A condensation independent role of condensin may be involved in rDNA segregation (Lavoie *et al.*, 2004; Clemeite-Blanco 2009; Ide 2010).

Condensin does not appear to have a specific role in rDNA organisation in other species (Vagnarelli *et al.*, 2006). A more subtle role for condensin in rDNA organisation is seen during interphase in *Drosophila* (Cobbe *et al.*, 2006), and condensin is seen to localise to the nucleolus in human (Cabello *et al.*, 2001) and *Arabidopsis* (Fujimoto *et al.*, 2005) therefore suggesting a possible rDNA role. This is the first time that condensin in a higher eukaryote has been shown to be required for the organisation of the rDNA, in a similar manner to that seen in yeast.

4.3.5.3 Origin of the anaphase defects

Anaphase bridges have been described for condensin mutants in several species during mitotic and meiotic cell divisions (Yu and Koshland, 2003; Chan *et al.*, 2004; Vagnarelli *et al.*, 2006; Resnick *et al.*, 2009). The origin of these bridges has been suggested to be due to the inability to remove concatenation between chromosomes in *C. elegans* (Chan *et al.*, 2004), or to the inability to remove cohesion from the sites of COs in budding yeast (Yu and Koshland, 2005). Connections have also been seen between the rDNA loci where condensin appears to associate as strong foci

along the otherwise linear axial signal (Yu and Koshland, 2003). To further probe into the possible origin of the anaphase defects seen in *AtSMC4^{RNAi}* lines the *AtSMC4^{RNAi}* lines were crossed to *Atspo11* mutants. *Atspo11* plants have no recombination and therefore the role of recombination in the anaphase defects could be assessed. It was seen from this cross that *AtSMC4^{RNAi}* knock-down in an *Atspo11* background resulted in 10 discrete univalents at metaphase I, however at anaphase I the chromosomes appeared to lose compactness as the chromosomes segregated. This loss of compaction may be due to the sister chromatids of some univalents trying to segregate to each pole but being prevented. What may be preventing the sister chromatids from segregating neatly in these plants is not known but it could be due to an inability to remove cohesin from between the sisters, catenations between sisters or telomere entanglements. In addition to this the chromosome architecture itself may be lost as the chromosomes segregate, and this effect may be enhanced by the inability to resolve connections of some kind between segregating chromosomes. A 'catastrophic loss of chromosome architecture' occurs upon anaphase onset in condensin deficient chicken cells (Vagnarelli *et al.*, 2006).

How do the results from the *AtSMC4^{RNAi} Atspo11-1* cross relate to the thin threads of chromatin seen between segregating chromosomes in the *AtSMC4^{RNAi}* lines? It is possible that the anaphase defects in the *AtSMC4^{RNAi}* lines are a combination of a defect in the ability to maintain chromosome architecture upon segregation and an inability to resolve links between chromosome. Whether these connections are in the form of catenations in specific DNA regions, catenations over the entire chromosome

or even an inability to resolve COs/remove cohesin (from sites of COs or between sisters) remains unknown.

4.3.6 Future perspectives

No prophase I axis defects were observed in *AtSMC4^{RNAi}* lines however, it is possible that synapsis is delayed in these lines, therefore a time course analysis using 5-bromo-2'-deoxyuridine (BrdU) (Armstrong and Jones, 2003) or 5-ethynyl-2'-deoxyuridine (EdU) (Kotogany *et al.*, 2010) would be required in order to establish whether there is a delay in synapsis.

Further analysis onto the role of condensin in recombination may provide interesting further insight into the complex role of these proteins. Recombination rates in condensin depleted plants could be analysed using tetrad analysis (Copenhaver *et al.*, 1998) as well as chiasmata analysis in *AtSMC4^{+/-}* plants. Combined with this, immunolocalisation of antibodies specific to recombination proteins such as DMC1/RAD51, MSH5/4, MLH1 and the phosphorylated form of the meiotic histone H2AX which marks DSB sites, on *AtSMC4^{RNAi}* lines may help to establish which stage of recombination is affected by condensin knock-down. Scoring *AtMLH1* foci on pachytene cell in wild-type and *AtSMC4^{RNAi}* lines can also provide information on total CO numbers in these plants.

Further analysis will need to be carried out to be sure that the disorganised centromere DNA observed in condensin I deficient plants is due to a loss of structure

induced by the spindle. This could be investigated in *Arabidopsis* condensin I deficient plants by incorporating colchicine into meiocytes to inhibit the spindle. Plants with inhibited spindles would arrest at metaphase I without the pulling forces of the spindle being applied to the centromeres, thus allowing analysis of the effect of the spindle force on the centromeres to be assessed. Combining centromere FISH probes and tubulin antibody to mark the spindles could help to establish whether merotelic attachment is occurring in these lines or not. Centromeric specific histone mis-localisation is seen in condensin deficient budding yeast (Yong-Gonzalez *et al.*, 2007), human (Ono *et al.*, 2004; Samoshkin *et al.*, 2009), *Xenopus* (Wignall *et al.*, 2003; Bernad *et al.*, 2011) and *Drosophila* (Jager *et al.*, 2005). These studies suggest that condensin is required to organise the centromeric DNA into a structure to which centromere specific histones can be successfully recruited and maintained in position. Whether the same is true in *Arabidopsis* is unknown, therefore to investigate this immunolocalisation experiments using antibodies raised against centromere specific histone variants could be carried out in the AtSMC4^{RNAi} lines. In addition to this using a range of centromeric and pericentromeric FISH probes on the AtSMC4^{RNAi} lines may help to identify which region of the centromere is defective, this could also be combined with higher-resolution microscopy such as 3D-SIM.

This chapter has described how condensin is required for wild-type levels of compaction in repetitive DNA such as the rDNA and centromere regions. Telomeres are also regions of repetitive DNA which have not been investigated here. Condensin has been implicated in the correct segregation of the telomeric regions in budding and fission yeast (Yu and Koshland, 2003; Yu and Koshland, 2005; Motwani

et al., 2010) and *Drosophila* (Steffensen *et al.*, 2001) and condensin I is seen to be enriched at the subtelomeric regions in budding yeast (Wang and Strunnikov, 2008) and during meiosis in mouse (Viera *et al.*, 2007). Therefore it would be interesting to investigate whether condensin has a role in telomere segregation in *Arabidopsis*. This could be done using telomere-specific FISH probes. If the telomeres were involved in the anaphase 'bridges' they would be detected by this method.

4.3.7 Conclusions

In this chapter the AtSMC4 subunit, predicted to be part of both condensin I and condensin II complexes, was knocked-down by RNAi. Chromosomes appeared to condense at metaphase in these lines to form chromosomes with only slight structural differences to wild type. However at anaphase multiple thin threads of chromatin were seen to trail behind the segregation chromosomes. The centromere DNA also appeared to stretch as the chromosome were aligned on the metaphase late. These results suggest that condensin is required to maintain chromosome structure and not for initial compaction of the chromosomes. Condensin also appeared to have a role in the organisation of the rDNA. The phenotypes observed in these plants reflect a knock-down of total cellular condensin and not a knock-out; therefore in some cases the phenotypes may be more severe if no condensin was present. These results also do now allow the individual roles of the 2 complexes to be resolved. Chapters 5 and 6 focus on knock-down and knock-out plants of the condensin I and condensin II complexes respectively.

CHAPTER 5

5 PRODUCTION AND ANALYSIS OF RNAi LINES FOR DEPLETION OF THE *ATCAPD2* SUBUNIT OF CONDENSIN I

5.1 INTRODUCTION

AtSMC4 is a member of two complexes, condensin I and condensin II. Therefore the work described in the Chapters 3 and 4 has revealed the combined role of both condensin complexes during meiosis; however the contribution of the individual complexes to chromosome organisation remains unknown.

Work in other species has indicated that the two condensin complexes appear to differ in their mitotic roles. Condensin I subunits are seen to localise in vertebrate chromosomes only after NEBD i.e. at prometaphase (Hirota *et al.*, 2004). Reducing condensin I subunits in HeLa cells resulted in 'swollen' chromosomes which were distinct from chromosomes depleted in condensin II subunits (Ono *et al.*, 2003). Condensin I has also been shown to be required for the full removal of cohesin from chromosome arms and to promote longitudinal compaction of chromosomes in HeLa cells (Hirota *et al.*, 2004). The progression through prometaphase and metaphase was also delayed in condensin I deficient HeLa cells (Hirota *et al.*, 2004). Condensin I is also highly dynamic in its localisation to mitotic chromosomes in human (Gerlich *et al.*, 2006). In this system condensin I was shown to have an architectural role in maintaining chromosome stability instead of in chromosome compaction itself.

The condensin I complex in budding and fission yeast has been shown to have a specific role in the condensation, maintenance and segregation of the rDNA regions (Freeman *et al.*, 2000; Bhalla *et al.*, 2002; D'Amours *et al.*, 2004; Lavoie *et al.*, 2004; Machin *et al.*, 2004; Sullivan *et al.*, 2004; Wang *et al.*, 2004; Wang *et al.*, 2005a; Nakazawa *et al.*, 2008). However a role for condensin I in rDNA organisation in other species is less clear (Cabello *et al.*, 2001; Fujimoto *et al.*, 2005; Cobbe *et al.*, 2006; Vagnarelli *et al.*, 2006).

Condensin I has also been shown to be important for the structural integrity of the centromeres (Oliveira *et al.*, 2005; Yong-Gonzalez *et al.*, 2007). In many cases the pulling force of the spindle is thought to cause the 'stretching' of centromeres in condensin deficient cells (Oliveira *et al.*, 2005; Savvidou *et al.*, 2005; Gerlich *et al.*, 2006; Ribeiro *et al.*, 2009). However merotelic attachment of the spindle to the kinetochores has also been suggested as a cause of centromere defects in human cells (Samoshkin *et al.*, 2009).

Condensin I complexes have been studied in a variety of species during meiosis including budding yeast – in which only the canonical condensin I complex exists (Yu and Koshland 2003, 2005; Brito *et al.*, 2010), mouse (Viera *et al.*, 2007), fruit fly (Resnick *et al.*, 2009) and nematode worm (Tsai *et al.*, 2008; Mets and Meyer, 2009). Condensin in *S. cerevisiae* appears to have a role in mediating axial length compaction, axis organisation (as seen by the mis-loading of axis proteins Red1 and Hop1), SC assembly, homologue pairing and correct DSB processing (Yu and

Koshland, 2003, 2005). Ycs4 (the budding yeast homologue of CAP-D2) co-localised with the SC TF protein Zip1. Condensin was therefore suggested to be a component of the axial core on which other components are loaded (Yu and Koshland, 2003).

In *Drosophila* condensin I Cap-G mutants there is a delay in SC disassembly but SC assembly is unaffected (Resnick *et al.*, 2009). In *Drosophila dcap-g* mutants, at metaphase I the homologous chromosomes often separate prematurely and migrate towards the poles. This could be a result of a defect in COs, possibly due to a premature loss of arm cohesion (Resnick *et al.*, 2009). In *C. elegans* condensin also has a role in ensuring correct recombination between homologues. In *C. elegans*, DPY-28 (later found to be the CAPD2 homologue), restricts COs by limiting the number of DSBs formed and also alters CO distribution (Tsai *et al.*, 2008).

In addition to a role in prophase I, condensin I has been shown to be required for accurate chromosome segregation at both meiotic divisions in budding yeast (Yu and Koshland, 2003), and for anaphase II segregation in *Xenopus* (Watrinn *et al.*, 2003). In these organisms condensin depletion results in bridges at anaphase I and II. The cause of these bridges is still unclear, but in *S. cerevisiae* they have been suggested to be due to improper resolution of recombination dependent linkages (Yu and Koshland, 2005).

To address whether the two complexes have different roles in meiosis in higher plants, analysis of plants deficient in *AtCAP-D2* of condensin I was carried out. This

chapter describes the attempts to find T-DNA insertion lines in condensin I subunits and the production and cytological analysis of *AtCAPD2^{RNAi}* lines. Analysis of the rDNA regions using probes for 45S and 5S as well as analysis of the centromeres has been carried out on the *AtCAPD2^{RNAi}* lines produced. Figure 5.1 shows the predicted subunit arrangement of the condensin I complex.

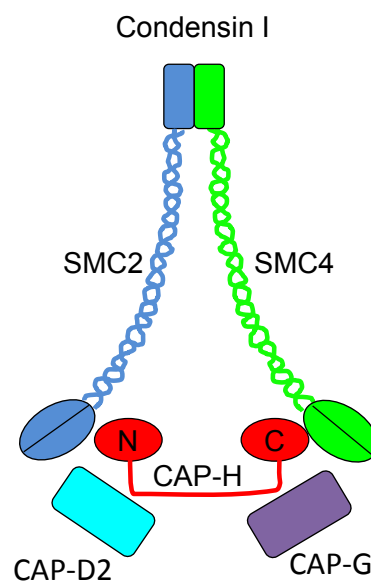


Figure 5.1: Schematic representation of the condensin I complex. Both condensin I and condensin II complexes share the same SMC2/SMC4 backbone but differ in their regulatory subunits. Condensin I comprises CAP-H, CAP-D2 and CAP-G.

5.2 RESULTS

5.2.1 Search for T-DNA insertion lines of condensin I subunits.

The NASC database was screened for lines with T-DNA inserts in each of the three non-SMC subunits of condensin I. The following lines were identified and ordered: *AtCAPD2* (*At3g57060*, *Sail_065716*, *Salk_044796*), *AtCAPH* (*At2g32590*, *Salk_013559*) and *AtCAPG* (*At5g37630*, *Salk_064009*). Seeds were planted and plants tested for the presence of inserts by PCR using gene-specific primers and primers specific to the T-DNA left border. No inserts were found in either *AtCAPD2* line by PCR; 17 plants were tested for *Sail_065716* and 26 for line *Salk_044796*. In addition to this, no seeds grew on selective media. 23 plants were tested by PCR for line *Salk_013559 AtCAPH* and no inserts were found. These results lead to the conclusion that the desired inserts were not present in these lines. Plants of these lines were also left to set seed and no reduction in fertility was observed in any of the plants. Inserts were identified in the *AtCAP-G* line (*Salk_064009*). 27 plants were obtained which contained an insert, as ascertained by PCR using gene specific and T-DNA left border specific primers. However all of these plants were shown to be heterozygous. A Chi-squared analysis was carried out on the segregation of these lines which showed that the absence of homozygous plants in the *AtCAPG* lines was significant ($\chi^2 = 39.5$ $p < 0.001$). This led to the conclusion that plants homozygous for T-DNA inserts in this gene maybe lethal, as was the case for *Atsmc4* homozygous mutant plants.

5.2.2 Production of an RNAi construct to deplete AtCAPD2

Due to the unsuccessful search for homozygous T-DNA insertions in condensin I genes an RNAi approach was adopted using the same strategy that had been applied for *AtSMC4^{RNAi}* lines (section 4.2.5). The mechanism of RNAi is described in section 4.2.6. *AtCAPD2* was chosen as the target for gene knock down. A 702 bp region of *AtCAPD2* (between bases 1069 and 1771) was selected for the sense and antisense fragments. The sequence was used in a BLAST search to check for its similarity to other sequences in order to reduce the chances of “off-site” effects caused by the RNAi. This sequence was cloned into pHANNIBAL in sense and antisense orientation, the sense and antisense fragments, separated by the ~800 bp intron, and the NOS terminator were then subcloned into pPF408. The construct was transformed into *A. tumefaciens* then subsequently transformed into wild-type *Arabidopsis* plants.

5.2.3 Checking for the presence of the RNAi inserts by PCR

Seeds harvested from dipped plants were planted in soil and sprayed with BASTA to allow for selection of successfully transformed plants. In order to confirm the presence of the insert in the plants that survived selection, PCR was carried out using two independent sets of primers specific for the construct. The first set of primers amplified the sense fragment from the DMC1 promoter to the intron (using DMC pro primer- and pHan seq rev: see appendix, table 8.2) and the second reaction amplified the antisense fragment from the intron to the terminator (using primers pHan seq for and pHan seq rev 2: see appendix, table 8.2). Bands that were detected were gel purified and cloned into pDrive for sequence analysis to confirm

they contained the expected sequence. Figure 5.2 shows the sequence obtained which correspond to the sense and antisense *AtCAPD2* cDNA fragments used in the RNAi construct.

A

5'-TACCTGACTCGCTTCTCTCGTTTTATTTGTTTCCGATGATCTGATCTGTTGTGTGTTTCGGATTCATA
GAGCTGAAGAAACGAGATCTCTCGAGGGAGATATGAGTTCCAAGTCCCTTCGTCTGCGAACTAAGCA
AGCTATGTTGGAAATTTTGTCTGAACGCTGTAGAGATGTTTCAGCCTATAACAAGGAGCCGTGTTCTTC
AAGTGTGGGCTGAACTCTGTGAAGAGCATTCTGTTCAATTGGCCTATGGAATGAAGTTGCATCACT
ATCTGCTGGAAGACTGGAAGATAAGAGTGCAATTGTTAGAAAATCCGCATTGAATTTACTGATCATG
ATGTTGCAACATAACCCCTTTGGTCCACAGCTGCGGATAGCTTCATTTGAAGCAACCCTGGAGCAGTA
TAAAAGAAAACCTGAACGAACTTGAACCTACTGAGCATGCATCAAAGAGTCAACTTCAGATGGTGAA
TCCTGTAATGGAGATGGTGAATCGATGACTTGCATCTTGAACTACAATAAGATTCATCAAGATA
GTCTATCTGATAGCTGTCAGCCAGAGAATGGAGAAGAAATCAGTGAGAAGGATGTTTCTGTTCCAGA
TATTGGTAACGTTGAGCAAACCAAGGCTTTGATTGCTCCCTAGAGGCTGGATTGAGGTTCTCGAAG
TGCATGTCAGCCAGTATGCCAATCCTCGTTCAATTAATGGCTTCATCTTCTGCCACTGATGTTGAGAAT
GCTATTCTTTTGTGATGAGGTGTAAGCAGTTCCAAATTAACGGTGCAGAATTCGGTACCCAGCTTG
GTAAGGAAATAATTATTTCTTTTTCTTTTAGTATAAAAATAGTTAAGTGATGTTAATTAGTATGATT
ATAATAATATAGTTGTTATAATTGTAAAAAATAATTTATAAATATATTGTTTACATAAACACATAGT
AATGTAAAAAATATGACAAGTGAT-3'

B

5'-GACGAATTCAGATTCTAAATGGATTGACTATTAATTAATGAATTAGTCGAACATGAATAACAAG
GTAACATGATAGATCATGTCATTGTGTTATCATTGATCTTACATTTGGATTGATTACAGTTGGGAAGC
TGGGTTTCGAAATCGATAAGCTTCTGCACCGTCAATTTGGAAGTCTTACACCTCATCAGAAAAGAA
AGCATTCTCAACATCAGTGGCAGAAGATGAAGCCATTAATTGAACGAGGATTGGCATACTGGCTGAC
ATGCACTTCGAGAACCTCAATCCAGCCTCTAGGGAAGCAATCAAAGCCTTGTTTTGCTCAACGTTACC
AATATCTGGAACAGAAACATCCTTCTCACTGATTTCTTCTCCATTCTCTGGCTGACAGCTATCAGATAG
ACTATCTTGATGAATCTTAGTTGTAGTTTCAAGATGCAAGTCATCGATTTACCATTCTCCATTACAGGA
TTCACCATCTGAAGTTGACTCTTTGATGCATGCTCAGTAGGTTCAAGTTGTTTCTTTTATAC
TGCTCCAGGTTGCTTCAAATGAAGCTATCCGAGCTGTGGACCAAAGGGGTTATGTTGCAACATCA
TGATCAGTAAATTCAATGCGGATTTCTAACAATTGCACTCTTATCTTCCAGTCTTCCAGCAGATAGTG
ATGCAACTTCATTCCATAGGCCAATTGAAACAGAATGCTCTTACAGAGTTTCCAGCCACACTTGAAGA
ACACGGCTCCTTGATAGGCTGAAACATCTCTACAGCGTTTCGAGCAAATTTCAAACATAGCTTGCTTA
GTCGCAGACGAAGGGACTTGGAACTCAWATCCCTCGGATTCCTAGAGTCTGCTTAATGAGATA
TGCGAGACGCCTATGATCGCATGATATTTGCTTCATTCTGTTGTGCACGTTGAAAAACCTGAATCAC
GAATCTGA-3'

Figure 5.2: Sequence of PCR product obtained from *AtCAPD2*^{RNAi} plants using insert specific primers. **A** = DMC1 promoter - intron reaction (sense fragment). **B** = Intron-terminator reaction (antisense fragment). Green = DMC1 promoter sequence. Red = sense/antisense fragment. Light blue= intron sequence. Dark blue = terminator sequence. Restriction sites are highlighted in yellow (top to bottom: *XhoI*, *EcoRI*, *HindIII*, *BamHI*).

5.2.4 Cytological screening of *AtCAPD2^{RNAi}* lines

After BASTA selection of the *AtCAPD2^{RNAi}* lines, 54 plants were recovered and 12 of these plants had clearly reduced fertility. Any plant which appeared to have shorter siliques than wild-type or gaps in their siliques was scored for fertility by counting seed set. Figure 5.3 shows the range of fertility seen in the *AtCAPD2^{RNAi}* lines. These lines appeared similar to wild-type in their vegetative development. All plants with reduced fertility as well as a few which had normal fertility were chosen for cytological analysis.

DAPI stained chromosome spreads were made for chosen lines as well as wild-type. In wild-type meiosis, prophase I chromosomes were visible as thin threadlike structures; the homologous chromosomes start to synapse at zygotene, are fully synapsed at pachytene and desynapse at diplotene. As chromosomes condensed in diakinesis, 5 discrete bivalents were observed. At metaphase I bivalents aligned along the meiotic spindle ready to segregate at anaphase I. Chromosomes segregated at anaphase I to form a dyad cell. In prophase II the chromosomes decondensed before re-condensing to form 2 sets of 5 individual chromosome masses at metaphase II. Sister chromatids are separated at anaphase II to form a tetrad cell (Figure 5.5: A-E). A cytological screen of first generation BASTA-resistant plants revealed 14 lines (3.8, 8.4, 3.1, 2.2, 6.5, 8.11, 1.4, 4.2, 7.3, 3.5, 2.1, 1.3, 7.6, and 8.3) which appeared to share the same phenotype to varying degrees. 9 of these lines had reduced fertility (less than 40 seeds/silique), the remaining 5 lines had normal fertility and a weaker meiotic phenotype (3.5, 1.2, 1.3, 7.6 and 8.3). In these lines prophase I appeared normal and synapsis seemed to progress as in wild-type.

However when the chromosomes condensed at metaphase I the chromosomes in the *AtCAPD2^{RNAi}* lines appeared elongated compared to those of wild-type (Figure 5.5: compare B with G, L and Q). At anaphase I thin threads of chromatin were seen between segregating chromosomes (Figure 5.5: H, M, R). In some cases these threads of chromatin continued into prophase II where cells with thin connections spanning the cytoplasm between the two sets of chromosomes were observed (Figure 5.4). Chromosomes decondensed at prophase II as in wild-type and recondensed at metaphase II. However the metaphase II chromosomes were again stretched compared to wild-type and appeared oddly-shaped (Figure 5.5: compare D with I, N and S). Thin threads of chromatin between segregating chromosomes were again seen at anaphase II (Figure 5.5: J, O, T). These phenotypes are consistent with those seen in *AtSMC4^{RNAi}* lines. Figure 5.5 shows some of the phenotypes observed. Note that not all stages of meiosis were found for every line.

One of the 14 lines which shared the meiotic phenotype observed in *AtSMC4^{RNAi}* lines (line 8.4) had an additional phenotype. In this plant connections between bivalents were seen at metaphase I. These were reminiscent of those seen in the empty vector control (section 4.2.7). It was therefore decided that the metaphase I connections were potentially an artefact of the transformation procedure. Line 6.2 had a phenotype consistent with a translocation heterozygote in which a single thick connection was consistently seen between non-homologous chromosomes and accompanied by a chromosome fragment.

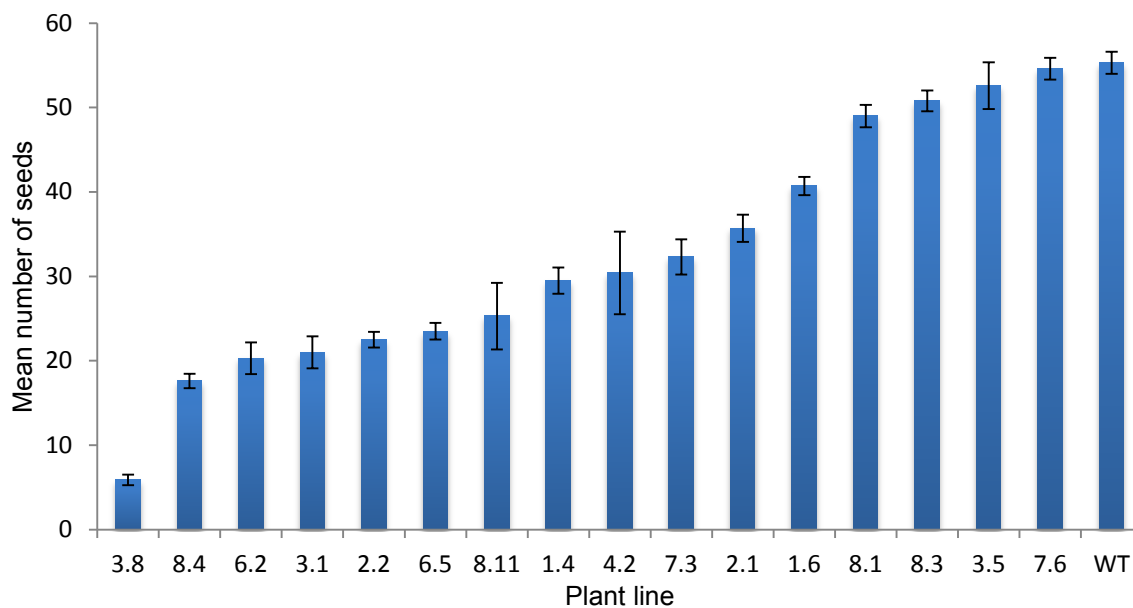


Figure 5.3: Mean seed set in *AtCAPD2^{RNAi}* lines which either showed signs of reduced fertility compared to wild-type or were analysed cytologically as ‘non reduced fertility controls’. Error bars = Standard error of the mean.

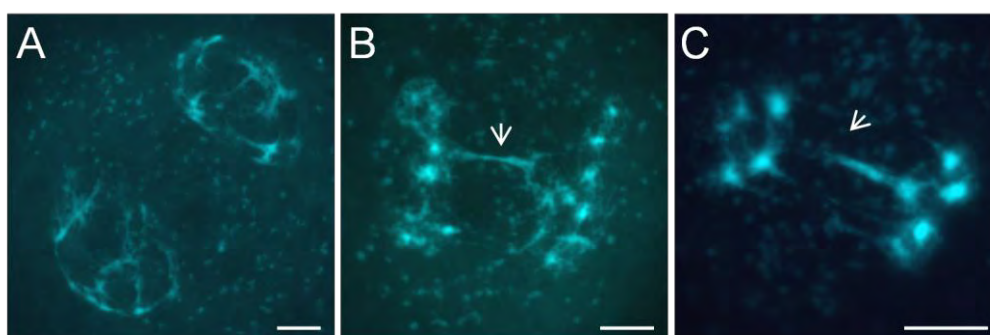


Figure 5.4: Meiotic prophase II cells in *AtCAPD2^{RNAi}* lines. Meiotic phenotypes observed in the *AtCAPD2^{RNAi}* lines in the cytological screen. Chromosomes stained with DAPI. **A** = wild-type; **B** = *AtCAPD2^{RNAi}* line 8.11; **C** = *AtCAPD2^{RNAi}* line 3.1. Arrowheads indicating connections. Scale bar 5µm.

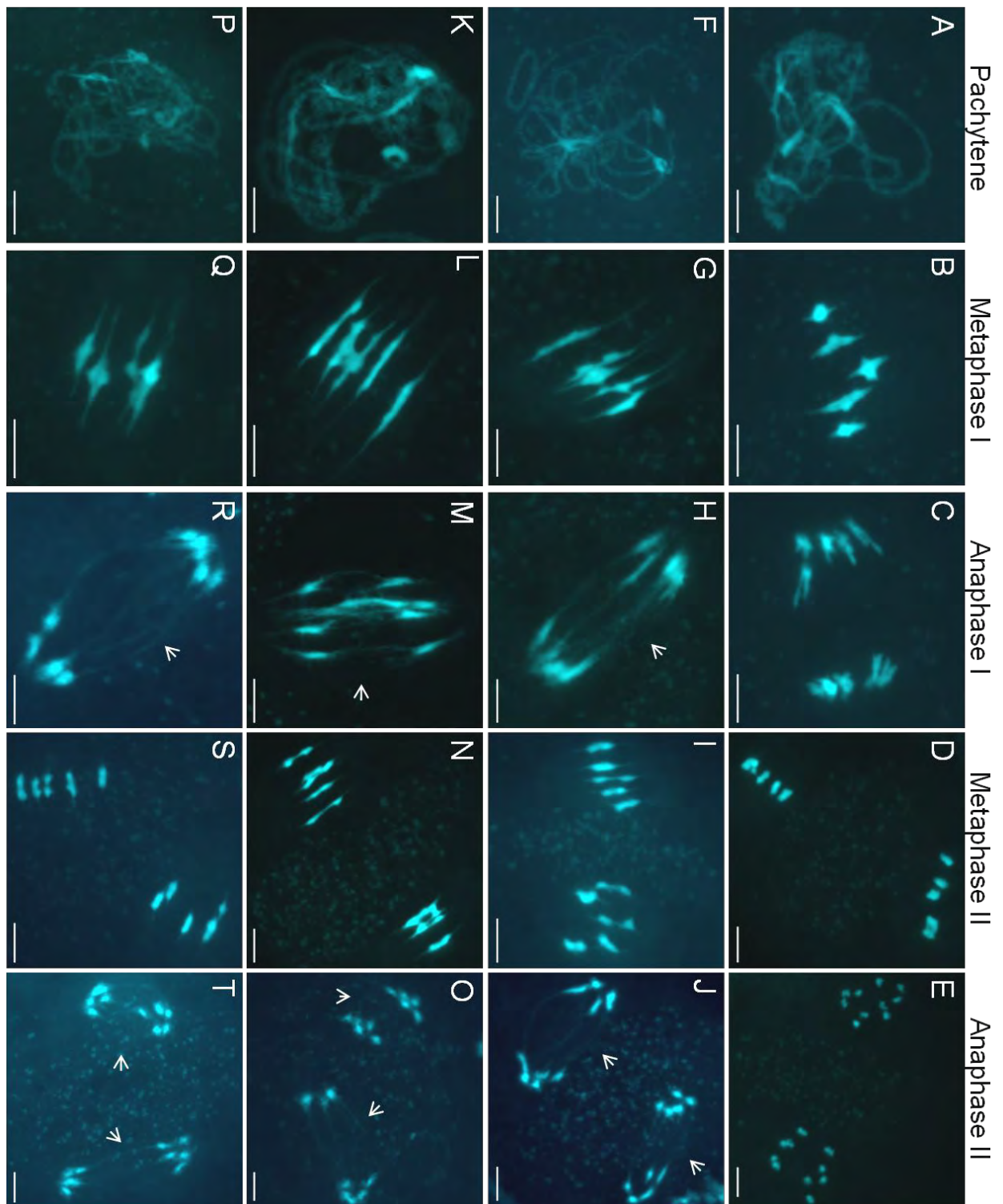


Figure 5.5: Meiotic phenotypes observed in the *AtCAPD2*^{RNAi} lines in the cytological screen. Chromosomes stained with DAPI. **A-E** = wild-type; **F-I** = *AtCAPD2*^{RNAi} line 8.11 (**J** = *AtCAPD2*^{RNAi} line 1.5); **K-O** = *AtCAPD2*^{RNAi} line 3.1; **P-Q** and **S-T** = *AtCAPD2*^{RNAi} line 2.2 (**R** = *AtCAPD2*^{RNAi} line 1.5). Arrowheads indicate thin threads of chromatin between chromosomes at anaphase I and II. Cell stages are indicated above columns. Scale bar 5µm.

5.2.5 *AtCAPD2^{RNAi}* lines have disorganised rDNA regions

Analysis of the rDNA in *AtSMC4^{RNAi}* lines in Chapter 4 revealed some defects in the organisation of the rDNA in these plants. However, *AtSMC4* functions in both condensin I and condensin II complexes, therefore it is not known whether the rDNA organisation role of *AtSMC4* is reflecting condensin I or condensin II function, or both. To address this, analysis of the 45S and 5S rDNA regions in *AtCAPD2^{RNAi}* lines was carried out using 45S and 5S specific FISH probes. Lines used for this analysis were 3.1 and 8.11 buds from the first generation of plants were used for each line.

FISH analysis of the rDNA regions in *AtCAPD2^{RNAi}* lines showed that, like *AtSMC4* deficient meiocytes, the rDNA regions appeared diffuse and disorganised. At metaphase I (and metaphase II) the 45S and 5S signals appeared abnormal. In particular the 5S signal was often spread out along the entire chromosome (Figure 5.6: D, G (F, I)). This contrasts with wild-type metaphase cells in which discrete 45S and 5S signals can be seen (Figure 5.6: A and C). At anaphase I the 5S rDNA signal is seen to stretch between the segregating chromosomes (Figure 5.6: E, H and K). These results phenocopy those seen in *AtSMC4^{RNAi}* lines (although the phenotype appears stronger in the *AtCAPD2^{RNAi}* lines). These results suggest that condensin I is required for the organisation of the rDNA. These results do not however rule out the possibility that condensin II also plays a role in rDNA organisation; this will be discussed in Chapter 6 (section 6.2.15).

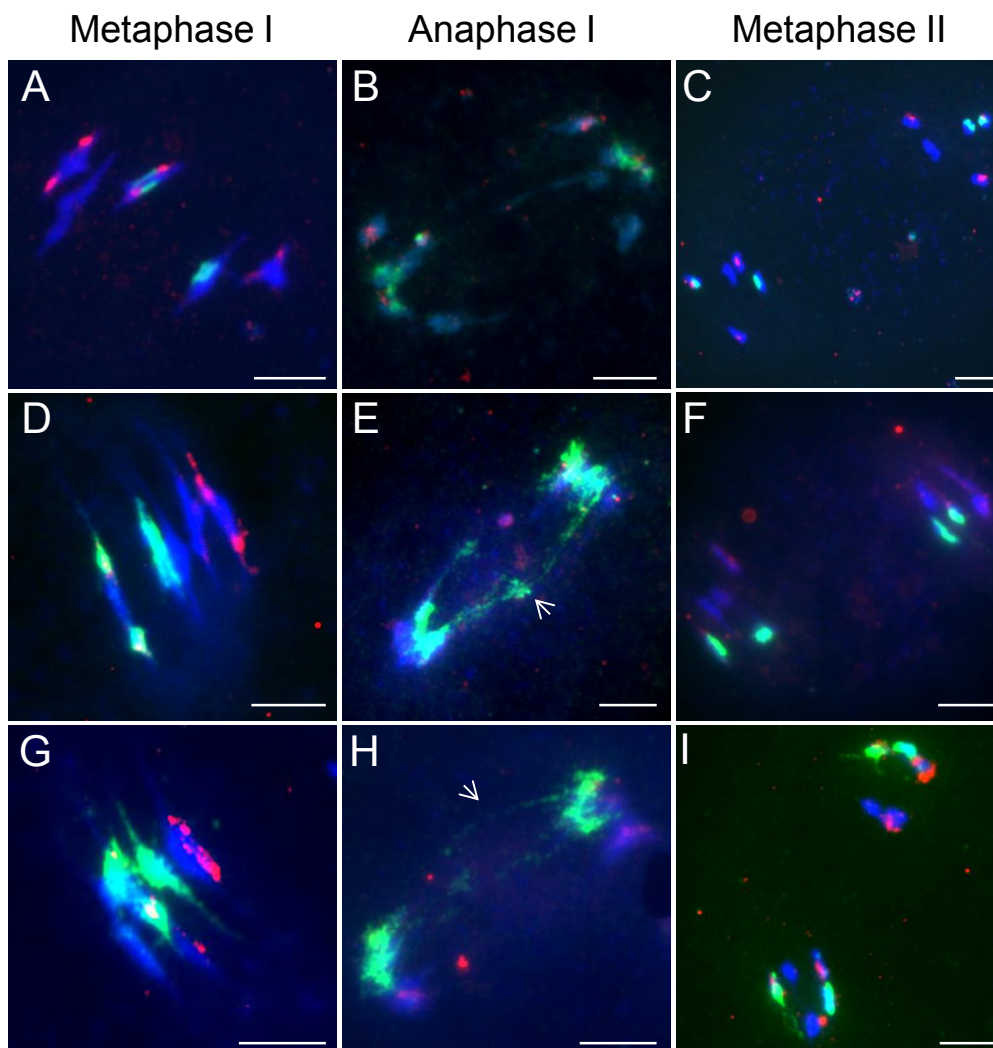


Figure 5.6: Analysis of the rDNA regions in *AtCAPD2^{RNAi}* lines and wild-type using 45S (red) and 5S (green) FISH probes. **A-C** = wild-type; **D-F** = *AtCAPD2^{RNAi}* line 8.11; **G-I** = *AtCAPD2^{RNAi}* line 3.1. Cell stage is indicated above column. Arrowheads indicate 5S rDNA signals between the segregating chromosomes. Scale bar = 5 μ m.

5.2.6 AtCAPD2^{RNAi} lines have defective centromeric DNA

In Chapter 4 it was seen that the centromeric DNA appeared disorganised in plants deficient in condensin. AtSMC4 antibody is also seen to localise to the centromeres of mitotic (and possibly meiotic) cells (sections 3.2.8 and 3.2.9). However from these results we cannot establish which of the two condensin complexes is primarily involved in the organisation of the centromeres. In budding yeast (Yong-Gonzalez *et al.*, 2007), *Drosophila* (Oliveira *et al.*, 2005) and human (Ribeiro *et al.*, 2009), the condensin I complex is required for centromere organisation. To investigate whether condensin I has a role in centromere organisation in *Arabidopsis*, FISH analysis using the centromere probe pAL38 was carried out on AtCAPD2^{RNAi} lines 3.1, 8.11 and 2.2. Again buds from the first generation of plants were used for each line.

During prophase I of meiosis the centromeres appeared as discrete signals which did not differ in their appearance from wild-type (Figure 5.7). However, by metaphase I when the chromosomes have been aligned along the metaphase plate by the spindle, the centromeres have a 'stretched' appearance. This was observed in all three AtCAPD2^{RNAi} lines assayed (Figure 5.8). This phenotype is the same as that seen in the AtSMC4^{RNAi} lines (section 4.2.16) and suggests that the condensin I complex is involved in the organisation or maintenance of the centromeric DNA.

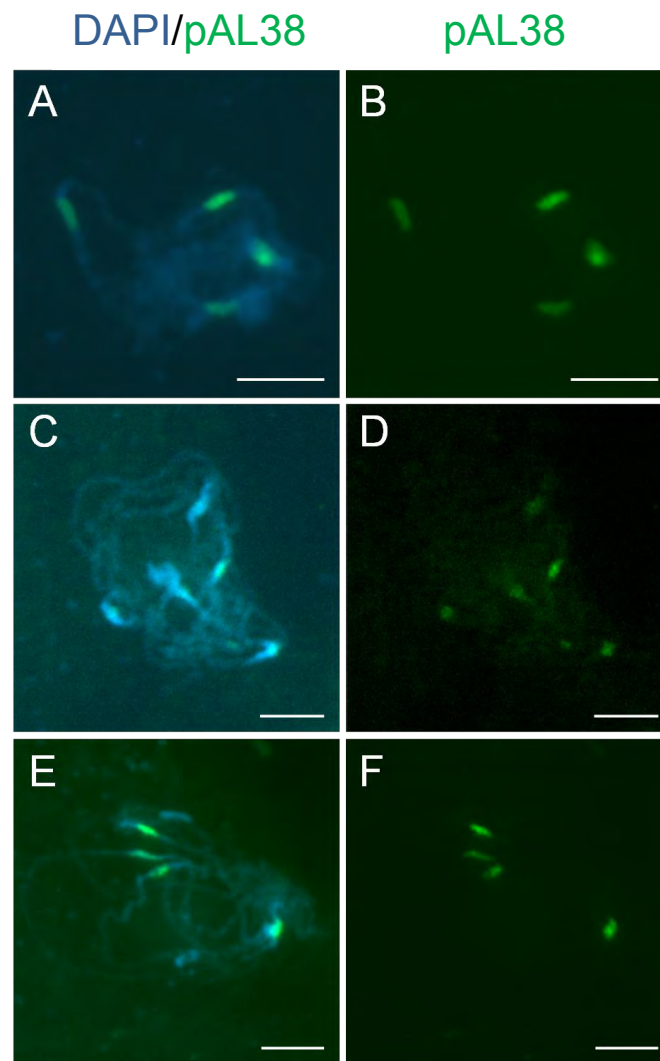


Figure 5.7: Analysis of centromere regions in *AtCAPD2^{RNAi}* lines at pachytene. PMCs hybridised with centromere specific FISH probe pAL38. **A - B** = wild-type; **C - D** = *AtCAPD2^{RNAi}* line 8.11; **E - F** = *AtCAPD2^{RNAi}* line 2.2. **A, C** and **E** = DAPI/Pal 38 (FITC) merge; **B, D** and **F** = pAL38. Scale Bar = 5 μ m.

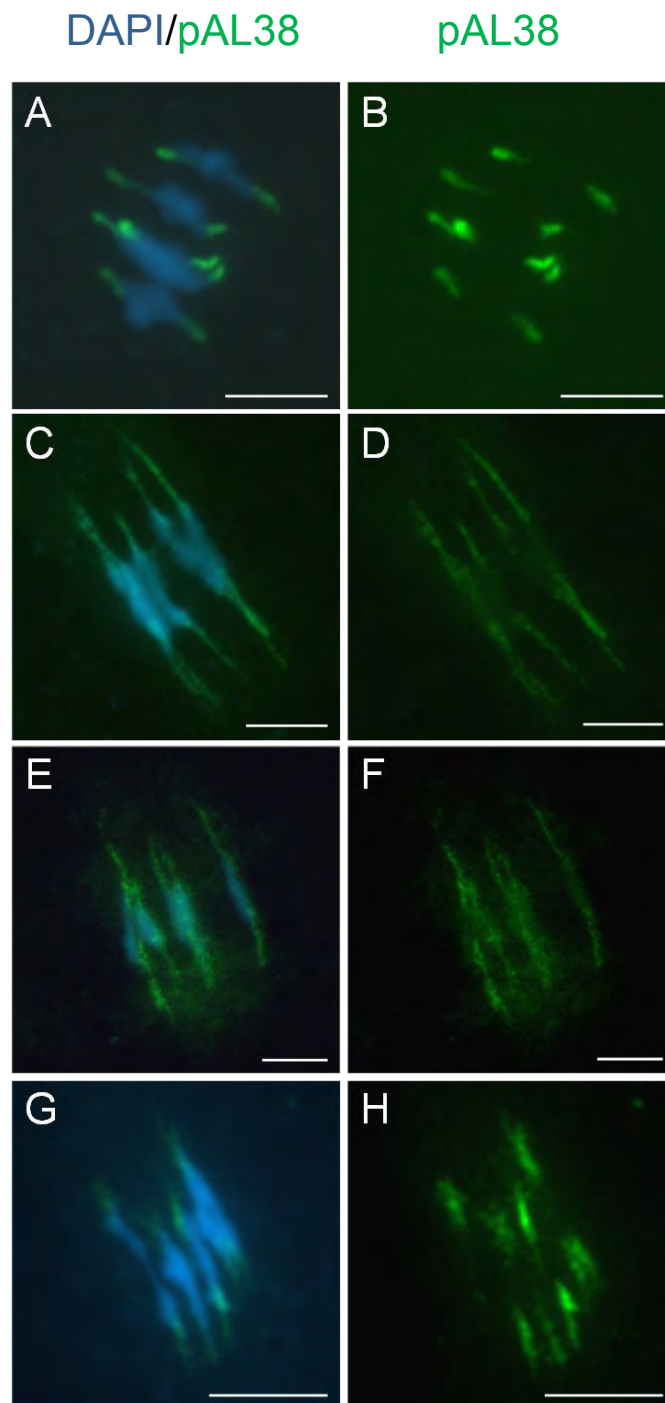


Figure 5.8: Analysis of centromere regions in *AtCAPD2^{RNAi}* lines at metaphase I. PMCs hybridised with centromere specific FISH probe pAL38. **A - B** = wild-type; **C - D** = *AtCAPD2^{RNAi}* line 3.1; **E - F** = *AtCAPD2^{RNAi}* line 8.11; **G - H** = *AtCAPD2^{RNAi}* line 2.2. **A, C, E and G** = DAPI/Pal 38 (FITC) merge; **B, D, F and H** = pAL38. Scale Bar = 5 μ m.

5.3 DISCUSSION

5.3.1 An *Atcapg* homozygote insertion mutant appears to be lethal

Attempts were made to identify T-DNA insertion lines in condensin I subunits. No inserts were identified in *AtCAPH* or *AtCAPD2* in any line tested. An insert was identified in one *AtCAPG* line, however only heterozygous plants were recovered. The lack of homozygous plants was statistically significant as shown by a Chi-squared test, suggesting that *Atcapg* homozygote insertion lines are lethal. Similar lethality was seen for *Atsmc4* insertion lines (Siddiqui *et al.*, 2006; and this study section 4.2.3). As *AtCAPG* functions in the same complex as *AtCAPD2* and *AtCAPH*, it is assumed that mutations in these subunits are also lethal. Condensin subunits are essential for viability in other species, for example *C. elegans* (Lieb *et al.*, 1998; Hagstrom *et al.*, 2002), *Drosophila* (Bhat *et al.*, 1996; Steffensen *et al.*, 2001), fission yeast (Saka *et al.*, 1994) and budding yeast (Strunnikov *et al.*, 1995; Freeman *et al.*, 2000).

5.3.2 Chromosome organisation in the *AtCAPD2^{RNAi}* lines

As with the *AtSMC4^{RNAi}* lines the chromosomes in the *AtCAPD2^{RNAi}* lines had abnormalities in chromosome organisation. In these plants prophase I appears indistinguishable from wild-type, as seen in DAPI stained chromosome spreads. However at metaphase I the structure of the chromosome appears altered compared to wild-type; metaphase I chromosomes in the *AtCAPD2^{RNAi}* lines appear more elongated in *AtCAPD2^{RNAi}* plants than wild-type, this results resembles the longer

metaphase I chromosomes seen in *AtSMC4^{RNAi}* plants. Abnormal centromere structure may be largely responsible for the elongated chromosome observed.

5.3.3 Condensin I is required for the structural stability of the centromeres

FISH analysis using the centromere probe pAL38 revealed that the condensin I complex is required for correct centromere architecture. A similar phenotype was observed in the *AtSMC4^{RNAi}* lines. The results showed that the centromeres appeared stretched when the chromosomes became attached to the spindle, suggesting that the pulling force of the spindle may be responsible for the stretching of the centromeres and that condensin is required in order to maintain centromere structure. This phenotype is consistent with those seen in budding yeast (Yong-Gonzalez *et al.*, 2007), *Drosophila* condensin I (Oliveira *et al.*, 2005; Savvidou *et al.*, 2005; Gerlich *et al.*, 2006) and chicken condensin complexes (Ribeiro *et al.*, 2009), where the spindle force is thought to be responsible for stretching the centromeric chromatin. However merotelic attachment of the spindles may also be responsible for the stretching of the centromeres seen in condensin depleted cells (Samoshkin *et al.*, 2009).

5.3.4 Condensin I is required for correct organisation of the rDNA in

Arabidopsis

Analysis of the rDNA regions using the FISH probes 45S and 5S showed that *AtCAPD2^{RNAi}* lines did not have discrete, compact rDNA signals at metaphase I or II, as is seen in wild-type cells. The rDNA regions were also seen to span the gap

between segregating chromosomes at both meiotic anaphases. These results are similar to those seen in *AtSMC4^{RNAi}* lines, however the disorganised rDNA signals at metaphase appear more severe in the *AtCAPD2^{RNAi}* lines than the *AtSMC4^{RNAi}* lines. As discussed in Chapter 4 (section 4.3.5.2), condensin may be required more specifically at the rDNA due to the repetitive nature of the DNA sequence and high transcription rates which make it unstable and prone to homologous recombination.

Condensin I has been implicated in rDNA maintenance in yeast (Freeman *et al.*, 2000; Bhalla *et al.*, 2002; Lavoie *et al.*, 2002; D'Amours *et al.*, 2004; Machin *et al.*, 2004; Sullivan *et al.*, 2004; Wang *et al.*, 2004; Wang *et al.*, 2005; Tsang *et al.*, 2007; D'Ambrosio *et al.*, 2008a; Nakazawa *et al.*, 2008). However, condensin does not appear to have a specific role in rDNA organisation in higher eukaryotes (Vagnarelli *et al.*, 2006), although a subtle role for condensin in rDNA organisation has been suggested in interphase in *Drosophila* (Cobbe *et al.*, 2006). Results presented in this chapter and in Chapter 4 represent the first time condensin I has been shown to be required for the organisation of the rDNA in a higher eukaryote. These results do not rule out the possibility that condensin II may also have a role in rDNA organisation.

5.3.5 Chromosome segregation defects are seen in condensin I-deficient cells

During chromosome segregation at anaphase I and II a veil of lagging chromatin was seen in *AtCAPD2^{RNAi}* lines which was absent in wild-type. These anaphase defects appeared similar to those seen in *AtSMC4^{RNAi}* lines. Anaphase bridges have been described in condensin mutants in several species during meiosis and mitosis (Yu

and Koshland, 2003; Chan *et al.*, 2004; Resnick *et al.*, 2009). The origin of these bridges has been suggested to be due to the inability to remove concatenation between chromosomes in *C. elegans* (Chan *et al.*, 2004), to be recombination-related (Yu and Koshland, 2003) or to be the result of a “catastrophic loss of individual chromosome architecture” when the chromosomes try to segregate at anaphase (Vagnarelli *et al.*, 2006). Connections have also been suggested to be between the rDNA loci where condensin appears to associate as strong foci along an otherwise linear axial signal (Yu and Koshland, 2003). The anaphase bridges in *AtCAPD2^{RNAi}* plants appear to be at least in part due to defects in the rDNA.

In Chapter 4 an *AtSMC4^{RNAi}* line was crossed to *Atspo11-1*. Plants homozygous for *Atspo11.1* and which also contained an *AtSMC4^{RNAi}* construct had a similar phenotype to *Atspo11.1* at, what in wild-type would constitute metaphase I, with 10 univalents present. However, when the chromosomes came to segregate at anaphase I chromosome appeared to de-condense. It was suggested from these results that condensin may be required to maintain chromatin structure at anaphase and possibly also resolve linkage between chromosomes. These results support previous studies in chicken DT40 cells (Vagnarelli *et al.*, 2006).

5.3.6 Future perspectives

The level of *AtCAPD2* depletion has not been assessed in the *AtCAPD2^{RNAi}* lines, therefore transcript analysis or western blot analysis using an antibody specific to *AtCAPD2* needs to be carried out in order to be sure that the phenotype observed is

due to reduced levels of *AtCAPD2*. However, since the phenotype of the *AtCAPD2^{RNAi}* lines is similar to that of the *AtSMC4^{RNAi}* lines, which has been shown to be due to a reduction in *AtSMC4* protein, it seems reasonable to assume that the phenotypes of the *AtCAPD2^{RNAi}* lines are due to a reduction in *AtCAPD2* protein.

Further analysis of the centromeres in the *AtCAPD2^{RNAi}* plants will provide interesting insight into the cause of the stretched appearance. As with *AtSMC4^{RNAi}* lines the role of the spindle apparatus in centromere structure in these lines could be investigated by arresting *AtCAPD2*-deficient meiocytes at metaphase I by inhibiting the spindle using colchicine. This would allow assessment of the effect of the spindle force on the centromeres. Investigation of centromere histone localisation could also be carried out on these plants using antibodies raised against centromere specific histones.

The localisation of condensin I specific subunits has not been investigated here. In Chapter 3 the localisation of *AtSMC4*, which is a subunit of both complexes, was assayed. However this did not allow any insight into the localisation of the two individual condensin complexes during meiosis. Therefore it would be interesting to investigate the localisation of the two complexes individually during a meiotic (and mitotic) cell division.

This chapter, and Chapter 4, have described how condensin I is required for wild-type levels of compaction in repetitive DNA such as the rDNA and centromere regions. Telomeres are also regions of repetitive DNA but have not been investigated here. Condensin has been implicated in the correct segregation of the telomeric regions in budding and fission yeast (Yu and Koshland, 2003; Yu and Koshland, 2005; Motwani *et al.*, 2010) and *Drosophila* (Steffensen *et al.*, 2001) and condensin I is seen to be enriched at the subtelomeric regions in budding yeast (Wang and Strunnikov, 2008) and during meiosis in mouse (Viera *et al.*, 2007). Therefore it would be interesting to investigate whether condensin has a role in telomere segregation in *Arabidopsis* using telomere specific FISH probes.

5.3.7 Conclusions

AtSMC4 and *AtCAPD2* are both subunits in the condensin I complex. Consistent with this, RNAi lines of both genes shared a very similar phenotype. Plants from both lines had elongated metaphase I and II chromosomes and thin thread-like bridges between segregating chromosomes at both meiotic divisions. Further analysis of both lines revealed that both proteins were required for organisation of repetitive DNA such as the rDNA and centromeres. Analysis of condensin I specific subunits has shed light onto the role of the individual complexes in chromosome organisation. However it is not known what specific part condensin II plays in the organisation of the meiotic chromosomes. Chapter 5 describes the analysis of a mutant in the condensin II subunit, *AtCAPD3*.

CHAPTER 6

6 ANALYSIS OF AN *ATCAPD3* T-DNA LINE AND *ATCAPD3*^{RNAi} LINES

6.1 INTRODUCTION

AtCAPD3 is a member of the condensin II complex found in metazoans. Condensin I and II are thought to play different roles during mitotic cell divisions. Depleting condensin I and condensin II specific subunits independently produces distinct phenotypes in HeLa cells, with condensin II depleted chromosomes appearing 'curly' (Ono *et al.*, 2003). During human mitotic divisions condensin II has been shown to have a role in prophase condensation (Hirota *et al.*, 2004, Ono *et al.*, 2004; Gerlich *et al.*, 2006). Prophase condensation was significantly delayed in cell deficient in condensin II subunits, whereas later stages of mitosis appeared unaffected (Hirota *et al.*, 2004). Condensin II has been suggested to be involved in mitotic chromosome shortening, and the loading of condensin II on chromosomes also appeared to be inversely proportional to the amount of cohesin remaining (Shintomi and Hirano, 2011).

Consistent with a role for condensin II in prophase condensation, condensin II subunits are enriched on the chromosomes at mitotic prophase (Hirota *et al.*, 2004; Ono *et al.*, 2004; Gerlich *et al.*, 2006). Using FRAP (fluorescence recovery after photobleaching) experiments this association on prophase chromosomes appeared to be stable (Gerlich *et al.*, 2006). Condensin II was subsequently shown to remain

enriched in the chromatid axis from prometaphase until anaphase (Gerlich *et al.*, 2006).

The role of condensin II in meiotic cell divisions has been less well studied, nevertheless a few studies have looked into the specific roles of condensin II in meiosis (Chan *et al.*, 2004; Hartl *et al.* 2008a; Mets and Meyer 2009). *C. elegans* condensin II subunits were seen to be enriched in pachytene nuclei (Mets and Meyer, 2009) and to localise on the chromosomes at diplotene and diakinesis (Chan *et al.*, 2004). During prophase I in *C. elegans*, pachytene chromosome axis length is increased in condensin II deficient cells compared to wild-type. This axis length increase is accompanied by an increase in DSBs and a subsequent increase in COs (Mets and Meyer, 2009). In addition to a role in pachytene axis length and CO distribution, *C. elegans* condensin II also has a role in chromosome compaction at diplotene and diakinesis and chromosome segregation. Clear DNA bridges were observed between segregating chromosomes at both meiotic divisions (Chan *et al.*, 2004). Chromosome segregation defects have also been observed in condensin II mutants in *Drosophila* (Hartl *et al.*, 2008a). These flies had abnormal chromosome territory formation in prophase I, suggesting a conserved role in prophase I chromosome organisation between worms and flies (Hartl *et al.*, 2008a). The role of condensin II during meiosis has not been investigated in plants. Plants differ from *Drosophila* and particularly *C. elegans* in their control of meiotic events such as recombination/CO formation and synapsis. Therefore it is likely that condensin II will play a slightly different role during meiosis in *Arabidopsis*.

This Chapter focuses on the role of *AtCAPD3*, a subunit of condensin II, in meiotic chromosome organisation. Figure 6.1 shows the predicted subunit arrangement of the condensin II complex. Both T-DNA knock out lines and RNAi lines of *AtCAPD3* have been analysed for their roles in meiosis. The aim of this work, together with work in Chapter 5 was to distinguish between the roles of the two condensin complexes during meiosis. This chapter also describes the endeavours to produce an *AtCAPD3* recombinant protein for antiserum production.

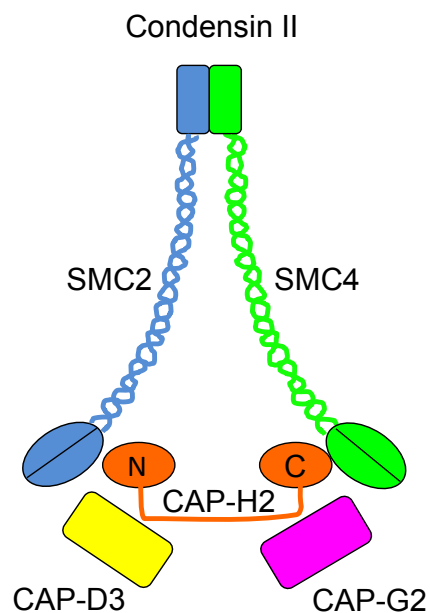


Figure 6.1: Schematic representation of the condensin II complex. Both condensin I and condensin II complexes share the same SMC2/SMC4 back bone but differ in their regulatory subunits. Condensin II comprises CAP-H2, CAP-D3 and CAP-G2.

6.2 RESULTS

6.2.1 Isolation and characterisation of *AtCAPD3* T-DNA lines

In order to ascertain the role of *AtCAPD3* and therefore the condensin II complex in meiosis a *Atcapd3* mutant was required. The NASC database was screened for insertion lines in the *AtCAPD3* gene, At4G15890. The T-DNA insertion mutant line Sail_826_B06 was ordered for analysis. A T-DNA insert was detected in this line using gene specific and insert specific primers (D3BO6_Rp and D3B06_Lp or Sail_LB1 and D3BO6_Rp respectively). Plants containing homozygous T-DNA inserts in this gene were identified. Figure 6.2 shows the position of the T-DNA insert in the first exon of the *AtCAPD3* gene as predicted by NASC.

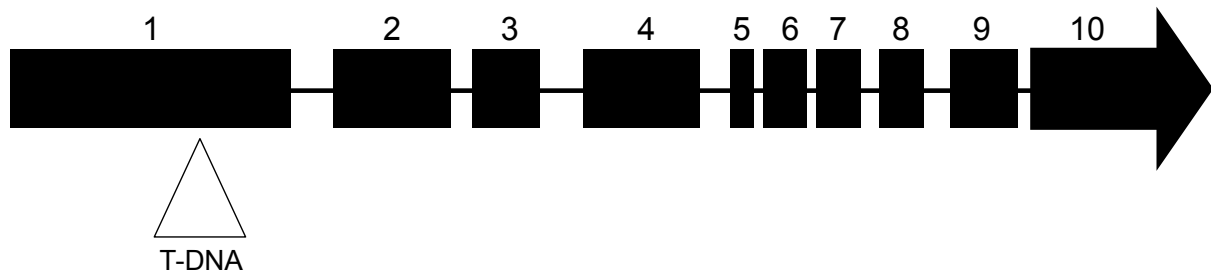


Figure 6.2: Position of the T-DNA insert in the Sail_826_B06 line. Insert in the 1st exon of the *AtCAPD3* gene At4G15890. Black bars represent exons, spaces represent introns. Exons are numbered.

6.2.2 Confirming the position of the T-DNA insertion site

The position of the T-DNA insert is predicted in the Sail_826_B06 line to be in the first exon of the *AtCAPD3* gene. To confirm this, the PCR product from the Sail-LB1/D3BO6_Rp reaction (for primer information see appendix, table 8.2) was excised from the gel, cloned into pDrive and sequenced. The sequence obtained confirmed that the T-DNA insert was in the first exon of the *AtCAPD3* gene. Figure 6.3 shows the sequence obtained.

```

5'-GTGACTATAGATCAGCGGCCGCGAGCTCGGGCCCCACACGTGTGGTCTAGAGCTAGCCTAGGCT
CGAGAAGCTTGTGCGACGAATTCAGATGCCTTTTCAGAAATGGATAAATAGCCTTGCTTCCTATTATAT
CTTCCCAAATTACCAATACATTACACTAGCATCTGAATTCATAACCAATCTCGATACACCAAATCGAA
TTCAATTCGGCGTTAATTCAGTACATTA AAAACGTCCGCAATGTGTTATTAAGTTGTCTAAGCGTCAA
TTTGTTTTCTTGGGTTGTATTGATGCTTTAGTTCAGCGGTGTT CAGACACGAGCGCTTTGATTAGAGC
TCGAGCTTTGTCCAACCTGGCTCAAGTTGTGGAGTTCTTGTCTGGTGATGAAAGGAGTAGGTCGATC
CTGAAACGAGCCCTTGGGTTTAACGGTGAGACTTCAGAGGGAAAAGGTGCAGTAACTGACCTTTTG
AAGAAAAGATGTGTGGATGAGAAGGCGGCTGTAAGGAGAGCAGCTCTTCTTCTGGTGACAAAATTG
ACATCGCTTATGGGTGGTTGCTTTGATGGTAGTATCCTAAAGACAATGGGTACATCTTGTTCTGATCC
GCTAATAAGTATAAGAAAGGCTGCAGTTTCAGCTATTTCCGAATCACGAATTCGGATCCGATACGTA
ACGCGTCTGCAGCATGCGTGGTACCGAGCTTCCCTATAGTGAGTCGTATTAGAGCTTGGCGTAATC
ATGGTCATAGCTGTTTCCTGTGTGAAATTGTTATCCGCTCACAAATCCACACAACATACGAGCCGGAA
GCATAAAGTGTAAGCCTGGGGTGCCTAATGAGTGAGCTAACTCACATTAATTGCGTTGCGCTCACT
GCCCGCTTCCAGTCGGGAAACCTGTCGTGCCAGCTGCATT-3'

```

Figure 6.3: Sequence obtained from cloning the PCR band of the insert reaction of *Atcapd3* T-DNA line Sail-826_B06. Green, T-DNA insert sequence. Red; *AtCAPD3* At4G15890 gene sequence. Blue pDrive sequence. Sail_LB1 primer (green) and D3BO6_Rp primer (red) are underlined. Yellow highlight shown positions of two EcoRI sites in pDrive

6.2.3 Confirming the number of inserts in the *Atcapd3* insertion line

Many T-DNA lines have more than one insert present in their genomes. It is predicted in the Salk institute website, T-DNA express, that Sail_826_B06 only contains one insert. To confirm this, FISH analysis was carried in *Atcapd3* plants on spread PMCs at pachytene stage of meiosis using a probe specific to the T-DNA insertion sequence. This experiment confirmed that there was only one T-DNA insert present in this line, most likely corresponding to the insert detected in PCR experiments (see 6.2.2). Figure 6.4 shows a pachytene cell with only 1 homozygote T-DNA insert

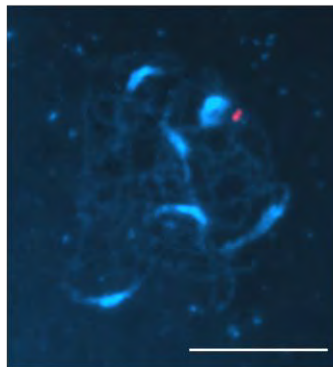


Figure 6.4: Pachytene cell from a homozygous plant of the *Atcapd3* T-DNA knock out line Sail-826_B06 showing one homozygous insert present (red). Scale bar 10 μ m

6.2.4 Analysis of AtCAPD3 transcript levels in wild-type and *Atcapd3* plants

To determine if the *AtCAPD3* transcript was expressed in the *Atcapd3* homozygous plants, RT-PCR analysis was carried out. RNA from leaf and bud tissue from both wild-type and *Atcapd3* homozygous plants was used to compare the levels of *AtCAPD3* transcript between wild-type and *Atcapd3* plants. For each sample tissue from several plants was pooled to make RNA. The housekeeping gene *GAPD* was used as a control. *AtCAPD3* gene specific primers were designed either side of the T-DNA insert. Both *AtCAPD3* and *GAPD* primer sets were designed so they span an intron, this way the primers should not amplify the genomic (gene) sequence. The predicted sizes of the *GAPD* band and the *AtCAPD3* band are 541 nt and 611 nt respectively. RT-PCR analysis revealed that *AtCAPD3* transcript is only detected in buds in wild-type and was absent from leaf samples. *AtCAPD3* transcript was absent from both leaf and bud in the *Atcapd3* homozygous insertion plant (Figure 6.5:A), thus suggesting that these plants are likely to be null mutants of *AtCAPD3*. PCR reactions of leaf for both wild-type and *Atcapd3* were re-amplified (1µl of original reaction amplified in a new reaction for a further 20 cycles). However no band was detected in the re-amplified sample for wild-type or *Atcapd3* plants, this reaction was repeated 3 times with the same outcome (Figure 6.5:B).

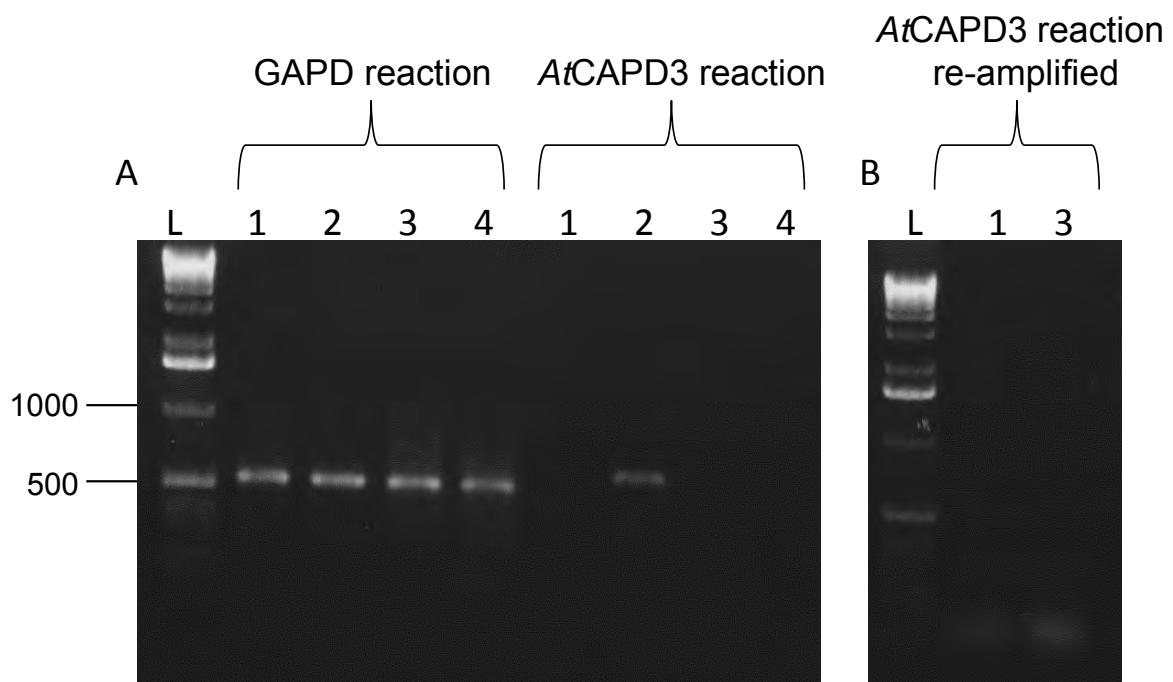


Figure 6.5: RT-PCR analysis of *AtCAPD3* transcript in *Atcapd3* homozygous and wild-type plants: L= 1kb ladder, 1000 and 500mbp are indicated. **A** = RT-PCR reaction showing products from GAPD and *AtCAPD3* primers (1 = Wild-type leaf; 2 = wild-type bud; 3 = *Atcapd3* leaf; 4 = *Atcapd3* bud. **B** =Re-amplification of *AtCAPD3* reaction on: 1 wild-type and 2 *Atcapd3* leaf samples.

6.2.5 *Atcapd3* mutants have developmental defects

Atcapd3 mutants exhibited a distinct vegetative phenotype. Plants were short in stature compared to wild-type and had smaller rosette leaves. Figure 6.6 shows the vegetative phenotype of wild-type and *Atcapd3*. Plants heterozygous for the T-DNA insertion (*AtCAPD3*^{+/-}) showed no somatic defects when compared to wild-type plants grown at the same time. Both *AtCAPD3*^{+/-} and *Atcapd3* plants had gaps in their siliques, indicating possible defects during meiosis.



Figure 6.6: Vegetative defects in *Atcapd3* plants. **A**= Wild-type and *Atcapd3* plants approximately 45 days after planting. **B** = Wild-type and *Atcapd3* rosette stage plants approximately 30 days after planting

6.2.6 Fertility was reduced in *Atcapd3* and *AtCAPD3*^{+/-} plants

Fertility of the *AtCAPD3*^{+/-} and *Atcapd3* plants as well as wild-type was scored at approximately 60 days after planting, when the siliques had dried out. Seed set was counted for each line. *Atcapd3* and *AtCAPD3*^{+/-} plants both had gaps in their siliques indicating reduced fertility. Figure 6.7 shows average seed set for wild-type, *Atcapd3* and *AtCAPD3*^{+/-} plants. Analysis shows that both *Atcapd3* and *AtCAPD3*^{+/-} plants had a similar reduction in fertility compared to wild-type (~50% reduction in fertility for both compared to wild-type).

Pollen viability was assessed in *Atcapd3* and *AtCAPD3*^{+/-} plants using Alexander stain (Alexander, 1969). For this analysis three plants from each genotype (Wild-type, *Atcapd3* and *AtCAPD3*^{+/-}) were used. Wild-type pollen had a ratio of non-viable: viable of 1:144 (n=1882), the ratio for *Atcapd3* was 1:25 (n=1506) whereas the ratio of non-viable to viable in *AtCAPD3*^{+/-} plants was 1:2.7 (n= 1684).

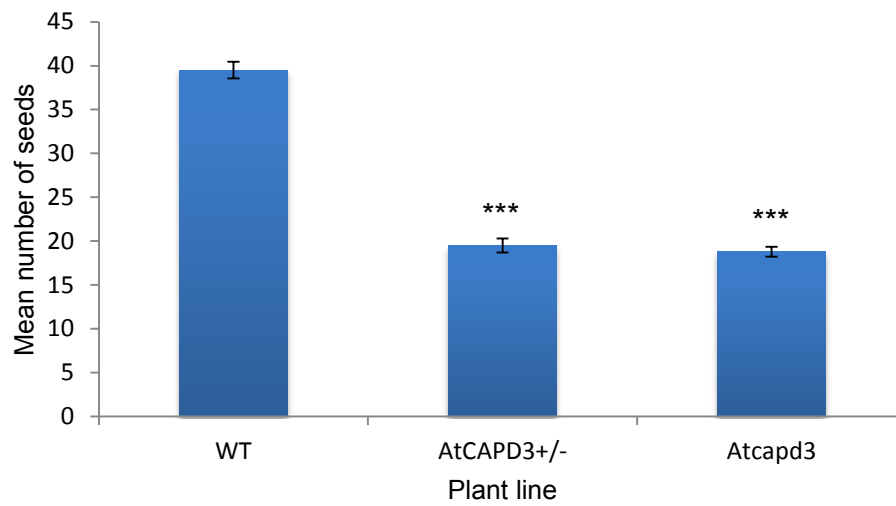


Figure 6.7: Mean seed set in *AtCAPD3*^{+/-} and *Atcapd3* compared to wild-type (WT). 5 plants were scored for each line. 10 siliques from each plant were scored. *** = $p < 0.005$. Error bars = Standard error of the mean.

6.2.7 *Atcapd3* plants had a reduced seed germination frequency compared to wild-type and *AtCAPD3*^{+/-} plants.

As both the heterozygous and homozygous T-DNA insertion plants for *AtCAPD3* appeared to have a similar reduction in fertility, a germination assay was carried out to determine whether all of the seeds from these lines were viable. Indeed many of the *Atcapd3* homozygous seeds appeared misshapen. Seeds from 4 plants of wild-type, *Atcapd3* and *AtCAPD3*^{+/-} were planted on MS agar plates. Germination was scored 14 days after planting when all seeds from wild-type had germinated. Wild-type seeds had a 100% germination rate (N=400), seeds from the *AtCAPD3*^{+/-} plants had a germination rate of 99% (N=400) and *Atcapd3* seeds had a germination rate of 63.75% (N=400). Seedlings of *Atcapd3* plants appeared to be smaller and slower growing than those of the *AtCAPD3*^{+/-} or wild-type. Therefore to be sure that the *Atcapd3* seeds were not simply slower to germinate, plants were left to grow for a further 7 days. However no further seeds germinated from the *Atcapd3* plants. Figure 6.8 shows seeds from wild-type, *AtCAPD3*^{+/-} and *Atcapd3* plants on MS medium 14 days after germination.

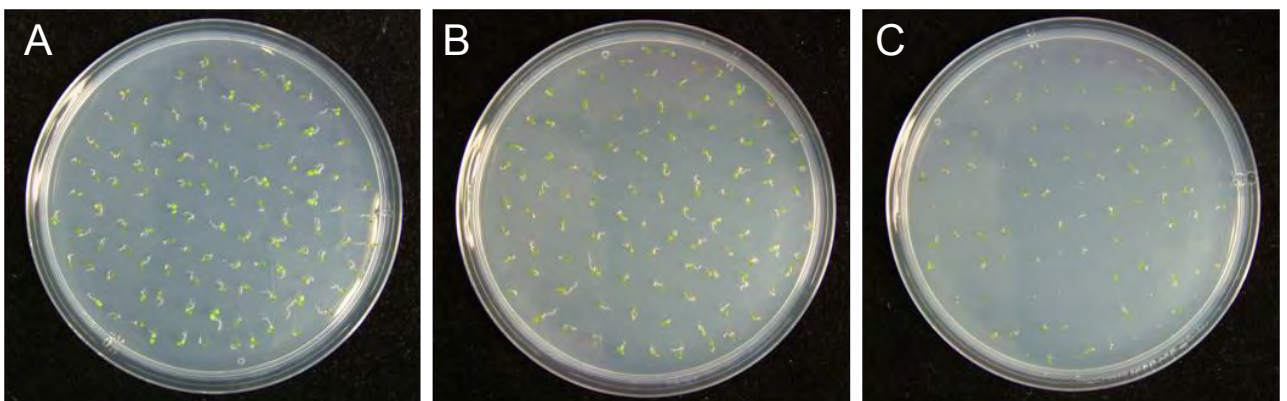


Figure 6.8: Germination assay. **A** = Seeds from wild-type; **B** = seeds from *AtCAPD3*^{+/-} plants; **C** = seeds from *Atcapd3* plants. Seeds were planted on MS media and scored for germination 14 days after planting.

6.2.8 Cytological analysis of *Atcapd3* and *AtCAPD3*^{+/-}

A cytological analysis of PMCs of *Atcapd3* and *AtCAPD3*^{+/-} was carried out alongside wild-type. In wild-type meiosis, early prophase I chromosomes were seen as thin threadlike structures, which start to synapse at zygotene, fully synapsed homologous chromosomes were seen at pachytene and homologous desynapsed at diplotene. As the chromosomes condensed in diakinesis, 5 discrete bivalents were observed. At metaphase I bivalents aligned along the meiotic spindle ready to segregate at anaphase I. Chromosomes segregated synchronously at anaphase I to form a dyad cell. In prophase II the chromosomes de-condensed before re-condensing to form 2 sets of 5 individual chromosome masses at metaphase II. Sister chromatids are separated at anaphase II to form a tetrad cell (Figure 6.9: A-F).

6.2.9 *AtCAPD3*^{+/-} plants had a mild meiotic phenotype

A cytological analysis was carried out on *AtCAPD3*^{+/-} plants to try to identify the cause of the reduced fertility and reduction in pollen viability. Cells in prophase I of meiosis were indistinguishable from those in wild-type. Homologous chromosomes appeared to fully synapse along their length (Figure 6.9: G). *AtCAPD3*^{+/-} chromosomes condensed into discrete metaphase I bivalents as in wild-type (Figure 6.9: compare B and H). However, a few metaphase I cells (2/8) had univalents (Figure 6.9: I). All other stages of meiosis appeared normal (Figure 6.9: J-L). No mis-segregation was observed out of the 15 metaphase II cells analysed.

6.2.10 *Atcapd3* plants had misshapen chromosomes and connections between chromosomes at metaphase I.

In *Atcapd3* plants various abnormalities were observed during meiosis. The chromosomes in prophase I appeared indistinguishable from wild-type with homologous chromosomes completing synapsis at pachytene. However at metaphase I chromosomes in *Atcapd3* appeared thin and elongated, multiple chromosome masses often involving all 5 bivalents were observed in the majority of cells (30/33) (Figure 6.10: B-D). Chromosome fragments were also observed in some cells (2/33) (see arrow head Figure 6.10: C) which may have arisen due to breakages caused as a result of a defects in resolving the multiple chromosome masses or due to unrepaired DSBs. In many metaphase I cells it appeared as if the sisters chromatids of each bivalent had separated from each other (Figure 6.10: E, arrowhead). Some metaphase I cells appeared more like wild-type in that they appeared closer to the length and width of wild-type bivalents (compare Figure 6.10: B and D). The chromosomes in these cells did still appear oddly shaped compared to those of wild-type. It is possible that these more ordered metaphase I cells represent a later stage in the *Atcapd3* meiosis than the other, more disorganised metaphase I cells. At anaphase I as the chromosomes moved toward the two poles of the cell the chromosomes did not appear to be neatly together as is seen in wild-type, instead trailing chromosomes were seen as the homologues segregated (Figure 6.10: E and F). It is possible that the individual sister chromatids have separated from each other in these cells. In 4/13 anaphase I cells connections were seen between segregating chromosomes (Figure 6.10: F- arrow head). These anaphase defects were distinct from those seen in *AtSMC4* and *AtCAPD2^{RNAi}* lines. At metaphase II chromosomes

were misshapen compared to those of wild-type. The chromosomes appeared to have trouble condensing and connections were seen between chromatids (Figure 6.10: G and H). The chromosomes in these cells also appeared almost square with thin chromatin pieces extending away from the chromosomes at either end (Figure 6.10: K and L). Anaphase II chromosomes resembled those of anaphase I with trailing chromosomes between segregating sisters (Figure 6.10: I). No connections were observed in the anaphase II cells analysed (n=11) however a connection was seen in a tetrad cell (1/8) which presumably represented an anaphase II connection which was not resolved (Figure 6.10: J). In tetrad cells the de-condensing chromatin appeared as a fuzzy mass instead of the comparatively ordered chromosomes seen in wild-type (compare Figure 6.9: F and Figure 6.10: J).

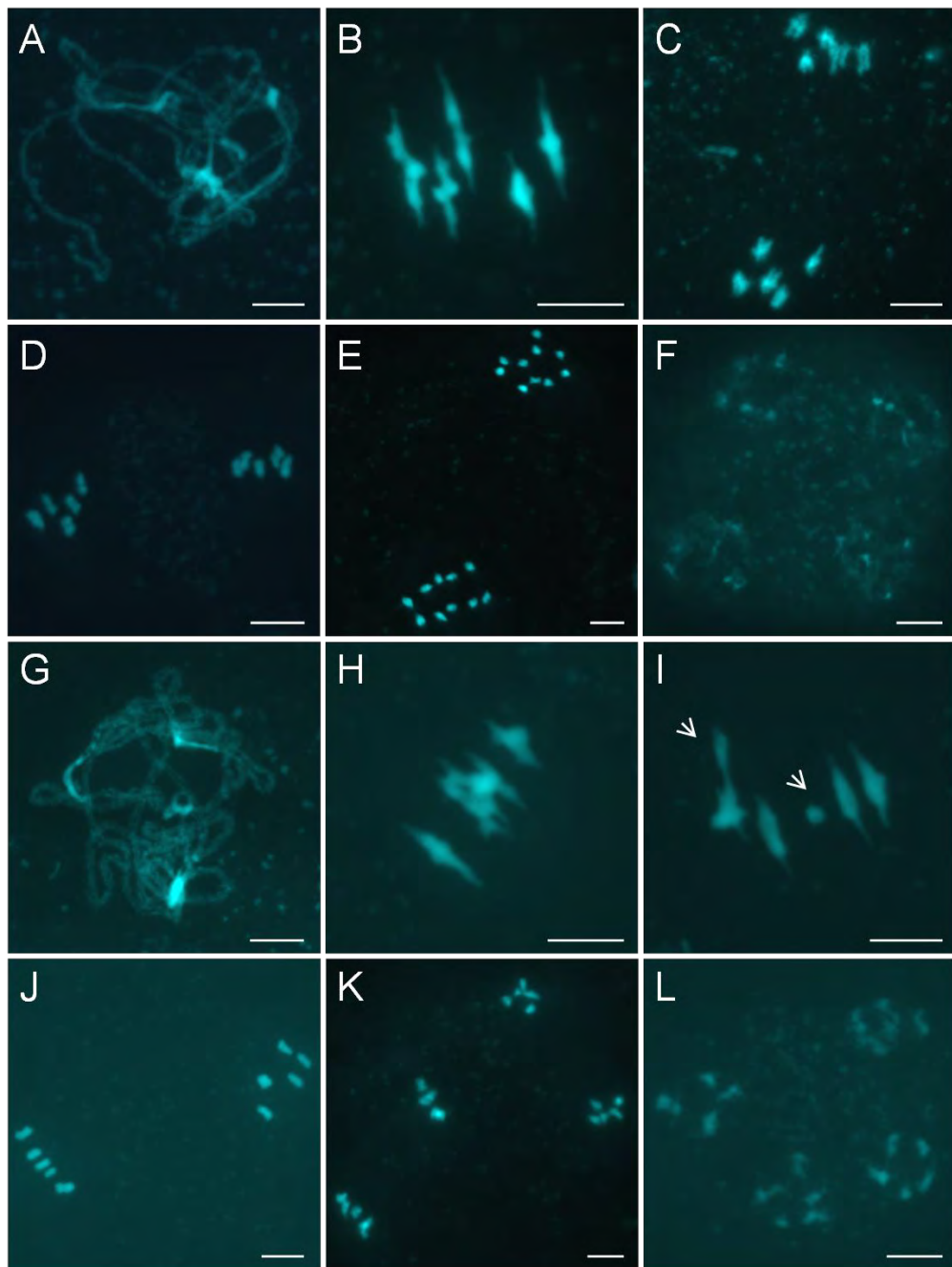


Figure 6.9: Wild-type and *AtCAPD3*^{+/-} meiosis. **A-F** = wild-type; **G-L** = *AtCAPD3*^{+/-}. **A** and **G** = Pachytene; **B**, **H** and **I** = metaphase I; **C** = anaphase I; **D** and **J** = metaphase II; **E** and **K** = anaphase II; **F** and **L** = tetrad. Arrowheads in **I** indicating fragments. Scale bar 5 μ m

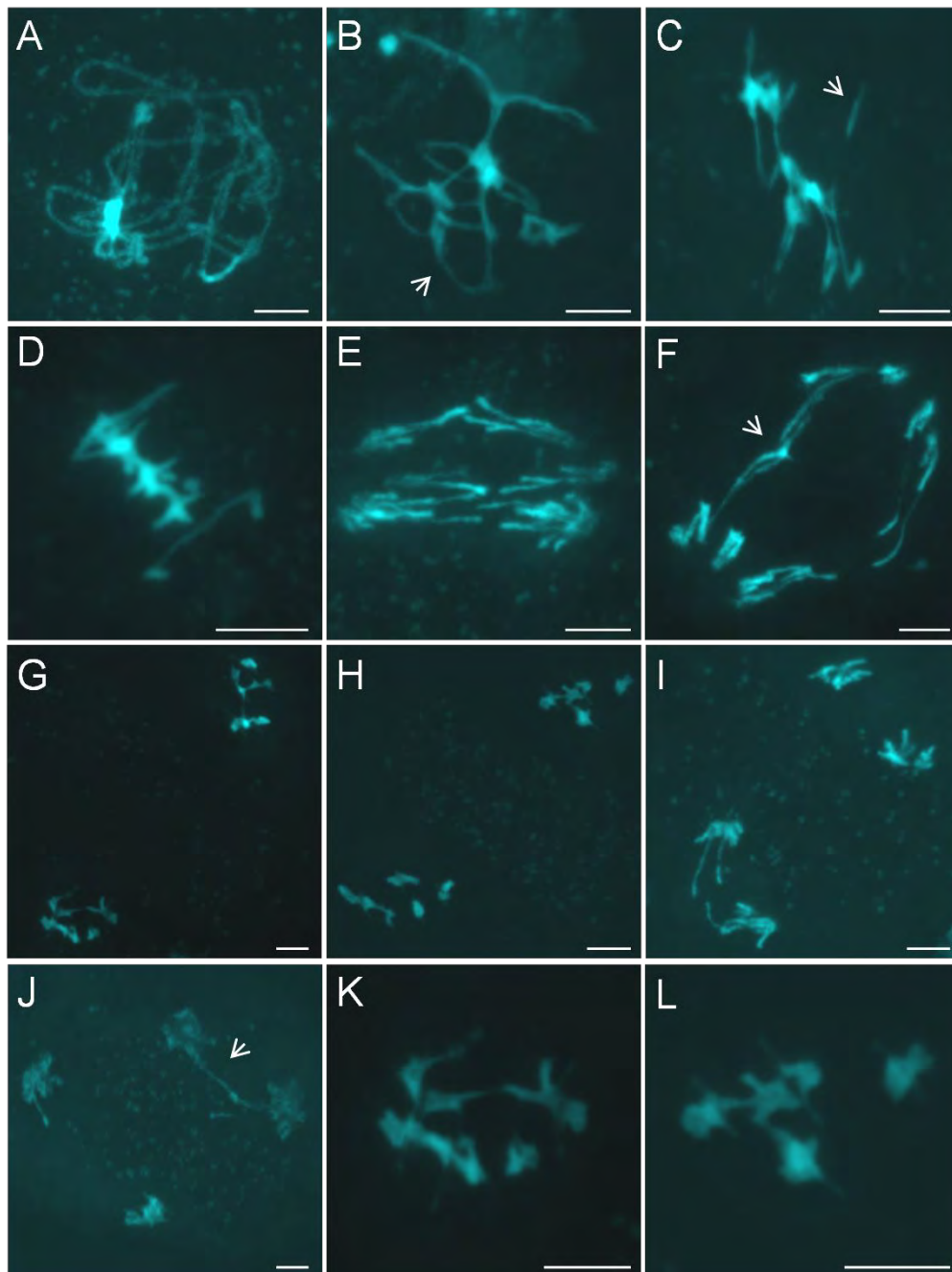


Figure 6.10: *Atcapd3* meiosis. **A** = pachytene; **B-D** = metaphase I (arrowhead in **C** indicating fragment); **E** and **F** = anaphase I (arrowhead in **F** indicating anaphase connection); **G** and **H** = metaphase II; **I** = anaphase II; **J** = tetrad (arrowhead indicating connection) **K** and **L** = enlarged metaphase II chromatids from **G** and **H**. Scale bar = 5 μ m.

6.2.11 Mitotic *Atcapd3* cells had anaphase defects

Condensin II is thought to act in both meiotic and mitotic cell divisions. Consistent with this, the *Atcapd3* plants showed developmental defects. To assess if the mitotically dividing chromosomes appeared abnormal in *Atcapd3* and *AtCAPD3*^{+/-} DAPI stained chromosome spreads were made on *Atcapd3*, *AtCAPD3*^{+/-} and wild-type buds and the mitotic cells analysed. Mitotic cells in *Atcapd3* plants appeared abnormal. At anaphase multiple connections were seen between dividing cells which were not detected in the wild-type cells (Figure 6.11: compare B and H). Chromosomes also appeared to trail behind segregating chromosomes in some cells (Figure 6.11: I). Mitotic cells in *AtCAPD3*^{+/-} plants appeared normal; consistent with these plants having normal vegetative development.

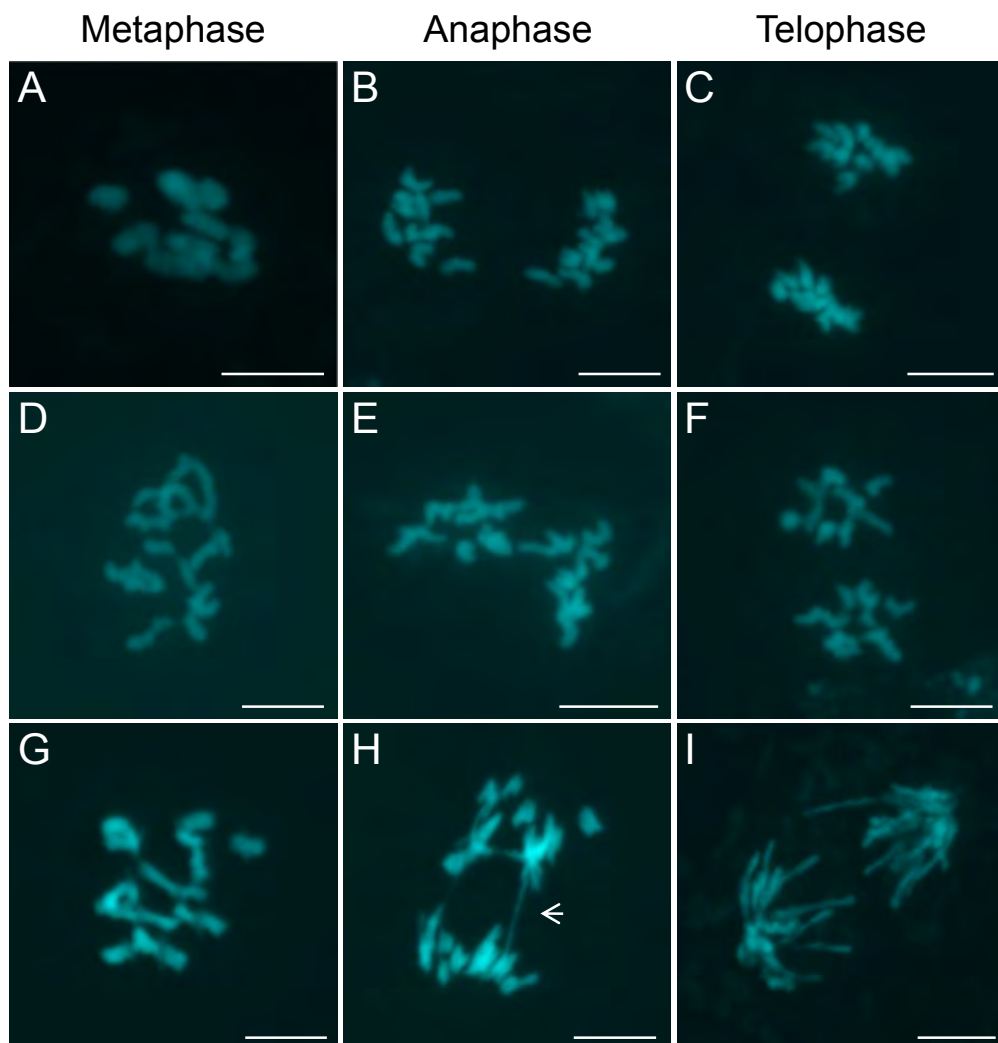


Figure 6.11: Mitotic cells of wild-type, *Atcapd3* and *AtCAPD3*^{+/-} plants. **A-C** = wild-type; **D-F** = *AtCAPD3*^{+/-}; **G-H** = *Atcapd3*. Cell stages are indicated above columns. Arrowhead indicates anaphase connection. Scale bar 5 μ m.

6.2.12 Producing *AtCAPD3*^{RNAi} lines

To further confirm that the phenotype observed in *Atcapd3* plants was due to the absence of *AtCAPD3*, an RNAi approach was adopted. *AtCAPD3*^{RNAi} plants were generated using the same DMC1 driven pPF408 vector which was used for *AtSMC4* and *AtCAPD2*^{RNAi} lines (Figure 4.7). The use of the DMC1 promoter can also dissect whether the observed phenotype is due to errors occurring in meiosis or a knock-on effect of previous erroneous mitotic divisions. The mechanism of RNAi is described in section 4.2.5.

To produce an RNAi construct targeted to *AtCAPD3* a 524 bp region of *AtCAPD3* mRNA was amplified from cDNA (2109 and 2633 bps relative to the ATG). This sequence was cloned into pHANNIBAL in sense and antisense orientations. The two inverted sequences separated by an intron, and the terminator were then sub-cloned into pPF408. The construct was transformed into *A. tumefaciens* then subsequently transformed into wild-type Col-0 *Arabidopsis* plants.

Seeds from transformed plants were grown on soil and sprayed with BASTA. 53 *AtCAPD3*^{RNAi} plants were recovered after selection.

6.2.13 Checking for the presence of the inserts by PCR and cloning the PCR

bands

In order to confirm the presence of the insert in the *AtCAPD3*^{RNAi} plants which survived BASTA, PCR was carried out using two independent sets of primers specific to the construct. The two sets of primers used were DMC-Pro-Primer with pHan seq

rev as well as pHan seq for and pHan seq rev 2. These two reactions will amplify both sense and antisense constructs independently. A band from each reaction was subsequently cloned and sequenced to confirm they contained the correct sequence (Figure 6.12).

A

5'-TTGTTTCGGATTCATAGAGCTGAAGAAACGAGATCTCTCGAGCCTGCTGCAGATCTGGCTGACAA
 TTTGCTGAAGAAAATCGAAAATTTTAACCTGCATTCTGCTGAGGTCGATGCACATGTCAAAGCATTAA
 AAACCTTTGTGCAAAAAGAAGGCAAGCACCTCTGAGGAGGCCGATATGCTTGTCAAGAAGTGGGTAG
 AACAAGTTTTCACTGAAAGCATCTAAGGTCCTGAGAAGTACATCGAGGGGGTTCCAGTCATAATCA
 TTCTTTTGTACACCAGCAACACTCGGAAGTAGAAGAAGCAAGAGACTGGATACTGTGTCCAAGAAA
 TTATCAAAGCAGTCACAGCAKTATACACCATTGGATCTTGTGTCATTATATATCCTTCAGCTGACACG
 ACCAAAATTGTTCCGTTCTTACATACTGTCATCACTTCAGGAAATTCAGACTCAAAGCTGAMAAACAA
 ACTGCCGCAAGCTAATGTTTGCTTGAAGCAAAAAGCTCCTTCTCTATAGTCAGTCTTGTTAACCAT
 GCGAAGATGTGTTTGGCTGACGGGAATTCGGTACCCASCCTTGGYAAGGAAATAATTATTTTCTTT
 TTTTCTTTTAGTATAAAATA-3'

B

5-ATAAACAAGGTAACATGATAGATCATGTCTATTGTGTTATCATTGATCTTACATTTGGATTGATTACA
 GTTGGGAAGCTGGGTTTCGAAATCGATAAGCTTCCCGTCAGCCAAACACATCTTCGCCATGGTTAACC
 AAGACTGACTATAGAGAAGAGGAGCTTTTTGCTTCAAGCAAACATTAGCTTGCGGCAGTTTGTTTTTC
 AGCTTTGAGTCTGAATTTCTGAAGTGATGACAGTATGTAAGAACGGAACAATTTTGGTCGTGTCAG
 CTGAAGGATATATAATGACACAAGATCCAATGGTGTATACTGCTGTGACTGCTTTTGATAATTTCTTG
 GACACAGTATCCAGTCTTGTCTTCTACTTCCGAGTGTTGCTGGTGTAAACAAAAGAATGATTATG
 ACTGAAACCCCTCGATGTACTTCTCAGTGACCTTAGATGCTTCAATGAACTTGTTCTACCCACTT
 CTTGACAAGCATATCGGCCTCCTCAGAGGTGCTTGCCTTCTTTTGCACAAAGTTTTTAATGCTTTGAC
 ATGTGCATCGACCTCAGCAGAATGCAGGTTAAAATTTTCGATTTTCTTTCAGCAAATTGTCAGCCAGAT
 CTGCAGCAGGCTCGGATCCTAGAGTCTGCTTAAATGAGATATGCGAGACGCCTATGATCGCATG
 ATATTTGCTTTCAATTCTGTTGTGCACGTTGTA-3'

Figure 6.12: Sequence of PCR product obtained from *AtCAPD3*^{RNAi} plants using insert specific primers. **A** = DMC1 promoter - intron reaction (sense fragment). **B** = Intron-terminator reaction (antisense fragment). Green = DMC1 promoter sequence. Red = sense and antisense *AtCAPD3* sequence. Light blue = intron sequence. Dark blue = terminator sequence. Restriction sites are highlighted in yellow (top to bottom: *XhoI*, *EcoRI*, *HindIII*, *BamHI*).

6.2.14 *AtCAPD3*^{RNAi} lines confirm the phenotype of *Atcapd3* plants

The vegetative development looked like wild-type in the majority of lines but 16 plants showed signs of reduced fertility, such as shorter siliques than wild-type or gaps in their siliques. Fertility was scored in any plant with signs of reduced fertility by scoring seed set when the seed pods had dried out. Figure 6.13 shows the range of fertilities observed. The plants which showed reduced fertility were assessed for meiotic phenotypes by making DAPI stained chromosome spreads. From the cytological screen, 11 lines were identified which shared to same meiotic phenotype to varying degrees (these were lines 3.6, 3.15, 4.2, 5.2, 5.5, 6.2, 8.10, 3.2, 5.8, 8.7 and 7.5). The plants which had a less severe reduction in fertility generally had weaker cytological phenotypes, except line 7.5 which had a weak meiotic phenotype and severely reduced fertility. In the 11 lines prophase I cells appeared essentially normal. However when the chromosomes came to condense at metaphase I multiple connections were seen between chromosomes and metaphase I chromosomes appeared long thin and misshapen compared to wild-type (Figure 6.14: compare B with F, J and N). Again it often appeared as if the sister chromatids in each bivalent were separating from each other. These cells resembled those of the *Atcapd3* mutant.

When the homologous chromosome came to segregate at anaphase I, problems occurred. Trailing chromosomes, which may represent separated sister chromatids, were seen between the segregating chromosomes (Figure 6.14: G, K, O) which resembled those seen in *Atcapd3* plants and were distinct from the anaphase defects in *AtSMC4* and *AtCAPD2*^{RNAi} lines. When the chromosomes condensed for

metaphase II, they again appeared misshapen. In many cells, masses of chromosomes were observed in which individual homologues could not be easily distinguished (Figure 6.14: H, L and P). These phenotypes resemble those seen in *Atcapd3* plants and therefore further confirm that the phenotype in the T-DNA insertion line is due to a reduction in *AtCAPD3*.

In addition to the plants which shared the same phenotype as the *Atcapd3* plants, 4 plants which had reduced fertility did not have any defects during meiosis (lines 2.1, 8.6, 5.3 and 7.2) therefore other factors may be contributing to their reduced fertility. One plant had metaphase I connections which resembled those seen in the empty vector control (line 3.12) (section 4.2.7).

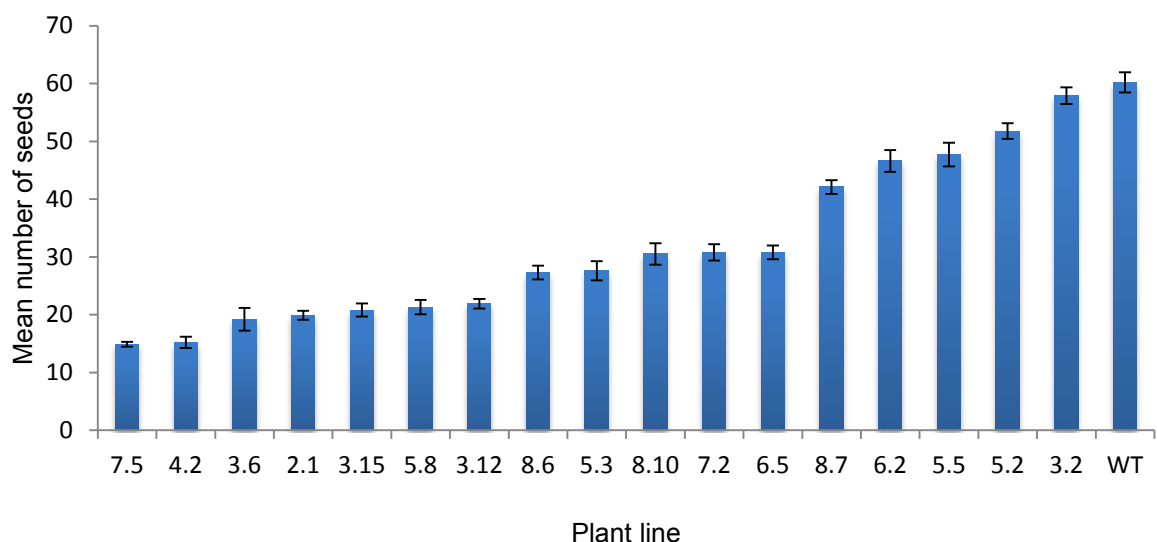


Figure 6.13: Mean seed set in *AtCAPD3*^{RNAi} transformants showing signs of reduced fertility. Seeds from 10 siliques were counted for each line. Error bars = Standard error of the mean.

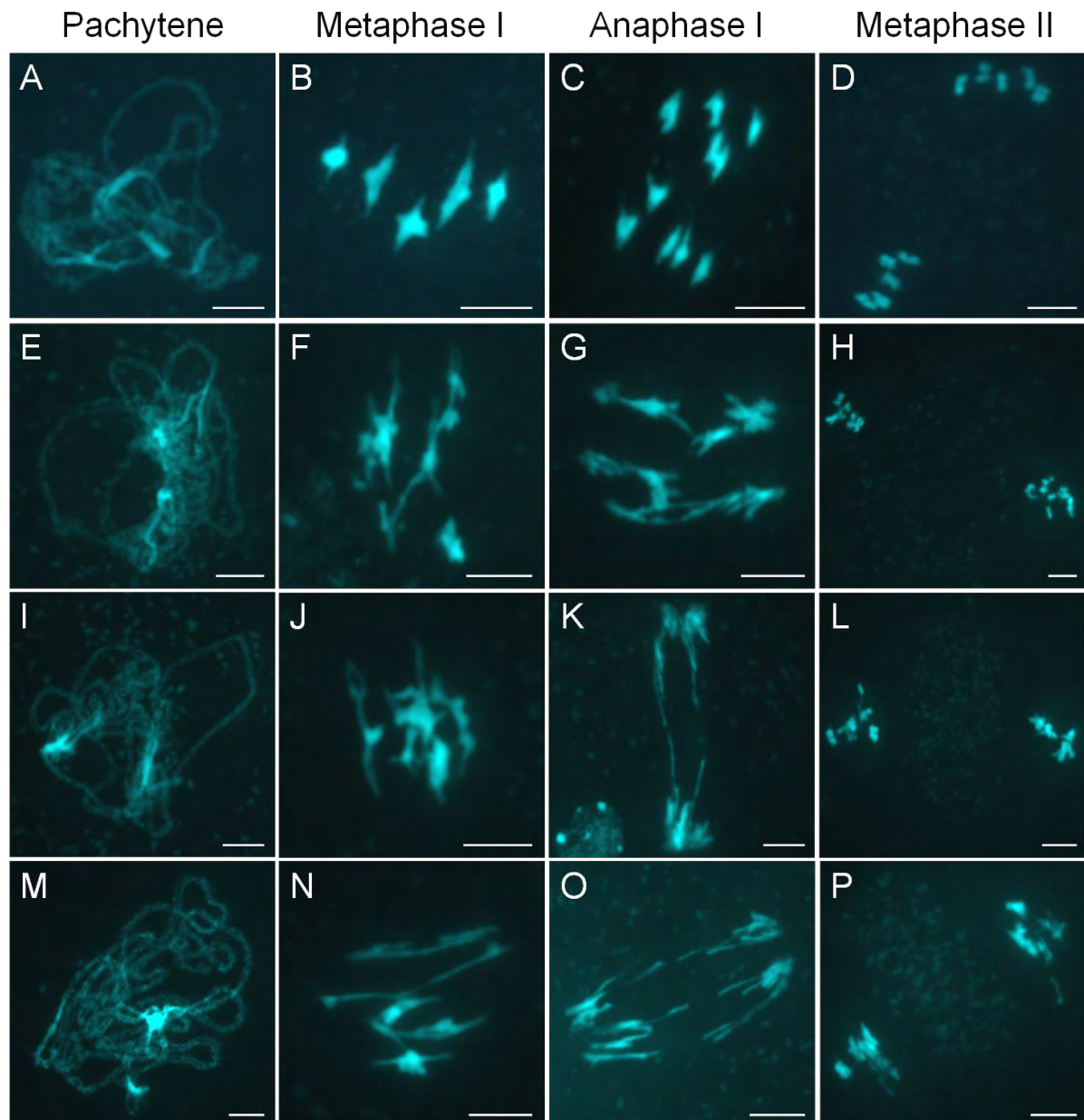


Figure 6.14: Meiotic phenotypes of *AtCAPD3*^{RNAi} lines and wild-type plants. **A-D** = wild-type; **E-H** = *AtCAPD3*^{RNAi} line 4.2; **I-L** = *AtCAPD3*^{RNAi} line 8.10; **M-P** = *AtCAPD3*^{RNAi} line 5.8. Scale bar = 5 μ m.

6.2.15 *Atcapd3* does not appear to be involved in rDNA organisation

In Chapters 4 and 5, RNAi lines of the condensin I subunit *AtCAPD2* and the condensin I and II subunit *AtSMC4* showed defects in the organisation of the rDNA. 45S and 5S signals were larger in these plants at metaphase I and II, than in wild-type controls. The rDNA was also seen to lag behind segregating chromosomes at anaphase I and II in both RNAi lines, possibly due to connections in the rDNA sequence. In budding and fission yeast the condensin I complex has been shown to be essential for the organisation of the rDNA (Freeman *et al.*, 2000; Bhalla *et al.*, 2002; Lavoie *et al.*, 2002; D'Amours *et al.*, 2004; Machin *et al.*, 2004; Sullivan *et al.*, 2004; Wang *et al.*, 2004; Wang *et al.*, 2005; Nakazawa *et al.*, 2008). To address whether defects in rDNA organisation were common to both condensin I and II deficient plants, FISH analysis using the 45S and 5S rDNA probes was carried out on *Atcapd3* plants. The rDNA signals in these lines did not appear unorganised or diffuse compared to wild-type. At metaphase I discrete 45S and 5S signals could be seen as in wild-type plants (Figure 6.15: compare B and E). This suggests that a role in rDNA organisation is unique to condensin I and not a role shared by condensin II.

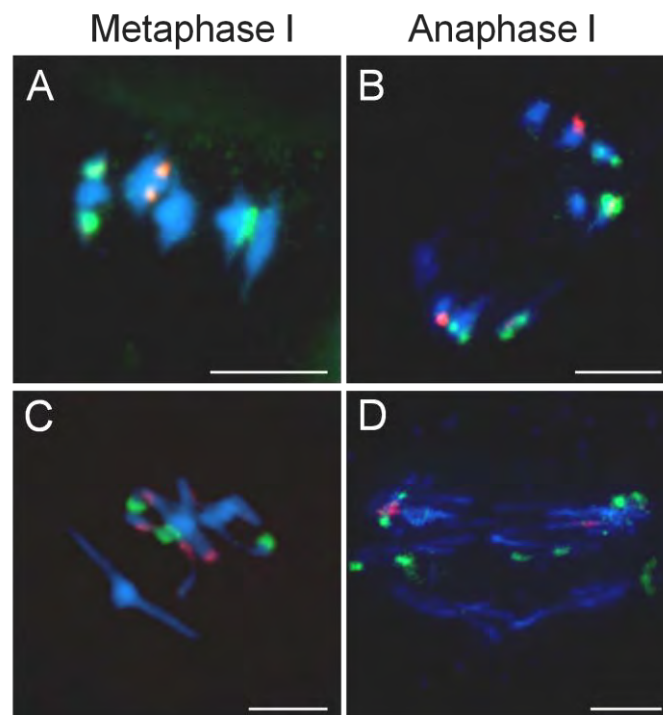


Figure 6.15: Analysis of the rDNA regions in *Atcapd3* mutants, using the rDNA probes; 45S (red) and 5S (green). DNA stained with DAPI. **A** and **B** = wild-type; **C** and **D** = *Atcapd3*. Cell stages are indicated above each column. Scale bar = 5 μ m.

6.2.16 Analysis of centromeric DNA in *Atcapd3* plants

Analysis of centromere organisation at metaphase I and II in *AtSMC4* and *AtCAPD2^{RNAi}* lines revealed that both subunits appeared to be required for the maintenance of centromere compactness at metaphase I (and II). In many species condensin I deficient cells appear to have centromere defects (Oliveira *et al.*, 2005; Savvidou *et al.*, 2005; Gerlich *et al.*, 2006; Yong-Gonzalez *et al.*, 2007). However some evidence suggests that the condensin II complex may also be required for centromere organisation. In human, CENP-A and CENP-E targeting to and maintenance at the centromeres is deficient in condensin II depleted cells (Ono *et al.*, 2004; Samoshkin *et al.*, 2009). In *Xenopus* CENP-A localisation to and retention at the centromeres required condensin II but not condensin I (Bernad *et al.*, 2011).

To investigate whether a centromere defect is seen in condensin II deficient plants a preliminary analysis of the centromere DNA was carried out in *Atcapd3* and wild-type plants using FISH probes specific to the centromere DNA, pAL38. The centromere signals in *Atcapd3* plants did not appear different to wild-type. In both plants the centromere signals at metaphase I appeared discrete and compact (Figure 6.16). These results suggest that in *Arabidopsis* meiosis condensin II does not have the same role in centromere organisation as condensin I.

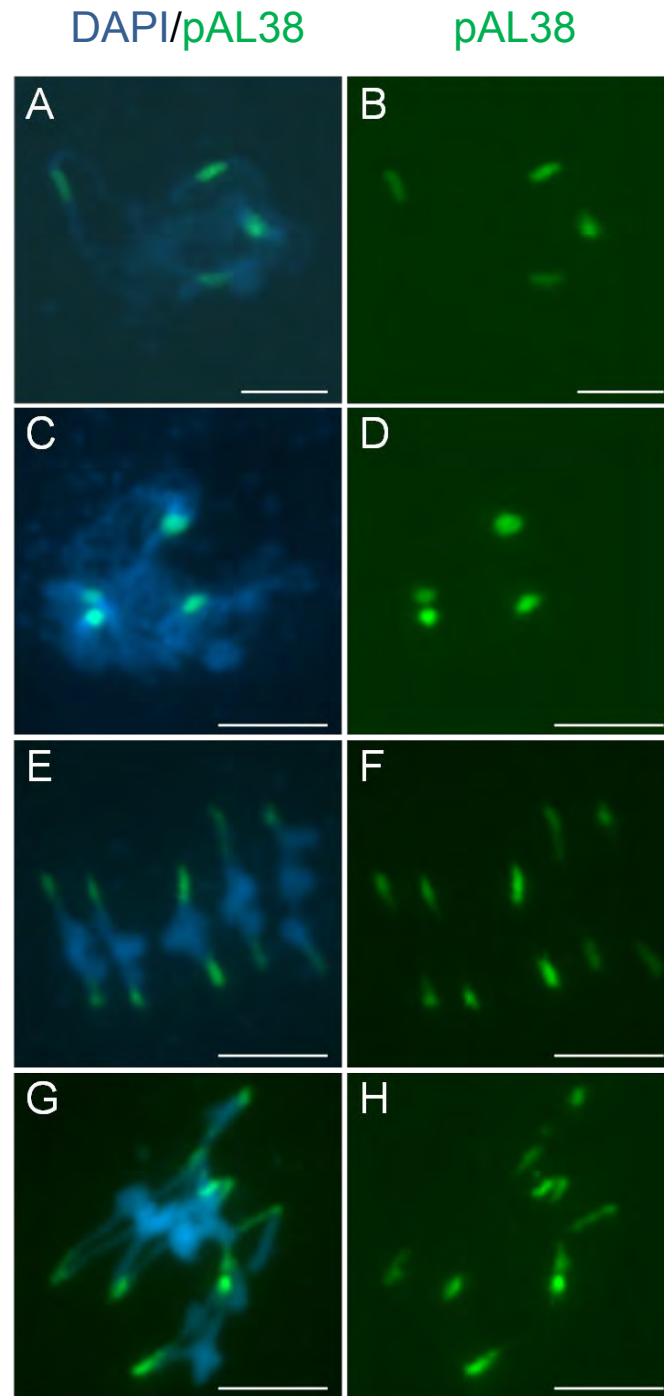


Figure 6.16: Analysis of the centromere regions in *Atcapd3* and wild-type PMCs, using centromeric FISH probe pAL38. DNA stained with DAPI. **A-D** = pachytene (**A** and **B** = wild-type; **C** and **D** = *Atcapd3*). **E-H** = metaphase I (**E** and **F** = wild-type; **G** and **H** = *Atcapd3*). **A, C, E** and **G** = DAPI/pAL38 (FITC: green) merge; **B, D, F** and **H** = pAL38. Scale bar = 5 μ m

6.2.17 Prophase I chromosome axes in *Atcapd3* plants appear normal

The multiple chromosomes masses seen at metaphase I may be due to prior prophase I defects, for example incomplete synapsis has been suggested to result in the incomplete removal of interlocks between homologous chromosomes (Reviewed by Zickler and Kleckner, 1999).

No prophase I defects were observed in a cytological screen of *Atcapd3* T-DNA lines or *AtCAPD3^{RNAi}* lines, however it is not always possible to detect axis defects during prophase I using basic cytological preparations. Therefore, to further analyse this stage in meiosis, axial organisation and synapsis were monitored in *Atcapd3* plants using the axis-associated protein *AtASY1* (Caryl *et al.*, 2000) and the SC transverse filament protein *AtZYP1* (Higgins *et al.*, 2005). In wild-type cells *AtASY1* was first seen on the chromatin at leptotene where it formed a linear signal along the chromosome axes. *AtASY1* remained associated with the axes from leptotene until pachytene. *AtZYP1* was first detected at leptotene as numerous foci marking the sites of DSBs, at zygotene *AtZYP1* was seen as multiple small stretches of protein as it started to polymerise. At pachytene *AtZYP1* was fully polymerized between the homologous chromosomes, at this stage *AtASY1* was seen as a more diffuse signal over the chromatin (Figure 6.17: A-F). Organisation of the chromosome axis, as seen by *AtASY1* localisation, appeared indistinguishable in *Atcapd3* plants from that of wild-type. Progression of synapsis also occurred as in wild-type, cells appeared fully synapsed at pachytene with no discontinuities in the SC (Figure 6.17: G-L).

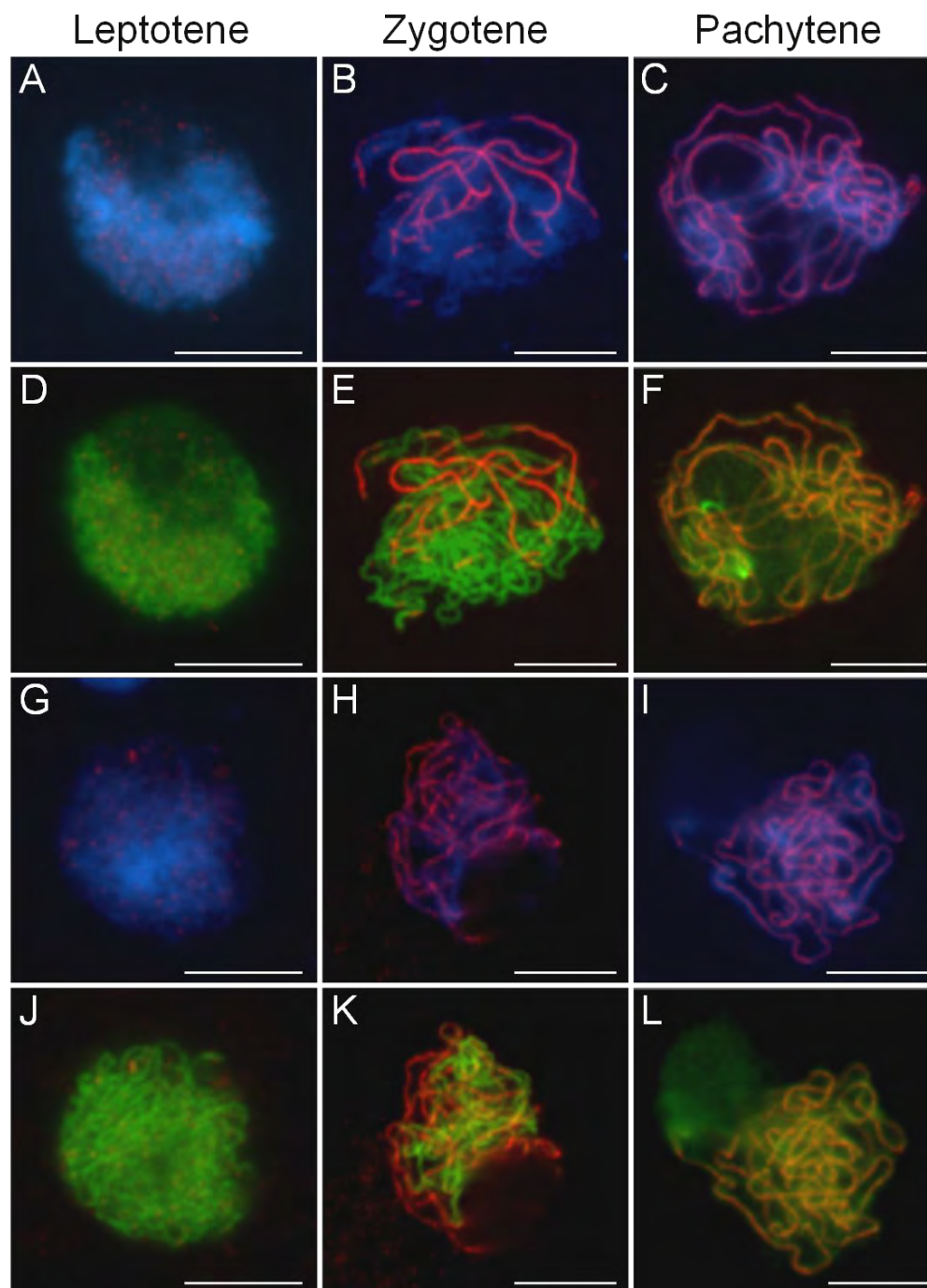


Figure 6.17: Immunolocalization of *AtASY1* (FITC green) and *AtZYP1* (Texas red) on *Atcapd3* and wild-type PMCs. Chromosomes were counter-stained with DAPI. **A-F** = wild-type; **G-L** = *Atcapd3*. **A-C** and **G-I** = DAPI/*AtZYP1* merge; **D-F** and **J-L** = *AtASY1/AtZYP1* merge. Cell stages are indicated above columns. Scale bar 5 μ m.

6.2.18 Attempting to make an *At*CAPD3 recombinant protein for antiserum production

*At*SMC4 antibody, discussed in Chapter 3, provided valuable information into the localisation of the condensin I and II complexes during a meiotic cell division. These results were however only informative in relation to the localisation of total cellular condensin and did not provide information into the distribution of condensin I and condensin II complexes individually. In vertebrates condensin II is seen to localise to interphase and prophase nuclei during mitotic divisions (Cabello *et al.*, 2001; Uzbekov *et al.*, 2003; Yeong *et al.*, 2003; Hirota *et al.*, 2004; Gerlich *et al.*, 2006). This localisation was stable and persisted through metaphase until anaphase. To investigate the localisation of *At*CAPD3 during a meiotic cell division in plants it was decided to make an antibody against *At*CAPD3.

To make an *At*CAPD3 specific antibody a 259 amino acid sequence at the C-terminus of *At*CAPD3 (corresponding to bases 1055 to 1313) was chosen for recombinant protein production. The C-terminus of *At*CAPD3 was chosen due to ease of amplification from cDNA and as successful antibodies have been raised against *At*CAPD3 C-terminus in other species, thereby reducing the likelihood of epitope masking occurring in this region of the protein. The desired sequence was amplified from cDNA using primers containing specific restriction sites not present in the selected sequence, namely *Nde*I and *Xho*I. The fragment obtained was cloned into pET21b so that the recombinant protein would be produced with a 6 residue histidine tag at the C-terminus, allowing for efficient purification of the protein. The construct was sequenced to ensure the protein and 6 residue HIS-tag were in frame.

pET21b-*AtCAPD3* was transformed into *E. coli* BL21 (DE3) expression cells. A test induction experiment was carried out in which protein expression was induced with IPTG and protein was extracted from both induced and uninduced colonies 4 hours after induction. Protein extracts were resolved on a 15% SDS-PAGE denaturing gel which was subsequently stained with Coomassie blue to allow visualisation of the protein. No obvious differences in the protein banding pattern were seen between induced and non-induced colonies. No distinct band around the predicted molecular weight of the protein (28 KDa) was detected in any of the 4 colonies analysed (Figure 6.18: A). These results indicate that the *AtCAPD3* C-terminus recombinant protein was not being expressed sufficiently under these conditions.

To determine whether the *AtCAPD3* recombinant protein was present at all, a western blot containing protein from induced and un-induced cultures was probed with an antibody specific to the HIS-tag of the recombinant protein. The HIS-Tag specific antibody was detected using alkaline phosphatase secondary antibody. A band was detected in induced colonies which corresponded to the predicted molecular weight of the recombinant protein (28 KDa). This band was absent from the non-induced control (Figure 6.18:B). This analysis confirmed that the *AtCAPD3* recombinant protein +HIS-tag was present in the soluble fraction of the induced samples at a low level. This low concentration of recombinant protein is not sufficient (for obtaining enough recombinant protein) to send for antiserum production.

To try to optimise expression of the *AtCAPD3* recombinant protein, further inductions were carried out at varying IPTG concentrations (0.1 M and 0.2 M) and induction times (2 – 8 hours) on multiple different colonies. However no improvement in expression of *AtCAPD3*-recombinant protein was observed. It was therefore decided that choosing an alternative section of *AtCAPD3* for recombinant protein production was the best approach. The central region of the *AtCAPD3* was amplified and cloned into pET21b, however due to time limitations this construct was not tested for expression of the protein.

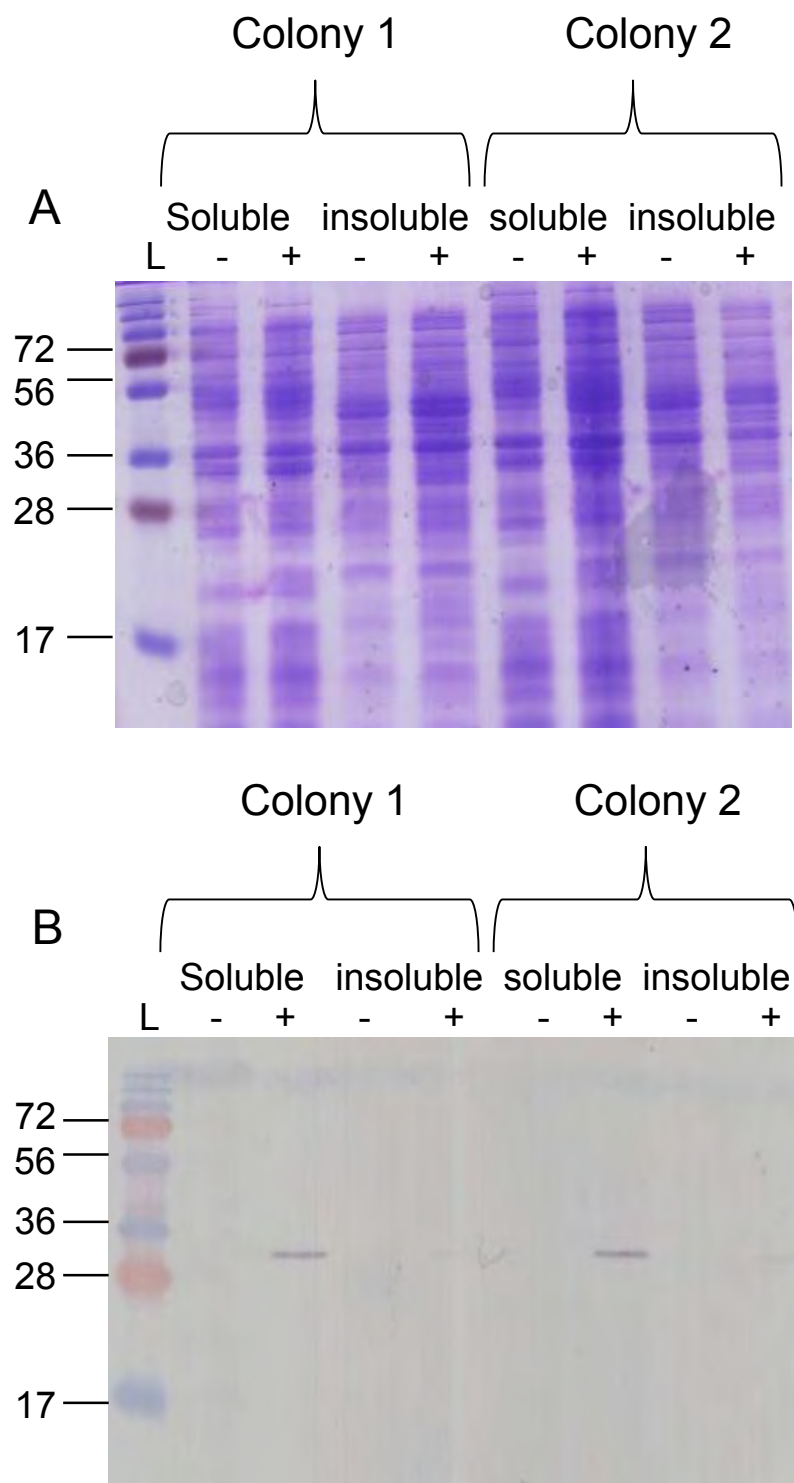


Figure 6.18. Expression of the *AtCAPD3* recombinant protein. **A** = Coomassie stained SDS-PAGE gel showing induced and un-induced colonies of BL21(DE3)-pET21b-*AtCAPD3*. **B** = western blot using anti-HIS antibody (1:5000) on induced and un-induced colonies of BL21(DE3)-pET21b-*AtCAPD3* antibody detected with alkaline phosphatase secondary (1:5000)

6.3 DISCUSSION

6.3.1 *Atcapd3* plants are viable and have developmental defects

Identification of a homozygous insertion line for the condensin II subunit *AtCAPD3* is described in this chapter. The insert site was cloned to confirm the insert was in the *AtCAPD3* gene and expression analysis was carried out to confirm that no *AtCAPD3* transcript was expressed in bud or leaf tissue in these plants. These results suggest that viable *Atcapd3* null plants were obtained. This contrasts results from the condensin *AtSMC4* subunit and the condensin I subunit *AtCAPG* in which homozygous insertion plants were lethal. In *Xenopus* eggs it has been shown that the ratio of condensin I to condensin II is 5:1 (Ono *et al.*, 2003). Consistent with this depletion of condensin I from chromosome has a more severe phenotype than the depletion of condensin II. This suggests that the primary condensin in these cells is condensin I. A similar situation may occur in *Arabidopsis* since mutants in condensin I subunits appear to be lethal, whereas condensin II mutants are viable, albeit with developmental defects. Therefore in plants condensin I may be the primary condensin required for chromosomes organisation (at least in mitosis) and condensin II may play more of a minor role as is seen in *Xenopus* (Ono *et al.*, 2003). However, due to the lack of an *AtCAPD3*-Ab it cannot currently be ruled out that a partially functional truncated *AtCAPD3* protein is present in these lines and is responsible for maintaining viability. Alternatively redundancy may exist between other condensin subunits or related proteins. Viable *dcapd3* mutants have been seen in *Drosophila*. Flies which contain homozygous inserts in the 3rd exon of the *dCAP-D3* gene were viable and interestingly completely male sterile (Savvidou *et al.*, 2005). However it is not clear if this mutant is actually a null knock-out. In *C. elegans* HCP-6 null alleles

are embryo lethal (Hagstrom *et al.*, 2006). These differences in viability of *capd3* null mutants may reflect differences in the relative contribution of the two complexes to chromosome organisation in these species. For example the ratio of condensin I to condensin II in *Xenopus* is 5:1, whereas in humans the ratio is 1:1 (Ono *et al.*, 2003).

Transcript analysis using RT-PCR showed that *AtCAPD3* did not appear to be expressed in wild-type leaf tissue. This result is surprising since it is assumed that all condensin subunits function in mitotic cell divisions in plants as they do in other species. In addition to this the *Atcapd3* plants had developmental defects and abnormalities in mitotic cell divisions which both suggest a role for *AtCAPD3* in mitosis. The apparent discrepancy seen in these results may be due to the tissue type used for RT-PCR analysis. RNA was extracted from leaf tissue from fully grown plants and therefore it is possible that *AtCAPD3* is no longer expressed in tissues which have ceased dividing. Indeed, *AtSMC4* protein levels were higher in young plants versus mature leaf (section 3.2.10). Also Siddiqui *et al.*, (2003) showed using promoter GUS analysis that *AtSMC2* was more highly expressed in developing tissues. Analysis of seedling material may therefore be more informative. Alternatively it is possible that a different splice variants of *AtCAPD3* is involved in mitotic and meiotic cell divisions and that the primers used here may be only amplifying the meiotic version. Primers in alternative positions of *AtCAPD3* may help to resolve these issues.

6.3.2 *AtCAPD3*^{+/-} and *Atcapd3* plants both had reduced fertility

Fertility was scored for both heterozygous and homozygous *AtCAPD3* T-DNA lines. Both *Atcapd3* and *AtCAPD3*^{+/-} plants had a similar reduction in fertility; however the pollen viability was much lower in *AtCAPD3*^{+/-} plants than *Atcapd3*. On the other hand, the seed germination assay shown that only 63.75% of the seeds from *Atcapd3* plants were viable compared to 99% of *AtCAPD3*^{+/-} seeds. This is likely to be due to a defect in embryo development. Interestingly *AtCAPD3*^{+/-} plants had univalents at metaphase I in a few cells, but other than this their meiosis appeared normal. The small number of cells with univalents (25% n=8) is unlikely to account for the 50% reduction in fertility observed. These results suggest that factors other than defects in meiosis may be causing the reduced fertility in *AtCAPD3*^{+/-} plants (and possibly also responsible for a proportion of the reduced fertility seen in *Atcapd3* plants). At this point it remains unknown what could be causing the reduced fertility in *AtCAPD3*^{+/-} plants, although the severe reduction in pollen viability suggests that the mitotic division which occurs prior to pollen maturation (reviewed by (McCormick, 1993)) may be defective. Interestingly a small number of cells (10% n=20) in *AtSMC4*^{+/-} plants also had univalents at metaphase I; however no univalents were seen in the *Atcapd3* or the *AtSMC4*^{RNAi} lines. The reason for this is unknown but it could be reflecting a dosage effect of the condensin complex in chromosome organisation. Haploinsufficiency is seen in condensin mutants in *C. elegans* (Tsai *et al.*, 2008).

6.3.3 *Atcapd3* does not appear to have prophase I defects

Connections at metaphase I are often a result of defects during prophase I of meiosis, such as unresolved interlocks (reviewed by Zickler and Kleckner, 1999). It was therefore thought that the connections seen at metaphase I in *Atcapd3* plants may be due to prior defects in synapsis. Cytological analysis of *Atcapd3* T-DNA lines did not reveal any defects in prophase I, however mild defects in synapsis are often difficult to detect with the standard cytological technique. Therefore immunolocalisation analysis on spread meiotic cells using antibodies specific to the axis associated *AtASY1* and the SC TF protein *AtZYP1* was carried out. No defects were detected in synapsis in this experiment, confirming the results of the cytological analysis. However, these results do not rule out the possibility that unresolved interlocks are causing the metaphase I connections in the *Atcapd3* plants as interlocks are not always easy to detect with these techniques. Analysis using 3D-SIM would help establish whether interlocks are present in *Atcapd3* lines at pachytene. It is also possible that synapsis or desynapsis is delayed in these lines as this was not addressed here.

6.3.4 Chromosome organisation problems in *Atcapd3* plants

Connections are observed at metaphase I and II in *Atcapd3* mutants. Condensin has been implicated in the removal of connections between chromosomes working in conjunction with TopoII. TopoII is able to remove aberrant connections between chromosomes by breaking and mending DNA, however it can also introduce connections in this fashion if the DNA is not kept tidy (Wang, 2002). It is thought that condensin may work alongside Topo II in *C. elegans* in order to prevent additional

connections being formed (Chan *et al.*, 2004). It is therefore possible that the metaphase I connections in *Atcapd3* plants are due to the inability to successfully remove, or the accidental introduction of, connections between chromosomes. It has been suggested that connections occur during the transient decondensation and recondensation of the chromosomes which occurs after pachytene exit in HCP-6 deficient cells (Chan *et al.*, 2004). Therefore a similar situation may be occurring in *Atcapd3* plants. Topo II staining on the *Atcapd3* plants would provide valuable insight into the cause of these connections.

Many of the metaphase I connections observed here appear to be resolved before anaphase since only a low frequency of connections are seen between segregating chromosomes at anaphase. Consistent with this, some metaphase I cells in *Atcapd3* plants appeared more ordered and had less connections between homologous chromosomes than others. These cells may reflect a later stage of the *Atcapd3* meiotic pathway when many of the chromosome connections have been resolved. What may be responsible for resolving these connections is unknown but the condensin I complex is one possible candidate, possibly in conjunction with Topo II.

In many of the late diakinesis/metaphase I cells it appeared as if the two sister chromatids of each bivalent may be coming apart. At anaphase I trails of chromatin were also seen behind segregating chromosome which may be due to separated sisters. However these were also seen at anaphase II, and therefore may represent a more general loss of chromatin structure upon anaphase. A link between condensin

and the related cohesin complex has been seen in a few other studies. However it often appears that the relative amount of one of the complexes on the chromosomes is inversely proportional to the other (Lavoie 2002, 2004; Shintomi and Hirano, 2011). Investigating the localisation of cohesin in the *Atcapd3* lines may shed some light on to the origin of this phenomenon.

6.3.5 Condensin II does not play a role in rDNA or centromeric organisation

Atcapd3 plants did not appear to have a defect in the compaction or organisation of the rDNA regions or the centromeric DNA, unlike plants with reduced levels of *AtSMC4* or *AtCAPD2*. This suggests that condensin I and not condensin II is required for the organisation of the repetitive DNA. These results are consistent with results from other species. Yeast only has the canonical condensin I complex and this is required for the organisation and segregation of the rDNA, and in many species it is condensin I which appears to play more of a role in maintaining the structure of the centromeres (Oliveira *et al.*, 2005; Savvidou *et al.*, 2005; Gerlich *et al.*, 2006; Yong-Gonzalez *et al.*, 2007). However, in human, CENP-A and CENP-E targeting to and maintenance at the centromeres is deficient in condensin I and II depleted cells (Ono *et al.*, 2004; Samoshkin *et al.*, 2009) and in *Xenopus* CENP-A localisation to and retention at the centromeres requires condensin II but not condensin I (Bernad *et al.*, 2011), therefore it is possible that condensin II may have a role in centromere organisation which was not detected in condensin II deficient cells analysed here.

6.3.6 *Atcapd3* plants appear to lose chromosome integrity at anaphase

As the chromosomes in the *Atcapd3* and *AtCAPD3^{RNAi}* plants came to segregate at anaphase, they appeared to lose structural integrity and trail behind the segregating chromosomes. Anaphase defects are a common phenotype in condensin deficient cells in other species. The cause of these defects is still unclear, although several studies have suggested possible causes. These trails of chromatin may be due to a loss of condensation as the chromosomes segregate. A loss of chromosome architecture at anaphase has been suggested as a cause of the anaphase defects seen in chicken SMC2 deficient cells (Vagnarelli *et al.*, 2006).

The anaphase defects seen in *Atcapd3* plants are different to those seen in the *AtSMC4* or *AtCAPD2^{RNAi}* lines where thin threads of chromatin lagged behind each pair of segregating chromosomes at anaphase I and II. These thin threads of chromatin in the *AtSMC4^{RNAi}* (and presumably also in the *AtCAPD2^{RNAi}* lines) were thought to be due to a loss of chromosome architecture upon anaphase onset and possibly also some form of unresolved connections between chromosomes (section 4.2.17 and 4.3.5.3). In *Atcapd3*, instead of the thread-like bridges, thicker portions of trailing chromosomes are often seen between segregating chromosomes. In these cells it also appears as if the chromosomes lose some form of structural integrity as they segregate. It is possible that both condensin I and condensin II complexes are required to maintain chromatin architecture during anaphase and that the phenotypes observed are a result of the different chromosome packing mechanisms of the two complexes.

6.3.7 *Atcapd3* phenotypes differed from those of *AtSMC4* and *AtCAPD2^{RNAi}* lines

Cytological analysis of meiosis in *Atcapd3* mutants revealed that the chromosome defects observed were distinct from those seen in *AtSMC4^{RNAi}* lines. In the *AtSMC4^{RNAi}* lines it is assumed that both condensin I and condensin II complexes have been equally reduced and therefore it may be expected that the *AtSMC4^{RNAi}* lines would exhibit phenotypes which reflected both condensin I and condensin II knock-down. However, *Atcapd3* has a distinct phenotype to *AtSMC4* or *AtCAPD2^{RNAi}* plants. There are several possible explanations for this apparent discrepancy. First it is feasible that residual *AtSMC4* present in the *AtSMC4^{RNAi}* lines binds preferentially to the condensin II specific subunits thus allowing condensin II to function at the expense of the condensin I complex in these plants. Support for this comes from the observation that in human and *Xenopus*, condensin II acts earlier in mitotic chromosome condensation than condensin I (Ono *et al.*, 2003), therefore, condensin II specific subunits may monopolise the available *AtSMC4* protein in the *AtSMC4^{RNAi}* lines before condensin I is thought to be required. Moreover, condensin I is highly dynamic in its localisation to human mitotic chromosomes whereas condensin II loading is stable (Gerlich *et al.*, 2006), therefore residual *AtSMC4* may be locked up in stable condensin II complexes and not available for use in the more dynamic condensin I complex. Alternatively, *Atcapd3* may be functioning independently of the condensin complex as has been suggested for *Drosophila* CAPD3 (Longworth *et al.*, 2008). In addition condensin subunits in *C. elegans* are known to act outside the condensin complex in the structurally similar dosage compensation complex (Lieb *et*

al., 1996; Csankovszki *et al.*, 2009). Therefore it is possible that another SMC-like protein may act in the condensin II complex in place of AtSMC4.

6.3.8 AtCAPD3 C-terminal recombinant protein appeared to be lethal to the *E. coli* expression cells

Attempts were made to produce an antibody specific to AtCAPD3 in order to investigate the localisation of the protein during meiosis. The C-terminus of the AtCAPD3 protein was chosen for recombinant protein production and cloned into the expression vector pET21b. This expression of the recombinant protein was induced in BL21 (DE3) *E. coli* cells using IPTG. Only a small amount of AtCAPD3 C-terminal recombinant protein was expressed in these cells, as seen by western blot analysis using the anti-HIS antibody. Attempts to optimise expression were unsuccessful. These results suggest that the recombinant protein may be toxic to the *E. coli* cells. A second construct containing the central region of the AtCAPD3 protein was constructed however due to time constraints expression of this construct was not tested in this study.

6.3.9 Future perspectives

Prophase I defects were not observed in the *Atcapd3* mutant, however, light microscopy is limited in its resolution and therefore some defects in the axes may be undetected with the techniques used here. More detailed analysis using electron microscopy or 3D-SIM would allow a closer analysis of the axis in these lines and would also accurate analysis of whether interlocks are present in *Atcapd3* pachytene

cells. The analysis carried out on the prophase I axes here does not rule out the possibility that prophase I is delayed. A time course analysis using BrdU or EdU in conjunction with *AtZYP1* antibody would be required to establish whether there is a delay in synapsis. Pachytene axis length was measured in an *AtSMC4^{RNAi}* line and no difference in length to wild-type was detected. However it is possible that the prophase I axis length may be increased in *Atcapd3* plants as *AtSMC4^{RNAi}* does not appear to exhibit the phenotypes from reducing condensin II subunits. Therefore analysis of prophase I axis length could be carried out on *Atcapd3* plants.

A BrdU or EdU time course analysis may also help to establish whether the more ordered metaphase I cells in the *Atcapd3* plants are a later stage in the *Atcapd3* meiotic pathway or a reflecting a subset of cells which have a less severe phenotype. 3D-SIM (3 dimensional structural illumination microscopy) analysis would also be informative for helping to resolve the nature of the metaphase I configurations seen in the *Atcapd3* mutant.

Analysis of the *Atcapd3* homozygote and heterozygote mutants revealed unusual results regarding fertility and pollen viability. It would be desirable to analyse a second T-DNA line for *Atcapd3* to further investigate/confirm these findings as well as conduct complementation analysis.

Due to the unsuccessful attempts to produce an *AtCAPD3* recombinant protein for antibody production further work should be carried out on the second pET21b-*AtCAPD3* construct in order to purify enough recombinant protein to send for

antiserum production. An antibody against *AtCAPD3* would provide more insight into the functions of condensin II during a meiotic cell division. An *AtCAPD3* specific antibody would also be interesting for analysing potential proteins which interact with *AtCAPD3* by pull-down assays. Alternatively generating a GFP-fused *AtCAPD3* protein would provide information into the localisation of *AtCAPD3* if a suitable antibody cannot be generated or to back-up results obtained from immunolocalisation experiments.

6.3.10 Conclusions

This chapter describes analysis of an *Atcapd3* T-DNA mutant and *AtCAPD3*^{RNAi} lines. Analysis has revealed that condensin II appears to have a different role in chromosome organisation than condensin I (Chapter 5). Unlike condensin I deficient cells, *Atcapd3* mutants do not appear to be required for the organisation of repetitive DNA such as the DNA or centromeres.

CHAPTER 7

7 GENERAL DISCUSSION

7.1 Introduction

The structural integrity of the chromosomes is important for a successful meiotic division including the correct progression of meiotic recombination and the successful segregation of the chromosomes at anaphase I and II. The aim of this project was to study the importance of chromosome structure during meiosis. Condensin is thought to form an integral part of the chromosome axes and is involved in maintaining chromosome structure. Condensin has been studied for its role in chromosome organisation during mitosis and meiosis in many species, but equivalent studies in plants are lacking. This study describes the first in-depth analysis into the role of the condensin complexes in chromosome structure during plant meiosis.

To investigate the role of condensin in *Arabidopsis*, three condensin subunits were chosen for analysis. *AtSMC4*, which forms part of the SMC backbone of condensin, was chosen in order to assess the effect of reducing both condensin I and II complexes during *Arabidopsis* meiosis. The different roles of the two condensin complexes were also investigated by analysing condensin I and condensin II specific subunits, *AtCAPD2* and *AtCAPD3* respectively. *AtCAPD2* and *AtCAPD3* were chosen for this analysis as a meiotic role has been suggested for them in other species; however any of the three non-SMC subunits should show similar phenotypes since they are thought to act in the same complex. Due to the lethality of condensin I and *Atsmc4* homozygote T-DNA insertion mutants, an RNAi approach

was adopted using the meiosis specific DMC1 promoter to knock-down the levels of these proteins. A T-DNA knock-out line for *AtCAPD3* was also analysed. The phenotypes observed from targeting each condensin gene are summarised in Table 4 and Figure 7.1.

	Wild type	<i>AtSMC4^{RNAi}</i>	<i>AtCAPD2^{RNAi}</i>	<i>Atcapd3</i>
Prophase I	Chromosome organisation and synapsis appear normal	Chromosome organisation and synapsis appear normal	Chromosome organisation and synapsis appear normal	Chromosome organisation and synapsis appear normal
Metaphase I	Compact chromosomes with compact centromere and rDNA signals	Elongated chromosomes with stretched centromeres and large rDNA signals	Elongated chromosomes with stretched centromeres and large rDNA signals	Multiple connections between chromosomes, compact rDNA and centromere signals
Anaphase I	Chromosomes segregate neatly as compact entities	Thin thread-like bridges appear as chromosome segregate, threads often involve the rDNA regions. Chromosomes appear to lose compaction	Thin thread-like bridges appear as chromosome segregate, threads often involve the rDNA regions. Chromosomes appear to lose compaction	Chromosomes appear to unravel as they segregate creating trailing chromatin. Connections between homologs seen in some cells
Metaphase II	Compact spherical chromosomes	Elongated chromosomes	Elongated chromosomes	Misshapen chromosomes, distinct from cells in <i>AtSMC4</i> or <i>AtCAPD2 RNAi</i> lines
Anaphase II	Chromosomes segregate neatly as compact entities	Thin thread-like bridges appear as chromosome segregate, threads often involve the rDNA	Thin thread-like bridges appear as chromosome segregate. FISH analysis on rDNA not carried out	Chromosomes appear to unravel as they segregate creating trailing chromatin.
Tetrad	4 loosely organised groups of chromosome visible	4 loosely organised groups of chromosome visible	4 loosely organised groups of chromosome visible	4 groups of chromosomes seen but organisation appears altered compared to wild-type

Table 4: Summary of condensin phenotypes in *Arabidopsis thaliana* compared to wild-type

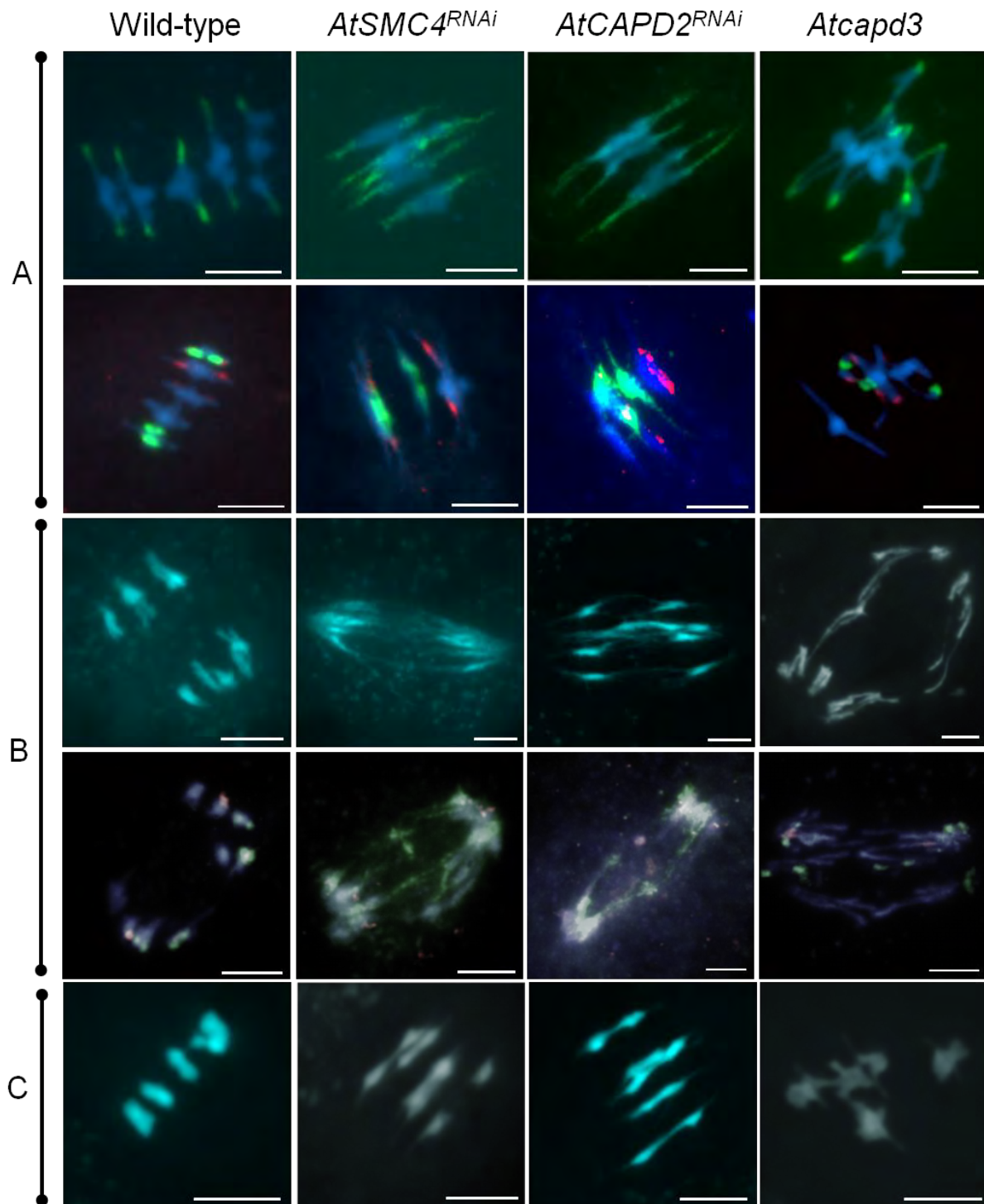


Figure 7.1: Summary of condensin phenotypes in *Arabidopsis thaliana* compared to wild-type. Genotype of plants is indicated above column. **Section A:** Metaphase cells. **Top row:** Centromere phenotypes of each line using the pAL38 centromere FISH probe. **Bottom row:** rDNA phenotype of each line using the 45S and 5S rDNA FISH probes. **Section B:** Anaphase cells. **Top row:** DAPI stained chromosome spreads showing anaphase phenotypes in each line. **Bottom row:** rDNA phenotypes at anaphase for each line using the 45S and 5S rDNA FISH probes. **Section C:** DAPI stained metaphase II chromosomes for each line, showing one set of bivalents. Scale bar = 5 μ m

7.2 Condensin does not appear to have a role in prophase I chromosome organisation

No apparent defects in prophase I organisation were observed in knock-downs of any condensin subunit analysed. Prophase I chromosome appeared normal in DAPI-stained chromosome spreads in plants deficient in each of the three subunits studied. Further analysis of the chromosome axes in the form of immunolocalisation using antibodies raised against the axis-associated *AtASY1* and the SC TF protein *AtZYP1* was carried out in *AtSMC4^{RNAi}* and *Atcapd3* plants; however no defects in the localisation of these proteins was observed compared to wild-type. Pachytene axis length was also investigated in *AtSMC4^{RNAi}* lines; no difference in axis length was observed in these lines compared to wild-type. These results suggest that factors other than condensin are required to organise the prophase I chromosome axes. Alternatively incomplete knock-down of the *AtSMC4* or *AtCAPD2* condensin subunits may be responsible for the lack of phenotype observed in these plants.

7.3 A role for condensin in recombination

Recombination between homologous chromosomes occurs during prophase I of meiosis and its progression is closely linked to the organisation of the chromosomes. The recombination rate was analysed in condensin *AtSMC4^{RNAi}* lines by scoring chiasmata at metaphase I. The results revealed that there was a slight reduction in COs in the condensin deficient plants compared to wild-type. This reduction in COs appeared to be mainly focused on chromosome 1 and 4, whereas chromosome 2 had an increase in COs in one line. In addition to this, occasional univalents were observed in both *AtSMC4^{+/-}* and *AtCAPD3^{+/-}* plants. Taken together these results

suggest that there may be a role for condensin in recombination: however, this role is minor and possibly requires a certain threshold of condensin. The role that condensin plays in recombination remains unknown. However, it may be that condensin acts on higher order chromatin structure to alter the number of DSBs (as in seen in *C. elegans* (Tsai *et al.*, 2008; Mets and Meyer, 2009)), albeit with a different outcome (more versus fewer COs). The results presented here also highlight that the individual chromosome appears to act differently in regards to COs. This has been seen previously in *AtSPO11* deficient plants (Nicola Roberts, Unpublished). It is possible that incomplete RNAi is partially responsible for the lack of a more prominent recombination phenotype in this study.

7.4 A role for condensin in maintaining chromosome architecture

All three of the condensin deficient plants analysed here show some form of chromosome abnormality during meiosis, however in all three cases the chromosomes are able to condense into metaphase I bivalents with only minor compaction defects. This suggests that condensin in *Arabidopsis*, unlike in *Xenopus* and yeast (Saka *et al.*, 1994; Strunnikov *et al.*, 1995; Lieb *et al.*, 1996; Hirano *et al.*, 1997; Sutani *et al.*, 1999; Freeman *et al.*, 2000; Ouspenski *et al.*, 2000; Lavoie *et al.*, 2002; Yu and Koshland, 2003) is not essential for the compaction of the chromosomes. This leads to the conclusion that other factors, distinct from condensin, may be required for chromosome condensation and that condensin may be required more in maintaining chromosome architecture rather than in compaction itself. In support of this, the *AtSMC4*-Ab was first seen to localise to the chromatin at

late diakinesis when the chromosomes had already largely condensed. Furthermore, it was observed that the metaphase I chromosomes in condensin deficient plants became more diffuse when fixed bud material of these lines was incubated in water overnight. This phenomenon was not seen in wild-type buds under the same conditions. These results reflect those seen in human in which hypotonic treatment of the chromosomes results in more severe defects. The authors suggest that condensin is required to maintain chromosome structure when swelling pressure is applied (Ono *et al.*, 2003). In addition to this in the *AtCAPD2* and *AtSMC4^{RNAi}* lines thin threads of chromatin were seen to trail behind segregating chromosomes at anaphase I and II. In chicken it has been suggested that condensin is required to maintain chromosome structure as the chromosomes segregate at anaphase (Vagnarelli *et al.*, 2006). The phenotypes observed in the *AtSMC4^{RNAi}* x *Atspo11* cross lead to the conclusion that the condensin in *Arabidopsis*, like in chicken is required to maintain the architecture of the chromosome upon segregation at anaphase. In these plants at metaphase 10 univalents were observed. However as they came to segregate at anaphase each chromosome seemed to lose structural integrity. This loss of chromosome architecture is likely to be accompanied or encouraged by the existence of some form of connection between segregating chromosomes. A role for the condensin I complex in maintaining chromosome structure was also seen at the centromeres (below).

7.5 Condensin I and II have different roles in meiotic chromosome organisation

The chromosome phenotypes seen in the *AtSMC4* and *AtCAPD2^{RNAi}* lines were distinct from those seen in the *Atcapd3* mutants, indicating that the two complexes play different roles in chromosome organisation. This is consistent with results from other species where the two condensin complexes are depleted separately (Ono *et al.*, 2003; Gerlich *et al.*, 2006; Shintomi and Hirano, 2011). Further distinction between the two complexes was seen with analysis of the repetitive DNA; the rDNA and the centromere DNA. FISH analysis of the rDNA regions 5S and 45S in the *AtSMC4* and *AtCAPD2^{RNAi}* lines revealed that the rDNA appear disorganised in these plants forming large signals at metaphase and bridges at anaphase I and II, whereas the 45S and 5S signals in *Atcapd3* appeared like wild-type. Maintenance of the rDNA has been suggested as a role of condensin in yeast (Tsang *et al.*, 2007; D'Ambrosio *et al.*, 2008a). However no obvious role of condensin in rDNA organisation has been observed in any higher eukaryote. The rDNA comprises a large amount of repetitive DNA and presents a huge logistical problem for the dividing cell in terms of maintaining a compact rDNA unit during cell division. It is therefore conceivable that when condensin, a complex involved in maintaining the structure of DNA, is depleted one of the most striking affects is the subsequent disorganisation of the rDNA repeats.

The centromeres are also large regions of repetitive DNA which have been highlighted as specific chromosome regions in which condensin is crucial (Stear and Roth, 2002; Oliveira *et al.*, 2005; Savvidou *et al.*, 2005; Yong-Gonzalez *et al.*, 2007;

Ribeiro *et al.*, 2009; Samoshkin *et al.*, 2009). Here, the centromere specific FISH probe pAL38 was hybridised to cells from all three condensin deficient lines. The results revealed that the *AtSMC4* and *AtCAPD2^{RNAi}* plants had defects in the structure of the centromeres, whereas the *Atcapd3* mutants appeared to have centromeres which compacted as in wild-type. This further distinguishes between the roles of the two complexes in chromosome organisation. The disorganised centromeres in the *AtCAPD2^{RNAi}* and *AtSMC4^{RNAi}* lines appeared like wild-type during prophase I but became stretched and disorganised at metaphase I when wild-type centromeres remained as discrete entities. These results appear to show that the centromeres in condensin deficient plants are unable to resist the pulling force of the spindle and as a result lose structural integrity. These stretched centromeres are however still able to segregate the chromosome to the opposite poles of the cells although it is likely that there is a delay in this process since a high number of anaphase I and II cells are detected in these lines compared to wild-type. These results support the view that condensin has a role in maintaining chromosome architecture rather than in the compaction itself. These results are also consistent with results from condensin deficient cells in other species, where the pulling force of the spindle has been suggested to result in the reversible (Gerlich *et al.*, 2006; Ribeiro *et al.*, 2009) or irreversible (Oliveira *et al.*, 2005; Savvidou *et al.*, 2005) stretching of the centromeric DNA. The role of condensin in centromere organisation may be due to the mis-localisation of centromere histones. It has been suggested that condensin is required to fold the DNA into a structure in which the centromere specific histones can load (Jager *et al.*, 2005). Alternatively, merotelic attachment

has been suggested as a cause of the centromere defects in condensin deficient worm (Stear and Roth, 2002) and human cells (Samoshkin *et al.*, 2009).

7.6 Future perspectives

The analysis carried out on the prophase I cells in each line in this study do not rule out the possibility that there is a delay in the progression of synapsis which is not apparent from cytological or immunohistochemical analysis. Therefore a time course experiment using the thymidine analogue BrdU or EdU could be carried out in order to assess this possibility. It is also possible that subtle axis defects are not detectable by the standard cytological techniques, therefore further analysis using EM or 3D-SIM would allow a closer look at the prophase I axes in these plants.

In condensin II mutants the metaphase I chromosome appeared misshapen with multiple connections between chromosomes. What role condensin II plays in shaping the metaphase I chromosomes is an interesting area of further analysis. This could involve higher-resolution microscopical analysis using 3D-SIM as well as a more detailed analysis into the organisation of the chromosomes. Multiple FISH probes could be used in order to try to decipher the complex chromosome masses seen in these plants.

Here condensin I has been shown to be required for maintenance of chromosome structure. Further probing into its role in the process in the form of micromanipulation and further hypotonic treatment will provide an interesting challenge for the future.

The results presented here suggest that neither of the two condensin complexes are primarily required for the condensation of meiotic chromosomes but are instead required for the maintenance of chromosome structure. This raises the question as to what protein or proteins are required to condense the chromosomes from prophase until metaphase. Currently no one candidate stands out as the single chromosome organiser, therefore it is likely that a complex interplay between multiple proteins is required to arrange the chromosomes into the highly organised structures seen at metaphase. Investigation into possible candidates for this role is an interesting and valuable area of future work.

Total condensin localisation was analysed here and provided useful information into the role of these proteins during meiosis. Investigation into the localisation of the two condensin complexes individually in *Arabidopsis* meiosis remains an important area for further research. This will provide valuable insights into the roles of the individual complexes.

A possible role for condensin in recombination was highlighted here. In what capacity condensin affects recombination is an interesting question for further work. Analysis of chiasmata frequency in *AtCAPD2^{RNAi}* and *Atcapd3* plants may prove informative as well as a more thorough analysis on the recombination rates in these plants using tetrad analysis in the quartet mutant (Copenhaver *et al.*, 1998).

Finally, pull-down assays using different condensin subunits may provide valuable insight into the function of these complexes. The identification of candidates with which condensin subunits interact may provide interesting avenues for future analysis.

7.7 Concluding remarks

The results presented here represent the first major insight into the role of condensin I and condensin II during meiosis in *Arabidopsis* and pave the way for further analysis into the complex roles of these proteins in chromosome organisation. The proteins and mechanisms which shape the metaphase chromosomes during both meiosis and mitosis remain to be elucidated in any species. Andrew Belmont described the folding of the metaphase chromosomes as 'A riddle wrapped in a mystery inside an enigma'. With the advent of ever increasing cytological and molecular techniques this remains an exciting and important area of further research.

CHAPTER 8

8 REFERENCE LIST

- Abe, S., Nagasaka, K., Hirayama, Y., Kozuka-Hata, H., Oyama, M., Aoyagi, Y., Obuse, C. and Hirota, T.** (2011) The initial phase of chromosome condensation requires Cdk1-mediated phosphorylation of the CAP-D3 subunit of condensin II. *Gene Dev*, **25**, 863-874.
- Adachi, Y., Luke, M. and Laemmli, U.K.** (1991) Chromosome assembly in vitro: topoisomerase II is required for condensation. *Cell*, **64**, 137-148.
- Alani, E., Thresher, R., Griffith, J.D. and Kolodner, R.D.** (1992) Characterization of DNA-binding and strand-exchange stimulation properties of γ -RPA, a yeast single-strand-DNA-binding protein. *J Mol Biol*, **227**, 54-71.
- Alexander, M.P.** (1969) Differential staining of aborted and nonaborted pollen. *Stain Technol*, **44**, 117-122.
- An, G., Watson, B.D. and Chiang, C.C.** (1986) Transformation of Tobacco, Tomato, Potato, and Arabidopsis thaliana Using a Binary Ti Vector System. *Plant Physiol*, **81**, 301-305.
- Anderson, D.E., Losada, A., Erickson, H.P. and Hirano, T.** (2002) Condensin and cohesin display different arm conformations with characteristic hinge angles. *J Cell Biol*, **156**, 419-424.
- Anderson, L.K., Hooker, K.D. and Stack, S.M.** (2001) The distribution of early recombination nodules on zygotene bivalents from plants. *Genetics*, **159**, 1259-1269.
- Armstrong, S.J., Caryl, A.P., Jones, G.H. and Franklin, F.C.** (2002) Asy1, a protein required for meiotic chromosome synapsis, localizes to axis-associated chromatin in Arabidopsis and Brassica. *J Cell Sci*, **115**, 3645-3655.
- Armstrong, S.J. and Jones, G.H.** (2003) Meiotic cytology and chromosome behaviour in wild-type Arabidopsis thaliana. *J Exp Bot*, **54**, 1-10.
- Bachellier-Bassi, S., Gadal, O., Bourouta, G. and Nehrbass, U.** (2008) Cell cycle-dependent kinetochore localization of condensin complex in *Saccharomyces cerevisiae*. *J Struct Biol*, **162**, 248-259.
- Bailis, J.M. and Roeder, G.S.** (1998) Synaptonemal complex morphogenesis and sister-chromatid cohesion require Mek1-dependent phosphorylation of a meiotic chromosomal protein. *Gene Dev*, **12**, 3551-3563.
- Ball, A.R., Jr., Schmiesing, J.A., Zhou, C., Gregson, H.C., Okada, Y., Doi, T. and Yokomori, K.** (2002) Identification of a chromosome-targeting domain in the human condensin subunit CNAP1/hCAP-D2/Eg7. *Mol Cell Biol*, **22**, 5769-5781.
- Bannister, L.A., Reinholdt, L.G., Munroe, R.J. and Schimenti, J.C.** (2004) Positional cloning and characterization of mouse mei8, a disrupted allele of the meiotic cohesin Rec8. *Genesis*, **40**, 184-194.
- Baudat, F.** (2010) PRDM9 is a major determinant of meiotic recombination hotspots in humans and mice *Science*, **328**, 690-690.
- Baulcombe, D.** (2004) RNA silencing in plants. *Nature*, **431**, 356-363.

- Bazett-Jones, D.P., Kimura, K. and Hirano, T.** (2002) Efficient supercoiling of DNA by a single condensin complex as revealed by electron spectroscopic imaging. *Mol Cell*, **9**, 1183-1190.
- Beenders, B., Watrin, E., Legagneux, V., Kireev, I. and Bellini, M.** (2003) Distribution of XCAP-E and XCAP-D2 in the *Xenopus* oocyte nucleus. *Chromosome Res*, **11**, 549-564.
- Berchowitz, L.E. and Copenhaver, G.P.** (2008) Fluorescent *Arabidopsis* tetrads: a visual assay for quickly developing large crossover and crossover interference data sets. *Nat Protoc*, **3**, 41-50.
- Berchowitz, L.E., Francis, K.E., Bey, A.L. and Copenhaver, G.P.** (2007) The role of AtMUS81 in interference-insensitive crossovers in *A.thaliana*. *PLoS Genet*, **3**, 1355-1364.
- Berchowitz, L.E., Hanlon, S.E., Lieb, J.D. and Copenhaver, G.P.** (2009) A positive but complex association between meiotic double-strand break hotspots and open chromatin in *Saccharomyces cerevisiae*. *Genome Res*, **19**, 2245-2257.
- Bernad, R., Sanchez, P., Rivera, T., Rodriguez-Corsino, M., Boyarchuk, E., Vassias, I., Ray-Gallet, D., Arnaoutov, A., Dasso, M., Almouzni, G. and Losada, A.** (2011) *Xenopus* HJURP and condensin II are required for CENP-A assembly. *J Cell Biol*, **192**, 569-582.
- Bhalla, N., Biggins, S. and Murray, A.W.** (2002) Mutation of YCS4, a budding yeast condensin subunit, affects mitotic and nonmitotic chromosome behavior. *Mol Biol Cell*, **13**, 632-645.
- Bhat, M.A., Philp, A.V., Glover, D.M. and Bellen, H.J.** (1996) Chromatid segregation at anaphase requires the barren product, a novel chromosome-associated protein that interacts with Topoisomerase II. *Cell*, **87**, 1103-1114.
- Bhatt, A.M., Lister, C., Page, T., Franz, P., Findlay, K., Jones, G.H., Dickinson, H.G. and Dean, C.** (1999) The DIF1 gene of *Arabidopsis* is required for meiotic chromosome segregation and belongs to the REC8/RAD21 cohesin gene family. *Plant J*, **19**, 463-472.
- Bishop, D.K.** (2006) Multiple mechanisms of meiotic recombination. *Cell*, **127**, 1095-1097.
- Bishop, D.K., Park, D., Xu, L.Z. and Kleckner, N.** (1992) Dmc1 - a Meiosis-Specific Yeast Homolog of Escherichia-Coli RecA Required for Recombination, Synaptonemal Complex-Formation, and Cell-Cycle Progression. *Cell*, **69**, 439-456.
- Blat, Y., Protacio, R.U., Hunter, N. and Kleckner, N.** (2002) Physical and functional interactions among basic chromosome organizational features govern early steps of meiotic chiasma formation. *Cell*, **111**, 791-802.
- Bleuyard, J.Y., Gallego, M.E., Savigny, F. and White, C.I.** (2005) Differing requirements for the *Arabidopsis* Rad51 paralogs in meiosis and DNA repair. *Plant J*, **41**, 533-545.
- Bleuyard, J.Y., Gallego, M.E. and White, C.I.** (2004) Meiotic defects in the *Arabidopsis* rad50 mutant point to conservation of the MRX complex function in early stages of meiotic recombination. *Chromosoma*, **113**, 197-203.
- Bleuyard, J.Y. and White, C.I.** (2004) The *Arabidopsis* homologue of Xrcc3 plays an essential role in meiosis. *EMBO J*, **23**, 439-449.

- Borde, V., Robine, N., Lin, W., Bonfils, S., Geli, V. and Nicolas, A.** (2009) Histone H3 lysine 4 trimethylation marks meiotic recombination initiation sites. *EMBO J*, **28**, 99-111.
- Borner, G.V., Barot, A. and Kleckner, N.** (2008) Yeast Pch2 promotes domainal axis organization, timely recombination progression, and arrest of defective recombinosomes during meiosis. *P Natl Acad Sci USA*, **105**, 3327-3332.
- Borner, G.V., Kleckner, N. and Hunter, N.** (2004) Crossover/noncrossover differentiation, synaptonemal complex formation, and regulatory surveillance at the leptotene/zygotene transition of meiosis. *Cell*, **117**, 29-45.
- Brito, I.L., Yu, H.G. and Amon, A.** (2010) Condensins promote coorientation of sister chromatids during meiosis I in budding yeast. *Genetics*, **185**, 55-64.
- Bundock, P. and Hooykaas, P.** (2002) Severe developmental defects, hypersensitivity to DNA-damaging agents, and lengthened telomeres in Arabidopsis MRE11 mutants. *Plant Cell*, **14**, 2451-2462.
- Cabello, O.A., Eliseeva, E., He, W.G., Youssoufian, H., Plon, S.E., Brinkley, B.R. and Belmont, J.W.** (2001) Cell cycle-dependent expression and nucleolar localization of hCAP-H. *Mol Biol Cell*, **12**, 3527-3537.
- Cai, X., Dong, F.G., Edelmann, R.E. and Makaroff, C.A.** (2003) The Arabidopsis SYN1 cohesin protein is required for sister chromatid arm cohesion and homologous chromosome pairing. *J Cell Sci*, **116**, 2999-3007.
- Carpenter, A.T.** (1975) Electron microscopy of meiosis in *Drosophila melanogaster* females: II. The recombination nodule--a recombination-associated structure at pachytene? *P Natl Acad Sci USA*, **72**, 3186-3189.
- Caryl, A.P., Armstrong, S.J., Jones, G.H. and Franklin, F.C.H.** (2000) A homologue of the yeast HOP1 gene is inactivated in the Arabidopsis meiotic mutant *asy1*. *Chromosoma*, **109**, 62-71.
- Celerin, M., Merino, S.T., Stone, J.E., Menzie, A.M. and Zolan, M.E.** (2000) Multiple roles of Spo11 in meiotic chromosome behavior. *EMBO J*, **19**, 2739-2750.
- Chan, K.L., Hickson, I.D.** (2011) New insights into the formation and resolution of ultra-fine anaphase bridges. *Semin Cell Dev Biol*, **22**, 906-912.
- Chan, R.C., Severson, A.F. and Meyer, B.J.** (2004) Condensin restructures chromosomes in preparation for meiotic divisions. *J Biol Chem*, **167**, 613-625.
- Chelysheva, L., Grandont, L., Vrielynck, N., le Guin, S., Mercier, R. and Grelon, M.** (2010) An Easy Protocol for Studying Chromatin and Recombination Protein Dynamics during Arabidopsis thaliana Meiosis: Immunodetection of Cohesins, Histones and MLH1. *Cytogenet Genome Res*, **129**, 143-153.
- Chelysheva, L., Vezon, D., Belcram, K., Gendrot, G. and Grelon, M.** (2008) The Arabidopsis BLAP75/Rmi1 homologue plays crucial roles in meiotic double-strand break repair. *PLoS Genet*, **4**, e1000309.
- Chen, S.Y., Tsubouchi, T., Rockmill, B., Sandler, J.S., Richards, D.R., Vader, G., Hochwagen, A., Roeder, G.S. and Fung, J.C.** (2008) Global analysis of the meiotic crossover landscape. *Dev Cell*, **15**, 401-415.
- Clavente, A., Viera, A., Page, J., Parra, M.T., Gomez, R., Suja, J.A., Rufas, J.S. and Santos, J.L.** (2005) DNA double-strand breaks and homology search: inferences from a species with incomplete pairing and synapsis. *J Cell Sci*, **118**, 2957-2963.

- Cobbe, N., Savvidou, E. and Heck, M.M.** (2006) Diverse mitotic and interphase functions of condensins in *Drosophila*. *Genetics*, **172**, 991-1008.
- Coelho, P.A., Queiroz-Machado, J. and Sunkel, C.E.** (2003) Condensin-dependent localisation of topoisomerase II to an axial chromosomal structure is required for sister chromatid resolution during mitosis. *J Cell Sci*, **116**, 4763-4776.
- Collas, P., Le Guellec, K. and Tasken, K.** (1999) The A-kinase-anchoring protein AKAP95 is a multivalent protein with a key role in chromatin condensation at mitosis. *J Cell Biol*, **147**, 1167-1180.
- Copenhaver, G.P., Browne, W.E. and Preuss, D.** (1998) Assaying genome-wide recombination and centromere functions with *Arabidopsis* tetrads. *P Natl Acad Sci USA*, **95**, 247-252.
- Copenhaver, G.P., Housworth, E.A. and Stahl, F.W.** (2002) Crossover interference in *Arabidopsis*. *Genetics*, **160**, 1631-1639.
- Couteau, F., Belzile, F., Horlow, C., Grandjean, O., Vezon, D. and Doutriaux, M.P.** (1999) Random chromosome segregation without meiotic arrest in both male and female meiocytes of a *dmc1* mutant of *Arabidopsis*. *Plant Cell*, **11**, 1623-1634.
- Csankovszki, G., Collette, K., Spahl, K., Carey, J., Snyder, M., Petty, E., Patel, U., Tabuchi, T., Liu, H., McLeod, I., Thompson, J., Sarkeshik, A., Yates, J., Meyer, B. and Hagstrom, K.** (2009) Three Distinct Condensin Complexes Control *C. elegans* Chromosome Dynamics. *Curr Biol*, **19**, 176-176.
- Cuvier, O. and Hirano, T.** (2003) A role of topoisomerase II in linking DNA replication to chromosome condensation. *J Cell Biol*, **160**, 645-655.
- Cuylen, S. and Haering, C.H.** (2011) Deciphering condensin action during chromosome segregation. *Trends Cell Biol*, **21**, 552-559.
- Cuylen, S., Metz, J. and Haering, C.H.** (2011) Condensin structures chromosomal DNA through topological links. *Nat Struct Mol Biol*, **18**, 894-901.
- D'Ambrosio, C., Kelly, G., Shirahige, K. and Uhlmann, F.** (2008a) Condensin-dependent rDNA decatenation introduces a temporal pattern to chromosome segregation. *Curr Biol*, **18**, 1084-1089.
- D'Ambrosio, C., Schmidt, C.K., Katou, Y., Kelly, G., Itoh, T., Shirahige, K. and Uhlmann, F.** (2008b) Identification of cis-acting sites for condensin loading onto budding yeast chromosomes. *Gene Dev*, **22**, 2215-2227.
- D'Amours, D., Stegmeier, F. and Amon, A.** (2004) Cdc14 and condensin control the dissolution of cohesin-independent chromosome linkages at repeated DNA. *Cell*, **117**, 455-469.
- d'Erfurth, I., Jolivet, S., Froger, N., Catrice, O., Novatchkova, M. and Mercier, R.** (2009) Turning Meiosis into Mitosis. *PLoS Biol*, **7**.
- Daniel, K., Lange, J., Hached, K., Fu, J., Anastassiadis, K., Roig, I., Cooke, H.J., Stewart, A.F., Wassmann, K., Jasin, M., Keeney, S. and Toth, A.** (2011) Meiotic homologue alignment and its quality surveillance are controlled by mouse *HORMAD1*. *Nat Cell Biol*, **13**, 599-610.
- de la Barre, A.E., Gerson, V., Gout, S., Creaven, M., Allis, C.D. and Dimitrov, S.** (2000) Core histone N-termini play an essential role in mitotic chromosome condensation. *EMBO J*, **19**, 379-391.
- de los Santos, T., Hunter, N., Lee, C., Larkin, B., Loidl, J. and Hollingsworth, N.M.** (2003) The *Mus81/Mms4* endonuclease acts independently of double-

- holliday junction resolution to promote a distinct subset of crossovers during meiosis in budding yeast. *Genetics*, **164**, 81-94.
- De Muyt, A., Pereira, L., Vezon, D., Chelysheva, L., Gendrot, G., Chambon, A., Laine-Choinard, S., Pelletier, G., Mercier, R., Nogue, F. and Grelon, M.** (2009) A High Throughput Genetic Screen Identifies New Early Meiotic Recombination Functions in *Arabidopsis thaliana*. *PLoS Genet*, **5**.
- De Muyt, A., Vezon, D., Gendrot, G., Gallois, J.L., Stevens, R. and Grelon, M.** (2007) AtPRD1 is required for meiotic double strand break formation in *Arabidopsis thaliana*. *EMBO J*, **26**, 4126-4137.
- Dej, K.J., Ahn, C. and Orr-Weaver, T.L.** (2004) Mutations in the *Drosophila* condensin subunit dCAP-G: defining the role of condensin for chromosome condensation in mitosis and gene expression in interphase. *Genetics*, **168**, 895-906.
- Dernburg, A.F., McDonald, K., Moulder, G., Barstead, R., Dresser, M. and Villeneuve, A.M.** (1998) Meiotic recombination in *C.elegans* initiates by a conserved mechanism and is dispensable for homologous chromosome synapsis. *Cell*, **94**, 387-398.
- Dion, E., Li, L., Jean, M. and Belzile, F.** (2007) An *Arabidopsis* MLH1 mutant exhibits reproductive defects and reveals a dual role for this gene in mitotic recombination. *Plant J*, **51**, 431-440.
- Doutriaux, M.P., Couteau, F., Bergounioux, C. and White, C.** (1998) Isolation and characterisation of the RAD51 and DMC1 homologs from *Arabidopsis thaliana*. *Mol Gen Genet*, **257**, 283-291.
- Drouaud, J., Camilleri, C., Bourguignon, P.Y., Canaguier, A., Berard, A., Vezon, D., Giancola, S., Brunel, D., Colot, V., Prum, B., Quesneville, H. and Mezard, C.** (2006) Variation in crossing-over rates across chromosome 4 of *Arabidopsis thaliana* reveals the presence of meiotic recombination "hot spots". *Genome Res*, **16**, 106-114.
- Dunoyer, P.** (2010) Small RNA duplexes function as mobile silencing signals between plant cells. *Science*, **328**, 1229-1229.
- Earnshaw, W.C., Halligan, B., Cooke, C.A., Heck, M.M. and Liu, L.F.** (1985) Topoisomerase II is a structural component of mitotic chromosome scaffolds. *J Cell Biol*, **100**, 1706-1715.
- Earnshaw, W.C. and Migeon, B.R.** (1985) Three related centromere proteins are absent from the inactive centromere of a stable isodicentric chromosome. *Chromosoma*, **92**, 290-296.
- Eijpe, M., Offenberger, H., Jessberger, R., Revenkova, E. and Heyting, C.** (2003) Meiotic cohesin REC8 marks the axial elements of rat synaptonemal complexes before cohesins SMC1 beta and SMC3. *J Cell Biol*, **160**, 657-670.
- Fire, A., Xu, S., Montgomery, M.K., Kostas, S.A., Driver, S.E. and Mello, C.C.** (1998) Potent and specific genetic interference by double-stranded RNA in *Caenorhabditis elegans*. *Nature*, **391**, 806-811.
- Franklin, A.E., McElver, J., Sunjevaric, I., Rothstein, R., Bowen, B. and Cande, W.Z.** (1999) Three-dimensional microscopy of the Rad51 recombination protein during meiotic prophase. *Plant Cell*, **11**, 809-824.

- Franklin, F.C.H., Higgins, J.D., Sanchez-Moran, E., Armstrong, S.J., Osman, K.E., Jackson, N. and Jones, G.H. (2006) Control of meiotic recombination in Arabidopsis: role of the MutL and MutS homologues. *Biochem Soc T*, **34**, 542-544.
- Freeman, L., Aragon-Alcaide, L. and Strunnikov, A. (2000) The condensin complex governs chromosome condensation and mitotic transmission of rDNA. *J Cell Biol*, **149**, 811-824.
- Fujimoto, S., Yonemura, M., Matsunaga, S., Nakagawa, T., Uchiyama, S. and Fukui, K. (2005) Characterization and dynamic analysis of Arabidopsis condensin subunits, AtCAP-H and AtCAP-H2. *Planta*, **222**, 293-300.
- Fung, J.C., Rockmill, B., Odell, M. and Roeder, G.S. (2004) Imposition of crossover interference through the nonrandom distribution of synapsis initiation complexes. *Cell*, **116**, 795-802.
- Gallego, M.E. and White, C.I. (2005) DNA repair and recombination functions in Arabidopsis telomere maintenance. *Chromosome Res*, **13**, 481-491.
- Gerlich, D., Hirota, T., Koch, B., Peters, J.M. and Ellenberg, J. (2006) Condensin I stabilizes chromosomes mechanically through a dynamic interaction in live cells. *Curr Biol*, **16**, 333-344.
- Gerlach, W.L., Bedbrook, J.R. (1979) Cloning and characterization of ribosomal RNA genes from wheat and barley. *Nucleic Acids Res*, **7**, 1869-1885.
- Gerton, J.L., DeRisi, J., Shroff, R., Lichten, M., Brown, P.O. and Petes, T.D. (2000) Global mapping of meiotic recombination hotspots and coldspots in the yeast *Saccharomyces cerevisiae*. *P Natl Acad Sci USA*, **97**, 11383-11390.
- Giet, R. and Glover, D.M. (2001) *Drosophila* Aurora B kinase is required for histone H3 phosphorylation and condensin recruitment during chromosome condensation and to organize the central spindle during cytokinesis. *J Cell Biol*, **152**, 669-681.
- Glynn, E.F., Megee, P.C., Yu, H.G., Mistrot, C., Unal, E., Koshland, D.E., DeRisi, J.L. and Gerton, J.L. (2004) Genome-wide mapping of the cohesin complex in the yeast *Saccharomyces cerevisiae*. *PLoS Biol*, **2**, 1325-1339.
- Gregan, J., Riedel, C.G., Pidoux, A.L., Katou, Y., Rumpf, C., Schleiffer, A., Kearsey, S.E., Shirahige, K., Allshire, R.C., Nasmyth, K. (2007) The kinetochore proteins Pcs1 and Mde4 and heterochromatin are required to prevent merotelic orientation. *Curr Biol*, **17**, 1190-1200.
- Grelon, M., Vezon, D., Gendrot, G. and Pelletier, G. (2001) AtSPO11-1 is necessary for efficient meiotic recombination in plants. *EMBO J*, **20**, 589-600.
- Guacci, V., Hogan, E. and Koshland, D. (1994) Chromosome condensation and sister chromatid pairing in budding yeast. *J Cell Biol*, **125**, 517-530.
- Haering, C.H., Farcas, A.M., Arumugam, P., Metson, J. and Nasmyth, K. (2008) The cohesin ring concatenates sister DNA molecules. *Nature*, **454**, 297-U219.
- Haering, C.H., Lowe, J., Hochwagen, A. and Nasmyth, K. (2002) Molecular architecture of SMC proteins and the yeast cohesin complex. *Mol Cell*, **9**, 773-788.
- Hagstrom, K.A., Holmes, V.F., Cozzarelli, N.R. and Meyer, B.J. (2002) *C. elegans* condensin promotes mitotic chromosome architecture, centromere organization, and sister chromatid segregation during mitosis and meiosis. *Gene Dev*, **16**, 729-742.

- Hamant, O., Ma, H. and Cande, W.Z.** (2006) Genetics of meiotic prophase I in plants. *Annu Rev Plant Biol*, **57**, 267-302.
- Hamilton, A.J. and Baulcombe, D.C.** (1999) A species of small antisense RNA in posttranscriptional gene silencing in plants. *Science*, **286**, 950-952.
- Hartl, T.A., Sweeney, S.J., Knepler, P.J. and Bosco, G.** (2008a) Condensin II Resolves Chromosomal Associations to Enable Anaphase I Segregation in Drosophila Male Meiosis. *PLoS Genet*, **4**.
- Hartsuiker, E., Mizuno, K., Molnar, M., Kohli, J., Ohta, K. and Carr, A.M.** (2009b) Ctp1CtIP and Rad32Mre11 nuclease activity are required for Rec12Spo11 removal, but Rec12Spo11 removal is dispensable for other MRN-dependent meiotic functions. *Mol Cell Biol*, **29**, 1671-1681.
- Hartsuiker, E., Neale, M.J. and Carr, A.M.** (2009a) Distinct requirements for the Rad32(Mre11) nuclease and Ctp1(CtIP) in the removal of covalently bound topoisomerase I and II from DNA. *Mol Cell*, **33**, 117-123.
- Hartung, F. and Puchta, H.** (2000) Molecular characterisation of two paralogous SPO11 homologues in Arabidopsis thaliana. *Nucleic Acids Res*, **28**, 1548-1554.
- Hartung, F. and Puchta, H.** (2001) Molecular characterization of homologues of both subunits A (SPO11) and B of the archaeobacterial topoisomerase 6 in plants. *Gene*, **271**, 81-86.
- Hartung, F., Suer, S., Knoll, A., Wurz-Wildersinn, R. and Puchta, H.** (2008) Topoisomerase 3alpha and RMI1 suppress somatic crossovers and are essential for resolution of meiotic recombination intermediates in Arabidopsis thaliana. *PLoS Genet*, **4**, e1000285.
- Hartung, F., Wurz-Wildersinn, R., Fuchs, J., Schubert, I., Suer, S. and Puchta, H.** (2007) The catalytically active tyrosine residues of both SPO11-1 and SPO11-2 are required for meiotic double-strand break induction in Arabidopsis. *Plant Cell*, **19**, 3090-3099.
- Henderson, K.A. and Keeney, S.** (2004) Tying synaptonemal complex initiation to the formation and programmed repair of DNA double-strand breaks. *P Natl Acad Sci USA*, **101**, 4519-4524.
- Higgins, J.D., Armstrong, S.J., Franklin, F.C.H. and Jones, G.H.** (2004) The Arabidopsis MutS homolog AtMSH4 functions at an early step in recombination: evidence for two classes of recombination in Arabidopsis. *Gene Dev*, **18**, 2557-2570.
- Higgins, J.D., Buckling, E.F., Franklin, F.C.H. and Jones, G.H.** (2008b) Expression and functional analysis of AtMUS81 in Arabidopsis meiosis reveals a role in the second pathway of crossing-over. *Plant J*, **54**, 152-162.
- Higgins, J.D., Vignard, J., Mercier, R., Pugh, A.G., Franklin, F.C. and Jones, G.H.** (2008a) AtMSH5 partners AtMSH4 in the class I meiotic crossover pathway in Arabidopsis thaliana, but is not required for synapsis. *Plant J*, **55**, 28-39.
- Hirai, S., Oka, S., Adachi, E. and Kodama, H.** (2007) The effects of spacer sequences on silencing efficiency of plant RNAi vectors. *Plant Cell Rep*, **26**, 651-659.
- Hirano, M., Anderson, D.E., Erickson, H.P. and Hirano, T.** (2001) Bimodal activation of SMC ATPase by intra- and inter-molecular interactions. *EMBO J*, **20**, 3238-3250.

- Hirano, T.** (2000) Chromosome cohesion, condensation, and separation. *Annu Rev Biochem*, **69**, 115-144.
- Hirano, T.** (2001) Chromosome cohesion and condensation in mitosis. *Mol Biol Cell*, **12**, 131A-131A.
- Hirano, T.** (2005) Condensins: Organizing and segregating the genome. *Curr Biol*, **15**, R265-R275.
- Hirano, T.** (2010) How to separate entangled sisters: interplay between condensin and decatenase. *P Natl Acad Sci USA*, **107**, 18749-18750.
- Hirano, T., Kobayashi, R. and Hirano, M.** (1997) Condensins, chromosome condensation protein complexes containing XCAP-C, XCAP-E and a Xenopus homolog of the Drosophila Barren protein. *Cell*, **89**, 511-521.
- Hirano, T. and Mitchison, T.J.** (1993) Topoisomerase II does not play a scaffolding role in the organization of mitotic chromosomes assembled in Xenopus egg extracts. *J Cell Biol*, **120**, 601-612.
- Hirano, T. and Mitchison, T.J.** (1994) A heterodimeric coiled-coil protein required for mitotic chromosome condensation in vitro. *Cell*, **79**, 449-458.
- Hirota, T., Gerlich, D., Koch, B., Ellenberg, J. and Peters, J.M.** (2004) Distinct functions of condensin I and II in mitotic chromosome assembly. *J Cell Sci*, **117**, 6435-6445.
- Holmes, V.F. and Cozzarelli, N.R.** (2000) Closing the ring: links between SMC proteins and chromosome partitioning, condensation, and supercoiling. *P Natl Acad Sci USA*, **97**, 1322-1324.
- Hudson, D.F., Vagnarelli, P., Gassmann, R. and Earnshaw, W.C.** (2003) Condensin is required for nonhistone protein assembly and structural integrity of vertebrate mitotic chromosomes. *Dev Cell*, **5**, 323-336.
- Hulten, M.A.** (2011) On the origin of crossover interference: A chromosome oscillatory movement (COM) model. *Mol Cytogenet*, **4**, 10.
- Ide, S., Miyazaki, T., Maki, H., Kobayashi, T.** (2010) Abundance of ribosomal RNA gene copies maintains genome integrity Science, **327**, 693-696.
- Ip, S.C., Rass, U., Blanco, M.G., Flynn, H.R., Skehel, J.M. and West, S.C.** (2008) Identification of Holliday junction resolvases from humans and yeast. *Nature*, **456**, 357-361.
- Ivanov, D. and Nasmyth, K.** (2005) A topological interaction between cohesin rings and a circular minichromosome. *Cell*, **122**, 849-860.
- Jackson, N., Sanchez-Moran, E., Buckling, E., Armstrong, S.J., Jones, G.H. and Franklin, F.C.H.** (2006) Reduced meiotic crossovers and delayed prophase I progression in AtMLH3-deficient Arabidopsis. *EMBO J*, **25**, 1315-1323.
- Jager, H., Rauch, M. and Heidmann, S.** (2005) The Drosophila melanogaster condensin subunit Cap-G interacts with the centromere-specific histone H3 variant CID. *Chromosoma*, **113**, 350-361.
- Jeffreys, A.J., Kauppi, L. and Neumann, R.** (2001) Intensely punctate meiotic recombination in the class II region of the major histocompatibility complex. *Nat Genet*, **29**, 217-222.
- Jones, G.H., Armstrong, S.J., Caryl, A.P. and Franklin, F.C.** (2003) Meiotic chromosome synapsis and recombination in Arabidopsis thaliana; an integration of cytological and molecular approaches. *Chromosome Res*, **11**, 205-215.

- Jones, G.H. and Franklin, F.C.H.** (2006) Meiotic crossing-over: Obligation and interference. *Cell*, **126**, 246-248.
- Keeney, S.** (2001) Mechanism and control of meiotic recombination initiation. *Curr Top Dev Biol*, **52**, 1-53.
- Keeney, S., Giroux, C.N. and Kleckner, N.** (1997) Meiosis-specific DNA double-strand breaks are catalyzed by Spo11, a member of a widely conserved protein family. *Cell*, **88**, 375-384.
- Ketting, R.F.** (2011) The many faces of RNAi. *Dev Cell*, **20**, 148-161.
- Kim, K.P., Weiner, B.M., Zhang, L., Jordan, A., Dekker, J. and Kleckner, N.** (2010) Sister cohesion and structural axis components mediate homolog bias of meiotic recombination. *Cell*, **143**, 924-937.
- Kimura, K., Cuvier, O. and Hirano, T.** (2001) Chromosome condensation by a human condensin complex in *Xenopus* egg extracts. *J Biol Chem*, **276**, 5417-5420.
- Kimura, K., Hirano, M., Kobayashi, R. and Hirano, T.** (1998) Phosphorylation and activation of 13S condensin by Cdc2 in vitro. *Science*, **282**, 487-490.
- Kimura, K. and Hirano, T.** (1997) ATP-dependent positive supercoiling of DNA by 13S condensin. *Mol Biol Cell*, **8**, 1855-1855.
- Kimura, K. and Hirano, T.** (2000) Dual roles of the 11S regulatory subcomplex in condensin functions. *P Natl Acad Sci USA*, **97**, 11972-11977.
- Kireeva, N., Lakonishok, M., Kireev, I., Hirano, T., Belmont, A.S.** (2004) Visualization of early chromosome condensation: a hierarchical folding, axial glue model of chromosome structure. *J Cell Biol*, **166**, 775-785.
- Kitajima, T.S., Yokobayashi, S., Yamamoto, M., Watanabe, Y.** (2003) Distinct cohesin complexes organize meiotic chromosome domains. *Science*, **300**, 1152-1155.
- Kleckner, N.** (2006) Chiasma formation: chromatin/axis interplay and the role(s) of the synaptonemal complex. *Chromosoma*, **115**, 175-194.
- Kleckner, N., Zickler, D., Jones, G.H., Dekker, J., Padmore, R., Henle, J. and Hutchinson, J.** (2004) A mechanical basis for chromosome function. *P Natl Acad Sci USA*, **101**, 12592-12597.
- Klein, F., Mahr, P., Galova, M., Bonomo, S.B.C., Michaelis, C., Nairz, K. and Nasmyth, K.** (1999) A central role for cohesins in sister chromatid cohesion, formation of axial elements, and recombination during yeast meiosis. *Cell*, **98**, 91-103.
- Klimyuk, V.I. and Jones, J.D.** (1997) AtDMC1, the Arabidopsis homologue of the yeast DMC1 gene: characterization, transposon-induced allelic variation and meiosis-associated expression. *Plant J*, **11**, 1-14.
- Kobayashi, T., Heck, D.J., Nomura, M., Horiuchi, T.** (1998) Expansion and contraction of ribosomal DNA repeats in *Saccharomyces cerevisiae*: requirement of replication fork blocking (Fob1) protein and the role of RNA polymerase I. *Genes Dev*, **12**, 3821-3830.
- Koshland, D. and Strunnikov, A.** (1996) Mitotic chromosome condensation. *Annu Rev Cell Dev Biol*, **12**, 305-333.
- Kotogany, E., Dudits, D., Horvath, G.V. and Ayaydin, F.** (2010) A rapid and robust assay for detection of S-phase cell cycle progression in plant cells and tissues by using ethynyl deoxyuridine. *Plant Methods*, **6**.

- Kugou, K., Fukuda, T., Yamada, S., Ito, M., Sasanuma, H., Mori, S., Katou, Y., Itoh, T., Matsumoto, K., Shibata, T., Shirahige, K. and Ohta, K.** (2009) Rec8 guides canonical Spo11 distribution along yeast meiotic chromosomes. *Mol Biol Cell*, **20**, 3064-3076.
- Lavoie, B.D., Hogan, E. and Koshland, D.** (2002) In vivo dissection of the chromosome condensation machinery: reversibility of condensation distinguishes contributions of condensin and cohesin. *J Cell Biol*, **156**, 805-815.
- Lavoie, B.D., Hogan, E. and Koshland, D.** (2004) In vivo requirements for rDNA chromosome condensation reveal two cell-cycle-regulated pathways for mitotic chromosome folding. *Gene Dev*, **18**, 76-87.
- Lavoie, B.D., Tuffo, K.M., Oh, S., Koshland, D. and Holm, C.** (2000) Mitotic chromosome condensation requires Brn1p, the yeast homologue of Barren. *Mol Biol Cell*, **11**, 1293-1304.
- Lee, J., Ogushi, S., Saitou, M. and Hirano, T.** (2011) Condensins I and II are essential for construction of bivalent chromosomes in mouse oocytes. *Mol Biol Cell*, **22**, 3465-3477.
- Legagneux, V., Cubizolles, F. and Watrin, E.** (2004) Multiple roles of Condensins: a complex story. *Biol Cell*, **96**, 201-213.
- Lehmann, A.R., Walicka, M., Griffiths, D.J., Murray, J.M., Watts, F.Z., McCready, S. and Carr, A.M.** (1995) The rad18 gene of *Schizosaccharomyces pombe* defines a new subgroup of the SMC superfamily involved in DNA repair. *Mol Cell Biol*, **15**, 7067-7080.
- Lengronne, A., Katou, Y., Mori, S., Yokobayashi, S., Kelly, G.P., Itoh, T., Watanabe, Y., Shirahige, K. and Uhlmann, F.** (2004) Cohesin relocation from sites of chromosomal loading to places of convergent transcription. *Nature*, **430**, 573-578.
- Li, W., Chen, C., Markmann-Mulisch, U., Timofejeva, L., Schmelzer, E., Ma, H. and Reiss, B.** (2004) The Arabidopsis AtRAD51 gene is dispensable for vegetative development but required for meiosis. *P Natl Acad Sci USA*, **101**, 10596-10601.
- Li, W.X., Yang, X.H., Lin, Z.G., Timofejeva, L., Xiao, R., Makaroff, C.A. and Ma, H.** (2005) The AtRAD51C gene is required for normal meiotic chromosome synapsis and double-stranded break repair in Arabidopsis. *Plant Physiol*, **138**, 965-976.
- Lichten, M.** (2001) Meiotic recombination: Breaking the genome to save it. *Curr Biol*, **11**, R253-R256.
- Lieb, J.D., Albrecht, M.R., Chuang, P.T. and Meyer, B.J.** (1998) MIX-1: an essential component of the *C. elegans* mitotic machinery executes X chromosome dosage compensation. *Cell*, **92**, 265-277.
- Lieb, J.D., Capowski, E.E., Meneely, P. and Meyer, B.J.** (1996) DPY-26, a link between dosage compensation and meiotic chromosome segregation in the nematode. *Science*, **274**, 1732-1736.
- Lin, Y., Larson, K.L., Dorer, R. and Smith, G.R.** (1992) Meiotically induced rec7 and rec8 genes of *Schizosaccharomyces pombe*. *Genetics*, **132**, 75-85.
- Lipp, J.J., Hirota, T., Poser, I. and Peters, J.M.** (2007) Aurora B controls the association of condensin I but not condensin II with mitotic chromosomes. *J Cell Sci*, **120**, 1245-1255.

- Lorenz, A., West, S.C. and Whitby, M.C.** (2010) The human Holliday junction resolvase GEN1 rescues the meiotic phenotype of a *Schizosaccharomyces pombe* mus81 mutant. *Nucleic Acids Res*, **38**, 1866-1873.
- Losada, A. and Hirano, T.** (2005) Dynamic molecular linkers of the genome: the first decade of SMC proteins. *Gene Dev*, **19**, 1269-1287.
- Lupo, R., Breiling, A., Bianchi, M.E. and Orlando, V.** (2001) *Drosophila* chromosome condensation proteins Topoisomerase II and Barren colocalize with Polycomb and maintain Fab-7 PRE silencing. *Mol Cell*, **7**, 127-136.
- Ma, J., Wing, R.A., Bennetzen, J.L., Jackson, S.A.** (2007) Plant centromere organisation: a dynamic structure with conserved functions. *Trends Genet*, **23**, 134-139.
- Machin, F., Paschos, K., Jarmuz, A., Torres-Rosell, J., Pade, C. and Aragon, L.** (2004) Condensin regulates rDNA silencing by modulating nucleolar Sir2p. *Curr Biol*, **14**, 125-130.
- Maddox, P.S., Portier, N., Desai, A. and Oegema, K.** (2006) Molecular analysis of mitotic chromosome condensation using a quantitative time-resolved fluorescence microscopy assay. *P Natl Acad Sci USA*, **103**, 15097-15102.
- Mahadevaiah, S.K., Turner, J.M.A., Baudat, F., Rogakou, E.P., de Boer, P., Blanco-Rodriguez, J., Jasin, M., Keeney, S., Bonner, W.M. and Burgoyne, P.S.** (2001) Recombinational DNA double-strand breaks in mice precede synapsis. *Nat Genet*, **27**, 271-276.
- Mansoor, S., Amin, I., Hussain, M., Zafar, Y. and Briddon, R.W.** (2006) Engineering novel traits in plants through RNA interference. *Trends Plant Sci*, **11**, 559-565.
- Martinez-Zapater, J.M., Estelle, M.A., and Somerville, C.R.** (1986). A highly repeated DNA sequence in *Arabidopsis thaliana*. *Mol. Gen. Genet*, **204**, 417-423.
- Masclaux, F., Charpentreau, M., Takahashi, T., Pont-Lezica, R. and Galaud, J.P.** (2004) Gene silencing using a heat-inducible RNAi system in *Arabidopsis*. *Biochem Biophys Res Commun*, **321**, 364-369.
- Matoba, K., Yamazoe, M., Mayanagi, K., Morikawa, K. and Hiraga, S.** (2005) Comparison of MukB homodimer versus MukBEF complex molecular architectures by electron microscopy reveals a higher-order multimerization. *Biochem Biophys Res Commun*, **333**, 694-702.
- McCormick, S.** (1993) Male Gametophyte Development. *Plant Cell*, **5**, 1265-1275.
- McKim, K.S., Green-Marroquin, B.L., Sekelsky, J.J., Chin, G., Steinberg, C., Khodosh, R. and Hawley, R.S.** (1998) Meiotic synapsis in the absence of recombination. *Science*, **279**, 876-878.
- McVean, G. and Myers, S.** (2010) PRDM9 marks the spot. *Nat Genet*, **42**, 821-822.
- Melby, T.E., Ciampaglio, C.N., Briscoe, G. and Erickson, H.P.** (1998) The symmetrical structure of structural maintenance of chromosomes (SMC) and MukB proteins: Long, antiparallel coiled coils, folded at a flexible hinge. *J Cell Biol*, **142**, 1595-1604.
- Meneely, P.M., Farago, A.F. and Kauffman, T.M.** (2002) Crossover distribution and high interference for both the X chromosome and an autosome during oogenesis and spermatogenesis in *Caenorhabditis elegans*. *Genetics*, **162**, 1169-1177.

- Mercier, R., Jolivet, S., Vezon, D., Huppe, E., Chelysheva, L., Giovanni, M., Nogue, F., Doutriaux, M.P., Horlow, C., Grelon, M. and Mezard, C.** (2005) Two meiotic crossover classes cohabit in Arabidopsis: One is dependent on MER3, whereas the other one is not. *Curr Biol*, **15**, 692-701.
- Mets, D.G. and Meyer, B.J.** (2009) Condensins Regulate Meiotic DNA Break Distribution, thus Crossover Frequency, by Controlling Chromosome Structure. *Cell*, **139**, 73-86.
- Moens, P.B., Kolas, N.K., Tarsounas, M., Marcon, E., Cohen, P.E. and Spyropoulos, B.** (2002) The time course and chromosomal localization of recombination-related proteins at meiosis in the mouse are compatible with models that can resolve the early DNA-DNA interactions without reciprocal recombination. *J Cell Sci*, **115**, 1611-1622.
- Moens, P.B., Marcon, E., Shore, J.S., Kochakpour, N. and Spyropoulos, B.** (2007) Initiation and resolution of interhomolog connections: crossover and non-crossover sites along mouse synaptonemal complexes. *J Cell Sci*, **120**, 1017-1027.
- Molnar, M., Bahler, J., Sipiczki, M. and Kohli, J.** (1995) The Rec8 Gene of Schizosaccharomyces-Pombe Is Involved in Linear Element Formation, Chromosome-Pairing and Sister-Chromatid Cohesion During Meiosis. *Genetics*, **141**, 61-73.
- Mora-Bermúdez, F., Gerlich, D., Ellenberg, J.** (2007) Maximal chromosome compaction occurs by axial shortening in anaphase and depends on Aurora kinase. *Nat Cell Biol*, **9**, 822-831.
- Motwani, T., Doris, R., Holmes, S.G. and Flory, M.R.** (2010) Ccq1p and the condensin proteins Cut3p and Cut14p prevent telomere entanglements in the fission yeast Schizosaccharomyces pombe. *Eukaryot Cell*, **9**, 1612-1621.
- Myers, S., Freeman, C., Auton, A., Donnelly, P. and McVean, G.** (2008) A common sequence motif associated with recombination hot spots and genome instability in humans. *Nat Genet*, **40**, 1124-1129.
- Nacry, P., Camilleri, C., Courtial, B., Caboche, M. and Bouchez, D.** (1998) Major chromosomal rearrangements induced by T-DNA transformation in Arabidopsis. *Genetics*, **149**, 641-650.
- Nairz, K. and Klein, F.** (1997) mre11S - a yeast mutation that blocks double-strand-break processing and permits nonhomologous synapsis in meiosis. *Gene Dev*, **11**, 2272-2290.
- Nakazawa, N., Mehrotra, R., Ebe, M. and Yanagida, M.** (2011) Condensin phosphorylated by the Aurora-B-like kinase Ark1 is continuously required until telophase in a mode distinct from Top2. *J Cell Sci*, **124**, 1795-1807.
- Nakazawa, N., Nakamura, T., Kokubu, A., Ebe, M., Nagao, K. and Yanagida, M.** (2008) Dissection of the essential steps for condensin accumulation at kinetochores and rDNAs during fission yeast mitosis. *J Cell Biol*, **180**, 1115-1131.
- Neale, M.J. and Keeney, S.** (2006) Clarifying the mechanics of DNA strand exchange in meiotic recombination. *Nature*, **442**, 153-158.
- Neuwald, A.F. and Hirano, T.** (2000) HEAT repeats associated with condensins, cohesins, and other complexes involved in chromosome-related functions. *Genome Res*, **10**, 1445-1452.

- Nicolette, M.L., Lee, K., Guo, Z., Rani, M., Chow, J.M., Lee, S.E. and Paull, T.T.** (2010) Mre11-Rad50-Xrs2 and Sae2 promote 5' strand resection of DNA double-strand breaks. *Nat Struct Mol Biol*, **17**, 1478-1485.
- Novak, I., Wang, H., Revenkova, E., Jessberger, R., Scherthan, H. and Hoog, C.** (2008) Cohesin Smc1 beta determines meiotic chromatin axis loop organization. *J Cell Biol*, **180**, 83-90.
- Oh, S.D., Lao, J.P., Taylor, A.F., Smith, G.R. and Hunter, N.** (2008) RecQ helicase, Sgs1, and XPF family endonuclease, Mus81-Mms4, resolve aberrant joint molecules during meiotic recombination. *Mol Cell*, **31**, 324-336.
- Ohta, K., Shibata, T. and Nicolas, A.** (1994) Changes in chromatin structure at recombination initiation sites during yeast meiosis. *EMBO J*, **13**, 5754-5763.
- Oliveira, R.A., Coelho, P.A. and Sunkel, C.E.** (2005) The condensin I subunit Barren/CAP-H is essential for the structural integrity of centromeric heterochromatin during mitosis. *Mol Cell Biol*, **25**, 8971-8984.
- Onn, I., Aono, N., Hirano, M. and Hirano, T.** (2007) Reconstitution and subunit geometry of human condensin complexes. *EMBO J*, **26**, 1024-1034.
- Ono, T., Fang, Y., Spector, D.L. and Hirano, T.** (2004) Spatial and temporal regulation of Condensins I and II in mitotic chromosome assembly in human cells. *Mol Biol Cell*, **15**, 3296-3308.
- Ono, T., Losada, A., Hirano, M., Myers, M.P., Neuwald, A.F. and Hirano, T.** (2003) Differential contributions of condensin I and condensin II to mitotic chromosome architecture in vertebrate cells. *Cell*, **115**, 109-121.
- Osakabe, K., Yoshioka, T., Ichikawa, H. and Toki, S.** (2002) Molecular cloning and characterization of RAD51-like genes from *Arabidopsis thaliana*. *Plant Mol Biol*, **50**, 71-81.
- Osman, F., Dixon, J., Doe, C.L. and Whitby, M.C.** (2003) Generating crossovers by resolution of nicked Holliday junctions: A role for Mus81-Eme1 in meiosis. *Mol Cell*, **12**, 761-774.
- Osman, K., Higgins, J.D., Sanchez-Moran, E., Armstrong, S.J. and Franklin, F.C.** (2011) Pathways to meiotic recombination in *Arabidopsis thaliana*. *New Phytol*, **190**, 523-544.
- Osman, K., Sanchez-Moran, E., Mann, S.C., Jones, G.H. and Franklin, F.C.H.** (2009) Replication protein A (AtRPA1a) is required for class I crossover formation but is dispensable for meiotic DNA break repair. *EMBO J*, **28**, 394-404.
- Ouspenski, II, Cabello, O.A. and Brinkley, B.R.** (2000) Chromosome condensation factor Brn1p is required for chromatid separation in mitosis. *Mol Biol Cell*, **11**, 1305-1313.
- Page, S.L. and Hawley, R.S.** (2003) Chromosome choreography: The meiotic ballet. *Science*, **301**, 785-789.
- Park, P.U., Defossez, P.A., Guarente, L.** (1999) Effects of mutations in DNA repair genes on formation of ribosomal DNA circles and life span in *Saccharomyces cerevisiae*. *Mol Cell Biol*, **19**, 3848-3856.
- Pek, J.W. and Kai, T.** (2011) A Role for Vasa in Regulating Mitotic Chromosome Condensation in *Drosophila*. *Curr Biol*, **21**, 39-44.

- Peoples, T.L., Dean, E., Gonzalez, O., Lambourne, L. and Burgess, S.M.** (2002) Close, stable homolog juxtaposition during meiosis in budding yeast is dependent on meiotic recombination, occurs independently of synapsis, and is distinct from DSB-independent pairing contacts. *Gene Dev*, **16**, 1682-1695.
- Petersen, J. and Hagan, I.M.** (2003) *S. pombe* aurora kinase/survivin is required for chromosome condensation and the spindle checkpoint attachment response. *Curr Biol*, **13**, 590-597.
- Preuss, D., Rhee, S.Y. and Davis, R.W.** (1994) Tetrad Analysis Possible in Arabidopsis with Mutation of the Quartet (Qrt) Genes. *Science*, **264**, 1458-1460.
- Puizina, J., Siroky, J., Mokros, P., Schweizer, D. and Riha, K.** (2004) Mre11 deficiency in Arabidopsis is associated with chromosomal instability in somatic cells and Spo11-dependent genome fragmentation during meiosis. *Plant Cell*, **16**, 1968-1978.
- Ravi, M. and Chan, S.W.L.** (2010) Haploid plants produced by centromere-mediated genome elimination. *Nature*, **464**, 615-U180.
- Renshaw, M.J., Ward, J.J., Kanemaki, M., Natsume, K., Nedelec, F.J. and Tanaka, T.U.** (2010) Condensins promote chromosome recoiling during early anaphase to complete sister chromatid separation. *Dev Cell*, **19**, 232-244.
- Resnick, T.D., Dej, K.J., Xiang, Y., Hawley, R.S., Ahn, C. and Orr-Weaver, T.L.** (2009) Mutations in the chromosomal passenger complex and the condensin complex differentially affect synaptonemal complex disassembly and metaphase I configuration in Drosophila female meiosis. *Genetics*, **181**, 875-887.
- Revenkova, E., Eijpe, M., Heyting, C., Hodges, C.A., Hunt, P.A., Liebe, B., Scherthan, H. and Jessberger, R.** (2004) Cohesin SMC1 beta is required for meiotic chromosome dynamics, sister chromatid cohesion and DNA recombination. *Nat Cell Biol*, **6**, 555-562.
- Ribeiro, S.A., Gatlin, J.C., Dong, Y., Joglekar, A., Cameron, L., Hudson, D.F., Farr, C.J., McEwen, B.F., Salmon, E.D., Earnshaw, W.C. and Vagnarelli, P.** (2009) Condensin regulates the stiffness of vertebrate centromeres. *Mol Biol Cell*, **20**, 2371-2380.
- Rockmill, B., Engebrecht, J.A., Scherthan, H., Loidl, J. and Roeder, G.S.** (1995) The yeast MER2 gene is required for chromosome synapsis and the initiation of meiotic recombination. *Genetics*, **141**, 49-59.
- Rockmill, B. and Roeder, G.S.** (1990) Meiosis in Asynaptic Yeast. *Genetics*, **126**, 563-574.
- Roeder, G.S.** (1997) Meiotic chromosomes: it takes two to tango. *Gene Dev*, **11**, 2600-2621.
- Ross, K.J., Franz, P., Armstrong, S.J., Vizir, I., Mulligan, B., Franklin, F.C. and Jones, G.H.** (1997) Cytological characterization of four meiotic mutants of Arabidopsis isolated from T-DNA-transformed lines. *Chromosome Res*, **5**, 551-559.
- Saitoh, Y. and Laemmli, U.K.** (1994) Metaphase Chromosome Structure - Bands Arise from a Differential Folding Path of the Highly at-Rich Scaffold. *Cell*, **76**, 609-622.

- Saka, Y., Sutani, T., Yamashita, Y., Saitoh, S., Takeuchi, M., Nakaseko, Y. and Yanagida, M.** (1994) Fission yeast cut3 and cut14, members of a ubiquitous protein family, are required for chromosome condensation and segregation in mitosis. *EMBO J*, **13**, 4938-4952.
- Sakai, A., Hizume, K., Sutani, T., Takeyasu, K. and Yanagida, M.** (2003) Condensin but not cohesin SMC heterodimer induces DNA reannealing through protein-protein assembly. *EMBO J*, **22**, 2764-2775.
- Samoshkin, A., Arnaoutov, A., Jansen, L.E., Ouspenski, I., Dye, L., Karpova, T., McNally, J., Dasso, M., Cleveland, D.W. and Strunnikov, A.** (2009) Human condensin function is essential for centromeric chromatin assembly and proper sister kinetochore orientation. *PLoS One*, **4**, e6831.
- Sanchez-Moran, E., Alfaro, D., Martinez, M. and Santos, J.L.** (2001) A comparative analysis of chiasma frequencies in different ecotypes of *Arabidopsis thaliana* (L.). *Chromosome Res*, **9**, 132.
- Sanchez-Moran, E., Armstrong, S.J., Santos, J.L., Franklin, F.C.H. and Jones, G.H.** (2002) Variation in chiasma frequency among eight accessions of *Arabidopsis thaliana*. *Genetics*, **162**, 1415-1422.
- Sanchez-Moran, E., Santos, J.L., Jones, G.H. and Franklin, F.C.H.** (2007) ASY1 mediates AtDMC1-dependent interhomolog recombination during meiosis in *Arabidopsis*. *Gene Dev*, **21**, 2220-2233.
- Savidou, E., Cobbe, N., Steffensen, S., Cotterill, S. and Heck, M.M.S.** (2005) *Drosophila* CAP-D2 is required for condensin complex stability and resolution of sister chromatids. *J Cell Sci*, **118**, 2529-2543.
- Schleiffer, A., Kaitna, S., Maurer-Stroh, S., Glotzer, M., Nasmyth, K. and Eisenhaber, F.** (2003) Kleisins: A superfamily of bacterial and eukaryotic SMC protein partners. *Mol Cell*, **11**, 571-575.
- Schueler, M. G., Sullivan, B.A.** (2006) Structural and functional dynamics of human centromeric chromatin. *Annu Rev Genomics Hum Genet*, **7**, 301-313.
- Schmiesing, J.A., Ball, A.R., Jr., Gregson, H.C., Alderton, J.M., Zhou, S. and Yokomori, K.** (1998) Identification of two distinct human SMC protein complexes involved in mitotic chromosome dynamics. *P Natl Acad Sci USA*, **95**, 12906-12911.
- Schmiesing, J.A., Gregson, H.C., Zhou, S. and Yokomori, K.** (2000) A human condensin complex containing hCAP-C-hCAP-E and CNAP1, a homolog of *Xenopus* XCAP-D2, colocalizes with phosphorylated histone H3 during the early stage of mitotic chromosome condensation. *Mol Cell Biol*, **20**, 6996-7006.
- Severson, A.F., Ling, L., van Zuylen, V. and Meyer, B.J.** (2009) The axial element protein HTP-3 promotes cohesin loading and meiotic axis assembly in *C. elegans* to implement the meiotic program of chromosome segregation. *Gene Dev*, **23**, 1763-1778.
- Shinohara, A., Ogawa, H. and Ogawa, T.** (1992) Rad51 Protein Involved in Repair and Recombination in *Saccharomyces-Cerevisiae* Is a RecA-Like Protein. *Cell*, **69**, 457-470.
- Shintomi, K. and Hirano, T.** (2011) The relative ratio of condensin I to II determines chromosome shapes. *Gene Dev*, **25**, 1464-1469.

- Shroff, R., Arbel-Eden, A., Pilch, D., Ira, G., Bonner, W.M., Petrini, J.H., Haber, J.E. and Lichten, M.** (2004) Distribution and dynamics of chromatin modification induced by a defined DNA double-strand break. *Curr Biol*, **14**, 1703-1711.
- Siaud, N., Dray, E., Gy, I., Gerard, E., Takvorian, N. and Doutriaux, M.P.** (2004) Brca2 is involved in meiosis in *Arabidopsis thaliana* as suggested by its interaction with Dmc1. *EMBO J*, **23**, 1392-1401.
- Siddiqui, N.U., Rusyniak, S., Hasenkampf, C.A. and Riggs, C.D.** (2006) Disruption of the *Arabidopsis* SMC4 gene, AtCAP-C, compromises gametogenesis and embryogenesis. *Planta*, **223**, 990-997.
- Siddiqui, N.U., Stronghill, P.E., Dengler, R.E., Hasenkampf, C.A. and Riggs, C.D.** (2003) Mutations in *Arabidopsis* condensin genes disrupt embryogenesis, meristem organization and segregation of homologous chromosomes during meiosis. *Development*, **130**, 3283-3295.
- Sinclair, D.A., Guarente, L.** (1997) Extrachromosomal rDNA circles – a cause of aging in yeast. *Cell*, **91**, 1033-1042.
- Snowden, T., Acharya, S., Butz, C., Berardini, M. and Fishel, R.** (2004) hMSH4-hMSH5 recognizes Holliday Junctions and forms a meiosis-specific sliding clamp that embraces homologous chromosomes. *Mol Cell*, **15**, 437-451.
- Somma, M.P., Fasulo, B., Siriaco, G. and Cenci, G.** (2003) Chromosome condensation defects in barren RNA-interfered *Drosophila* cells. *Genetics*, **165**, 1607-1611.
- St-Pierre, J., Douziech, M., Bazile, F., Pascariu, M., Bonneil, E., Sauve, V., Ratsima, H. and D'Amours, D.** (2009) Polo Kinase Regulates Mitotic Chromosome Condensation by Hyperactivation of Condensin DNA Supercoiling Activity. *Mol Cell*, **34**, 416-426.
- Stacey, N.J., Kuromori, T., Azumi, Y., Roberts, G., Breuer, C., Wada, T., Maxwell, A., Roberts, K. and Sugimoto-Shirasu, K.** (2006) *Arabidopsis* SPO11-2 functions with SPO11-1 in meiotic recombination. *Plant J*, **48**, 206-216.
- Stahl, F.W., Foss, H.M., Young, L.S., Borts, R.H., Abdullah, M.F. and Copenhagen, G.P.** (2004) Does crossover interference count in *Saccharomyces cerevisiae*? *Genetics*, **168**, 35-48.
- Stear, J.H. and Roth, M.B.** (2002) Characterization of HCP-6, a *C. elegans* protein required to prevent chromosome twisting and merotelic attachment. *Gene Dev*, **16**, 1498-1508.
- Steen, R.L., Cubizolles, F., Le Guellec, K. and Collas, P.** (2000) A kinase-anchoring protein (AKAP)95 recruits human chromosome-associated protein (hCAP)-D2/Eg7 for chromosome condensation in mitotic extract. *J Cell Biol*, **149**, 531-536.
- Steffensen, S., Coelho, P.A., Cobbe, N., Vass, S., Costa, M., Hassan, B., Prokopenko, S.N., Bellen, H., Heck, M.M.S. and Sunkel, C.E.** (2001) A role for *Drosophila* SMC4 in the resolution of sister chromatids in mitosis. *Curr Biol*, **11**, 295-307.
- Storlazzi, A., Gargano, S., Ruprich-Robert, G., Falque, M., David, M., Kleckner, N. and Zickler, D.** (2010) Recombination Proteins Mediate Meiotic Spatial Chromosome Organization and Pairing. *Cell*, **141**, 94-106.

- Storlazzi, A., Tesse, S., Gargano, S., James, F., Kleckner, N. and Zickler, D.** (2003) Meiotic double-strand breaks at the interface of chromosome movement, chromosome remodeling, and reductional division. *Gene Dev*, **17**, 2675-2687.
- Strunnikov, A.V., Hogan, E. and Koshland, D.** (1995) SMC2, a *Saccharomyces cerevisiae* gene essential for chromosome segregation and condensation, defines a subgroup within the SMC family. *Gene Dev*, **9**, 587-599.
- Sullivan, M., Higuchi, T., Katis, V.L. and Uhlmann, F.** (2004) Cdc14 phosphatase induces rDNA condensation and resolves cohesin-independent cohesion during budding yeast anaphase. *Cell*, **117**, 471-482.
- Sumner, A.T.** (1996) The distribution of topoisomerase II on mammalian chromosomes. *Chromosome Res*, **4**, 5-14.
- Sun, H., Treco, D., Schultes, N.P. and Szostak, J.W.** (1989) Double-Strand Breaks at an Initiation Site for Meiotic Gene Conversion. *Nature*, **338**, 87-90.
- Sutani, T., Yuasa, T., Tomonaga, T., Dohmae, N., Takio, K. and Yanagida, M.** (1999) Fission yeast condensin complex: essential roles of non-SMC subunits for condensation and Cdc2 phosphorylation of Cut3/SMC4. *Gene Dev*, **13**, 2271-2283.
- Sym, M. and Roeder, G.S.** (1994) Crossover interference is abolished in the absence of a synaptonemal complex protein. *Cell*, **79**, 283-292.
- Tada, K., Susumu, H., Sakuno, T. and Watanabe, Y.** (2011) Condensin association with histone H2A shapes mitotic chromosomes. *Nature*, **474**, 477-483.
- Takemoto, A., Kimura, K., Yanagisawa, J., Yokoyama, S. and Hanaoka, F.** (2006) Negative regulation of condensin I by CK2-mediated phosphorylation. *EMBO J*, **25**, 5339-5348.
- Takemoto, A., Kimura, K., Yokoyama, S. and Hanaoka, F.** (2003) Analysis of regulation of human condensin during the cell cycle. *Cell Struct Funct*, **28**, 338.
- Takemoto, A., Kimura, K., Yokoyama, S. and Hanaoka, F.** (2004) Cell cycle-dependent phosphorylation, nuclear localization, and activation of human condensin. *J Biol Chem*, **279**, 4551-4559.
- Takemoto, A., Maeshima, K., Ikehara, T., Yamaguchi, K., Murayama, A., Imamura, S., Imamoto, N., Yokoyama, S., Hirano, T., Watanabe, Y., Hanaoka, F., Yanagisawa, J. and Kimura, K.** (2009) The chromosomal association of condensin II is regulated by a noncatalytic function of PP2A. *Nat Struct Mol Biol*, **16**, 1302-1308.
- Takemoto, A., Murayama, A., Katano, M., Urano, T., Furukawa, K., Yokoyama, S., Yanagisawa, J., Hanaoka, F. and Kimura, K.** (2007) Analysis of the role of Aurora B on the chromosomal targeting of condensin I. *Nucleic Acids Res*, **35**, 2403-2412.
- Tay, Y.D. and Wu, L.** (2010) Overlapping roles for Yen1 and Mus81 in cellular Holliday junction processing. *J Biol Chem*, **285**, 11427-11432.
- Tease, C. and Hulten, M.A.** (2004) Inter-sex variation in synaptonemal complex lengths largely determine the different recombination rates in male and female germ cells. *Cytogenet Genome Res*, **107**, 208-215.

- Terasawa, M., Ogawa, H., Tsukamoto, Y., Shinohara, M., Shirahige, K., Kleckner, N. and Ogawa, T.** (2007) Meiotic recombination-related DNA synthesis and its implications for cross-over and non-cross-over recombinant formation. *P Natl Acad Sci USA*, **104**, 5965-5970.
- Tesse, S., Storlazzi, A., Kleckner, N., Gargano, S. and Zickler, D.** (2003) Localization and roles of Ski8p protein in *Sordaria* meiosis and delineation of three mechanistically distinct steps of meiotic homolog juxtaposition. *P Natl Acad Sci USA*, **100**, 12865-12870.
- Torres-Rosell, J., Sunjevaric, I., De Piccoli, G., Sacher, M., Eckert-Boulet, N., Reid, R., Jentsch, S., Rothstein, R., Aragón, L., Lisby, M.** (2007) The Smc5-Smc6 complex and SUMO modification of Rad52 regulates recombinational repair at the ribosomal gene locus. *Nat Cell Biol*, **9**, 923-931.
- Tremethick, D.J.** (2007) Higher-order structure of chromatin: the elusive 30 nm fibre. *Cell*, **128**, 651-654.
- Tsai, C.J., Mets, D.G., Albrecht, M.R., Nix, P., Chan, A. and Meyer, B.J.** (2008) Meiotic crossover number and distribution are regulated by a dosage compensation protein that resembles a condensin subunit. *Gene Dev*, **22**, 194-211.
- Uanschou, C., Siwec, T., Pedrosa-Harand, A., Kerzendorfer, C., Sanchez-Moran, E., Novatchkova, M., Akimcheva, S., Woglar, A., Klein, F. and Schlogelhofer, P.** (2007) A novel plant gene essential for meiosis is related to the human CtIP and the yeast COM1/SAE2 gene. *EMBO J*, **26**, 5061-5070.
- Uemura, T., Ohkura, H., Adachi, Y., Morino, K., Shiozaki, K. and Yanagida, M.** (1987) DNA topoisomerase II is required for condensation and separation of mitotic chromosomes in *S. pombe*. *Cell*, **50**, 917-925.
- Usui, T., Ohta, T., Oshiumi, H., Tomizawa, J., Ogawa, H. and Ogawa, T.** (1998) Complex formation and functional versatility of Mre11 of budding yeast in recombination. *Cell*, **95**, 705-716.
- Uzbekov, R., Timirbulatova, E., Watrin, E., Cubizolles, F., Ogereau, D., Gulak, P., Legagneux, V., Polyakov, V.J., Le Guellec, K. and Kireev, I.** (2003) Nucleolar association of pEg7 and XCAP-E, two members of *Xenopus laevis* condensin complex in interphase cells. *J Cell Sci*, **116**, 1667-1678.
- Vagnarelli, P., Hudson, D.F., Ribeiro, S.A., Trinkle-Mulcahy, L., Spence, J.M., Lai, F., Farr, C.J., Lamond, A.I. and Earnshaw, W.C.** (2006) Condensin and Repo-Man-PP1 co-operate in the regulation of chromosome architecture during mitosis. *Nat Cell Biol*, **8**, 1133-U1161.
- Verkade, H.M., Bugg, S.J., Lindsay, H.D., Carr, A.M. and O'Connell, M.J.** (1999) Rad18 is required for DNA repair and checkpoint responses in fission yeast. *Mol Biol Cell*, **10**, 2905-2918.
- Viera, A., Gomez, R., Parra, M.T., Schmiesing, J.A., Yokomori, K., Rufas, J.S. and Suja, J.A.** (2007) Condensin I Reveals New Insights on Mouse Meiotic Chromosome Structure and Dynamics. *PLoS One*, **2**, Article No.: e783.
- Voinnet, O.** (2005) Non-cell autonomous RNA silencing. *FEBS Lett*, **579**, 5858-5871.
- Wang, B.D., Eyre, D., Basrai, M., Lichten, M. and Strunnikov, A.** (2005a) Condensin binding at distinct and specific chromosomal sites in the *Saccharomyces cerevisiae* genome. *Mol Cell Biol*, **25**, 7216-7225.

- Wang, B.D., Eyre, D., Basrai, M., Lichten, M. and Strunnikov, A.** (2005b) Condensin binding at distinct and specific chromosomal sites in the *Saccharomyces cerevisiae* genome. *Mol Cell Biol*, **25**, 7216-7225.
- Wang, B.D. and Strunnikov, A.** (2008) Transcriptional homogenization of rDNA repeats in the episome-based nucleolus induces genome-wide changes in the chromosomal distribution of condensin. *Plasmid*, **59**, 45-53.
- Wang, B.D., Yong-Gonzalez, V. and Strunnikov, A.V.** (2004) Cdc14p/FEAR pathway controls segregation of nucleolus in *S. cerevisiae* by facilitating condensin targeting to rDNA chromatin in anaphase. *Cell Cycle*, **3**, 960-967.
- Wang, C.J., Carlton, P.M., Golubovskaya, I.N. and Cande, W.Z.** (2009) Interlock formation and coiling of meiotic chromosome axes during synapsis. *Genetics*, **183**, 905-915.
- Wang, J.C.** (2002) Cellular roles of DNA topoisomerases: a molecular perspective. *Nat Rev Mol Cell Biol*, **3**, 430-440.
- Wang, M., Wang, K., Tang, D., Wei, C., Li, M., Shen, Y., Chi, Z., Gu, M. and Cheng, Z.** (2010) The central element protein ZEP1 of the synaptonemal complex regulates the number of crossovers during meiosis in rice. *Plant Cell*, **22**, 417-430.
- Wang, X. and Haber, J.E.** (2004) Role of *Saccharomyces* single-stranded DNA-binding protein RPA in the strand invasion step of double-strand break repair. *PLoS Biol*, **2**, 104-112.
- Waterworth, W.M., Altun, C., Armstrong, S.J., Roberts, N., Dean, P.J., Young, K., Weil, C.F., Bray, C.M. and West, C.E.** (2007) NBS1 is involved in DNA repair and plays a synergistic role with ATM in mediating meiotic homologous recombination in plants. *Plant J*, **52**, 41-52.
- Watrin, E., Cubizolles, F., Osborne, H.B., Le Guellec, K. and Legagneux, V.** (2003) Expression and functional dynamics of the XCAP-D2 condensin subunit in *Xenopus laevis* oocytes. *J Biol Chem*, **278**, 25708-25715.
- Watrin, E. and Legagneux, V.** (2005) Contribution of hCAP-D2, a non-SMC subunit of condensin I, to chromosome and chromosomal protein dynamics during mitosis. *Mol Cell Biol*, **25**, 740-750.
- Wei, Y., Yu, L., Bowen, J., Gorovsky, M.A. and Allis, C.D.** (1999) Phosphorylation of histone H3 is required for proper chromosome condensation and segregation. *Cell*, **97**, 99-109.
- Wignall, S.M., Deehan, R., Maresca, T.J. and Heald, R.** (2003) The condensin complex is required for proper spindle assembly and chromosome segregation in *Xenopus* egg extracts. *J Cell Biol*, **161**, 1041-1051.
- Wojtasz, L., Daniel, K., Roig, I., Bolcun-Filas, E., Xu, H., Boonsanay, V., Eckmann, C.R., Cooke, H.J., Jasin, M., Keeney, S., McKay, M.J. and Toth, A.** (2009) Mouse HORMAD1 and HORMAD2, two conserved meiotic chromosomal proteins, are depleted from synapsed chromosome axes with the help of TRIP13 AAA-ATPase. *PLoS Genet*, **5**, e1000702.
- Woodcock, C.L., Ghosh, R.P.** (2010) Chromatin higher-order structure and dynamics. *Cold Spring Harb Perspect Biol*, **2**, a000596.
- Wu, T.C. and Lichten, M.** (1994) Meiosis-induced double-strand break sites determined by yeast chromatin structure. *Science*, **263**, 515-518.

- Xu, H.L., Beasley, M.D., Warren, W.D., van der Horst, G.T.J. and McKay, M.J.** (2005) Absence of mouse REC8 cohesin promotes synapsis of sister chromatids in meiosis. *Dev Cell*, **8**, 949-961.
- Xu, L.H., Weiner, B.M. and Kleckner, N.** (1997) Meiotic cells monitor the status of the interhomolog recombination complex. *Gene Dev*, **11**, 106-118.
- Yeong, F.M., Hombauer, H., Wendt, K.S., Hirota, T., Mudrak, I., Mechtler, K., Loregger, T., Marchler-Bauer, A., Tanaka, K., Peters, J.M. and Ogris, E.** (2003) Identification of a subunit of a novel kleisin-beta/SMC complex as a potential substrate of protein phosphatase 2A. *Curr Biol*, **13**, 2058-2064.
- Yong-Gonzalez, V., Wang, B.D., Butylin, P., Ouspenski, I. and Strunnikov, A.** (2007) Condensin function at centromere chromatin facilitates proper kinetochore tension and ensures correct mitotic segregation of sister chromatids. *Genes Cells*, **12**, 1075-1090.
- Yoshimura, S.H., Hizume, K., Murakami, A., Sutani, T., Takeyasu, K. and Yanagida, M.** (2002) Condensin architecture and interaction with DNA: Regulatory non-SMC subunits bind to the head of SMC heterodimer. *Curr Biol*, **12**, 508-513.
- Yu, H.G., Hiatt, E.N., Dawe, R.K.** (2000) The plant kinetochore. *Trends Plant Sci*, **5**, 543-547.
- Yu, H.G. and Koshland, D.** (2005) Chromosome morphogenesis: Condensin-dependent cohesin removal during meiosis. *Cell*, **123**, 397-407.
- Yu, H.G. and Koshland, D.E.** (2003) Meiotic condensin is required for proper chromosome compaction, SC assembly, and resolution of recombination-dependent chromosome linkages. *J Cell Biol*, **163**, 937-947.
- Zickler, D. and Kleckner, N.** (1999) Meiotic chromosomes: Integrating structure and function. *Annu Rev Genet*, **33**, 603-754.
- Zickler, D., Moreau, P.J., Huynh, A.D. and Slezec, A.M.** (1992) Correlation between pairing initiation sites, recombination nodules and meiotic recombination in *Sordaria macrospora*. *Genetics*, **132**, 135-148.

9 APPENDIXES

9.1 BUFFERS

ALEXANDER STAIN

Ethanol 95% 10 ml

Malachite green (1% in 95% Ethanol) 1 ml

Fuchsin acid (1% in water) 5 ml

Orange G (1% in water) 0.5 ml

Phenol 5 g

Chloral hydrate 5 g

Glacial acetic acid 2 ml

Glycerol 25 ml

Distilled water 50 ml

CITRATE BUFFER

Citric acid 0.1 M

Sodium citrate 0.1 M

diluted 1:10 with sterile distilled water
pH 5.4

COOMASSIE BLUE

Coomassie Blue R-2500 1 %

SDW 45 % (v/v)

Methanol 45 % (v/v)

Glacial acetic acid 10%

DESTAIN

Methanol 30 % (v/v)

Glacial acetic acid 10 % (v/v)

DILUTION BUFFER

3x BSA in water (Bovine serum
albumin)

DNA EXTRACTION BUFFER

KCL 0.25 M

EDTA 10 mM

Tris-HCL 100 mM

pH 9.5

DNA LOADING BUFFER

Bromophenol blue 50 µl

1 Kb ladder (Invitrogen) 12 µl

SDW 138 µl

ELUTION BUFFER

Tris HCL 50 mM

NaCl 300 mM

Urea 8 M

Varying concentrations of Imidazol,
pH 8

HYBRIDISATION MIX

Detran sulphate 1 g
 Deionised formamide 5 ml
 20xSSC 1 ml
 to 7ml with water, pH

IP-BUFFER:

20 mM Tris-HCL, pH 7.7
 150 mM NaCl
 10 % glycerol
 2 mM EDTA

1x PBS

Phosphate saline buffer 1 tablet per
 100ml pH 7

LB MEDIUM

1-1bacto-tryptone 10 g
 1-1 bacto-yeast extract 5 g
 NaCl 10 g

LYSIS BUFFER

50 mM Tris
 300 mM NaCl (pH 8)
 20 mM Imidazole

LYSOGENY BROTH (LB) AGAR

1-1bacto-tryptone 10 g
 1-1 bacto-yeast extract 5 g

NaCl 10 g

Bacto-agar 15 g

Media was prepared in SDW and
 sterilised by autoclaving at 15 psi
 at 121 °C for 20 minutes.

MILK BLOCK

PBS 1x
 Milk powder 5 % (w/v)

MS MEDIA (Murashige and Skoog,
 1962)

2.2g MS basal salt powder with
 Gamborg'e vitamins (Sigma)/ litre
 SDW

pH 5.6-5.8 (with KOH)

10g^l⁻¹ agar (Sigma)

5X PROTEIN LOADING BUFFER (PLB)

Tris-HCL (pH 6.8) 12.5% (v/v)

SDS 2% (w/v)

Glycerol 10% (v/v)

B-Mercatoethanol 5% (v/v)

Bromophenol blue 0.001% (w/v)

RESERVOIR BUFFER 1X

Tris 25 mM

Glycine 192 mM

SDS 0.1 % (w/v)

pH 8.3

20 x SSC

3 M NaCl

300 mM trisodium citrate

Made to pH 7 using HCl

5x TBE

Tris 0.445 M

Boric acid 0.445 M

EDTA 0.01 M

WESTERN TRANSFER BUFFER

Methanol 20 % (v/v)

Sodium hydrogen carbonate 0.01 M

Sodium carbonate 3.0 mM

9.2 TABLE OF PRIMERS

Primer name	Primer sequence 5' to 3'	Tm (°C)
T7 promoter	TAATACGACTCACTATAGGG	45.6
M13 forward	TGACCGGCAGCAAATG	58.7
M3 reverse	AACAGCTATGACCATG	42.0
Oligo dt	TTTTTTTTTTTTTTTTTTTTTTTTTT	42.2
SMC4Ab-g_F	CCGCTAGCGAACTGGCGAAAAGCCAAAG	69.5
SMC4Ab_R	GCGGCCGCTTTCAGATCACAA	61.8
SMC4_86_D2_LP	AAGCTCAGACCGGTAACCTTC	59.8
SMC4_86_D2_RP	CAAATGGTCAAATTAGCGGAG	55.9
SAILLB	GCCTTTTCAGAAATGGATAAATAGCCTTGCTTCC	71.2
LBa.1	TGGTTCACGTAGTGGGCCATCG	67.9
Cap-gSALK009LP	GGCATTATCAACCCTTCACTCAA	58.9
Cap-gSALK009RP	GTAATTCAGACGGTGACTCCG	59.8
Capd2_734_lp	TTGAAGTTTTCACATACCGCC	55.9
Capd2_734_rp	TCTGCATCCTCATCAATCTCC	57.9
CAPD2-796_lp	GTAGAGGTTCCACTTTTGCCC	59.8
CAPD2-796_rp	AACATAACCCCTTTGGTCCAC	57.9
Caph2_339LP	TTCCGCTCTCTTCAACAGTC	57.9
Caph2_339RP	AAGGTTGGGAAATGGCTATTG	55.9
SMC4RNAi EcoR1	CGCAATTCCTTTGCCACAACAGTGTTTC	71.1
SMC4RNAi Xho1	CGCTCGAGAAGAGTCAGAATGAGG	64.6
SMC4RNAiHindIII	GCAAGCTTTGCCACAACAGTGTTT	65.2
SMC4RANI BamHI	CGGGATCCGAGAAGAGTCAGAATGAGG	70.3
CAPD2_bamh1_f1	GGGATCCGAGGGAGATATGAGTTC	66.3
CAPD2_xho1_f2	GCTCGAGGGAGATATGAGTTCC	62.1
CAPD2_hind3_r3	GAAGCTTCTGACCGTCAATTTGG	62.7
CAPD2_ecor1	GGAATTCGACCGTCAATTTGG	60.6
CAPD3_bamh1_f1	GGGATCCGAGCCTGCTGCAGATCGGA	72.6
CAPD3_xho1_f2	GCTCGAGCCTGCTGCAGATCTGGC	69.6
CAPD3_hind3_r3	GAAGCTTCCCGTCAGCCAAACACATC	66.4
CAPD3_ecor1_r4	GGAATTCCTGTCAGCCAAACACATC	64.6
DMC Pro Primer	GTTTCGGATTCATAGAGCTGAAG	58.9
pHan seq for	AGTGGATTGATGTGACATCTC	53.2
pHan seq for 2	CTAAATGGATTGACTATTAAT	44.4
pHan seq rev	TCAGGTTTTTTACAACGTGC	54.9
pHan seq rev 2	TTTATAAATTATTTTTTTCAC	40.9
D3B06_Lp	CTGAAGAAGGTGGATTTGATGCG	60.6
D3B06_Rp	CGGAAATAGCTGAAACTGCAGCC	62.4
D3 RTPCRf	CCTGAGAAGGCCGAGCCGCGTGG	71.3
D3 RTPCRr	CATATTCTGAATGCCTCGGAAATAGC	61.6
GAPD-N	CTTGAAGGGTGGTGCCAAGAAGG	66.7
GAPD-C	CCTGTTGTCGCCAACGAAGTCAG	66.8
CapD3_AB_F	CCCATATGGCCCCAGAACACCTTTTGG	68.0
CapD3_AB_R	CCCTCGAGACTCTCATCATCAGACATG	66.5
D3ABfor2	CCCATATGTCCAACCTTGCTCAAGTTGTGG	68.1

D3ABrev2	CCCTCGAGCAAGCAACTGCCAATGATGG	69.5
SPO11 F4	GAGGATATCCAGATGTCTC	54.5
SPO11 R1	AGGAGAGCTTACTTCACGAC	52.2
WISCLB	AACGTCCGCAATGTGTTAAGTTGT	62.2

Table 5: Table of primers. Restriction sites are highlighted in red

Condensin subunit	Gene name	T-DNA line	Outcome
AtSMC4	At5G48600	Sail_86_D2	Homozygote lethal
AtCAPD2:	At3G57060:	Salk_158734	No inserts found
		Salk_044796	No inserts found
AtCAPG	At5G37630	Salk_064009	Homozygote lethal
AtCAPH	At2G32590	Salk_013559	No inserts found
AtCAPD3	At4G15890	Sail_826_B06	Homozygote viable

Table 6: Table of T-DNA lines